Gondwana Research 128 (2024) 161–263

Contents lists available at ScienceDirect

Gondwana Research

journal homepage: www.elsevier.com/locate/gr

GR Focus Review

Finding Argoland: Reconstructing a microcontinental archipelago from the SE Asian accretionary orogen

Eldert L. Advokaat [a,b,*], Douwe J.J. van Hinsbergen [a]

[a] Department of Earth Sciences, Utrecht University, 3584 CB Utrecht, The Netherlands
[b] School of Geography, Earth and Environmental Sciences, University of Birmingham, Birmingham B15 2TT, United Kingdom

ARTICLE INFO

Article history:
Received 20 March 2023
Revised 27 September 2023
Accepted 12 October 2023
Available online 19 October 2023
Handling Editor: D. Nance

Keywords:
GPlates
Plate tectonic reconstruction
Sundaland
Argo Abyssal Plain
Australia

ABSTRACT

Based on the marine magnetic anomalies identified in the Argo Abyssal Plain offshore northwestern Australia, the conceptual continent of Argoland must have rifted off in the Late Jurassic (~155 Ma) and drifted northward towards SE Asia. Intriguingly, in SE Asia there are no intact relics of a major continent such as India, but instead the region displays an intensely deformed, long-lived accretionary orogen that formed during more than 100 million years of oceanic and continental subduction. Within this orogen, there are continental fragments that may represent parts of Argoland. After accretion of these fragments, the orogen was further deformed. We compiled the orogenic architecture and the history of post-accretionary deformation of SE Asia, as well as the architecture and history of the NW Australian passive margin. We identified the Gondwana-derived blocks and mega-units of SW Borneo, Greater Paternoster, East Java, West Burma, and Mount Victoria Land as fragments that collectively may represent fragments of Argoland. These fragments are found between sutures with relics of Late Triassic to Middle Jurassic oceanic basins that all pre-date the break-up of Argoland. We systematically restore deformation within SE Asia in the upper plate system above the modern Sunda trench, use this to estimate where Gondwana-derived continental fragments accreted at the Sundaland (Eurasian) margin in the Cretaceous (~110–85 Ma), and subsequently reconstruct their tectonic transport back to the Australian-Greater Indian margin. Our reconstruction shows that Argoland originated at the northern Australian margin between the Bird's Head in the east and Wallaby-Zenith Fracture Zone in the west, south of which it bordered Greater India. We show that the lithospheric fragment that broke off northwest Australia in the Late Jurassic consisted of multiple continental fragments and intervening Triassic to Middle Jurassic oceanic basins, which we here call Argopelago. Argoland broke up into Argopelago during the Late Triassic rifting of Lhasa from the northern margin of Gondwana, and consisted of multiple continental fragments that were surrounded by oceanic basins, similar to Zealandia offshore modern east Australia, and the reconstructed history of Greater Adria in the Mediterranean.

Contents

1. Introduction . . . 162
2. The case for Argoland based on the tectonic evolution of the NW Australian margin . . . 163
3. Reconstruction philosophy and protocol . . . 167
4. Kinematic constraints from SE Asian orogenic architecture . . . 169
   4.1. Modern plates, plate boundaries, and the Sundaland core of the SE Asian accretionary orogen . . . 170
   4.2. Late Cretaceous to Cenozoic deformation of Sundaland . . . 172
   4.3. Longzi Block of the Tethyan Himalayas; West Burma block; Indo-Burman ranges; Mount Victoria Land . . . 173
   4.4. Woyla Arc; Andaman-Nicobar ophiolites; Ciletuh Complex . . . 175
   4.5. Sagaing Fault; Andaman Sea region; Sumatran Fault System . . . 176

* Corresponding author at: Department of Earth Sciences, Utrecht University, 3584 CB Utrecht, The Netherlands.
E-mail address: E.L.Advokaat@uu.nl (E.L. Advokaat).

https://doi.org/10.1016/j.gr.2023.10.005
1342-937X/

4.6. SW Borneo Mega-Unit; Kuching Zone; OPS sequences in Sarawak and Sabah . . . 177
4.7. Meratus Complex; Klaten-Banyuwangi Suture; East Java Block . . . 180
4.8. Greater Paternoster Mega-Unit; Makassar Straits Basin; Flores Basin; Timor Allochthon . . . 182
4.9. Bantimala Mélange Belt . . . 185
4.10. Celebes Sea Basin; North Sulawesi Arc; Gorontalo Bay Basin; East Sulawesi Ophiolite; SE Sulawesi accretionary complex . . . 186
4.11. Sula Spur fragments; Banda basins . . . 189
4.12. Accreted Australian plate units of Timor and the Outer Banda Islands . . . 193
4.13. Sulu Arc; Sulu Sea; Cagayan Arc; Palawan Accretionary Complex; Rajang-Crocker Accretionary Complex . . . 195
4.14. South China Sea Basin . . . 198
4.15. Active margins with Panthalassa/Pacific-derived plates . . . 199
5. Kinematic restoration tested against paleomagnetic data . . . 205
5.1. Paleomagnetic database of SE Asia . . . 205
5.2. Paleomagnetic tests of the reconstruction . . . 205
6. Stepwise reconstruction of SE Asia: Finding Argoland . . . 209
6.1. Zanclean – 5 Ma . . . 209
6.2. Chattian – 25 Ma . . . 212
6.3. Lutetian – 45 Ma . . . 217
6.4. Santonian – 85 Ma . . . 222
6.5. Valanginian – 135 Ma . . . 227
6.6. Kimmeridgian – 155 Ma . . . 231
6.7. Norian – 215 Ma . . . 234
7. Discussion . . . 237
7.1. Argopelago destruction and subduction initiation in SE Asia . . . 238
7.2. Argoland and the pre-late Jurassic width of Greater India . . . 241
7.3. Implications of Argoland reconstruction for continental subduction . . . 244
8. Summary and conclusions . . . 245
Declaration of Competing Interest . . . 245
Acknowledgements . . . 245
Appendix A. Supplementary Material . . . 246
References . . . 246

1. Introduction

A paradigm underlying plate tectonics and paleogeographic reconstructions is that whilst aging oceanic crust becomes denser than the mantle and will eventually subduct, continental crust escapes subduction due to its buoyancy (e.g. Vlaar and Wortel, 1976). In the last decades, evidence has mounted that this paradigm requires some modification: geological reconstructions and numerical models have shown that continental lower crust and lithospheric mantle may subduct, but that its upper crust is offscraped and accreted as nappes to the upper plate, forming orogenic belts (Capitanio et al., 2010; Jolivet and Brun, 2010; Toussaint et al., 2004; van Hinsbergen et al., 2005; van Hinsbergen and Schouten, 2021). This mechanism provides an explanation for the long-lived balance between the amount of continental crust that is formed by arc magmatism and tectonic accretion, and destroyed by subduction into the mantle since the onset of plate tectonics (Cawood et al., 2013; Hawkesworth et al., 2019; Scholl and von Huene, 2009; Spencer et al., 2017). These new insights define the basic paradigm underlying the reconstruction of supercontinents and their cyclicity (Dewey and Burke, 1974; Wilson, 1966) is that the crust of ancient continents is still largely present today, as lithospheric fragments in continental interiors, or as deformed upper crustal slivers in accretionary orogens. In this respect it is interesting, and for paleogeographic reconstructions worrisome, that the proposed continent of Argoland that once formed the conjugate margin to northwestern Australia (Gibbons et al., 2012; Veevers et al., 1991) potentially poses a challenge to this concept.

Argoland is a conceptual continent that must have broken off northwestern Australia in the Late Jurassic (~160 Ma) (Gartrell et al., 2022, 2016; Longley et al., 2002; von Rad et al., 1992) and drifted north towards SE Asia. In the orogenic belt of SE Asia, from Myanmar to eastern Indonesia, deformed continental rocks are widespread, but no intact relics of a major continent, such as India, is present. Instead, SE Asia exposes an intensely deformed, long-lived accretionary orogen that formed during more than 130 million years of subduction (Hall, 2009; Parkinson et al., 1998; Wakita, 2000). This orogen hosts accreted remnants of continental crust that possibly represent parts of Argoland (Hall and Sevastjanova, 2012; Metcalfe, 2013a; Smyth et al., 2007). Kinematic reconstructions of the region have restored the Cenozoic deformation of the SE Asian orogen (Hall, 2002, 1996; Lee and Lawver, 1995; Rangin et al., 1990b), but reconstructions that focus on the Late Jurassic break-up history of NW Australia (e.g. Hall, 2012; Zahirovic et al., 2016, 2014) have so far only restored continental fragments exposed on SE Asian islands that have a much smaller area than the predicted size of Argoland along the Australian margin.

In addition to the areal mismatch, also the timing of rifting recorded in the interpreted Argoland relics does often not match the Late Jurassic rifting age recorded in the geology and marine geophysics of western Australia (Gibbons et al., 2012; Veevers et al., 1991). The fragments so far identified as Argoland (e.g. Hall, 2012; Hall et al., 2009a; Metcalfe, 2013a; Zahirovic et al., 2016, 2014) are found between geological relics of ocean basins that are of Late Triassic to Middle Jurassic age (Böhnke et al., 2019; Coggon et al., 2011; Wakita et al., 1998). This challenges the concept that these fragments were part of a coherent Jurassic continent and raise the question what 'Argoland' looked like, or whether it existed at all. Other continental fragments that may have been derived from the northwestern Australian margin are found in Myanmar (the West Burma Block and Mount Victoria Land in the Indo-Burman Ranges (Aitchison et al., 2019; Mitchell, 1986), but these have also not been unequivocally interpreted as part of the Australian or Eurasian margin in the Mesozoic

(Naing et al., 2023; Sevastjanova et al., 2016; Yao et al., 2017; Zhang et al., 2020b). Global plate reconstructions (e.g., Müller et al., 2019) thus struggle with the conceptual Argoland continent, rifting it off northwestern Australia in the Late Jurassic, but removing it from the reconstruction from the mid-Cretaceous onwards. Other authors have suggested that the indications for Jurassic break-up are misinterpreted and that western Australia was entirely conjugate to the Greater Indian continental promontory that as part of the Indian plate broke off Australia in the early Cretaceous (e.g. Ingalls et al., 2016). The vast majority of such an enormous conceptual Greater Indian promontory with an area equivalent in size to present-day Arabia (van Hinsbergen et al., 2019a) would then have entirely subducted below Eurasia in the Cenozoic (e.g. Ingalls et al., 2016; Rowley and Ingalls, 2017; Rowley, 2019a, 2019b), because from a period between the early Eocene and latest Oligocene, no accretionary record is known from the Himalaya (van Hinsbergen, 2022; van Hinsbergen et al., 2012). If correct, this would show that the basic paradigm of paleogeography and plate tectonics – that continents do not subduct without an accretionary record – is incorrect, which would make reconstructing paleogeography and supercontinents, or dating continental collision, very challenging (van Hinsbergen, 2022; van Hinsbergen and Schouten, 2021). It is therefore important to identify the paleogeographic and plate tectonic evolution of the continental fragments contained in the SE Asian orogen, to evaluate to what extent these may or may not be representative of Argoland, and if so, what paleogeographic evolution must be inferred to satisfy the discrepancy between the conceptual Argoland model, and the geological reality of SE Asia's orogenic architecture.

In this paper, we therefore aim to reconstruct the plate tectonic and paleogeographic evolution of the plates that carried the SE Asian continental fragments from the Gondwana margin to their modern position since the early Mesozoic. We systematically review the modern architecture of the western and northwestern Australian margin, and the SE Asian accretionary orogen (Hall, 2009), which is defined as the deformed belt that encompasses Myanmar and Indochina, Indonesia and Malaysia, bounded from the Pacific/Panthalassa-derived oceanic plates by the Philippine Mobile Belt (Figs. 1 and 2). We cast our reconstruction in plate kinematic reconstructions of Australia-Eurasia motion. We use this to kinematically restore deformation within SE Asia in the wider upper plate system between the modern Sunda trench and stable China and estimate when and where Gondwana-derived continental fragments arrived and accreted to the SE Asian orogen. We then reconstruct their trajectory back to the Australian margin. We focus our search for Argoland in a region from the eastern Himalaya in the west to the Panthalassa Ocean-derived geological records of the Philippines, Halmahera, and New Guinea in the east (Fig. 1). We review available constraints from marine magnetic anomalies and structural and paleomagnetic constraints quantifying past motions using GPlates software (Müller et al., 2018) and applying a systematic reconstruction protocol that was also applied to regions with similar tectonic complexity (Boschman et al., 2014; Vaes et al., 2019; van Hinsbergen et al., 2020, 2019a). We will use our results to evaluate whether continental crust must have subducted in its entirety in the eastern Neotethys or is accounted for in the orogenic belts of SE Asia.

2. The case for Argoland based on the tectonic evolution of the NW Australian margin

The concept of Argoland was derived from the final Late Jurassic breakup history recorded in the northwestern Australian margin and the adjacent ocean floor. But the margin also contains evidence for older deformation phases, that the conceptual Argoland continent may also have experienced when it was still adjacent to the modern Australian margin. In this section, we thus review the constraints on the tectonic history of the western and northwestern Australian margin and explain how the Argoland concept has come about in the literature.

The **Australian Northwest Shelf** (AGSO, 1994; Heezen and Tharp, 1965) forms part of the northern Australian continental margin (Figs. 1, 2 and S1) that displays evidence for a protracted history of extension and continental thinning. The shelf comprises Precambrian continental basement overlain by intra-cratonic basins that started to accumulate sediments in the early Paleozoic (AGSO, 1994 and references therein). Rifting occurred in the Late Carboniferous (Kasimovian/Gzelian) to Early Permian (Sakmarian) (Gartrell et al., 2022). This extension has been generally been assumed to be NW-SE to N-S directed (AGSO, 1994; Etheridge and O'Brien, 1994; Gartrell et al., 2022). This extension was accommodated in the upper crust by NE-SW striking normal faults and N-S and E-W striking transtensional accommodation zones, whereas the lower crust was thinned from a presumed initial thickness of 35–45 km corresponding to non-extended Australia (Drummond et al., 1991) to 5–20 km, i.e. 100–500 % extension, accommodated along detachment zones that exhumed lower crust and lithospheric mantle (Bellingham and Mcdermott, 2014; Deng and McClay, 2019; Etheridge and O'Brien, 1994). Post-rift thermal subsidence following this extension created accommodation space for several kilometers of Lower Permian (Kungurian) to Upper Permian (Wuchiapingian) clastic sediments (Etheridge and O'Brien, 1994; Gartrell et al., 2022), after which the enigmatic 'Bedout movement' and 'Fitzroy movements' in the Upper Permian (Changhsingian) to Late Triassic (early Norian: ~225 Ma) led to inversion and shortening (Gartrell et al., 2022; Longley et al., 2002; Smith et al., 1999). Renewed *syn*-rift sedimentation commenced in the Late Triassic (Norian: ~215 Ma) (Gartrell et al., 2022, 2016; Gradstein, 1992; Longley et al., 2002; von Rad et al., 1992) and was associated with emplacement of volcanic rocks with K–Ar whole rock ages of 213–192 Ma along the margin of the Australian Northwest Shelf (von Rad and Exon, 1982) (Fig. 3). Extension in the shelf continued until the Late Jurassic (Oxfordian: ~160 Ma) after which its termination is marked by a break-up unconformity (Gartrell et al., 2016; Longley et al., 2002; Norvick et al., 2001) related to the onset of ocean spreading in the adjacent Argo Abyssal Plain (AGSO, 1994). Late Triassic (Norian/Rhaetian) to Late Jurassic (Oxfordian) extension in the Australian margin was accommodated in the upper crust by normal faulting, mainly focused along the continent-ocean boundary, and up to ~10 % extension farther away from the continent-ocean boundary, equaling ~15 km extension. Lower crustal thinning accounted for 20–55 % extension that reflects long wavelength strain partitioning extending 300–500 km from the continent-ocean transition, equaling at least 15–60 km extension (Baxter et al., 1999; Chen et al., 2002) (see Supplementary Information 2, Table S1).

The **Argo Abyssal Plain**, located outboard of the Australian Northwest Shelf (Figs. 1 and 2), is floored by oceanic crust. The basaltic basement at ODP site 765 (Figs. 2 and 3) in the southern part of the Argo Abyssal Plain yields disparate $^{40}Ar/^{39}Ar$ ages of 156 ± 3 Ma and 111 ± 2 Ma. A celadonite vein from the same site yields a conventional K–Ar age of 155.3 ± 3.4 Ma, that is interpreted to represent the timing of low-temperature alteration of the oceanic crust (Ludden, 1992), and provides only a minimum age for the oceanic crust (Peterson et al., 1986; Staudigel et al., 1986, 1981). The lowest nannofossil bearing sedimentary rocks above the volcanic basement in the southern Argo Abyssal Plain yields a Tithonian (152.1–145.0 Ma) age range (Bown, 1992; Kaminski et al., 1992). The lowest sedimentary rocks in the northern part at DSDP site 261 (Figs. 2 and 3) were initially dated as late Oxfordian (163.5–157 Ma) (Bolli, 1978; Veevers and Heirtzler,

1974), but re-examination of the sample yields a Kimmeridgian to Tithonian (157.3–145.0 Ma) age range (Bown, 1992). ENE-WSW striking marine magnetic anomalies in the Argo Abyssal Plain were initially interpreted as M26 to M16 (156.56–140.42 Ma) from southeast to northwest (Fullerton et al., 1989; Sager et al., 1992), but were later re-interpreted as M25–M22A (156.04–151.92 Ma)

Fig. 1. Geographic map of SE Asia.

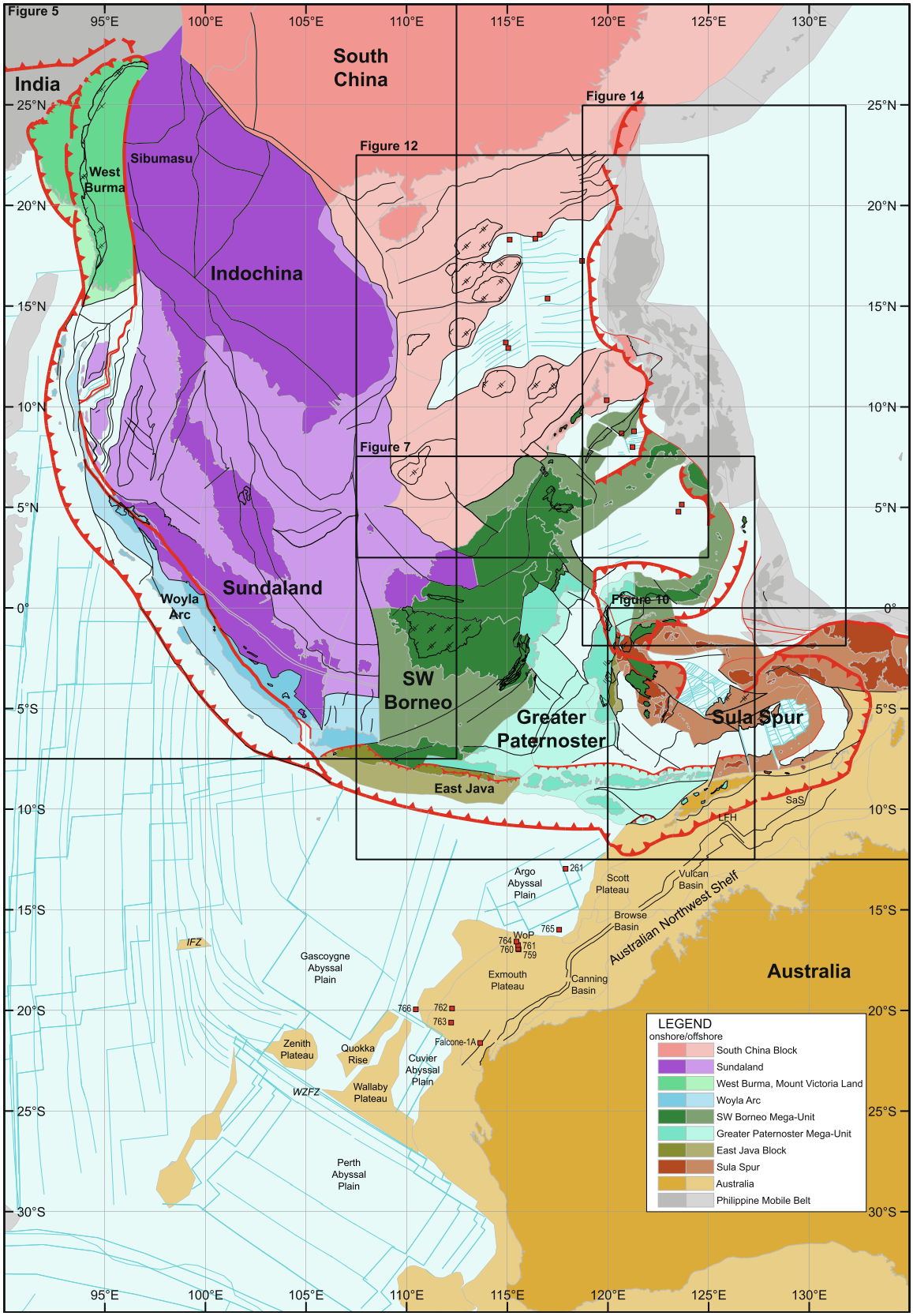

Fig. 2. Tectonic map of SE Asia showing lithotectonic blocks and mega-units (outlined in Sections 1, 2, and 4), major structural features (Barber et al., 2005b; Ren et al., 2013), and marine magnetic anomalies in the Indian Ocean (Gibbons et al., 2012), Andaman Sea (Raju et al., 2004), South China Sea (Li et al., 2014), Sulu Sea (Roeser, 1991; Schlüter et al., 1996), Celebes Sea (Weissel, 1980), North Banda Basin (Hinschberger et al., 2000), and South Banda Basin (Hinschberger et al., 2001). See Fig. S1 for A2-size version. Abbreviations: IFZ, Investigator Fracture Zone; LFH, Laramia-Flamingo High; SaS, Sahul Shelf; WoP, Wombat Plateau; WZFZ, Wallaby-Zenith Fracture Zone.

(Heine et al., 2004; Heine and Müller, 2005) and M26–M21 (156.56–148.44 Ma) (Gibbons et al., 2012). Collectively, these data suggest that NW Australia underwent a long history of continental extension since the late Paleozoic, intervened by an enigmatic period of Triassic shortening and inversion, after which final break-up and ocean spreading separated a (probably deformed) (micro-) continental block from the NW Australian margin sometime between the Oxfordian (163.5–157.3 Ma) and the base of anomaly M26 (156.56 Ma). This conceptual continental block is known as 'Argoland' (Veevers et al., 1991).

To the northeast of the Argo Abyssal Plain, the Australian margin has undergone late Neogene collision with the deformed orogenic and oceanic crust of SE Asia, intruded and overlain by the Banda Arc (Figs. 1 and 2). As a result, the sediments of the northwest Australian margin have been thrusted and uplifted and are available for field study, most notably on the island of Timor (Audley-Charles, 1968; Bird and Cook, 1991; Charlton et al., 2009, 2002; Davydov et al., 2014, 2013; Haig et al., 2014, 2022, 2018, 2017; Haig and McCartain, 2010; Sawyer et al., 1993; Tate et al., 2017, 2015) and the Outer Banda Islands east of Timor (Charlton et al., 1991a, 1991c; Kaneko et al., 2007) (Fig. 1). These Gondwana-derived units are intensely deformed, as will be described later in this paper in more detail (Section 4.12), but their stratigraphic evolution has revealed a similar break-up history as the Australian Northwest Shelf (Charlton, 1989). The stratigraphy of Timor is subdivided into a metamorphosed Aileu complex, a 'Gondwana Sequence' and a 'Kolbano Sequence' (Fig. 3), presently separated by two decollement horizons formed in Upper Carboniferous and Upper Triassic–Middle Jurassic clay intervals (Tate et al., 2015). The *Aileu Complex* is presently the structurally highest, and paleogeographically most northern Australian margin-derived unit exposed on Timor and comprises metamor-

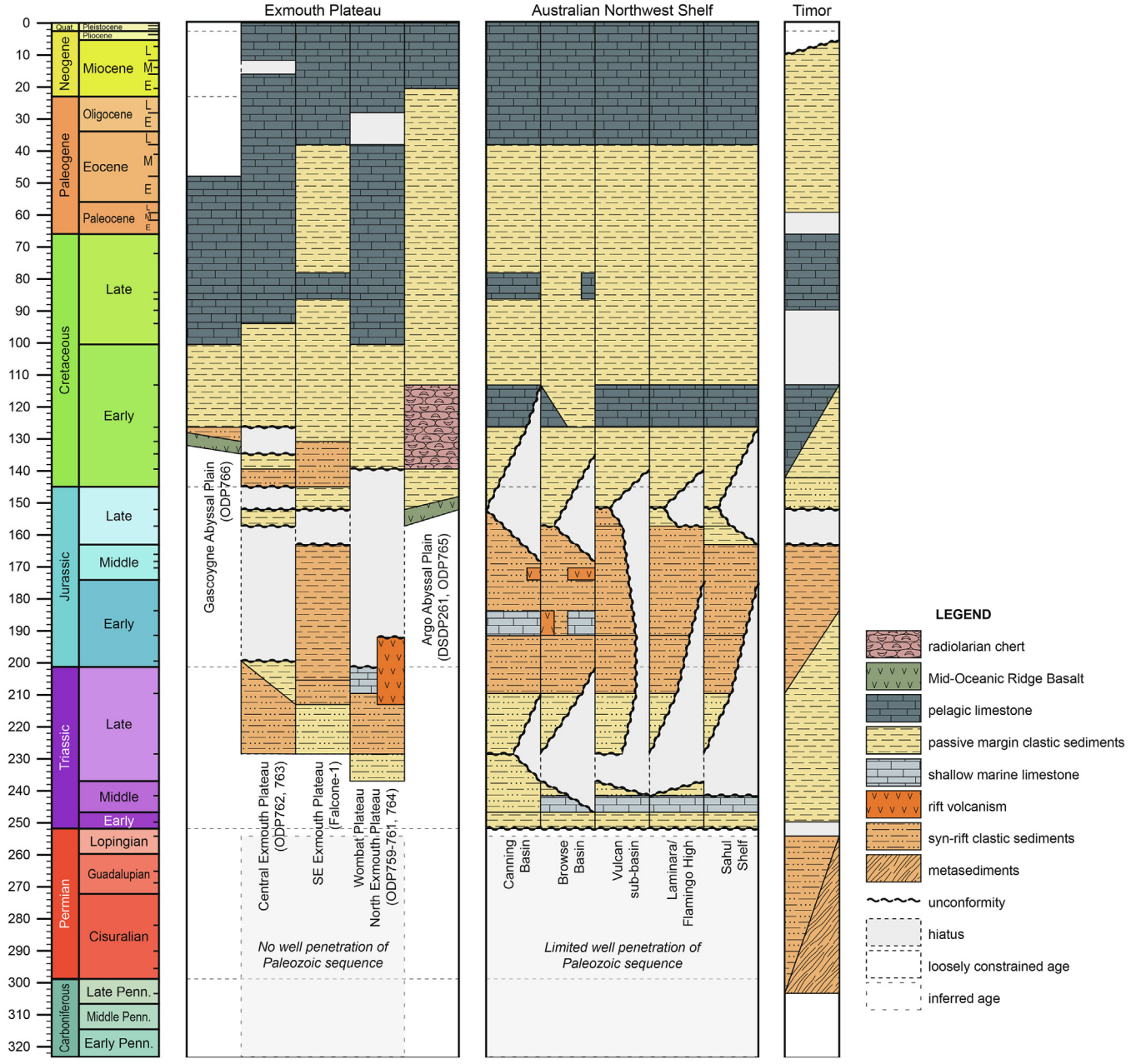

Fig. 3. Stratigraphy of the Exmouth Plateau, Australian Northwest Shelf (modified from Longley et al., 2002) and Timor. Geologic Time Scale from Gradstein et al. (2012).

phosed basalts, limestones, and clastic rocks (Tate et al., 2015). Audley-Charles (1965) assigned a Permian protolith age for fossiliferous low-grade parts of these metasedimentary rocks that correlate well with time-equivalent series in the Gondwana Sequence (Prasetyadi and Harris, 1996; Tate et al., 2015). Locally peridotite bodies and gabbros are emplaced into the Aileu sequence (Harris, R., Long, 2000), interpreted by Tate et al. (2015) to reflect a former continent-ocean transition. The Upper Carboniferous (Gzhelian) to Middle Jurassic (Callovian) *Gondwana Sequence* (Harris et al., 1998) is interpreted as strata deposited in horsts and grabens of an intracontinental rift basin on the Australian margin prior to Gondwana break-up (Bird and Cook, 1991; Charlton et al., 2002) that consists of three parts. The basal sequence comprises Upper Carboniferous (Gzhelian) to Upper Permian (Wuchiapingian) ammonite- and crinoid-bearing limestone, shale, subordinate sandstone and occasional basaltic lava (Audley-Charles, 1968, 1965; Charlton et al., 2002; Davydov et al., 2014, 2013; Haig et al., 2022, 2018, 2017). This sequence is unconformably overlain by Lower Triassic (Olenekian) to Lower Jurassic (Sinemurian–Pliensbachian) shale, siltstone, micaceous sandstone, and deep shelf limestones (Audley-Charles, 1968; Bird and Cook, 1991; Charlton et al., 2009; Haig and McCartain, 2007) and grades into the upper part of the Gondwana Sequence that consists of now intensely deformed Upper Triassic (Rhaetian) to Middle Jurassic (Callovian) shales (Audley-Charles, 1968; Haig and McCartain, 2010; Sawyer et al., 1993). The *Kolbano Sequence* was interpreted as a deep-marine Australian passive margin sequence with Upper Jurassic (Tithonian) to Lower Cretaceous (Berrasian) sandstone, Lower Cretaceous (Berriasian–Aptian) shales, mudstones and limestones, and Lower Cretaceous (Berriasian–Aptian) and Upper Cretaceous (Coniacian–Maastrichtian) planar bedded limestones (Munasri and Sashida, 2018; Sawyer et al., 1993). The top of the sequence comprises limestone, clay and chert that span the Late Paleocene (Thanetian) to late Miocene (~9.8 Ma) (Keep and Haig, 2010) in East Timor, whereas the top of the sequence in West Timor is of Early Pliocene (Zanclean) age (Sawyer et al., 1993). This sequence is widely interpreted to reflect a Late Jurassic break-up of northern Australia (Charlton, 1989), synchronous with the break-up recorded in the Argo Abyssal Plain, suggesting that Argoland continued towards the modern Banda region.

To the south of the Argo Abyssal Plain, the western Australian margin contains extensive evidence for Late Triassic (Rhaetian) to Late Jurassic (Oxfordian) continental extension (AGSO, 1994; Gartrell et al., 2022, 2016; Stagg and Colwell, 1994; von Rad et al., 1992), and Early Cretaceous (Berriasian–Valanginian) extension, hyperextension, oceanization, and separation of microcontinental fragments that still reside in the ocean floor to the west of Australia (Gibbons et al., 2012 and references therein). Sea floor spreading ages in the Gascoygne and Cuvier abyssal plains (Figs. 1–3) were most recently estimated to start at M10 (134.22 Ma) by Gibbons et al. (2012) based on marine magnetic anomalies, in conjunction with earlier estimates (Fullerton et al., 1989; Robb et al., 2005; Sager et al., 1992). These ages coincide with the age of break-up of the SW Australian margin, where the modern Indian continent restores in Gondwana fits (e.g. Williams et al., 2012). The shortening recorded in the continent-derived Himalayan fold-thrust belt demonstrate that continental India was wider during Early Cretaceous break-up than today and must have been conjugate to the margin of the Perth Abyssal Plain (Ali and Aitchison, 2005; van Hinsbergen et al., 2019a; Williams et al., 2012) and perhaps beyond (Fig. 2).

There is an ongoing debate on how wide Greater India may have been in Early Cretaceous time. Shortening estimates of the Himalaya suggest that Greater India must have contained at least ~600 to perhaps 900 km more continental crust (from N-S) than today (Long et al., 2011 and references therein). Paleomagnetic data from Lower Cretaceous and older rocks of the northernmost Himalayan rocks (the Tibetan Himalaya) are consistent with such an Early Cretaceous dimension of Greater India (Ali and Aitchison, 2005; van Hinsbergen et al., 2019a), as is the modern width of Indian lithosphere that horizontally underthrusted Tibet (Agius and Lebedev, 2013; van Hinsbergen et al., 2019a). Such a dimension would suggest that Greater India extended to the NW-SE striking **Wallaby-Zenith Fracture Zone** that forms the southern border of the Gascoygne and Cuvier abyssal plains, and the Wallaby and Zenith plateaus, which are two continental slivers modified by magma from seafloor spreading (Nelson et al., 2009; Planke et al., 2002; Stilwell et al., 2012; Symonds et al., 1998) (Figs. 1, 2, and S1). Others, however, have suggested that Greater India extended considerably farther north, even more than 2500 km wide to occupy the Gascoygne Abyssal Plain and reach the Argo Abyssal Plain, and then assumed that most of this continent entirely subducted below Tibet in the Cenozoic (Hall, 2012; Ingalls et al., 2016; Rowley, 2019a).

In their kinematic reconstruction of the western Australian margin, Gibbons et al. (2012) argued that the Greater Indian margin did not extend beyond the Wallaby-Zenith Fracture Zone. Dredging on the N-S striking Investigator Fracture Zone (Figs. 1, 2, and S1), which forms the northern continuation of the Wallaby-Zenith Fracture Zone, recovered a sample of volcanic glass with a $^{40}Ar/^{39}Ar$ whole rock plateau age of 153.1 ± 3.4 Ma. This sliver of oceanic lithosphere is trapped in oceanic lithosphere of Chron C34 that is interpreted to be ~99 Ma (Gibbons et al., 2012). Based on the age of this sliver, and its geographic and structural configuration, Gibbons et al. (2012) interpreted that the extent of spreading ridge responsible for the formation of the Argo Abyssal Plain, and thereby the extent of Argoland, reached as far south as the Wallaby-Zenith Fracture Zone (Figs. 1 and 2) and was likely also conjugate to the eastern part of Greater India. If correct, Argoland must have been considerably larger than only the width of the Argo Abyssal Plane, finally breaking off Australia in the Late Jurassic (~160 Ma), from the Wallaby Fracture zone in the south, to the Banda Arc and the Bird's Head in the north (Figs. 1 and 2).

3. Reconstruction philosophy and protocol

The separation of Argoland from Australia was accommodated by the formation of oceanic crust of the Neotethyan Ocean north of Greater India (i.e. the original Indian continent that existed before its underthrusting below Asia – the Himalaya fold-thrust belt contains the accreted relics of Greater India (e.g., Hodges, 2000)), and the east Indian ocean offshore northwestern Australia. If Argoland did not entirely subduct, then its relics must therefore now reside to the north of the trench that accommodates Indian oceanic crustal subduction, i.e. in in the SE Asian orogen to the west of the Philippines (which entirely consist of oceanic lithosphere of Paleo-Pacific origin (Hall, 2002; Yumul et al., 2003; van de Lagemaat and van Hinsbergen, 2024)), and to the south and southeast of the Himalaya, where no continental crustal relics are known that could be candidates of Argoland relics. The SE Asian orogen, from Myanmar to eastern Indonesia, contains abundant continental crust-derived fold-thrust belts and intervening sutures and we uncover these relics and restore them into their pre-orogenic, pre-subduction tectonic configuration. To this end, we take the following, 7-step approach that has been used in complex fold-thrust belts elsewhere for kinematic restoration of accretionary orogens (Boschman et al., 2014; van Hinsbergen et al., 2020, 2019a; van Hinsbergen and Schouten, 2021).

Step 1 in our reconstruction provides key boundary conditions for net area gain and area loss in SE Asia between India, Australia, and Eurasia based on marine magnetic anomaly and fracture zone-based plate reconstructions. India-Eurasia motion is constrained using a Eurasia – North America – Africa – India plate circuit with marine magnetic anomalies in the North Atlantic Ocean using Euler rotations of Vissers and Meijer (2012a, 2012b) and DeMets et al. (2015), NW Africa-North America rotations of Müller et al. (1997), Labails et al. (2010), DeMets et al., (2015), van Hinsbergen et al. (2020) and, Gürer et al., 2022, NW Africa-Somalia rotations of DeMets & Merkouriev (2016), and Indian Ocean rotations of Molnar et al. (1988), Merkouriev and DeMets (2006), and Gaina et al. (2015). For Australia-Eurasia motion, East Antarctica-Somalia rotations were used of Royer and Chang (1991), Bernard et al. (2005), Cande et al. (2010), and Mueller and Jokat (2019) and Australia-East Antarctica rotations of Cande and Stock (2004), Whittaker et al. (2013, 2007), and Williams et al. (2011). Marine magnetic anomalies were also used for ocean basins within the SE Asian collage, but those will be explained in the detailed sections below.

Orogenic deformation was restored using structural geology-based estimates of displacement accommodated by continental extension (**step 2**), transform and strike-slip faults (**step 3**) and tectonic shortening (**step 4**), after which we developed a geometrically consistent reconstruction relative to the stable, surrounding continents (Australia, Eurasia) (**step 5**). This reconstruction was then placed in a paleomagnetic reference frame (Vaes et al., 2023) and tested against compiled paleomagnetic data from SE Asian blocks to test predictions of paleolatitude and vertical axis rotation, and the reconstruction was iterated where necessary, within structural geological constraints (**step 6**). Finally, the reconstruction follows the basic rules of plate tectonics, i.e. all plates are surrounded by plate boundaries that end in triple junctions (**step 7**).

Key in the reconstruction is to determine when paleogeographic units – continents, arcs, or oceans – arrived in the trenches where they accreted to the SE Asian collage. To kinematically reconstruct the motions of the plates that hosted these paleogeographic units for the time periods prior to accretion, it is key to determine where continental fragments were separated from each other by ocean basins, and what the ages of these basins were. To extract the relevant information to this end from the geological record of SE Asia, we review stratigraphic, metamorphic, and selected geochemical constraints from accreted units.

For ocean-derived units, we analyze the relics of ocean plate stratigraphy (OPS) (Isozaki et al., 1990; Wakita, 2015; Wakita and Metcalfe, 2005): the minimum age of the subducted ocean floor may be derived from the oldest pelagic sediments (typically radiolarian cherts) in the OPS sequence, and the age of arrival of this sequence at the trench follows from the age of trench-fill deposits at the top of the sequence (Fig. 4). A minimum age of accretion may further be inferred from ages of metamorphic parts of an OPS sequence, and/or the age of unconformably overlying sediments (Isozaki et al., 1990). If the lavas underlying the OPS sequence have an island arc or ocean island geochemical signature, the oldest sediments of the OPS sequence only give a minimum age of the underlying ocean floor. For basalts with a mid-ocean ridge, back-arc basin, or supra-subduction zone geochemical signature, the actual age of the subducted ocean floor may be estimated (Isozaki et al., 1990; van Hinsbergen and Schouten, 2021).

For continent-derived units, we compile 'continental plate stratigraphy' (CPS) (van Hinsbergen and Schouten, 2021): although continental crust has a longer and more complex history than oceanic crust, the stratigraphy of continental units typically consists of a deformed, often crystalline basement related to an earlier orogeny, a *syn*-rift sequence marking break-up, a pelagic or hemipelagic passive margin sequence marking the drift period, and a trench-fill or foreland basin flysch-molasse sequence marking the arrival in a trench/collision zone (Fig. 4). As for OPS, the timing of accretion of CPS, as nappe, or following subduction termination and possibly relocation, follows from the age of the youngest upper plate-derived terrestrial or volcaniclastic sediments deposited in a trench or foreland basin setting on the CPS sequence, the oldest burial-related metamorphism, and unconformably covering sediments.

Upper plate-derived units are either older accretionary orogenic units that formed along the fringes of Eurasia, or upper plate oceanic units preserved as ophiolites. From such ophiolites, the geochemical signature indicates timing of formation relative to subduction initiation (SSZ ophiolites forming (typically shortly) after, and MORB ophiolites having formed before subduction initiation) and the timing of metamorphic sole formation or cooling provides the (minimum age of) subduction initiation (van Hinsbergen and Schouten, 2021; and references therein).

The reconstruction is bounded in the southwest and south by the Indian and Australian plate, and to the northeast by South China that is part of the Eurasian plate since ~130 Ma. We follow the reconstruction of minor, Neogene South China-Eurasia motion of Replumaz and Tapponnier (2003), as in van Hinsbergen et al. (2011). For Triassic to Early Cretaceous times, South China is reconstructed relative to Siberia following the reconstruction of van der Voo et al. (2015) as implemented in Torsvik and Cocks (2016). Rifting of the western Australian margin is restored using the reconstruction of Gibbons et al. (2012). We adopt the kinematic reconstruction of the orogenic belts of the Himalaya, Tibet, as well as the Cenozoic extrusion tectonics of Indochina (Figs. 2, 5, S1) as detailed in van Hinsbergen et al. (2019a, 2011) and Li et al. (2017) that followed the same reconstruction protocol and data selection approach as used in this paper.

To compare our positions of blocks in the reconstructions with paleomagnetic data from those blocks, we rotate the global paleomagnetic reference frame of Vaes et al. (2023) in coordinates of the reconstructed blocks using the approach outlined in Li et al. (2017), using the online paleomagnetic analysis tool www.paleomagnetism.org (Koymans et al., 2020, 2016).

Our reconstruction systematically applies the Geologic Time Scale of Gradstein et al. (2012), which we also apply to marine magnetic anomaly ages. Many tectonic phases in SE Asia are loosely confined to an epoch level in the Geologic Time Scale based on biostratigraphic constraints. In such cases and in absence of further constraints, we distribute associated motions equally over the entire time period as defined in the Geologic Time Scale (Gradstein et al., 2012), whereby we note that such motions may have occurred more rapidly, in a shorter period of time within that epoch. In addition, we acknowledge the long-standing debate on the age of the base of the Cretaceous Quiet Zone in marine magnetic anomalies, which is dated by Gradstein et al. (2012) at ~126.3 Ma, whereas the marine magnetic anomaly community prefers an age of ~121 Ma (e.g. Midtkandal et al., 2016). For this reason, marine magnetic anomaly-based plate circuits tend to use the magnetic polarity timescale of Gee and Kent (2007). However, that timescale does not include ages for biostratigraphy that lie at the basis of many field-based kinematic constraints, and we therefore use the timescale of Gradstein et al. (2012) everywhere for consistency.

Our GPlates reconstruction uses where possible rigid polygons. Where distributed continental deformation is reconstructed, we apply polylines that move relative to one another. For a detailed description of restoring orogenic deformation using GPlates, we refer the reader to van Hinsbergen and Schmid (2012).

Finally, we note that the uncertainty of restorations of orogenic architecture is difficult to quantify, even though quantitative esti-

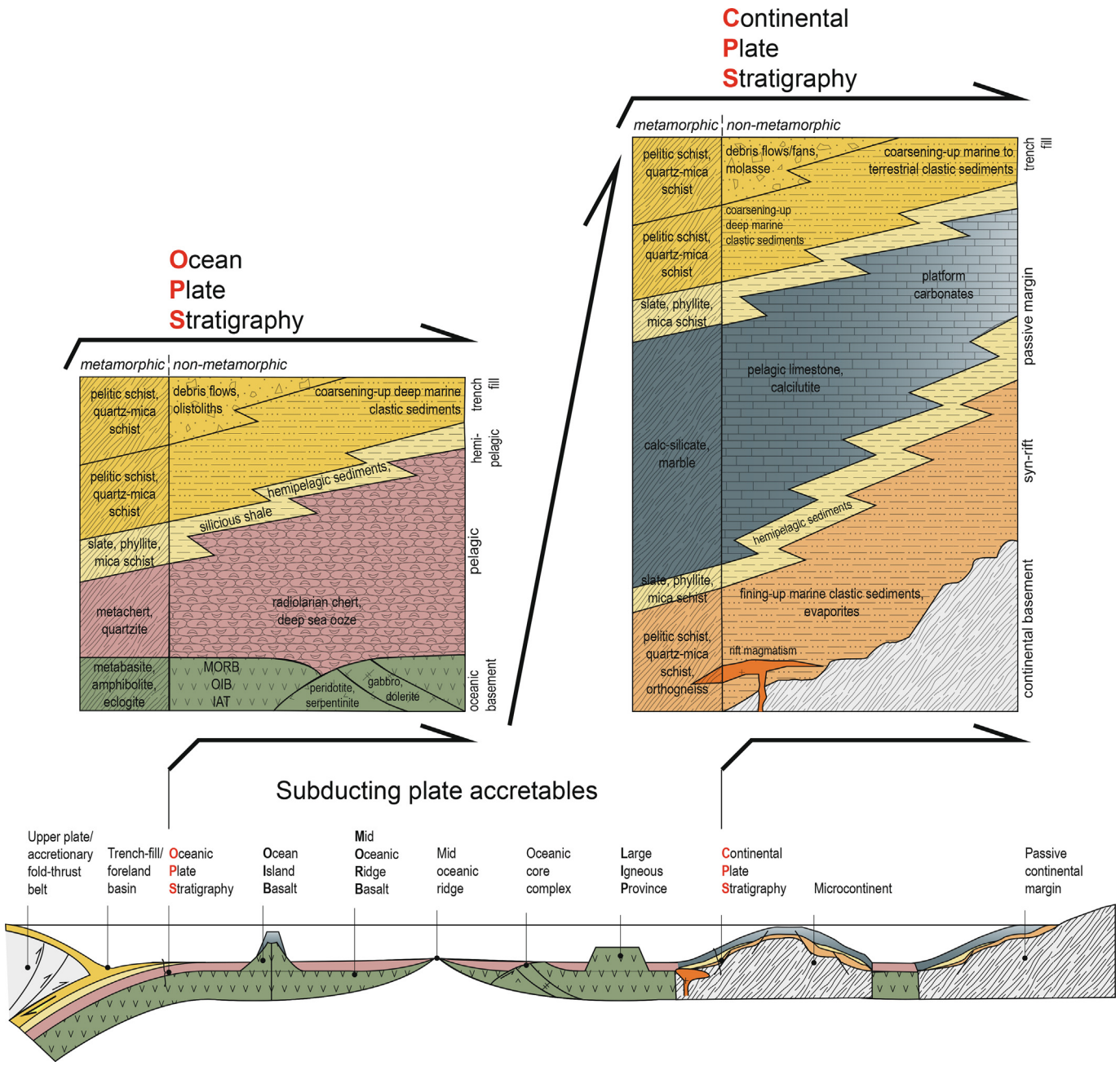

Fig. 4. Accretable units from downgoing plates, shown as metamorphic and non-metamorphic equivalents as preserved in accretionary complexes as Ocean Plate Stratigraphy (OPS) and Continental Plate Stratigraphy (CPS). Modified from van Hinsbergen and Schouten (2021).

mates for fault displacements or timing of extension or tectonic accretion are used. In our review of orogenic architecture below, we indicate data uncertainty where we can. In many places, fault displacements are estimates without quantified uncertainty. Age uncertainties come in many different flavors, from analytical to biostratigraphic. But most importantly, there are at present no ways to propagate uncertainties into a paleotectonic or paleogeographic reconstruction, and the final result that we present is therefore the sum of all our choices – and this is presently valid for all paleogeographic reconstructions. However, our analysis systematically follows the steps above, and the effects of different choices can this way be evaluated. We will return to this subject in the discussion.

4. Kinematic constraints from SE Asian orogenic architecture

Below, we review the tectonic architecture of the SE Asian orogen and identify the quantitative kinematic constraints that form the basis of our reconstruction. First, we give a brief outline of pre-Jurassic assemblage of the Sundaland continental promontory that forms the core of the SE Asian orogen. We then describe Cenozoic deformation in Sundaland and follow with describing the deformation of the accreted terranes in a counterclockwise fashion, starting with the West Burma Block to the NW of Sundaland, continuing via the west Sunda margin and the Banda Arc to eastern Indonesia and the South China Sea. Our review is focused on tectonic architecture rather than modern geography, and we describe the geology per tectonic unit rather than per island or island group.

We adopt the term 'Mega-Unit' (Schmid et al., 2020, 2008) for tectonic units that share a similar CPS and are surrounded by sutures, but that are now spread out over multiple regions and islands, because they are for example cut by younger extensional basins (e.g., the Sibumasu Mega-Unit). For tectonic units that are still confined to a single land area, we use the term 'Block' as commonly used in literature (e.g., West-Burma Block). The geographic locations mentioned in the text are given in Fig. 1, the locations of tectonic elements are shown on the tectonic map of Figs. 2 and S1 (and detailed maps outlined in Fig. 2), and the quantitative constraints for our reconstruction are summarized in Table S1.

4.1. Modern plates, plate boundaries, and the Sundaland core of the SE Asian accretionary orogen

The SE Asian orogen is located between the major plates of Eurasia, Indo-Australia and the Pacific and its basement contains elements derived from subducted portions of these, as well as entirely subducted, once intervening plates (Hall, 2002; Hall and Sevastjanova, 2012) (Fig. 2). The modern SE Asian orogen is still mostly surrounded by active margins. The northwestern margin, in Myanmar, is characterized by subduction of the Indian plate, and the NE Indian continental margin and the overlying Bengal Fan on that plate, below the West Burma Block (Fig. 5). The southwestern margin, bounding the Andaman Sea and the Andaman-Nicobar archipelago, Sumatra and Java, is the oceanic Sunda subduction zone consuming Indo-Australian oceanic lithosphere. To the southeast, in the Banda Sea region, lies the collision zone where the northern Australian continental margin entered the trench, all along the curved Banda Arc (Figs. 1 and 2). To the east, on Halmahera and the Philippines, the Pacific Ocean-derived Philippine Sea plate is obliquely thrusting over the SE Asian orogen. To the north, a former active margin delineates northern Borneo and Palawan. This subduction zone is no longer active, and the South China Sea ocean basin presently shares passive margins with the SE Asian orogen and the South China and Indochina blocks (Figs. 1 and 2). Because our reconstruction aims to identify Gondwana-derived continental terranes, we have not restored the tectonic and plate kinematic history of the Philippines and Halmahera in detail.

The core the SE Asian orogen is the biogeographic area named Sundaland (Figs. 1 and 2), which consists of an accretionary orogen that hosts late Paleozoic to early Mesozoic sutures and contains continental and arc fragments that accreted in this period. Most of Sundaland consists of the Indochina and East Malaya blocks that are separated by a suture from the South China Block, and the Sibumasu block that runs from Sumatra towards Tibet, where it continues as the Qiangtang terrane, and the West Sumatra Block (Metcalfe, 2013a) (Fig. 2).

The **Indochina-East Malaya** Mega-Unit covers much of Indochina and part of the Thai-Malay Peninsula (Figs. 1, 2 and 5). The Indochina-East Malaya Mega-Unit is separated from South China Block by the Late Devonian–Early Carboniferous Song Ma suture (Gatinsky and Hutchison, 1986; Hutchison, 1989a, 1989b) that demarcates the original amalgamation of the two blocks, and elsewhere by the Late Triassic Song Da Suture (Şengör et al., 1988) that was interpreted as Permo-Triassic rift basins that closed in the Late Triassic (Metcalfe, 1996), and that may also have older histories of deformation (Cawood et al., 2020). These suture zones were reactivated in the Cenozoic as the NW-SE trending Ailao Shan-Red River Fault Zone (Peltzer and Tapponnier, 1988) (Fig. 5) that has been active as sinistral strike-slip zone between ~30 Ma to ~20 Ma (Searle et al., 2010; Wang et al., 2000). In the northwestern segment, the estimated displacement is 700 ± 200 km (Chung et al., 1997; Leloup et al., 1995), whilst the southeastern segment shows no more than 250 km displacement (Fyhn et al., 2009; Wang and Burchfiel, 1997). The difference is accommodated by E-W shortening (Wang and Burchfiel, 1997) and block rotations in northwestern Sundaland (Li et al., 2018, 2017) that we reconstruct following Li et al. (2017). The Ailao Shan-Red River Fault Zone was reactivated as dextral strike-slip fault, with an estimated displacement of ~40 km since ~8 Ma (Replumaz et al., 2001; Schoenbohm et al., 2006), included in the Tibet reconstruction of van Hinsbergen et al. (2011) that we adopt for the northwestern part of our study area.

The Indochina-East Malaya Mega-Unit is separated from the **Sibumasu** Mega-Unit by the Bentong-Billiton Accretionary Complex (Figs. 2 and 5) that formed in Late Permian to Late Triassic time and is interpreted as a former branch of the Paleo-Tethys Ocean (Barber and Crow, 2009, 2003; Harbury et al., 1990; Metcalfe, 2013b, 2000; Sevastjanova et al., 2011; Sone and Metcalfe, 2008). Sibumasu is traced from the Yunnan region in north to southeast Sumatra in the south (Metcalfe, 2013a, 1984). It is underlain by a Precambrian continental basement (Hall and Sevastjanova, 2012; Liew and McCulloch, 1985; Sevastjanova et al., 2011) and a Cambrian (and on Sumatra Carboniferous) to Permian clastic sedimentary cover (Aung and Cocks, 2017; Barber et al., 2005a; Barber and Crow, 2009; Cai et al., 2017; Hassan et al., 2014; Lee, 2009) that includes pebbly mudstones, interpreted as deep-marine glacial diamictites that are hence interpreted as Gondwana-derived (Stauffer and Lee, 1986). These are overlain by Permian to Triassic limestones (Barber et al., 2005a; Barber and Crow, 2009; Oo et al., 2002; Win et al., 2017).

The western part of Sibumasu in Myanmar is the Shan Plateau, which is bounded to the west by the Mogok-Mandaley-Mergui Belt (MMM Belt) comprising Paleozoic metasedimentary rocks of upper amphibolite to granulite facies intruded by deformed arc-granitoids and pegmatites (Barley et al., 2003; Mitchell et al., 2012, 2007; Searle et al., 2020, 2017, 2007). The MMM belt accommodated intense ductile deformation for nearly 200 Ma: U–Pb monazite ages in metasedimentary rocks recorded a first metamorphic event at ~200 Ma (Yonemura et al., 2013) and U–Pb zircon ages from deformed granitoids recorded episodes of arc magmatism around ~170–163 Ma and ~124–120 Ma (Barley et al., 2003; Searle et al., 2020) followed by 114 ± 3 Ma and ~75 Ma metamorphic events (Mitchell et al., 2012; Searle et al., 2020; Yonemura et al., 2013). Extensive U–Pb zircon geochronology in the southern part of the MMM Belt suggest a protracted phase of arc magmatism between ~84 Ma and ~48 Ma (Crow and Zaw, 2017; Gardiner et al., 2018, 2016; Jiang et al., 2017; Li et al., 2019; Searle et al., 2007). U–Pb monazite ages indicate granulite facies metamorphism (9 kbar, 870–970 °C) between 43 and 32 Ma, and upper amphibolite facies metamorphism peaking at 23–20 Ma (Lamont et al., 2021), both associated with syntectonic granitoid emplacement between 35 and 23 Ma (Barley et al., 2003; Searle et al., 2020, 2017, 2007; Yonemura et al., 2013). The Shan Scarp Fault that bounds the MMM Belt in the west exposes an exhumed dextral ductile shear zone. U–Pb monazite ages from the northern part show that a this part was not active before 20–18 Ma (Lamont et al., 2021), whilst $^{40}Ar/^{39}Ar$ biotite ages show a structural progression of fault activity with ages from 26.9 ± 1.0 Ma in the south to 15.8 ± 1.1 Ma in the north (Bertrand et al., 2001, 1999).

The MMM Belt is bounded to the west and northwest by ophiolitic lithologies. To the northwest is an extensive supra-subduction zone (SSZ) ophiolite in the Myitkyinia area (Figs. 1 and 5) (Liu et al., 2016b) with plagiogranites and gabbros yielding U–Pb zircon ages of 177–171 Ma and pillow lavas giving a U–Pb zircon age of 166 ± 3 Ma (Jingsui et al., 2012; Liu et al., 2016a), covered by Upper Jurassic (Tithonian) radiolarian chert (Maung et al., 2014). This ophiolite belt is interpreted as the eastward termination of the Bangong-Nujiang Suture Zone (Liu et al., 2016a) that bounds the Sibumasu/Qiangtang terrane from the south Tibetan

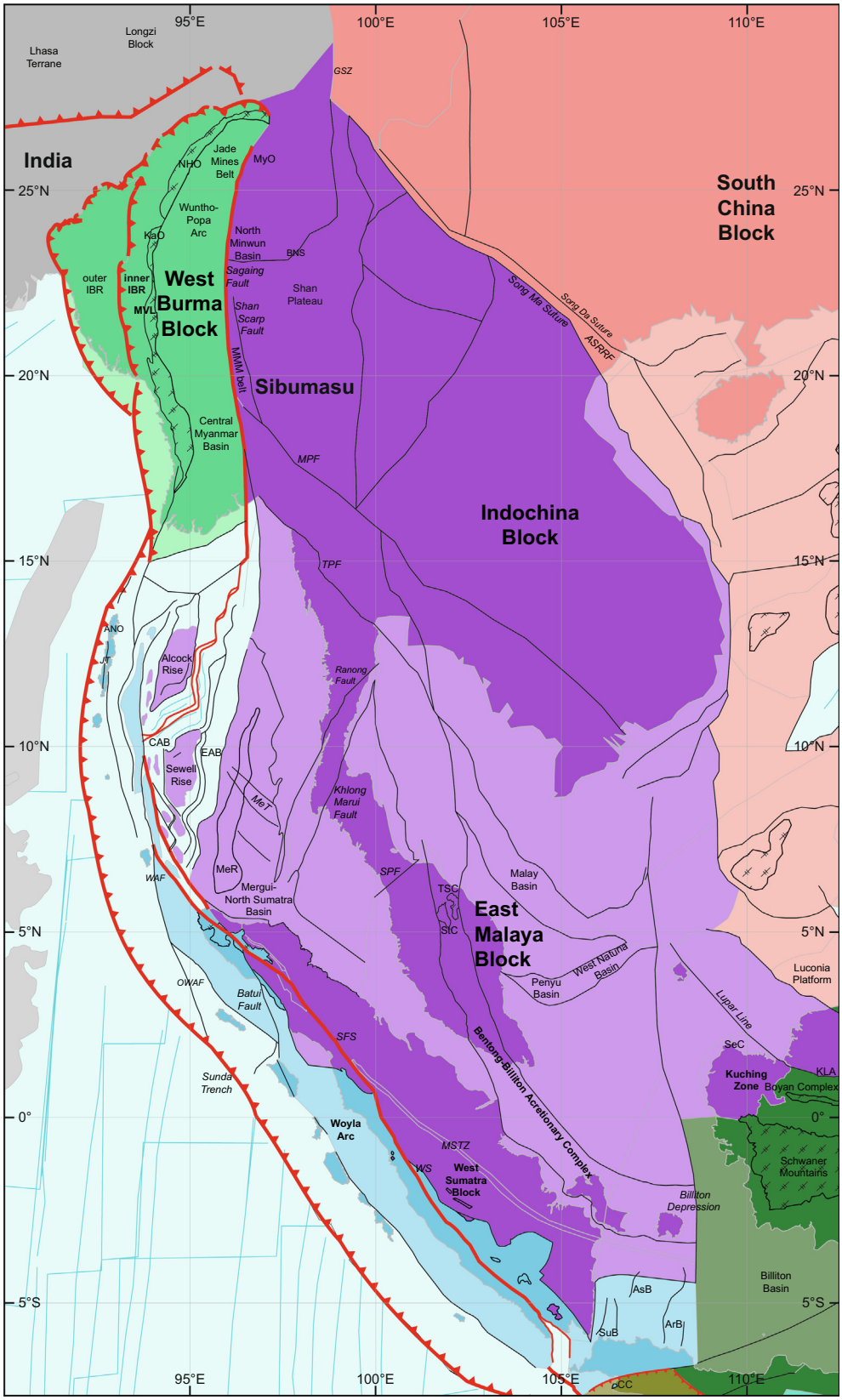

Fig. 5. Tectonic map of Sundaland, Indo-Burman Ranges, West Burma Block, Andaman Ophiolite, Woyla Arc, Boyan Complex and Kuching Zone. See Fig. 2 for location. Abbreviations: ANO, Andaman-Nicobar ophiolites; ArB, Arjuna Basin; AsB, Asri Basin; ASRRF, Aliao Shan-Red River Fault; BNS, Bangong-Nujiang Suture; CAB, Central Andaman Basin; CC, Ciletuh Complex; EAB, East Andaman Basin; GSZ, Gaoligong Shear Zone; IBR, Indo-Burman Ranges; JT, Jarawa Thrust; KaO, Kalaymyo Ophiolite; KLA, Kapuas-Lubok Antu Mélange; MeR, Mergui Ridge; MeT, Mergui Transform; MPF, Mae Ping Fault; MSTZ, Medial Sumatra Tectonic Zone; MyO, Myitkinya Ophiolite; NHO, Naga Hills Ophiolite; OWAF, Old West Andaman Fault; SeC, Serabang Complex; SFS, Sumatran Fault System; SPF, Songkla-Penang Fault; SuB, Sunda Basin; TPF, Three Pagodas Fault; WAF, West Andaman Fault; WS, Woyla Suture.

Lhasa Block that ends in the Yunnan region (Fig. 1). Along the Sagain Fault in the Minwun area in central Myanmar (Fig. 5) there are limited exposures of serpentinized peridotites (Morishita et al., 2023), Lower Cretaceous (Hauterivian) radiolarian chert (Suzuki et al., 2020), and amphibolites with U–Pb zircon ages of 117.1 ± 1.5 Ma and 96.6 ± 2.0 Ma (Lai et al., 2018) (Fig. 6). These ophiolitic lithologies reveal that subduction along the western MMM belt continued at least into the Late Cretaceous, and the arc magmatic and metamorphic records suggest subduction may have continued into the late Eocene or early Oligocene, after which the zone mainly accommodated dextral strike-slip motion.

The **West Sumatra Block** forms the westernmost part of the Sundaland core. It is juxtaposed against Sibumasu along the Medial Sumatra Tectonic Zone (MSTZ) that exposes a SE-NW striking belt of intensely deformed gneisses that runs from the Andaman Sea to the western Java Sea (Figs. 1 and 5). Syntectonic granites within the MSTZ with K–Ar muscovite and biotite ages of 198–186 Ma (Barber et al., 2005b; Rock et al., 1983) suggest motion continued into the Early Jurassic but undeformed Middle–Upper Triassic sedimentary rocks with similar facies and sequences on either side of the fault zone suggest most displacement predates the Middle Triassic (Barber and Crow, 2009). The MSTZ does not contain any ophiolitic or OPS components and it is thus unknown whether it represents a suture (Barber and Crow, 2009; Metcalfe, 2013a).

The West Sumatra Block exposes Lower Carboniferous limestone and Upper Carboniferous–Lower Permian clastic sedimentary rocks that are unconformably overlain by Upper Triassic shallow marine limestones and deep marine, *syn*-rift clastic sedimentary rocks. This sequence is intruded by Jurassic–Cretaceous arc granitoids (Cobbing, 2005; Li et al., 2020b; McCourt et al., 1996) and is overlain by Middle Jurassic–Lower Cretaceous quartzitic and calcareous sandstones and shales, and volcaniclastic sandstones (Fig. 6) that were interpreted to be deposited in a forearc basin (Barber et al., 2005a; Barber and Crow, 2009) revealing that it was located above a subduction zone in this time. The West Sumatra margin is partially metamorphosed, with metamorphic grades increasing westwards up to amphibolite facies conditions (Suwarna et al., 1994), where metamorphic rocks with K–Ar ages of 125–95 Ma (Andi Mangga et al., 1994; Koning, 1985) suggest that these became buried in a southwest dipping subduction zone below the adjacent Woyla Arc (Barber et al., 2005a) (see Section 4.4).

The Lower Permian tuffs and volcaniclastic sedimentary rocks of the West Sumatra Block contain fossilized tree trunks that do not contain growth rings (Booi et al., 2014; Vozenin-Serra, 1989), and intercalated limestones with fusuline foraminiferal assemblages that differ from contemporaneous faunas observed in northern Thailand and Yunnan (Stauffer and Lee, 1986; Ueno, 2003; de Boer et al., 2006). Based on these floral and faunal assemblages, the West Sumatra Block has been interpreted as a South China Block-derived fragment that originated at tropical latitudes (Barber and Crow, 2009, 2003; Hutchison, 1994). However, this Lower Permian flora may also be indicative of higher (subtropical) latitudes (van Waveren et al., 2007), whereby the lack of growth rings may also signal climatic fluctuations rather than tropical latitudes (van Waveren et al., 2018). Additional arguments for that latter interpretation are paleomagnetic data suggesting a Late Permian paleolatitude of West Sumatra of ~15° S (Haile, 1979; Sasajima et al., 1978), as well as U–Pb detrital zircon geochronology from Pre-Triassic sandstones in West Sumatra that have similar age populations as contemporaneous rocks of Sibumasu in east Sumatra (Zhang et al., 2018b). The West Sumatra Block was thus likely a part of Sibumasu that was dextrally displaced along the western Sibumasu margin during the Triassic–Early Jurassic, while being located above a subduction zone that lasted into the mid-Cretaceous, after which accretion of the Woyla Arc modified the active margin (see Section 4.4).

4.2. Late Cretaceous to Cenozoic deformation of Sundaland

During Late Cretaceous to Cenozoic time, the Sundaland orogen was re-deformed in strike-slip fault zones, fold-thrust belts, and extensional provinces (Morley et al., 2011; Pubellier and Morley, 2014) that we describe from north to south and west to east. Mainland Indochina hosts the NW-SE striking, sinistral Mae Ping Fault (also known as Wang Chao Fault) and Three Pagodas Fault (Fig. 5). Stratigraphic and seismic data from the basins in the Gulf of Thailand and the eastern Sunda Shelf (Fig. 1) suggest these faults were active in the late Eocene and Oligocene (~40–23 Ma), with estimated sinistral displacements of ~100 km per fault zone (Fyhn et al., 2010a, 2010b; Morley, 2007; van Hinsbergen et al., 2011). To the west, the Thai Peninsula exposes the **Ranong Fault** and **Khlong Marui Fault** that recorded 23 km and 6 km, respectively, of dextral shearing between 88 and 81 Ma, followed by 113 km and 31 km of dextral displacement, respectively, between 44 and 40 Ma (Table S1), after which they became reactivated as sinistral transpressional brittle faults with displacements of 66 km and 20 km, respectively, between 38 and 23 Ma (Kanjanapayont et al., 2012a, 2012b; Watkinson, 2009; Watkinson et al., 2011a, 2008) (Table S1). To the south, the **Songkla-Penang Fault** (Bunopas, 1982) accommodated differential, paleomagnetically constrained rotations between the Thai and Malai parts of the peninsula sometime in the Cenozoic (Richter et al., 1999) (see Section 5.2), but displacements have not been quantified. This differential rotation is also accommodated to the west of the Thai-Malay Pensinsula by the **Mergui-North Sumatra Basin**. This basin is floored by continental crust crosscut by the NW-SE striking Mergui Transform Fault Zone (Fig. 5). The continental basement is overlain by Lower–Upper Oligocene conglomerates and Lower Miocene shallow marine clastic sedimentary rocks and limestone. The top of the sequence consists of Middle Miocene to Holocene shales (Andreason et al., 1997; Kamili et al., 1976; Polachan and Racey, 1994). Curray (2005) estimated a crustal thickness of ~20 km, and assumed an initial crustal thickness of 30 km to calculate a stretching factor of 1.5, or 60 km of extension, in a NW-SE direction in the Oligocene (Table S1).

Upper Jurassic–Lower Cretaceous sedimentary rocks in the **Malay Peninsula** are folded (Harbury et al., 1990; Tjia, 1996) associated with ~(N)NW-(S)SE transtensional shearing of metamorphic and magmatic rocks in the Bentong-Billiton Accretionary Complex (Ali et al., 2016; Harun, 2002; Salmanfarsi et al., 2018; Sautter et al., 2019) and brittle strike-slip faulting (Morley, 2012; Tjia, 1972; van der Wal, 2015). The timing of this deformation event is estimated at ~46–23 Ma based on apatite fission track ages that recorded cooling due to ~80 km of NNW-SSE directed extension exhuming the Taku Schist Complex and the 70 km exhuming the Stong Complex at extensional step-overs dextral strike-slip faults along the Bentong-Billiton Accretionary Complex (Cottam et al., 2013; François et al., 2017; Krähenbuhl, 1991; van der Wal, 2015) (Table S1).

Within the **Gulf of Thailand** (Fig. 1), three sub-basins opened diachronously between the (Middle) Eocene and Middle Miocene. Stretching factors varying between 1.1 and 1.4 correspond to ~90 km E-W directed extension between the Thai Peninsula and Indochina (Kaewkor and Watkinson, 2017; Morley, 2001; Watcharanantakul and Morley, 2000) (Table S1). The **Malay Basin** to the south (Fig. 5) formed in the Late Eocene during ~100 km N-S directed extension between the Malay Peninsula and Indochina (Table S1) (Fyhn et al., 2010a; Madon, 1997; Mansor et al., 2014; Morley, 2001). Inversion of half grabens in the southern part of the Malay Basin during Early–Middle Miocene transpression

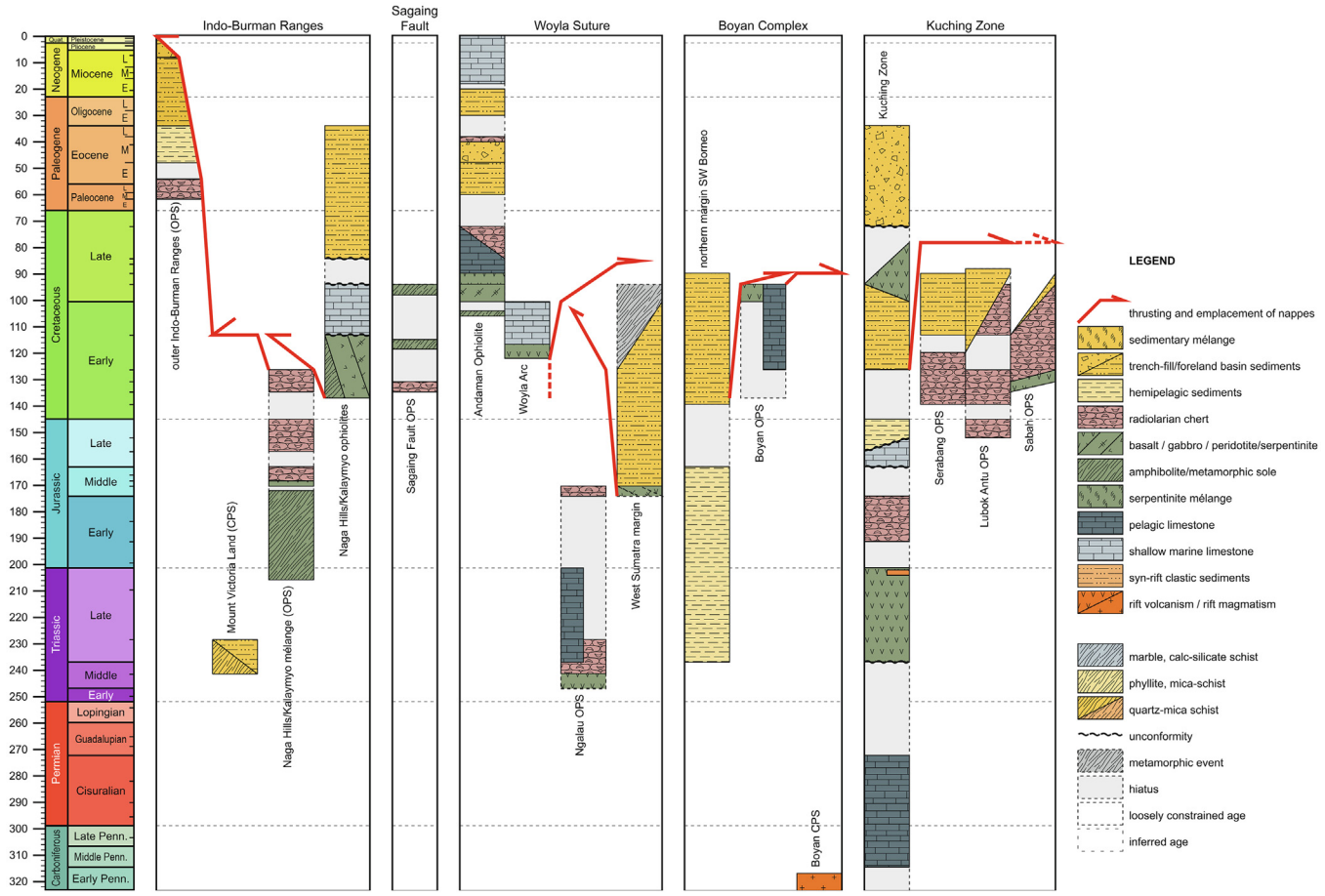

Fig. 6. Tectonostratigraphy of the inner Indo-Burman Ranges, Andaman Ophiolite and Woyla Suture, Boyan Complex, Kuching Zone, and the Serabang, Lubok Antu, and Sabah mélange complexes. Geologic Time Scale from Gradstein et al. (2012).

resulted in 10 km N-S shortening (Fyhn et al., 2010a; Jagger and McClay, 2018; Madon, 1997; Morley, 2001). The **Penyu** and **West Natuna basins** to the south of the Malay Basin (Fig. 5) also formed in the Middle Eocene as a result of ~100 km NNW-SSE directed dextral transtension between 44 Ma and ~30 Ma (Table S1) (Ginger et al., 1993; Madon, 1997; Manur and Jacques, 2014; Morley, 2001). Between 27 Ma and 15 Ma, these basins were inverted during sinistral transpression (Manur and Jacques, 2014).

The Sunda Shelf between Sumatra, Borneo, and Java is hosts the **Sunda, Asri, Arjuna and Billiton basins** that are bounded by N-S striking normal faults that accommodated E-W extension (Atkinson et al., 2004; Doust and Noble, 2008; Noble et al., 1997; Sukanto et al., 1998; Wight and Sudarmono, 1986). The basal conglomerates in the Arjuna, Asri and Billiton basins are inferred to be of Eocene age (Noble et al., 1997; Sukanto et al., 1998; van de Weerd and Armin, 1992), whereas rare age-diagnostic palynomorphs in the basal conglomerates of the Sunda Basin may be of Early Oligocene age (Wight and Sudarmono, 1986). In the Billiton Basin, the basal conglomerates are capped by an Early Oligocene unconformity (van de Weerd and Armin, 1992) that marks the end of the first phase of E-W rifting. Unconformably overlying Oligocene–Lower Miocene fluvio-deltaic sedimentary rocks were deposited during a second phase of E-W rifting, and are unconformably covered by Middle Miocene–Holocene post-rift sediments (Atkinson et al., 2004). We follow Advokaat et al. (2018b) assuming these episodes of extension were distributed across the western Java Sea.

4.3. Longzi Block of the Tethyan Himalayas; West Burma block; Indo-Burman ranges; Mount Victoria Land

The westernmost unit that has been interpreted as genetically related to Argoland is the **Longzi Block** (Fig. 5) in the eastern Tethyan Himalayas (Zhang et al., 2022b). The Tethyan Himalayas forms the northernmost nappe of the Himalayas that was the first to collide with Tibet, around 60 Ma according to Tibet-derived clastic sedimentary rocks in the top of its stratigraphy (An et al., 2021). The Tethyan Himalayas nappe extends along much of the strike of the Himalaya, and has a typical passive margin stratigraphy dominated by Mesozoic carbonate sequences (Jadoul et al., 1998). At the longitude of Nepal, the Tethyan Himalayan stratigraphy contains an Upper Carboniferous deepening sequence interpreted to record rifting, overlain by Permian basalts (the Nar Tsum spillites and Bhote Kosi Basalts) interpreted to record continental break-up along the north Gondwana margin (Garzanti et al., 1999). Recently, Zhang et al. (2022) reported evidence for Jurassic rifting and ~155–152 Ma magmatism in the eastern Tibetan Himalaya and they termed this part the Longzi Block. This Longzi Block contains Triassic sandstones that are consistent with a west Australian provenance (Cai et al., 2016), suggesting a paleogeographic position adjacent to northeastern India and western Australia. Zhang et al. (2022) thus interpreted the Longzi block as a passive margin of the synchronously opening Argo Abyssal Plain. They also showed evidence for ~130 Ma folding of the strata in the Longzi Block, which they interpreted as related to collision of the Longzi

Block with the West Burma Block, which was then located around the equator (Westerweel et al., 2019). Zhang et al. (2022) consequently interpreted the Longzi Block as part of Argoland rather than of the Tethyan Himalaya. However, there is no evidence for a suture between the Longzi Block and the Tethyan Himalayas, and recent paleomagnetic evidence show that around 75 Ma, the rocks the Longzi Block were still located around 20°S as part of the Tethyan Himalaya (Yuan et al., 2021), far south of position predicted by Zhang et al. (2022). Hence, we interpret the Longzi Block as part of the Tibetan Himalayan margin, from which Argoland broke off around 155–152 Ma. The Permian break-up recorded in the Tethyan Himalayas at the longitude of Nepal then constrains the maximum paleogeographic width of Argoland. We tentatively interpret the shortening recorded around 130 Ma in the Longzi Block as local deformation along the fracture zones that accommodated India-Australia separation. Rocks with affinities to the Tethyan Himalayas are also exposed near the northern termination of the Sagaing Fault (Min et al., 2022; Zhang et al., 2018a). These rocks record metamorphism starting at ~65 Ma, reaching peak conditions of 9.3 kbar and 510 °C at 45 Ma, and recording subsequent rapid cooling at 25 °C/Ma until ~30 Ma, and slower cooling at ~4 °C/Ma until 16–14 Ma (Min et al., 2022). Min et al. (2022) interpreted these rocks were buried, accreted, and exhumed in a subduction zone to the north of the West Burma Block (in present-day coordinates) that was subsequently reactivated in the Sagaing Fault.

To the southeast of the Himalaya, the **West Burma Block** is separated by the active, dextral Sagaing strike-slip fault from the Mogok-Mandaley-Mergui Belt (MMM Belt) of west Sibumasu in the east, and it is fringed in the north and west by ophiolites and the Indo-Burman Ranges fold-thrust belt (Figs. 2 and 5). As mentioned in Section 4.1, along the Sagaing Fault there are limited exposures of serpentinized peridotites (Morishita et al., 2023), Lower Cretaceous (Hauterivian) radiolarian chert (Suzuki et al., 2020), and amphibolites with U–Pb zircon ages of 117.1 ± 1.5 Ma and 96.6 ± 2.0 Ma (Lai et al., 2018) in mélanges that suggest that the Sagaing Fault reactivated a post-mid Cretaceous suture zone. The oldest rocks of the West Burma Block are Lower Ordivician metasedimentary rocks exposed as the highest structural unit of the inner **Indo-Burman Ranges** in the Naga Hills as well as in windows in the Central Myanmar Basin (Figs. 1 and 5). Detrital zircon age populations from these rocks are consistent with a NW Australian provenance (Aitchison et al., 2019).

In northern Myanmar, between the Indo-Burman Ranges to the west and the fault strands of the Sagaing Fault to the east, the Jades Mines Belt (Chhibber and Ramamirtham, 1934) exposes high-pressure metamorphic rocks, including jadietite and associated garnet- and phengite-bearing blueschist, serpentinized peridotite, and mafic schists that are interpreted to have been formed in an exhumed subduction channel (Nyunt et al., 2017). Due to the inaccessibility of the area, little is known about field relations of the rock units, and it may either be a window into a subduction channel that formed by subduction along the western margin of the West Burma Block or be associated with the SSZ Myitkyinia Ophiolite that forms the lateral continuation of the Bangong-Nujiang Suture Zone against which the West Burma Block became juxtaposed by Cenozoic motion along the Sagaing Fault. U–Pb zircon geochronological studies on jadietite retrieved Late Jurassic (163.2 ± 2.2 Ma, 158 ± 2 Ma, 146.5 ± 3.4 Ma) ages (Qiu et al., 2009; Shi et al., 2008), but Yui et al. (2013) showed that these ages come from inherited or incompletely recrystallized zircons. Subsequent $^{40}Ar/^{39}Ar$ geochronology on jadietite revealed a $^{40}Ar/^{39}Ar$ amphibole age of 134.8 ± 0.7 Ma and a $^{40}Ar/^{39}Ar$ jadeite age of 123.9 ± 3.4 Ma that were interpreted to record formation of the jadietite in a subduction channel (Qi et al., 2013). A $^{40}Ar/^{39}Ar$ amphibole age of 92.7 ± 1.2 Ma from associated amphibolite and a U–Pb zircon age of 77 ± 3 Ma from jadietite were interpreted to record later metasomatism (Qi et al., 2013; Yui et al., 2013). The above data indicate that subduction was either underway at ~135 Ma below either the West Burma Block or still active below the Myitkyinia SSZ ophiolite of the Bangong-Nujiang Suture Zone.

The West Burma Block is overlain by the Wuntho-Popa magmatic arc and an interfingering nearly-continuous sequence of mid-Cretaceous (Albian) to Quaternary sediments of the Central Myanmar Basin (Pivnik et al., 1998; Zhang et al., 2017b). In the Wuntho Massif in the northern part, volcanic members yield a K–Ar age of 71 Ma (UN, 1978) and a $^{40}Ar/^{39}Ar$ whole rock age of 100.9 ± 0.2 Ma (Westerweel et al., 2019). However, these ages are younger than the overlying mid-Cretaceous (Albian–Cenomanian) limestone (Mitchell, 2017) suggesting hydrothermal alteration may have reset these ages (Licht et al., 2020). These mid-Cretaceous (Albian–Cenomanian) limestones are overlain by mudstones and shale, and tuffs with $^{40}Ar/^{39}Ar$ whole rock ages of 91.2 ± 0.2 Ma and 85.0 ± 0.2 Ma, although also these ages may have been hydrothermally reset (Licht et al., 2020; Westerweel et al., 2019). The West Burma Block basement and the volcanogenic cover units are intruded by I-type batholiths with U–Pb zircon ages of 106–90 Ma (Barley et al., 2003; Gardiner et al., 2017; Li et al., 2020a; Licht et al., 2020) as well as by diorites and copper porphyries with U–Pb zircon ages of 40–31 Ma (Barley et al., 2003; Gardiner et al., 2016; Li et al., 2019). The Wuntho-Popa Arc continues ~1000 km farther south where it is poorly exposed and is mostly covered by Neogene fluvial sediments (Licht et al., 2019; Pivnik et al., 1998; Zhang et al., 2017b). To the south, the Wuntho-Popa Arc comprise I-type batholiths and andesites with U–Pb zircon ages of 105–98 Ma and 15–13 Ma (Gardiner et al., 2016; Lee et al., 2016; Mitchell et al., 2012), and also isolated Quaternary volcanic centers (Belousov et al., 2018; Lee et al., 2016; Maury et al., 2004). The Wuntho-Popa Arc is generally considered to have formed due to east-dipping subduction at the modern western side of the West Burma Block (Licht et al., 2020; Maury et al., 2004; Zhang et al., 2018a).

To the west, the West Burma Block overlies ophiolites that in turn overlie the Indo-Burman Ranges fold-thrust belt (Aitchison et al., 2019). The mantle section of the *Naga Hills Ophiolite* hosts rodingite dykes with U–Pb zircon ages of 137–114 Ma (Bidyananda et al., 2022), whilst plagiogranites in the crust of the Naga Hills ophiolite (Fig. 5) yield U–Pb zircon ages of 119–116 Ma (Aitchison et al., 2019; Singh et al., 2017). The ophiolite is nonconformably overlain by Mid–Upper Eocene conglomerates (Acharyya, 2015; Acharyya et al., 1986; Jena and Acharyya, 1986). The *Kalaymyo Ophiolite* (Fig. 5) comprises peridotites, amphibolites likely representing a metamorphic sole, gabbros, granite, and mafic volcanic rocks with a SSZ geochemical signature (Liu et al., 2016b, 2016a; Zhang et al., 2018a, 2017). Rodingite dykes within serpentinites yield U–Pb zircon ages of 126.6 ± 1.0 Ma and 125.8 ± 1.7 Ma (Liu et al., 2016a), gabbros yield U–Pb zircon ages of 133.1 ± 2.1 Ma and 131.1 ± 1.8 Ma, and a granitic intrusion within these gabbros yield a U–Pb age of 128.1 ± 1.9 Ma (Zhang et al., 2018a). Collectively, these data suggest that subduction below the western margin of the West Burma Block was underway by ~137 Ma (Fig. 6).

Sub-ophiolitc mélange below the Kalaymyo Ophiolite includes Middle Jurassic radiolarian chert and associated pillow basalts (Zhang et al., 2018a), metachert, and associated amphibolite with U–Pb zircon ages of 119 ± 3 Ma and 114.7 ± 1.4 Ma (Liu et al., 2016a; Zhang et al., 2017a) interpreted as reflecting ~119–114 Ma accretion of subducted Middle Jurassic OPS. Sub-ophiolitic mélange below the Naga Hills ophiolite mostly consists of OPS and contains eclogite blocks with U–Pb zircon ages of ~205 Ma, ~189–185 Ma and ~172 Ma interpreted to represent protolith ages (Rajkakati et al., 2019), and chert blocks with radio-

larian assemblages with Middle Jurassic (Bathonian–Callovian), Late Jurassic (Kimmeridgian–Tithonian) and Early Cretaceous (Hauterivian–Barremian) age ranges (Aitchison et al., 2019; Baxter et al., 2011). These data suggest subduction of an uppermost Triassic–Middle Jurassic oceanic crust with a Middle Jurassic to Lower Cretaceous pelagic sedimentary cover (Fig. 6).

The Kalaymyo Ophiolite and underlying mélange and OPS are thrust over thrust slices that contain Middle–Upper Triassic (Ladinian–Carnian) volcaniclastic sandstones and low-grade mica and chlorite schists (Bannert et al., 2012; Maurin and Rangin, 2009; Morley et al., 2020; Sevastjanova et al., 2016; Yao et al., 2017; Zhang et al., 2018a, 2017) (Fig. 6). These Triassic units were interpreted to be derived from a continental fragment named **Mount Victoria Land** (Mitchell, 1986). Provenance studies on these sandstone and schist units yielded contradictory interpretations. Sevastjanova et al. (2016) conducted a qualitative comparison between detrital zircons from these Upper Triassic sandstones and source terranes in Asia and Australia and suggested that Mount Victoria Land, and by inference the West Burma Block, was adjacent to Sundaland in the Triassic. Yao et al. (2017) conducted a statistical analysis to quantify the similarity between detrital zircons from these Upper Triassic sandstones and potential sources terrane in Greater India, Australia, and Asia and showed distinct differences from contemporaneous units in Indochina and Sibumasu, but similarity with NW Australia and Greater India. Yao et al. (2017) therefore instead concluded that these Upper Triassic volcaniclastic sandstones were deposited close to the paleogeographic junction between western Australia and northern Greater India, and this interpretation was subsequently adopted by Zhang et al. (2020b) and Naing et al. (2023).

The Kalaymyo Ophiolite as well as the Triassic units of Mount Victoria Land are both unconformably overlain by mid-Cretaceous (Albian–Cenomanian) limestones that contain clasts of metamorphic and ophiolitic rocks (Morley et al., 2020), from which we infer a ~115 Ma age for the accretion of the Mount Victoria Land Block below the ophiolite (Fig. 6). To the west, the Triassic units of Mount Victoria Land are unconformably overlain by Upper Cretaceous (Campanian–Maastrichtian) to Eocene forearc sedimentary rocks (Morley et al., 2020). The Cretaceous accretionary fold-thrust belt and mélange of the inner Indo-Burman Ranges overthrusts middle Paleocene (Selandian) to earliest Eocene (lower Ypresian) radiolarian cherts (Aitchison et al., 2019) and folded Middle–Upper Eocene turbidites (Lokho et al., 2004; Lokho and Tewari, 2011) that grade into shallow marine shale and sandstone of Oligocene–Miocene age (Vadlamani et al., 2015) that collectively form the outer Indo-Burman Ranges, which lie unconformably on NE India (Alam et al., 2003; Gupta and Biswas, 2000; Johnson and Nur Alam, 1991). The outer Indo-Burman Ranges have accommodated ~38.4 ± 16 km E-W shortening since ~8 Ma (Betka et al., 2018) in the north (latitude: 24°N), whereas further south E-W shortening decreases to 16 km (23°N) and 4.2 km (22°N) respectively (Hossain et al., 2022).

4.4. Woyla Arc; Andaman-Nicobar ophiolites; Ciletuh Complex

South of Myanmar lies the Andaman Sea flanked in the west by the Andaman-Nicobar Islands that expose the Andaman-Nicobar Ophiolites, in the east by the Thai-Malay peninsula that exposes the Sibumasu terrane, and in the south by the island of Sumatra that exposes the Woyla intraoceanic arc, juxtaposed against the West Sumatra Block. The intervening Andaman Sea is an Oligocene-Neogene extensional basin (Figs. 1 and 5).

The **Woyla Arc** comprises basaltic to andesitic volcanic rocks that include xenoliths of radiolarian chert, dykes, shales, and volcaniclastic sandstones lacking quartz, and there is no evidence for the presence of a continental basement (Barber, 2000; Barber et al., 2005a; Wajzer et al., 1991). Sparse radiometric dating of the volcanic rocks yield K–Ar ages of 122–105 Ma (Gafoer et al., 1992; Koning, 1985; Pulunggono and Cameron, 1984). In addition Lower Cretaceous (Aptian–Albian) limestones with volcanic detritus associated with basaltic to andesitic volcanic rocks (Advokaat et al., 2018a; Bennett et al., 1981; Gafoer et al., 1992; Yancey and Alif, 1977) are interpreted as reefs fringing volcanic edifices (Barber, 2000; Cameron et al., 1980; Wajzer et al., 1991) that date the onset of the arc in the Early Cretaceous (~130 Ma, Table S1, Fig. 6). A contemporaneous arc existed on the West Sumatra Block of Sundaland (Section 4.2), showing that a double, opposite verging subduction configuration existed with (south)westward subduction below the intra-oceanic Woyla Arc and (north)eastward subduction below the West Sumatra Block (Barber et al., 2005a), consuming a conceptual Ngalau Ocean in between (Advokaat et al., 2018a).

The Woyla Arc was thrusted over the western margin of the West Sumatra Block (Barber et al., 2005a) as inferred from metamorphism up to amphibolite facies in the West Sumatra margin (Suwarna et al., 1994) which was constrained by K–Ar ages between 125 and 95 Ma (Andi Mangga et al., 1994; Koning, 1985). Accreted rocks in the Woyla Suture between West Sumatra and the Woyla Arc comprise deformed serpentinites, gabbros, pillow basalts, cherts, red shales, volcanic breccia, and limestone (Barber, 2000). Cherts at two locations contain Middle–Upper Triassic (Ladinian–Carnian) and Middle Jurassic (Aalenian) radiolarian assemblages, respectively (McCarthy et al., 2001; Munasri and Putra, 2019), whilst a limestone block contained Upper Triassic foraminifera (Wajzer et al., 1991). These rocks show that the Ngalau ocean floor was at least Middle Triassic in age (Advokaat et al., 2018a). Collision of the Woyla Arc with the West Sumatra margin was completed around 95–85 Ma (Fig. 6) as suggested by the youngest K–Ar age of 95 ± 3 Ma in metamorphic rocks from the West Sumatra margin (Koning, 1985) and granites with K–Ar ages of ~87–85 Ma that pierce the Woyla Suture (Kanao, 1971; Rock et al., 1983; Wajzer et al., 1991). During collision of the Woyla Arc with the West Sumatra margin, the modern subduction system initiated west of the Woyla Arc, as suggested by renewed arc-related magmatism on Sumatra in the Late Cretaceous (Advokaat et al., 2018a; Barber et al., 2005a).

The mid-Cretaceous **Andaman and Nicobar ophiolites**, currently to the northwest of the Woyla Arc to the west of the Andaman Sea, are likely witnesses of this subduction polarity reversal (Bandyopadhyay et al., 2021; Plunder et al., 2020). These ophiolites and the narrow forearc ridge above the Sunda subduction zone, moved north relative to Sumatra during the Cenozoic opening of the Andaman Sea Basin (Curray, 2005) (see Section 4.5) (Figs. 1 and 5) from a restored position adjacent to the northwestern Woyla Arc (Advokaat et al., 2018a; van Hinsbergen et al., 2011). The ophiolitic suite consists of a mantle sequence with more and less depleted peridotites interpreted to have originally formed in back-arc basin setting, and subsequently modified in a supra-subduction zone setting (Bandyopadhyay et al., 2021, 2020; Ghosh et al., 2017), whereas the crust comprises a gabbroic magmatic sequence, plagiogranite intrusions with an arc geochemical signature (Jafri et al., 1995) and boninitic and island arc tholeiitic pillow lavas (Pal, 2011). In addition, isolated occurrences of andesitic agglomerates, in places together with abundant plagiogranite fragments, are found that indicate explosive arc magmatism (Bandyopadhyay et al., 2021). Gabbros and plagiogranites, including those associated with the andesitic agglomerates, yield U–Pb zircon ages ranging from 99 Ma to 93 Ma (Bandyopadhyay et al., 2021; Pedersen et al., 2010; Sarma et al., 2010). One gabbro contained an inherited U-Pb zircon core age of 105.3 ± 1.4 Ma (Bandyopadhyay et al., 2021), an age that coincides with a plagioclase xenocryst with a $^{40}Ar/^{39}Ar$ age of 106 ± 3 Ma contained in

Pleistocene volcanic rocks on nearby Barren Island (Ray et al., 2015) (Fig. 1), and $^{40}Ar/^{39}Ar$ hornblende ages on amphibolites of the metamorphic sole welded to the base of the ophiolites of 106.4 ± 2.1 Ma and 105.3 ± 1.6 Ma (Plunder et al., 2020). These findings suggest that supra-subduction zone spreading and associated metamorphic sole exhumation occurred around 106 Ma (Plunder et al., 2020). The 99–93 Ma magmatic rocks, originally interpreted as the age of the ophiolite (Pedersen et al., 2010) may rather represent a magmatic arc that developed upon subduction maturation (Bandyopadhyay et al., 2021). The ophiolite is overlain by Upper Cretaceous (Campanian) radiolarian cherts (Ling et al., 1996) with a geochemical signature that suggests deposition near a continental margin (Jafri et al., 1993). Collectively, subduction initiation below the Andaman ophiolites likely occurred at or before 106 Ma (Fig. 6) in a restored position immediately to the west of the Woyla Arc suggesting that these ophiolites recorded the subduction polarity reversal that occurred upon collision of the Woyla Arc with West Sumatra (Advokaat et al., 2018a; Bandyopadhyay et al., 2021; Plunder et al., 2020).

In Paleogene time (~60–40 Ma), the ophiolite was shortened and uplifted, and shallow marine, volcanic arc-derived sandstones were deposited (Bandopadhyay, 2012, 2005; Bandopadhyay et al., 2022, 2009; Bandopadhyay and Carter, 2017a, 2017b). These volcanic arc-derived sandstones contain abundant 60 Ma detrital zircons that are unknown from Sumatra. The Wuntho-Popo Arc of the West Burma Block was a more likely source (Bandopadhyay et al., 2022). During Middle–Late Eocene the Andaman ophiolites subsided, the sedimentary connection to an active arc source was lost, and radiolarian chert sedimentation resumed, followed by deposition of deep-marine, distal Sundaland-derived clastic sandstones in the Late Oligocene–Early Miocene (Bandopadhyay et al., 2022; Bandopadhyay and Carter, 2017b; Bandopadhyay and Ghosh, 2015; Limonta et al., 2017; Ling and Srinivasan, 1993). Finally, the Andaman ophiolites were uplifted since Middle Miocene, witnessed by the deposition of Upper Miocene shallow marine limestones (Bandopadhyay and Carter, 2017c). This uplift is likely related to the formation of an accretionary prism of clastic turbiditic sandstones and shales of poorly known but likely Neogene age that dominate the western part of the islands as well as the offshore region, separated from the ophiolites along the Jarawa Thrust (e.g. Bandopadhyay and Carter, 2018; Bhat et al., 2019). The accreted sedimentary rocks are thought to derive from the Bengal and Nicobar fan deposits for a large part derived from India and the Tibetan-Himalayan orogen (Bandopadhyay and Carter, 2017b; Bandopadhyay and Ghosh, 2015; Limonta et al., 2017). Offshore seismic sections to the west of the Andaman-Nicobar Ridge show that the accretionary prism below the Jarawa thrust extends to the modern plate boundary (Moeremans et al., 2014; Roy, 1992; Roy and Chopra, 1987).

To the southeast of the Andaman and Nicobar Ridge, the Mentawai islands (Figs. 1, 5, and 6) form the Sumatran forearc above the Sunda Trench, and are underlain by an ophiolite (Milsom et al., 1990). This ophiolite consists of a mantle sequence comprising of serpentinized peridotites, and a crust comprising gabbros, diorites, plagiogranties, dolerites, and basalt (Moore and Karig, 1980). E-MORB gabbros of this ophiolite yield K–Ar ages of 40.1 ± 2.7 Ma and 35.4 ± 3.6 Ma that record low-grade metamorphism (Kallagher, 1990). Commonly, the ophiolite is dismembered, and its components occur as clasts in a mélange. These clasts include garnet amphibolites, metasedimentary rocks (Kallagher, 1990; Moore and Karig, 1980), pelagic limestones, ochres, and cherts with Upper Cretaceous (Campanian) and Middle Eocene radiolarian assemblages (Samuel et al., 1997) suggesting these are accreted sub-ophiolitic units derived from the Indian Ocean (Barber and Crow, 2005). The ophiolite is overlain by deep marine turbidites, originally interpreted as Eocene in age based on reworked clast content (Pubellier et al., 1992), but later shown to be of mid-Oligocene–Miocene age (Samuel et al., 1997). This sequence is highly disrupted due to later shale diapirism and mud-volcanism (Samuel et al., 1997, 1995). This sequence is overlain by shallow marine diachronous Middle Miocene–Pliocene sandstones and mudstones that also include coral-algal limestone units (Samuel et al., 1997). Late Pliocene to recent siliciclastic sediments and reefal limestones rest unconformably on the underlying units (Samuel et al., 1997). We interpret that the ophiolite exposed on the Mentawai islands formed between the Woyla Arc and Andaman-Nicobar ophiolites and became disrupted in the Miocene-Pliocene when the outboard located Andaman-Nicobar ophiolites moved northward (Bandopadhyay et al., 2022).

Ophiolitic lithologies are also exposed in the **Ciletuh Complex** of West Java, located to the south of the Woyla Arc (Fig. 5). The Ciletuh Complex was first studied by Boachi (1856) and comprises a series of north dipping thrust slices (Ikhram et al., 2019), where the highest thrust slice is formed by a dismembered ophiolite that consists of amphibolite, serpentinized harzburgite and dunite, gabbro, and pillow basalt in close association with red clay (Endang Thayyib et al., 1977). Gabbros yield K–Ar ages between 56.0 and 42.7 Ma, that were likely partially reset by Eocene magmatic activity (Satyana et al., 2021; Schiller et al., 1991). Amphibolite associated with the peridotite likely represents a metamorphic sole and records P-T conditions of 5–6 kbar and 640–660 °C, whilst epidote amphibolite recorded retrograde P-T conditions of 4–5 kbar and 410–455 °C (Patonah and Permana, 2010). Structurally below the Ciletuh Ophiolite is a shale-hosted OPS mélange with fragments of chert, greywacke, and Upper Cretaceous limestone (Endang Thayyib et al., 1977). Endang Thayyib et al. (1977) also reported the presence of glaucophane schist, but later studies could not reproduce this observation (Ikhram et al., 2019; Satyana et al., 2021; Schiller et al., 1991). Sub-ophiolitic metamorphic rocks occur in close association with brecciated serpentinite and comprise greenschist facies phyllites, pelitic chlorite-muscovite schists, epidote-chlorite schists, and quartzites (Endang Thayyib et al., 1977; Ikhram et al., 2019). Chlorite-muscovite schist yields K–Ar ages between 55 and 38 Ma (Satyana et al., 2021), but it is likely these ages were also partially reset by Eocene magmatism (Schiller et al., 1991). The Ciletuh Complex is unconformably overlain by Middle Eocene conglomerates and volcaniclastic sandstones that rework the underlying lithologies. A basaltic pebble within this conglomerate yields a K–Ar plagioclase age of 89.6 ± 3.0 Ma, further suggesting a Late Cretaceous age of the Ciletuh Complex (Schiller et al., 1991). Collectively, the Ciletuh Complex is interpreted as a SSZ ophiolite that formed in the Late Cretaceous (Schiller et al., 1991), in a restored position to the southwest of the Woyla Arc (Advokaat et al., 2018b).

4.5. Sagaing Fault; Andaman Sea region; Sumatran Fault System

The highly oblique India-Sundaland plate motion is presently partitioned over the Sunda trench and Indo-Burman ranges fold-thrust belt that accommodate the E-W convergent component (Betka et al., 2018; Hossain et al., 2022; Maurin and Rangin, 2009), and the Sagaing Fault, Andaman Sea region, and faults on- and offshore Sumatra (Curray, 2005; Steckler et al., 2016) that accommodate most of the N-S strike-slip component of motion (Fig. 5). Together, these surround a forearc sliver that contains the West Burma Block and inner Indo-Burman Ranges, the Andaman-Nicobar forearc ridge, and part of Sumatra. In this section, we review the constraints on the formation and evolution of this forearc sliver.

Morley and Arboit (2019) showed that the North Minwun Basin, which forms a releasing splay at the northern termination of the Sagaing Fault, accommodated at least 100–120 km of extension

since 27.5 ± 0.42 Ma, and sedimentary sequences to the west of the Sagaing Fault record a Late Oligocene–Early Miocene phase of transpression (Westerweel et al., 2020), indicating that the Sagaing Fault must have been active since that time. In addition, the Shan Scarp Fault to the east of the Sagaing fault also accommodated strike-slip motion of unknown magnitude between ~27–16 Ma (Bertrand et al., 2001, 1999) (see Section 4.1, Fig. 5, Table S1). Apart from the minimum displacement constraints from the North Minwun Basin, rocks of the West Burma Block do not correlate to those in Sibumasu and offsets cannot be directly constrained along the fault itself. Van Hinsbergen et al. (2011) noted that the ~40–23 Ma old Three Pagodas and Mae Ping faults, with each ~100 km of displacement, do not continue into the West Burma Block and therefore inferred that the West Burma Block must have been located to the south of the Three Pagodas fault prior to its activity, requiring a northward displacement of the West Burma Block of at least 800 km.

To the north, the northern Indo-Burman Ranges fold-thrust belt and the Sagaing fault merge in a triple junction with the Gaoligong Shear Zone and related younger brittle faults that accommodate northward motion of India relative to Sibumasu (Lin et al., 2009; Tun and Watkinson, 2017; Wang et al., 2008). To the south, the Sagaing fault propagates into the **Andaman Sea**, where it presently connects to spreading ridge segments that accommodated N-S extension between the West Burma Block and Andaman and Nicobar forearc ridge in the north and west, and Sumatra and the Thai-Malay Peninsula in the south and east (Figs. 1 and 5), and that provides direct kinematic evidence for the northward displacement of the forearc sliver (Morley et al., 2023a). The Andaman Sea hosts the Central and East Andaman Basins.

The **Central Andaman Basin** contains oceanic crust, where marine magnetic anomalies C3, C2 and C1r.1r were recognized that reveal 118 km extension since 4.19 Ma (Curray, 2005; Raju et al., 2004). The spreading center forms an extensional step-over between the Sagaing Fault to the northeast, and the West Andaman and Old West Andaman Faults in the west that connect southward to the Sumatran Fault System (Fig. 5; see below). To the north and south of the Central Andaman Basin are the Alcock and Sewell Rises, respectively, which represent hyperextended island-arc crust (Morley and Alvey, 2015). Two dredged basalt samples from the Alcock Rise yield K–Ar ages of 20.5 ± 1.0 Ma and 19.8 ± 0.7 Ma (Curray, 2005; Rodolfo, 1969) and are interpreted to represent rift-related magmatism, showing that extension in the Andaman Sea was underway by Early Miocene time (Morley and Alvey, 2015). The bathymetry of the Alcock Rise reveals ENE-WSW trending faults, suggesting NNW-SSE oriented extension, parallel to the modern Andaman Sea spreading center (Chamot-Rooke and Rangin, 2000; Raju et al., 2004). Based on the current N-S extent of the Alcock and Sewell Rises and assuming their entire area represents extensionally exhumed rock, we reconstruct (a maximum of) 530 km of N-S directed extension between ~23 Ma and the onset of magmatic spreading at 4.19 Ma (Table S1).

The **East Andaman Basin** is located to the east of the Central Andaman Basin and the Alcock and Sewell Rises (Fig. 5). The western margin of the East Andaman Basin is floored by a narrow, 15 km wide zone of oceanic crust, and is separated from the Alcock and Sewell Rises by NNE-SSW striking normal faults that were interpreted to be active between 4.19 and 1.78 Ma (Table S1), in part coeval with oceanic spreading in the Central Andaman Basin (Curray, 2005). The East Andaman Basin itself is straddles the continent ocean transition between the Central Andaman Basin and the Mergui-North Sumatra Basin (Section 4.2) to the east (Figs. 1 and 5). WNW dipping listric normal faults form the eastern boundary with the Mergui Ridge to the east, and accommodated 100 km of NW-SE directed extension during the Early Miocene to early Middle Miocene (Table S1) (Curray, 2005; Mahattanachai et al., 2021; Morley, 2017a, 2016a; Morley and Alvey, 2015; Srisuriyon and Morley, 2014).

Collectively, it is feasible that the Central and East Andaman Sea basins accommodated the 800 km of extension, since ~27.5 Ma, that avoids overlap between the West Burma Block and the Three Pagodas and Mae Ping Faults. The West Andaman Fault that accommodated the northward displacement of the Andaman-Nicobar forearc ridge relative to Sumatra must thus have been connected to faults that ultimately transferred this displacement to the Sunda Trench. The presently most prominent of these faults is the active **Sumatran Fault System (SFS)**. This fault system runs from the West Andaman Fault over the island of Sumatra to the Sunda Strait (Fig. 5) and cuts through the Woyla Arc and the West Sumatra Block. It may have started as a normal fault system in the Middle Miocene and became reactivated as dextral strike-slip fault system in the Pliocene–Pleistocene (Barber et al., 2005a). Geomorphic indicators suggest at least ~20 km dextral motion (Sieh and Natawidjaja, 2000) since 2 Ma (Wang et al., 2023b), but correlation of Paleozoic basement units in the north of Sumatra suggest as much as 150 km dextral motion (McCarthy and Elders, 1997). Our reconstruction uses an estimate of ~80 km of extension that was accommodated since ~5 Ma in an extensional step-over in the **Sunda Strait**, where the Sumatra Fault System connects to the Sunda Trench in a trench-trench-transform triple junction (Huchon and Le Pichon, 1984; Lassal et al., 1989; Lelgemann et al., 2000; Sieh and Natawidjaja, 2000) (Table S1).

Prior to the Pliocene activity of the Sumatra Fault System, the West Andaman Fault was connected to the Sunda trench west of Sumatra along the **Batee Fault** (Fig. 5) and related splays. Beaudry and Moore (1985) estimated a ~65 km dextral offset during the Middle–Late Miocene for the Batee Fault (Table S1). We accommodated the remainder of Andaman Sea extension along faults that separate the Andaman-Nicobar Ridge from Sumatra (e.g. the Old West Andaman Fault (Curray, 2005)), but for these faults, no detailed displacement estimates are available.

4.6. SW Borneo Mega-Unit; Kuching Zone; OPS sequences in Sarawak and Sabah

Tectonic units to the east of Sumatra, in southern and eastern Indonesia, were accreted to the eastern margin of Sundaland. The most internal accreted block that is thought to originate from the southern Neotethys margin is the SW Borneo Mega-Unit, separated by the marine, N-S trending Billiton Depression from the Sundaland core to the west (Ben-Avraham and Emery, 1973). North of the SW Borneo Mega-Unit is the Kuching Zone that comprises a series of E-W striking accretionary complexes that are thought to have formed by subduction (of presumed Panthalassa-derived crust) below the SW Borneo Mega-Unit during the Mesozoic. The SW Borneo Mega-Unit is surrounded by accretionary complexes. The complexes of the Kuching Zone in NW Borneo are useful to constrain the arrival of the SW Borneo Mega-Unit against the Sundaland margin, and the relative motion history between the SW Borneo Mega-Unit, Sundaland, and presumed Panthalassic oceanic crust. We analyze the relationship of the SW Borneo Mega-Unit with the accreted SE Asian orogenic units to the south and east in following sections.

The **SW Borneo Mega-Unit** (Fig. 7) has a crystalline basement that is exposed in the Schwaner Mountains and comprises Devonian andesites with a U–Pb zircon age of 403 ± 11 Ma (Lai et al., 2021). The Schwaner Mountains also expose metasedimentary rocks with K–Ar ages of 242–199 Ma (Van de Weerd et al., 1987) and metamorphosed Triassic arc granitoids with U–Pb zircon ages of 236.4 ± 1.4 Ma, 233 ± 3 Ma and 213 ± 3 Ma (Batara and Xu, 2022; Hennig et al., 2017a; Setiawan et al., 2013b). Extensive U–Pb zircon geochronology and K–Ar hornblende and biotite geochronology on

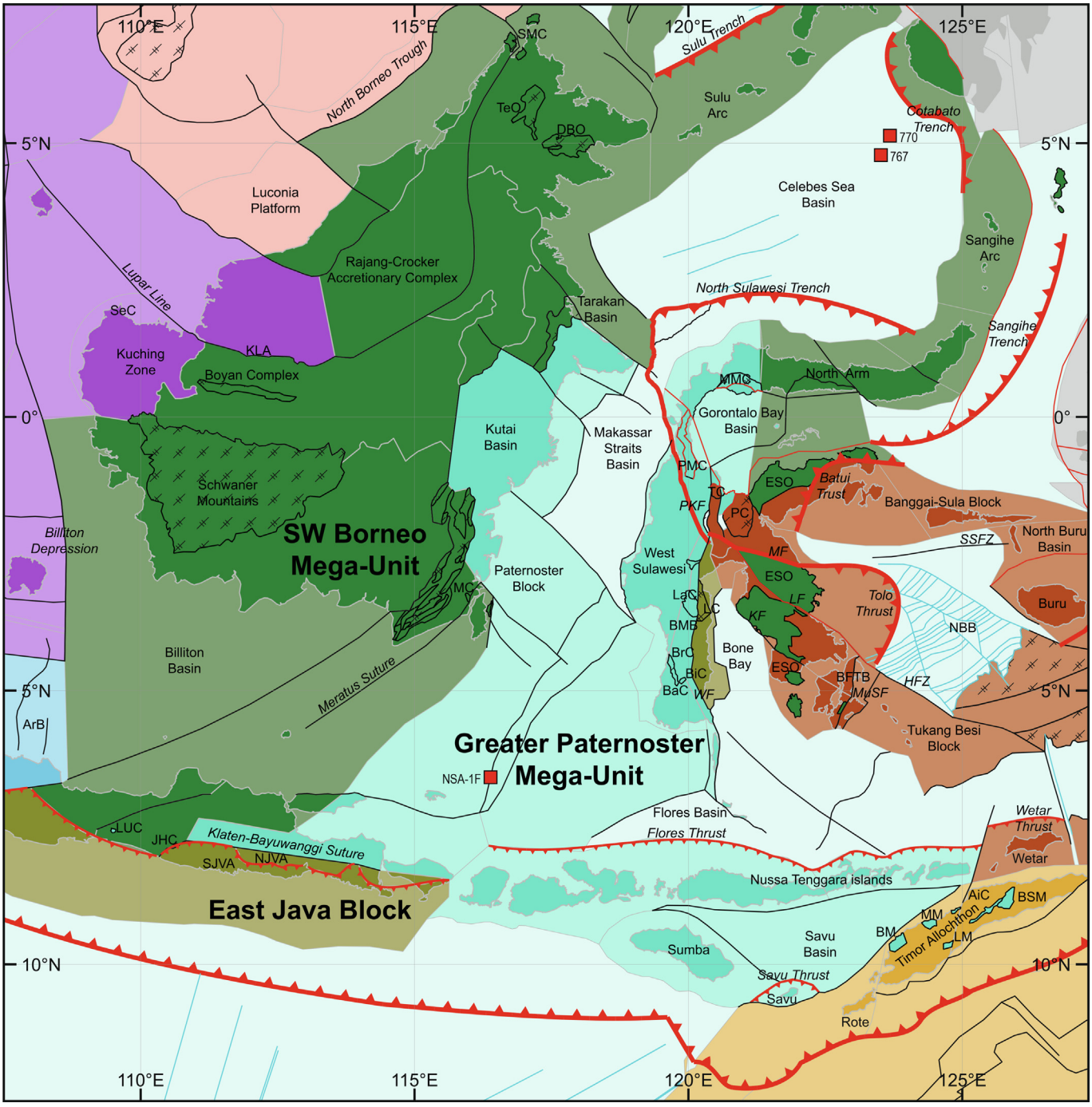

Fig. 7. Tectonic map of the central Indonesian accretionary complexes (Meratus Complex, Lok Ulo Complex, Jiwo Hills, Timor Allochthon, Bantimala Mélange Belt). See Fig. 2 for location. Abbreviations: AiC, Aileu Complex; ArB, Arjuna Basin; BaC, Bantimala Complex; BFTB, Buton Fold-Thrust Belt; BMB, Bantimala Mélange Belt; BiC, Biru Complex; BM, Boi Massif; BrC, Barru Complex; BSM, Bebe Susu Massif; DBO, Darvel Bay Ophiolite; ESO, East Sulawesi Ophiolite; HFZ, Hamilton Fracture Zone; JHC, Jiwo Hills Complex; KF, Kolaka Fault; KLA, Kapuas-Lubok Antu Mélange; LaC, Latimojong Complex; LC, Lamasi Complex; LF, Lawanopo Fault; LM, Lolotoi Massif; LUC, Lok Ulo Complex; MC, Meratus Complex; MF, Matano Fault; MM, Miomaffo Massif; MMC, Malino Metamorphic Complex; MuSF, Muna Straits Fault; NBB, North Banda Basin; NJVA, Northern Java Volcanic Arc; PC, Pompangeo Complex; PKF, Palu-Koro Fault; PMC, Palu Metamorphic Complex; SeC, Seranbang Complex; SJVA, Southern Java Volcanic Arc; SMC, Sabah mélange complexes; SSFZ, South Sulu Fault Zone; TC, Tokorondo Complex; TeO, Telupid Ophiolite; WF, Walanae Fault.

granitoids and volcanic rocks has revealed several pulses of Jurassic magmatism between 189 and 150 Ma that were interpreted to be related to rifting (Batara and Xu, 2022; Breitfeld et al., 2020; Davies et al., 2014; Haile et al., 1977; Van de Weerd et al., 1987; Wang et al., 2022b). Subsequent arc magmatism was interpreted to be subduction related and pulsed, starting at ~132 Ma and lasting until ~88 Ma (Breitfeld et al., 2020; Davies et al., 2014; Haile et al., 1977; Hennig et al., 2017a; Williams et al., 1988). However, Batara and Xu (2022) argued that 154–150 Ma granitoids also have an arc signature, suggesting the SW Borneo Mega-Unit may already have been in an upper plate position above a subduction zone by this time. The lack of inherited zircons in these arc rocks suggests either remelting of an immature arc, or a mantle derivation of their melts (Breitfeld et al., 2020). U–Pb zircon geochronology showed most of these igneous rocks underwent metamorphism between 92 and 86 Ma (Hennig et al., 2017a).Younger igneous rocks on

the SW Borneo, with ages of 89–72 Ma, were geochemically interpreted as within-plate magmatic rocks (Breitfeld et al., 2020; Haile et al., 1977; Hennig et al., 2017a), although Qian et al. (2022) argued that these igneous rocks also formed in an arc setting, suggesting subduction below the SW Borneo Mega-Unit continued in the Late Cretaceous (Campanian). Inherited zircons in crystalline rocks from the Schwaner Mountains are rare: igneous and meta-igneous rocks mostly contain Jurassic and Triassic inherited ages, and only a few pre-Mesozoic (Batara and Xu, 2022; Breitfeld et al., 2020; Davies et al., 2014; Hennig et al., 2017a; Wang et al., 2022b). Very few metamorphosed volcaniclastic rocks contain inherited zircon cores, with ages ranging from the Proterozoic to the Cretaceous (Davies et al., 2014; Wang et al., 2022b).

Mesozoic rocks of the SW Borneo Mega-Unit are also exposed on the island of Karimata and the Karimunjawa Islands (Fig. 1). Karimata Island directly west of Borneo forms the western margin of the SW Borneo Mega-Unit, and exposes granitoids with a Rb–Sr whole rock isochron age of 74 ± 2 Ma, and associated amphibolite with a K–Ar whole rock age of 78 ± 5 Ma (Priem et al., 1975). The Karimunjawa Islands in the eastern Java Sea form the southern boundary of the SW Borneo Mega-Unit with the Meratus Suture (Fig. 7, see Section 4.7) in the Java Sea (Granath et al., 2011; Hamilton, 1979). The Karimunjawa islands expose low-grade Upper Triassic meta-sandstone and conglomerate with Paleozoic, Proterozoic and Archean inherited zircons suggesting an Australian provenance (Witts et al., 2012). We trace the SW Borneo Mega-Unit farther towards east Borneo, where the Cenozoic Kutai Basin exposes Lower Devonian coral and stromatoporoid bearing limestones occurring in Permian debris flows (Rutten, 1940; Sugiaman and Andria, 1999). The western margin of the Tarakan Basin exposes predominantly low-grade metamorphosed clastic sedimentary rocks, including quartzose greywacke and a micaceous quartzite with a K–Ar age of ~190 Ma (Hamilton, 1979 and references therein). Towards the east, on the Magkalihat Peninsula, these rocks are bounded by mélange and arc lithologies (Hamilton, 1979; Hutchison, 1986) that we interpreted as northern continuation of the Meratus Suture (see Section 4.7) demarcating the eastern boundary of the SW Borneo Mega-Unit. Mesozoic rocks are also exposed in the Segama Valley in Sabah (NE Borneo), where they comprise intermediate to felsic intrusive and volcanic rocks, hornfels, and schist with widely dispersed K–Ar ages between 210 and 99.5 Ma (Graves et al., 2000; Kirk, 1968; Leong, 1974; Swauger et al., 1995). Recent U–Pb zircon geochronology on these felsic intrusions yields ages of clustering around 250–240 Ma, 210–203 Ma, and ~179 Ma that were interpreted to represent a Triassic to Jurassic magmatic arc (Burton-Johnson et al., 2020; Wang et al., 2023a), on par with the geology of the Schwaner Mountains, which we consider to be part of the SW Borneo Mega-Unit too. Collectively these data indicate that SW Borneo Mega-Unit is in part underlain by an igneous and metasedimentary basement of Devonian, Permian, and Triassic age with sediments that were derived from the Australian continent and with abundant Triassic, and Late Jurassic–Cretaceous arc magmatism.

The WNW-ESE striking **Kuching Zone** is located to the north of the Schwaner Mountains (Fig. 7). The tectonic contact with the SW Borneo Mega-Unit is obscured by batholiths (Williams et al., 1988). The northern margin of the SW Borneo Mega-Unit consists of intensely deformed Upper Triassic to Middle Jurassic (Callovian) ammonite-bearing calcareous shales (Schairer and Zeiss, 1992), and Lower–Upper Cretaceous (Valanginian–Turonian) turbiditic sequences and to the north is the steeply south-dipping *Boyan Complex* (Williams et al., 1988, 1986). This complex comprises a clay-rich matrix with blocks of chert, sandstone, greenschist, serpentinite, granite, quartzite, and mid-Cretaceous (Aptian–Cenomanian) *Orbitulina*-bearing limestone as well as tectonic slices of metamorphosed and unmetamorphosed ultramafic, mafic, and intermediate igneous rocks are hosted in a serpentinite matrix (Williams et al., 1986). A granitoid block in the Boyan Complex yields a K–Ar hornblende age of 320 ± 3 Ma, whereas volcanic rocks yield a K–Ar pyroxene age of 97.8 Ma (Williams et al., 1988, 1986). Collectively, this shows that the Boyan Complex is a Cretaceous suture between a terrane consisting of Paleozoic granites that likely belongs to the Sundaland core and the northern margin of the SW Borneo Mega-Unit (Fig. 6). Recently, Quek et al. (2023) interpreted the Boyan Complex as Carboniferous–Triassic in age, and combined detrital zircon records from either side of the complex into one collection to infer a paleogeographic affinity of both blocks with Sundaland since the Triassic. The age constraints of the Boyan Complex demonstrate that the SW Borneo Mega-Unit should be treated as a separate block that was mobile relative to Sundaland until the Late Cretaceous.

The Kuching Zone directly north of the Schwaner Mountains exposes Upper Carboniferous limestone and marble that are intruded by biotite granites with K–Ar hornblende and biotite ages of 320–204 Ma (Williams et al., 1988) and by mafic to intermediate arc-granitoids with U–Pb zircon ages of 154–130 Ma (Wang et al., 2022a, 2022b). Basaltic and andesitic volcanic rocks that are exposed between these arc granitoids yield U–Pb zircon ages of 138–130 Ma (Wang et al., 2022a). Directly north of this arc are Upper Jurassic metasandstones that were likely derived from this arc. Detrital zircons in these metasandstones are dominated by a Triassic–Late Jurassic populations, and a less pronounced ~1853 Ma population that may suggest derivation from Indochina-East Malaysia (Wang et al., 2022b). Williams et al. (1988) interpreted these granitoids as part of the SW Borneo Mega-Unit, implying a suture to the north, whereas Breitfeld et al. (2020, 2017), Hennig et al. (2017a) and Wang et al. (2022a, 2022b) interpreted them as part of Sundaland, inferring a N-S suture through the Schwaner Mountains for which field evidence is lacking. Instead, we consider this part of the Kuching Zone as part of Sundaland, whose fragments and sediments became incorporated in an E-W trending (in modern coordinates), south-dipping subduction zone directly north of the Schwaner Mountains in the Late Cretaceous.

Farther north, the Kuching Zone exposes phyllites and quartz-mica schists with U–Pb zircon ages of 462.4 ± 2.6 M and 453.3 ± 1. 9 Ma that represent their protolith age. These U–Pb zircon ages, in combination with Hf zircon isotopic data, suggest an affinity with the Indochina Mega-Unit (Zhu et al., 2022). $^{40}Ar/^{39}Ar$ white mica ages of 219.6 ± 3 Ma and 216.8 ± 1.2 Ma record later metamorphic events associated with arc magmatism (Breitfeld et al., 2017). This crystalline basement is unconformably overlain by Upper Carboniferous (Moscovian) to Lower Permian chert, shale, and limestone (Metcalfe, 1985) (Fig. 6). This sequence is intruded by granodiorite with a U–Pb zircon age of 208.3 ± 0.9 Ma (Breitfeld et al., 2017), and unconformably overlain by Upper Triassic basaltic-andesitic volcanic rocks, Lower Jurassic (Pliensbachian–T oarcian) tuffaceous radiolarian chert, and clastic sedimentary rocks (Jasin et al., 1996; Jasin and Said, 1999a). Breitfeld et al. (2017) interpreted this sequence as a Triassic–Early Jurassic accretionary complex on the east Sundaland margin. This accretionary complex is unconformably overlain by Upper Jurassic (Oxfordian–Kimmeridgian) shallow marine limestone (Kakizaki et al., 2013), Upper Jurassic (Kimmeridgian–Tithonian) mudstone and radiolarian chert, and Cretaceous (Aptian–Santonian) deep marine volcaniclastic rocks (Breitfeld et al., 2017; Jasin and Said, 1999b; Schmidtke et al., 1990; Zhang et al., 2022a) and intermediate basaltic and andesitic volcanic rocks with U–Pb zircon ages of 97–78.5 Ma and a $^{40}Ar/^{39}Ar$ whole rock plateau age of 77.1 ± 2.4 Ma (Wang et al., 2021b; Zhang et al., 2022a). This sequence is interpreted to record the transition from shallow marine (passive) continental margin in Late Jurassic (Oxfordian–Kimmeridgian) time to rapidly subsiding deep marine

forearc basin in Late Jurassic (Kimmeridgian) to Late Cretaceous (Campanian) time (Breitfeld et al., 2017). This sequence is intruded by Upper Cretaceous arc granitoids with U–Pb zircon ages of 83.6–77.5 Ma (Gan et al., 2022) and is unconformably overlain by Upper Cretaceous (Maastrichtian) to Upper Eocene fluvio-deltaic sedimentary rocks (Breitfeld et al., 2018; Metcalfe, 1990; Williams et al., 1988, 1986), suggesting subduction and arc magmatism ceased in during Late Cretaceous (Campanian) time (Breitfeld et al., 2017) (Fig. 6).

Along the northern boundary of the Kuching Zone are OPS-derived mélange complexes (Figs. 6 and 7). The Serabang Complex in the west exposes blocks of slate, sandstone, volcanic tuffs, and chert with Valanginian–middle Aptian radiolaria that have suffered regional metamorphism (Jasin and Madun, 1996). U–Pb zircon provenance on the trench-fill clastic rocks revealed maximum depositional ages between 111 and 90 Ma (Wang et al., 2021b). The Kapuas-Lubok Antu Mélange is exposed along the Lupar Line, and comprises blocks of Upper Jurassic (Tithonian), Lower Cretaceous (Valanginian–Barremian) and Lower–Upper Cretaceous (Albian–Cenomanian) chert (Jasin, 1996; Jasin and Haile, 1993; Tan, 1979). U–Pb zircon provenance on the trench-fill clastic rocks revealed maximum depositional ages of 119 Ma, 115 Ma, and 105 Ma based on the youngest zircon grain in each sample (Wang et al., 2021b; Zhao et al., 2021). Similar mélange complexes are also present in northern Sabah (Fig. 7), where they comprise thrust slices of gabbro with U–Pb ages of 123–112 Ma, plagiogranite, pillow basalt with $^{40}Ar/^{39}Ar$ plateau ages of 136–135 Ma, Lower–Upper Cretaceous (Barremian–Cenomanian) radiolarian chert, and trench-fill clastic rocks (Ismail et al., 2014; Jasin et al., 1985; Jasin and Tongkul, 2013; Omang et al., 1994; Wang et al., 2023a; van de Lagemaat et al., 2023). These mélanges are overlain by Middle Eocene sandstone (Haile, 1996; Jasin and Tongkul, 2013; Rahim et al., 2017).

Collectively the stratigraphy of the Kuching Zone and these mélange complexes record subduction and accretion during Late Jurassic (Kimmeridgian) to Late Cretaceous (Campanian) time of oceanic lithosphere of at least Late Jurassic (Tithonian) to Late Cretaceous (Cenomanian) age (Fig. 6). After the Campanian, there is a hiatus in accretion below North Borneo. The next units to accrete are the Upper Cretaceous (Maastrichtian) and younger rocks from the Rajang Crocker Accretionary Complex (Cullen, 2010; Tongkul, 1997), interpreted to relate to a younger and unrelated subduction zone whose geological record is traced farther east, towards the Palawan Ophiolite (see Section 4.13).

4.7. Meratus Complex; Klaten-Banyuwangi Suture; East Java Block

To the east of the SW Borneo Mega-Unit are accretionary complexes of the Meratus Suture. This suture separates the SW Borneo Mega-Unit from continent-derived, deformed and in part metamorphosed rocks, overlain and cut by Cenozoic basins, that are exposed across much of central and eastern Indonesia. These continent-derived rocks have different names on different islands, but because there is no evidence that they are separated by sutures, we include them all in the 'Greater Paternoster Mega-Unit', named after the Paternoster Block (Rose and Hartono, 1978; Samuel and Muchsin, 1975) that lies adjacent to the Meratus Suture on SE Borneo. The Greater Paternoster Mega-Unit is separated by the here defined Klaten-Banyuwangi Suture from the East Java Block to the south (Section 4.8), and by the Bantimala Mélange Belt from the East Sulawesi Ophiolite and underlying accreted units to the east (Section 4.9), and by the Rajang-Crocker Accretionary Complex and Palawan Accretionary Complex from the South China Sea and related microcontinental fragments to the north Section 4.12, Fig. 7). We correlate continent-derived rocks of SE Borneo, west Sulawesi, Sumba, Flores, and the highest structural units of Timor (the Mutis and Lolotoi complexes, see below) to the Greater Paternoster Mega-Unit (Figs. 7 and 8). Below, we describe the manifestations of these continental rocks on the different islands, their bounding sutures, and the basins and arcs that formed in and on the Greater Paternoster Mega-Unit.

The **Meratus Complex** on SE Borneo lends its name to the Meratus Suture that forms the eastern boundary of the SW Borneo Mega-Unit (Section 4.6). This suture continues southward through the Java Sea towards the Lok Ulo Complex in central Java (Section 4.8). On SE Borneo, the Meratus Complex exposes a series of NE-SW striking, east verging thrust slices (Monnier et al., 1999; Priyomarsono, 1985; Yuwono et al., 1988). The structurally highest thrust slice is the ~90 km wide Meratus Ophiolite (Figs. 7 and 8) comprising serpentinitized peridotites, pyroxenites, and variably metamorphosed mafic lavas (Idrus et al., 2022; Monnier et al., 1999; Pubellier et al., 1999). Metamorphic sole amphibolites and granulites record *P–T* conditions of 9.5–12 kbar and 765–900 °C, and yield a U–Pb zircon age of 136.8 ± 3.6 Ma (Soesilo, 2012; Soesilo et al., 2015) that is likely a more reliable minimum age for subduction initiation below the Meratus Ophiolite than an earlier K–Ar age of 145 Ma (Priyomarsono, 1985).

The structurally highest thrust slice below the ophiolite comprises low-grade phyllites and greenschist to amphibolite-facies schists yielding K–Ar phengite ages of 180 ± 9 Ma and 165 ± 9 Ma (Wakita et al., 1998) that are interpreted as a pre-burial metamorphic event (e.g., Jurassic rifting in the Australian margin), or may be attributed to excess Ar (Alfing et al., 2021; Kelley, 2002). The thrust slice below comprises epidote–amphibolite facies schists that recorded *P–T* conditions of up to 11–15 kbar and 545–690 °C, and overprinting from epidodite-amphibolite to greenschist facies (Setiawan et al., 2015). These schist yield K–Ar phengite ages 119–108.4 Ma (Sikumbang, 1986; Sikumbang and Heryanto, 1994; Wakita et al., 1998), and Rb–Sr ages of 115–110 Ma (Alfing et al., 2021), interpreted as the age of mica-recrystallization during epidote–amphibolite to greenschist facies retrogression (Alfing et al., 2021). We interpret this sequence as metamorphic OPS or distal content-derived sediments that arrived in the trench and were exhumed between 115 and 110 Ma (Fig. 8).

The structurally lowest tectonic slice exposed onshore SE Borneo is the Alino Arc (Fig. 8) that comprises mafic-intermediate plutonic and volcanic rocks with U–Pb zircon ages of 140–107 Ma (Wang et al., 2022c). Volcanic and volcaniclastic rocks are interbedded with Lower–Upper Cretaceous (Aptian–Cenomanian) radiolarian tuffaceous clay, turbidites, and calcareous mudstones with Lower Cretaceous (Aptian–Albian) foraminifera and Upper Cretaceous (Cenomanian) molluscs. These rocks are interpreted as a submarine volcanic arc that formed above a subduction zone (Sikumbang and Heryanto, 1994; Wakita et al., 1998) likely on the southern margin of the Greater Paternoster Mega-Unit (see Section 4.8). Deeper structural units are exposed on Laut Island (Figs. 1 and 7) and comprise mélange consisting of OPS lithologies embedded within a sheared shale matrix, including blocks of basalt, limestone, marl, manganese carbonate nodules, Middle Jurassic (Bajocian) to Upper Cretaceous (Cenomanian) radiolarian chert, and Lower Cretaceous (Valanginian–Aptian) radiolaria-bearing siliceous shale (Wakita et al., 1998) (Fig. 8). Collectively, these results show that an oceanic basin of at least Middle Jurassic (Bajocian) age, and an overlying volcanic arc of Early Cretaceous (Valanginian) age started to subduct around 137 Ma below the SW Borneo margin (Fig. 8), at which the Meratus Ophiolite formed in a supra-subduction zone setting. We will return to the implications of this arc in Section 4.8. The thrust slices of the Meratus Complex are intruded by dykes, and are unconformably covered by volcanic rocks with K–Ar ages of 87–72 Ma, and associated volcaniclastic sedimentary rocks of Late Cretaceous (late Turonian to Campanian/Maastrichtian) age (Yuwono et al., 1988), showing a

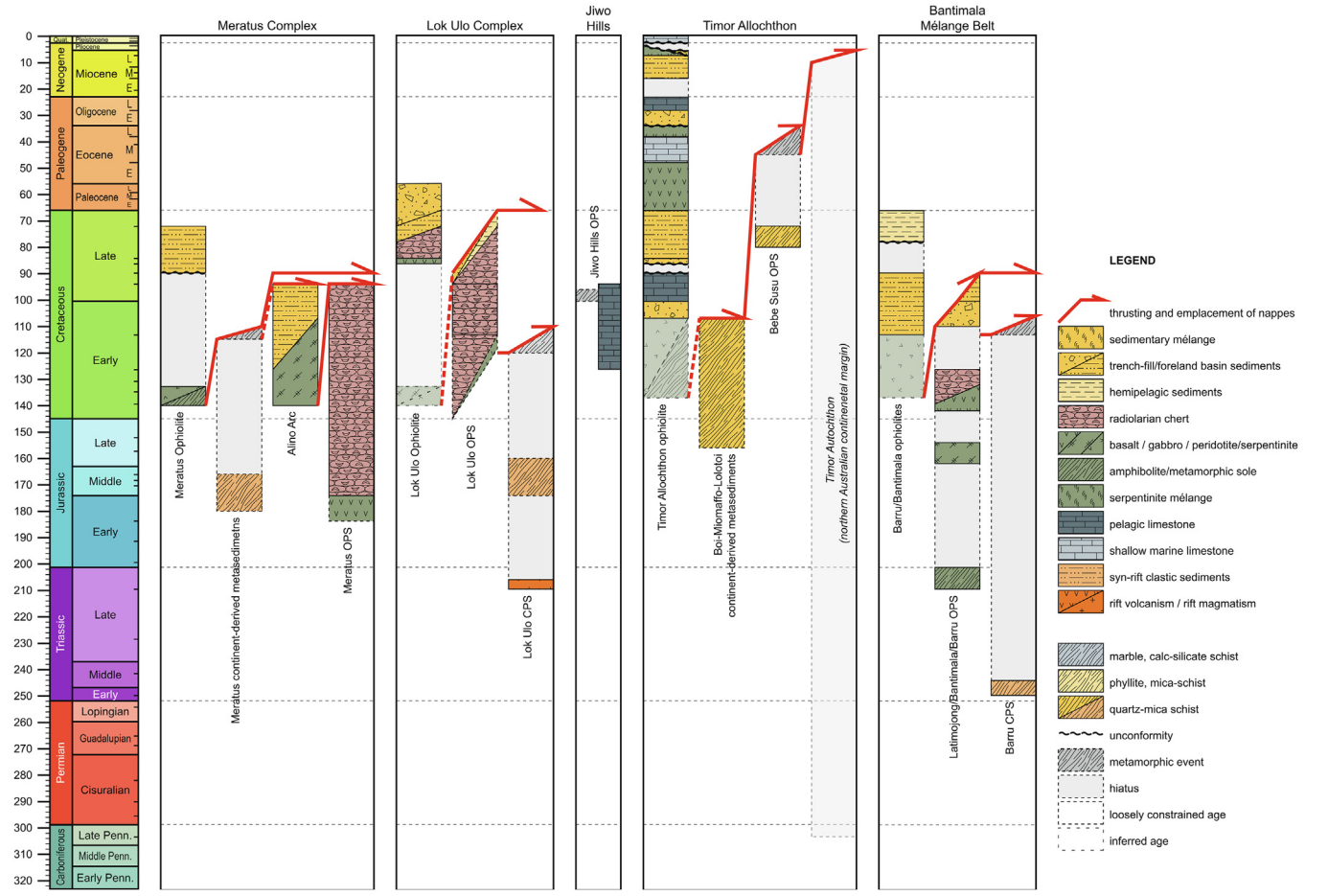

Fig. 8. Tectonostratigrahpy of the central Indonesian accretionary complexes (Meratus Complex, Lok Ulo Complex, Jiwo Hills, Timor Allochthon, Bantimala Mélange Belt). Geologic Time Scale from Gradstein et al. (2012).

minimum age for the end of accretion of ~90 Ma or shortly thereafter (Fig. 8).

The Meratus Suture is traced northwards towards the Mangkalihat Peninsula of east Borneo (Figs. 1 and 7), where radiolarian chert, basalt, serpentinite, peridotite, greenstone, and scaly clay are unconformably overlain by Eocene and younger sedimentary rocks (Hamilton, 1979; Hutchison, 1986). The Telupid and Darvel Bay ophiolites that are located adjacent to the SW Borneo Mega-Unit granitoids in eastern Sabah comprise supra-subduction zone ophiolites with a mantle sequence represented by serpentinized harzburgite (Omang, 1995; Omang et al., 1992) and a crustal sequence represented by gabbro, basalt with a K–Ar whole rock age of 137.5 ± 6 Ma (Rangin et al., 1990a), and Lower Cretaceous (Valanginian–Barremian) radiolarian chert (Jasin, 1992). Around Darvel Bay, gabbro with a U–Pb age of 84 ± 2 Ma and basalts with $^{40}Ar/^{39}Ar$ ages of 94–92 Ma are exposed (Wang et al., 2023a), which are similar ages as the volcanic and sedimentary cover of the Meratus Complex (Yuwono et al., 1988). The ophiolites in Sabah likely formed the northeastern continuation of the Meratus suture, at the junction with the Kuching Zone. Towards the SW, the Meratus Suture is also recognized in seismic sections in the eastern Java Sea (Bransden and Matthews, 1992; Granath et al., 2011), where boreholes recovered volcanic rocks and granites with disparate K–Ar ages between 140 and 74 Ma and low-grade metasedimentary rocks with K–Ar ages between 101 and 58 Ma that were correlated with the Meratus Suture (Hamilton, 1979). The thrust slices of the Meratus Suture are unconformably covered by Upper Cretaceous (Campanian–Maastrichtian) sedimentary rocks (Bransden and Matthews, 1992; Granath et al., 2011; Matthews and Bransden, 1995), consistent with a minimum age for the end of accretion farther north onshore Borneo.

Rocks correlated with the Meratus Suture are traced as far south as the Lok Ulo Complex of central Java. There it connects in a triple junction to the Klaten-Banyuwangi Suture that separates the SW Borneo and Greater Paternoster Mega-Units from the East Java Block. The **Lok Ulo Complex** in Central Java (Fig. 7) consists of a series of WSW-ENE trending thrust slices (Ketner et al., 1976; Miyazaki et al., 1998). The structurally highest thrust slice is formed by a dismembered ophiolite (Fig. 8) comprising serpentinized llherzolite, gabbro, and diabase and basaltic pillow lavas (Isyqi and Ansori, 2021). The ophiolite is undated, but a minimum age is provided by an overlying Upper Cretaceous (Coniacian–Campanian) radiolaria-bearing sequence of shale, chert, and basalt with K–Ar ages of 85 ± 4 Ma and 81 ± 4 Ma, and upper Campanian–Maastrichtian radiolaria-bearing terrigenous siliceous shale interpreted as forearc deposits (Suparka, 1988; Wakita et al., 1994a; Wakita and Metcalfe, 2005). For now, we tentatively correlate the Lok Ulo ophiolite with the Meratus Ophiolite of the SW Borneo fore-arc.

Below the Lok Ulo ophiolite are thrust slices and fault blocks that contain rhyolitic lava and tuff, chert interbedded with limestone, tuffaceous shale interbedded with volcaniclastic sandstone, basaltic pillow lava, and basaltic conglomerate (Wakita et al., 1991). These lithologies yield various radiolarian assemblages with Early–Late Cretaceous (Berriasian–Campanian) age ranges (Wakita et al., 1994a; Wakita and Metcalfe, 2005) (Fig. 8). Pebbly shales and

sandstones contain angular fragments of quartz, feldspar, mica, basic to felsic volcanic rocks, and schist, whereas mid-Cretaceous (Albian–Cenomanian) radiolarian shale contains thin rhyolitic tuff intercalations suggesting deep marine deposition near an explosive volcanic arc (Wakita et al., 1991), presumably the Alino Arc in the Meratus Complex.

The sub-ophiolitic thrust slices also contain high-pressure metamorphic rocks, including jadeite-quartz-glaucophane rock that recorded burial with *P–T* conditions of 22 ± 2 kbar and 530 ± 40 °C (Miyazaki et al., 1998), various eclogites that record peak conditions of 20.5–22.5 kbar and 365–410 °C and later epidote-blueschist-facies overprinting of 8–10 kbar and 350–400 °C (Kadarusman et al., 2007), and garnet amphibolite that records *P–T* conditions of 9–14 kbar and 560–600 °C (Setiawan et al., 2020). These HP metamorphic rocks yield K–Ar whole rock ages of 124–119 Ma (Parkinson et al., 1998) and more robustly constrained Rb–Sr ages of 119.1–117.2 Ma (Alfing et al., 2021; Hoffmann et al., 2019). These K–Ar and Rb–Sr ages are interpreted to record recrystallization and cooling during exhumation in a subduction channel setting (Hoffmann et al., 2019; Kadarusman et al., 2007; Miyazaki et al., 1998).

The lowest thrust slices (Fig. 8) comprise lithologically coherent felsic metasedimentary schists and blocks of epidote amphibolite (Alfing et al., 2021; Hoffmann et al., 2019; Miyazaki et al., 1998) that record burial to pressures of 15–16 kbar and temperatures of 380 °C (Soesilo et al., 2010). These schists yield K–Ar phengite ages of 117–110 Ma (Ketner et al., 1976; Miyazaki et al., 1998) and more robustly constrained Rb–Sr ages of 118.0 ± 0.8 Ma and 114.7 ± 1.3 Ma (Alfing et al., 2021). The epidote amphibolite yield a Rb–Sr age of 116.8 ± 0.7 Ma (Alfing et al., 2021). These ages were interpreted to record mica (re-)crystallization during peak-metamorphic conditions (Alfing et al., 2021). Detrital zircon ages in these metasedimentary schists are dominated by a large Triassic populations, and less pronounced Jurassic and Paleozoic populations and rare Proterozoic and Archean zircons (Hoffmann et al., 2019). Float samples of meta-granitoids yield U–Pb zircon ages of 208 ± 1 Ma and 207 ± 1 Ma (Wang et al., 2021a), which may explain the abundance of Triassic ages in the metasedimentary schists. These meta-granitoids also have inherited Silurian, Neo-Proterozoic and Archean zircons (Wang et al., 2021a). Triassic magmatism is known from SW Borneo (see Section 4.6), but Archean ages are only known from East Java (see below), suggesting these sediments and granitoids were derived from East Java.

The Lok Ulo Complex is unconformably overlain by an Upper Cretaceous (Maastrichtian) to Paleocene breccia formation (Fig. 8) that contains clasts of Upper Cretaceous (Campanian) radiolarian chert (Okamoto et al., 1994; Wakita et al., 1994a). Collectively, these results show that an oceanic basin with an age of at least Early Cretaceous (Berriasian) age subducted around 137 Ma below the Lok Ulo Complex. The arrival of the East Java continental margin in the trench occurred sometime between 118 and 110 Ma.

To the east, the **Jiwo Hills Complex** (Fig. 7) exposes an OPS-bearing mélange that includes limestone and radiolarian chert (Hamilton, 1979; Ketner et al., 1976; Sumarso, 1975). Metasedimentary and meta-mafic rocks include greenschist-facies phyllite, mica schist, calc-silicate schist, marble, as well as amphibolite and rare epidote-glaucophane blueschist all in close association with serpentinite (Setiawan et al., 2013c; Warmada et al., 2008), suggesting these rocks have been buried in a subduction zone. A quartz-mica schist yields K–Ar ages of 98.1 ± 2.1 Ma and 98.5 ± 1.5 Ma (Prasetyadi, 2007) that we interpret as cooling following burial. No age-indicative fossils were found in the sedimentary sequences in the mélange, but a limestone pebble from overlying Neogene conglomerate contained *Orbitulina* indicating an Early Cretaceous age (Bothe, 1929), consistent with the OPS in the Lok Ulo Complex (Fig. 8). The Jiwo Hills Complex is probably part of a poorly exposed E-W striking suture on eastern Java that is geophysically imaged as negative gravity anomaly (Clements et al., 2009; Smyth et al., 2005; Waltham et al., 2008) and continues in the Madura Strait where it was recognized in seismic sections and recovered by boreholes in the southeastern Java Sea (Bransden and Matthews, 1992; Matthews and Bransden, 1995). There, it is unconformably overlain by Campanian–Maastrichtian mudstones and interbedded siltstones and sandstones (Bransden and Matthews, 1992; Matthews and Bransden, 1995), consistent with the ages of the overlap sequence in the Lok Ulo complex. Smyth et al. (2005, 2007) inferred this suture as they found Cambrian, Proterozoic and Archean inherited zircons in Cenozoic volcanic rocks in southeastern Java, signaling underlying old continental crust, whereas Cenozoic volcanic rocks in northeast Java yield only Jurassic and Cretaceous inherited zircons, similar as observed in SW Borneo (Breitfeld et al., 2020; Davies et al., 2014; Hennig et al., 2017a). We define this suture here as the **Klaten-Banyuwangi Suture**, separating the Greater Paternoster Mega-Unit in the northeast and the SW Borneo Mega-Unit in the northwest from the **East Java Block** to the south. The East Java Block comprises 18–25 km thick continental crust (Van der Werff, 1996) between the Lok Ulo Complex in the west (Nugraha and Hall, 2012) and the island of Bali in the east (Curray et al., 1977; McCaffrey and Nabelek, 1987). Based on the presence of Archean–Cambrian inherited zircons, Smyth et al. (2005, 2007) interpreted a NW Australian cratonic provenance for the East Java Block.

The Lok Ulo and Jiwo Hills complexes and the Klaten-Nanyuwangi Suture are unconformably overlain by sedimentary rocks of the Kendeng Basin (Smyth et al., 2008). The Kendeng Basin comprises folded and thrusted Middle Eocene to Middle Miocene volcaniclastic sedimentary rocks (De Genevraye and Samuel, 1972; Smyth et al., 2008, 2007). Java hosts a major volcanic arc, in two belts. The **Southern Java volcanic arc** (Fig. 7), which is built on the East Java Block (Smyth et al., 2007; Van der Werff, 1996), started forming by the Middle Eocene (U–Pb zircon ages of 41.8 ± 1.6 and 42.7 ± 1.5 Ma; Smyth et al., 2008) and continued into the Early Miocene (Smyth et al., 2008; Soeria-Atmadja et al., 1994). The southern Java volcanic arc became overlain by Middle Miocene volcaniclastic turbidites and reefal limestones (Smyth et al., 2008). Arc volcanism migrated to the Upper Miocene and younger **Northern Java volcanic arc** (Fig. 7) that is built on the Kendeng Basin (Smyth et al., 2008; Soeria-Atmadja et al., 1994). The shift in arc location was coinciding with upper plate shortening: the Southern Java volcanic arc was thrusted northward over the Kendeng Basin in the Middle Miocene (Clements et al., 2009; Hall et al., 2007) and thrusting continues to present-day, as shown by seismicity on the Java Back-arc Thrust (Aribowo et al., 2022; Marliyani et al., 2016; Pena-Castellnou et al., 2019; Tsuji et al., 2009) (Fig. 7). Estimates of thrust displacement vary in magnitude between 10 km in east Java to as much as 100 km in west Java (Clements et al., 2009; Hall et al., 2007), which we reconstruct between the arrest of the Southern Java Arc around 16 Ma, and present-day (Table S1). South of the Southern Java volcanic arc, Middle Eocene–Upper Oligocene volcanic and volcaniclastic deposits and Miocene fine clastic and volcaniclastic rocks in the **Java forearc** rest with an angular unconformity on the pre-Cenozoic basement of the East Java Block. The East Java Block is bounded in the south by the present-day Sunda subduction zone (Bolliger and De Ruiter, 1975; Deighton et al., 2011; Nugraha and Hall, 2012).

4.8. Greater Paternoster Mega-Unit; Makassar Straits Basin; Flores Basin; Timor Allochthon

The **Paternoster Block** sensu stricto (Rose and Hartono, 1978; Samuel and Muchsin, 1975) comprises continent-derived rocks

that occupy the Paternoster Shelf in the southwestern Makassar Straits (Figs. 1 and 7) and was underthrust westwards (in modern coordinates) below the Meratus Complex (Granath et al., 2011). Seismic sections in the eastern Java Sea and southern Makassar Straits show a 30–35 km thick crystalline basement and ~8.5 km of supracrustal clastic sedimentary rocks assumed to be Precambrian to Permo-Triassic in age, but the basement was not penetrated by boreholes, and the supracrustal sedimentary rocks were only penetrated in one borehole (NSA-1F) that did not provide age control (Granath et al., 2011). This sequence is unconformably overlain by a folded sequence of mid-Cretaceous (upper Aptian–Cenomanian) fluvio-deltaic clastic sedimentary rocks that become shallower marine upward. Locally, a thin sequence of Upper Cretaceous (Campanian–Maastrichtian) sedimentary rocks unconformably covers the mid-Cretaceous sequence and thrust slices of the Meratus Complex (Bransden and Matthews, 1992; Emmet et al., 2009; Granath et al., 2011; Matthews and Bransden, 1995; Phillips et al., 1991). Granath et al. (2011) interpreted this sequence to constrain the arrival of the Paternoster Terrane to the Late Cretaceous (Turonian–Santonian). This sequence is unconformably covered by Middle Eocene sedimentary rocks (Bransden and Matthews, 1992; Emmet et al., 2009; Granath et al., 2011; Phillips et al., 1991).

Seismic sections of West Sulawesi reveal continental basement with a similar stratigraphy as below the eastern Java Sea and the southwestern Makassar Straits (Granath et al., 2011) and we include these regions in the **Greater Paternoster Mega-Unit**. Igneous rocks in boreholes in rift shoulders below the southern Makassar Straits and the northern Flores Basin yield K–Ar ages of ~100–92 Ma, and 65 Ma (Bransden and Matthews, 1992; Granath et al., 2011), which Granath et al. (2009) interpreted as a volcanic arc complex that developed on the southeastern margin of the Greater Paternoster Mega-Unit.

Between Borneo and Sulawesi lies the **Makassar Straits Basin** that formed by extension of Greater Paternoster Mega-Unit and is in part underlain by oceanic crust. Below the Mahakam delta in the central Makassar Straits (Figs. 1 and 7) is a continent-ocean-transition, and the northern Makassar Straits is floored by oceanic lithosphere (Hall et al., 2009b; Satyana, 2015). The Makassar Straits Basin underwent ~200 km NW-SE directed spreading (Hall et al., 2009b). There are no direct constraints on the age of the ocean floor in the Makassar Straits: the timing of opening of the Makassar Basin is instead interpreted to coincide with deposition of Middle–Upper Eocene (Lutetian–Priabonian) clastic sedimentary rocks in the adjacent Kutai Basin of eastern Borneo (Advokaat et al., 2018b; Moss et al., 1997; Witts et al., 2012, 2011), and Middle–Upper Eocene (upper Lutetian–Priabonian) clastic sedimentary rocks in West Sulawesi (Calvert and Hall, 2007) (Table S1). Inversion in the Kutai Basin on the western side of the Makassar Straits occurred since the Early Miocence (Armandita et al., 2015; Chambers and Daley, 1997; McClay et al., 2000), whereas the western margin of Sulawesi underwent inversion since the Pliocene (Bergman et al., 1996; Calvert and Hall, 2007; Coffield et al., 1993). In absence of quantified shortening estimates, we do not reconstruct Early Miocene and Pliocene inversion in detail.

Onshore Sulawesi, continental basement of the Greater Paternoster Mega-Unit is exposed in the Neck and western North Arm of Sulawesi (Figs. 1 and 7), in the Palu and Malino metamorphic complexes that comprise Devonian metaturbidites with abundant Proterozoic inherited zircons, and Lower Carboniferous and Upper Triassic arc metagranitoids with abundant Proterozoic, Devonian and Carboniferous inherited zircons, which were interpreted to have a northern Australian provenance (Hennig et al., 2016; van Leeuwen et al., 2016; Van Leeuwen et al., 2007) The continental crust of West Sulawesi is unconformably overlain by Upper Cretaceous (upper Campanian–lower Maastrichtian) turbidite sequences deposited in deep marine conditions (van Leeuwen, 1981; van Leeuwen and Muhardjo, 2005). These are unconformably overlain by Cenozoic sequences that include arc magmatic rocks. In the South Arm (Figs. 1 and 7), arc volcanism started in the Paleocene, as shown by a fission track zircon age of 63 ± 2 Ma and K–Ar whole rock ages of 61.4 ± 3.1 Ma and 59.2 ± 3 .0 Ma (Elburg et al., 2002; Polvé et al., 1997; van Leeuwen, 1981), whilst in central West Sulawesi arc magmatism started later, as suggested by Middle Eocene–Upper Oligocene volcaniclastic rocks and mafic intrusives with K–Ar ages of 46 ± 3.5 Ma and ~44.5 Ma (Calvert and Hall, 2007, 2003; Polvé et al., 1997; van Leeuwen et al., 2016; van Leeuwen and Muhardjo, 2005). In the South Arm, there is a markedly different stratigraphy to the west and east of the prominent Walanae Fault. To the west of the Walanae Fault, Eocene volcanic rocks are intercalated with and conformably covered by limestones, shales, and volcaniclastic sandstones, and platform carbonate deposition continued until the Middle Miocene (Van Leeuwen, 1981; Wilson and Bosence, 1996). To the east of the Walanae Fault, the stratigraphy is dominated by Oligocene volcanic rocks (Lamasi Complex) (Polvé et al., 1997; van Leeuwen et al., 2010; White et al., 2017), and here an Upper Oligocene-Lower Miocene angular unconformity exists that extends to central West Sulawesi and north Sulawesi, interpreted to reflect uplift contemporaneous with underthrusting of continental crustal nappes below the East Sulawesi Ophiolite (Section 4.10) (van Leeuwen, 1981; van Leeuwen et al., 2010; White et al., 2017). Following this uplift, extensional normal faulting in south Sulawesi culminated around 14–12 Ma and was focused in the transtensional Walanae Fault (van Leeuwen et al., 2010) (Fig. 7, Table S1). Sedimentation during this extensional period comprised Middle–Upper Miocene volcanic and volcaniclastic rocks, and mudstones, and reflect subsidence (Calvert and Hall, 2007, 2003; Nugraha and Hall, 2018; van Leeuwen et al., 2010; van Leeuwen and Muhardjo, 2005; White et al., 2017). Central West Sulawesi was intruded by Upper Miocene–Lower Pliocene granites that are crosscut by strike-slip shear zones and were exhumed in the latest Miocene to Early Pliocene (Bergman et al., 1996; Polvé et al., 2001; Polvé et al., 1997; Priadi, 1993; Priadi et al., 1994; White et al., 2017). Collectively, these data suggest that the Greater Paternoster Mega-Unit on West Sulawesi was in an upper plate position above a subduction zone and within a volcanic arc setting since at least the Paleocene.

Offshore southern Sulawesi lies the **Flores Basin** (Fig. 7). Its northern part is underlain by continental crust (Bransden and Matthews, 1992; Granath et al., 2011) of the Greater Paternoster Mega-Unit, whilst the southern part of the Flores Basin is underlain by oceanic crust (Curray et al., 1977; Granath et al., 2009). Seismic sections in the northern part show Paleocene *syn*-rift sediments in half-grabens that formed due to N-S extension and that are unconformably covered by Eocene and younger post-rift sediments (Emmet et al., 2009; Prasetyo, 1992) that constrain pre-drift extension. The oceanic crust of the Flores basin continues southward to the Nusa Tenggara Islands and widens towards the east (including Lombok, Sumbawa, and Flores, Fig. 1), where it is overlain by a volcanic arc leading to crustal thicknesses of 14–23 km (Udintsev, 1975). The oldest arc volcanic rocks on Flores yield K–Ar ages of 27.7–25.7 Ma (Hendaryono, 1998) providing a minimum age for the underlying Flores Basin oceanic crust. The arc has been intermittently active to present-day (Abbot and Chamalaun, 1981; Barberi et al., 1987; Muraoka et al., 2002; Nishimura et al., 1981). We reconstruct N-S to NW-SE opening of the Flores Basin with Paleocene pre-drift extension increasing from 50 km in the west to 140 km in the east, and Eocene oceanic spreading increasing from 100 km in the west to ~280 km in the east corresponding to the modern width of the ocean floor (Table S1). In the last 2 Ma, the prominent south-dipping Flores Thrust accommodated

about 30 km of shortening, which we include in our reconstruction (Silver et al., 1983c) (Table S1).

To the south of Flores Island, the **Savu Basin** and the island of Sumba are underlain by continental crust that was probably conjugate to the South Sulawesi margin (van der Werff et al., 1994) (Figs. 1 and 7), which we correlate to the Greater Paternoster Mega-Unit. The continental crust of the Savu Basin is only 12–14 km thick and is cut by NE-dipping normal faults (Rigg and Hall, 2012, 2011; Van der Werff, 1995; Reed, 1985). Such faults also bound the less extended, ~24 km thick crust underlying the island of **Sumba** (Chamalaun et al., 1981). Eastern Sumba exposes Upper Cretaceous intrusive and volcanic arc rocks with K–Ar whole rock ages of 85.4 Ma–76.9 Ma (Abdullah et al., 2000) and $^{40}Ar/^{39}Ar$ ages of 77.7 ± 0.3 Ma and 76.1 ± 0.3 Ma (Van Halen, 1996; Wensink, 1997), and Upper Cretaceous (Coniacian–lower Campanian) volcaniclastic deposits (Burollet and Salle, 1982; van Gorsel, 2012; Von der Borch et al., 1983). These Upper Cretaceous volcaniclastic rocks have a Sundaland sediment provenance (Zimmermann and Hall, 2019). The volcaniclastic rocks are intruded by plutons and dykes with K–Ar (whole rock and mineral) ages of 66.5 Ma–59.2 Ma (Abdullah et al., 2000; Chamalaun and Sunata, 1982) and an $^{40}Ar/^{39}Ar$ age of 64.9 ± 0.2 Ma (Van Halen, 1996; Wensink, 1997) that may be correlated with coeval magmatic activity on the northern rift shoulder of the Flores Basin (Bransden and Matthews, 1992; Granath et al., 2011) and south Sulawesi (Elburg et al., 2002; Polvé et al., 1997; van Leeuwen, 1981). Sumba records an Early-Middle Eocene phase of shortening: Upper Cretaceous-Paleocene rocks are folded (Laufer and Kraeff, 1957; Von der Borch et al., 1983) and unconformably covered by Middle–Upper Eocene nummulitic limestones (Caudri, 1934). Renewed arc volcanism is recorded from andesitic rocks with K–Ar whole rock ages of 43.5 Ma–31.3 Ma (Abdullah et al., 2000) and an $^{40}Ar/^{39}Ar$ age of 37.3 ± 0.2 Ma (Van Halen, 1996; Wensink, 1997). An Oligocene angular unconformity separates the Middle Eocene–Lower Oligocene sequence from Lower Miocene platform carbonates (Caudri, 1934). These limestones are overlain by Middle Miocene–Lower Pliocene deep marine marls that were deposited below the Carbonate Compensation Depth (Fortuin et al., 1997, 1992). The lower part of this sequence is characterized by extensional faulting and associated large scale slumping (Fortuin et al., 1992). This Middle-Late Miocene phase of extension is found across the Savu Basin: seismic sections show NE-dipping low angle normal faults that crosscut the basement (Rigg and Hall, 2012, 2011). In absence of borehole data, the stratigraphy of Sumba was extrapolated to seismic sections crossing the Suva Basin (Fortuin et al., 1997, 1992; van der Werff et al., 1994; Von der Borch et al., 1983) and using this, Rigg and Hall (2012, 2011) interpreted that Upper Cretaceous–Lower Miocene sedimentary rocks were separated by an unconformity from Middle Miocene to Quaternary sequences of deep marine sediments. They inferred that that a phase of major extension of the Savu Basin commenced in the latest Burdigalian. Based on its current width, we reconstruct 145 km of N-S directed extension in the Savu Basin between 16 and 2 Ma. During the Pleistocene (~2 Ma), the southern margin of the Savu Basin became emergent due northward thrusting along the Savu Thrust system (Harris et al., 2009; Rigg and Hall, 2011, 2012). This uplift is reflected by Middle Pleistocene coral reefs covering the Middle Miocene–Lower Pliocene marls that form terraces up to ~600 m above sea level (Bard et al., 1996; Nexer et al., 2015; Pirazzoli et al., 1993), and coincides with the shortening accommodated at the Flores Thrust (see above).

From Savu to Timor in the east, extended continental units that we correlate to Greater Paternoster are found as the highests structural unit above accreted Australian margin units (see Section 4.12) on the islands of e.g. Savu, Rote and Timor. This suggests that the Greater Paternoster Mega-Unit extends from Flores to the south and southeast, to the Sunda Trench. In the literature, the forearc rocks exposed as uppermost thrust unit of Savu, Rote, and Timor are collectively known as the Banda Terrane or Banda Forearc (Audley-Charles, 1986, 1968; Audley-Charles and Harris, 1990; Harris, 2006; Harris et al., 2009), but we prefer the term **Timor Allochthon** (Charlton et al., 1991a). The Timor Allochthon contains a record of intense Cretaceous to Neogene deformation and is in part oceanic, and in part continental in nature. We correlate the continental rocks to the Greater Paternoster Mega-Unit.

The two highest structural units of the Timor Allochthon are exposed in the *Boi*, *Miomaffo*, and *Lolotoi* massifs (Figs. 7 and 8). The upper unit represents an oceanic lithosphere and comprises from top to base tremolite serpentinite, mafic amphibolite, and greenschist-facies meta-basalt, -chert and -black shale (Brown and Earle, 1983) that likely represent a metamorphic sole. The lower unit represents continent-derived metasedimentary rocks and comprises amphibolitic and pelitic gneisses and schists that recorded burial to *P–T* conditions of 6.2–10 kbar and 600–750 °C, and later isothermal decompression to 2.3–4 kbar and 600–700 °C (Brown and Earle, 1983). The timing of peak metamorphism and subsequent exhumation is loosely constrained by a Rb–Sr whole rock age of 118 ± 38 Ma (Brown and Earle, 1983). The pelitic schists are sheared and brecciated towards the top, where they are in faulted and unconformable contact with weakly metamorphosed and strongly deformed volcanic breccia and agglomerate with coarse angular fragments of schists and igneous rocks, overlain by tuffaceous radiolarian cherts, interbedded andesitic volcanic and tuffaceous clastic rocks, and Upper Cretaceous (Cenomanian–Turonian) limestone and interbedded radiolarian chert (Earle, 1983, 1979; Haile et al., 1979; Munasri and Harsolumakso, 2020). The pelitic schists were already exhumed to a deep marine seafloor before or during deposition of volcanic rocks and sediments in the Early Cretaceous, given the presence of schist fragments in the lower part of this sequence, while deformation and metamorphism still continued (Earle, 1979). This sequence is unconformably overlain by conglomerate with fragments of greenschist, chert, and an andesite boulder with a U–Pb zircon age of 83 ± 2 Ma constraining the maximum age of deposition (Harris, 2006). These are overlain by Upper Cretaceous (Campanian–Maastrichtian) turbidites and Paleogene arc-related tuffs and lavas (Harris, 2006; Standley and Harris, 2009). The top of the sequence is formed by Middle Eocene shallow marine limestone (Audley-Charles and Carter, 1972; Carter et al., 1976). These limestones have a faunal assemblage consistent with a Sundaland affinity (Lunt, 2003) and are overlain by sandstones intercalated with basaltic to dacitic arc volcanic rocks with U–Pb zircon ages of ~35 Ma (Harris, 2006).

The Timor Allochthon is interpreted as a Cretaceous deep marine fore-arc basin, built on Lower Cretaceous oceanic crust. There are no geochemical analyses available, but the combination of ophiolite with an underlying sequence that is consistent with a metamorphic sole, and an overlying basin with arc-derived sedimentary rocks leads us to suspect that this sequence is an Early Cretaceous supra-subduction zone ophiolite (Fig. 8). Forearc extension occurred during the Late Cretaceous (Cenomanian–Turonian) when sediments subducted below the ophiolite were exhumed to the seafloor (Brown and Earle, 1983; Earle, 1983, 1979; Haile et al., 1979; Munasri and Harsolumakso, 2020). The volcaniclastic material in the forearc sequence is coeval with the arc found on Sumba and West Sulawesi, which was constructed on Greater Paternoster continental crust, and we thus infer that this forearc basin formed at the edge of Greater Paternoster, after initiation of an Early Cretaceous subduction zone. Subsequently the sequence was in a forearc position, not far from the arc, until at least late Eocene time.

Metasedimentary units in the Bebe Susu Massif (Figs. 7 and 8) on East Timor contain detrital zircons indicating a maximum depo-

sitional age of ~81 Ma (Standley and Harris, 2009). These metasedimentary units record burial to *P–T* conditions of 6–8 kbar and 530–680 °C and yield Lu–Hf garnet ages 45.4 ± 0.6 Ma that record the timing of peak-metamorphic conditions (Standley and Harris, 2009). These meta-sedimentary rocks likely represent foreland basin sediments that were buried below the leading edge of the overriding plate in the middle Eocene. Subsequent cooling, likely due to extensional exhumation, is recorded in metasedimentary units on West Timor that yield $^{40}Ar/^{39}Ar$ amphibole ages of 39–34 Ma, $^{40}Ar/^{39}Ar$ muscovite ages of 37–34 Ma and $^{40}Ar/^{39}Ar$ biotite ages of 34–33 Ma (Harris, 2006), coinciding with the extension in the Flores Basin.

Conglomerates reworking and overlying the metamorphosed Bebe Susu and Lolotoi units (Standley and Harris, 2009) are overlain by Upper Oligocene calcilutites (Audley-Charles and Carter, 1972) and Middle Miocene marls and intercalated ash layers (Carter et al., 1976). The top of this sequence is formed by Upper Miocene basaltic volcanic rocks with arc affinity (Harris, 1992) and unconformably overlying deep marine tuff and marl deposits containing uppermost Miocene (upper Messinian) microfauna (Carter et al., 1976) (Fig. 8). A basaltic dyke yields a K–Ar age of 6.1 ± 0.5 Ma (Abbot and Chamalaun, 1981), whereas basaltic pillow lavas yield K–Ar ages of 5–2 Ma (Abbot and Chamalaun, 1981) that are younger than the unconformably overlying sedimentary rocks (Carter et al., 1976), indicating that these K–Ar ages likely suffered Ar-loss (Harris, 1992). This sequence signals renewed subsidence in the Middle–Late Miocene, and recorded renewed extension of the forearc (Harris, 1992; Ishikawa et al., 2007). This overlaps with the younger extension history documented in the Savu Basin, as well as in the South Banda Basins to the northeast (see Section 4.11), and with arc magmatism documented on the islands to the north of Timor (7.8–3.0 Ma on Wetar, 3.5–3.1 Ma on Ataúro, to 2.5–1.4 Ma on Alor (Abbot and Chamalaun, 1981; Elburg et al., 2005; Ely et al., 2011; Hilton et al., 1992; Honthaas et al., 1998; Scotney et al., 2005)). The final uplift of the highly extended Paternoster units and the underlying, accreted Cretaceous and Paleocene metamorphic rocks that comprise the Timor Allochthon on the islands where it is exposed, is young: coral limestones varying in age between 0.8 Ma in Savu, 0.2 Ma in Rote, and 1.9 Ma in west Timor, are currently exposed at elevations of ~300 m, ~200 m, and ~1200 m respectively (Jouannic et al., 1988; Roosmawati and Harris, 2009; Rosidi et al., 1979) and is related to accretion and duplexing of Australian margin units below the Timor Allochthon (see Section 4.12).

4.9. Bantimala Mélange Belt

The Bantimala Mélange Belt forms the eastern boundary of the Greater Paternoster Mega-Unit (Fig. 7) and exposes an accretionary mélange with OPS and continent-derived metasedimentary rocks (Fig. 8). To the east of the Bantimala Mélange, on east Sulawesi, are Eocene ophiolites and an Oligo-Miocene accretionary complex of HP-LT metamorphic continent-derived nappes, i.e., much younger than the Bantimala Mélange. The architecture in east Sulawesi, and its field relation with the Bantimala Mélange will be discussed in the next section.

The N-S trending **Bantimala Mélange Belt** is exposed on central Sulawesi and South Sulawesi in the Tokorondo, Latimojong, Barru, Bantimala, and Biru complexes (Fig. 7). The Bantimala Mélange Belt may continue further north in the Palu Metamorphic Complex in the Neck of Sulawesi, where van Leeuwen et al. (2016) interpreted fault slices of amphibolite within gneiss as accreted remnants of oceanic crust, and extend as far north as in the Malino Metamorphic Complex in the western North Arm. The Bantimala Mélange Belt extends southward in the Timor Allochthon, where similar field relations as in the Bantimala Complex were observed (Section 4.7).

The western part of the *Tokorondo Massif* exposes N-S striking tectonic slices of serpentinite and metabasite with a K–Ar whole rock age of 114 ± 3.0 Ma, whereas the eastern part exposes graphitic marble, calcareous phyllite, graphitic quartzite, and quartz-mica schists with K–Ar mica ages of 112 ± 3.9 Ma and 108 ± 2.5 Ma (Parkinson, 1998a). The *Latimojong Complex* exposes high-pressure metamorphic rocks, including glaucophane-lawsonite blueschist, crossite-epidote metabasite and, possibly, eclogite (Parkinson et al., 1998) that record burial to pressures up to 12 kbar and temperatures of 300–415 °C (Hakim et al., 2022, 2018). Associated with the Latimojong Complex are sheared shale mélange occurences including blocks of OPS sequences consisting of feldspathic sandstone and siltstone, red chert and limestone, ultramafic rocks, altered gabbro, amphibolite, glaucophane-lawsonite schist and greenschist (Hamilton, 1979; White et al., 2017). Float of radiolarian chert to the west of the Latimojong Complex yielded an Early Cretaceous (possibly Albian) age (White et al., 2017). To the east of the Latimojong Complex, a basaltic dyke and gabbro with K–Ar whole rock ages of 158.50 ± 4.97 Ma and 137.17 ± 4.84 Ma, respectively (Polvé et al., 1997), and a sheared basaltic greenstone with a K–Ar plagioclase age of 120 ± 5 Ma (Bergman et al., 1996) are collectively interpreted to represent accreted OPS derived from oceanic crust of Late Jurassic to Early Cretaceous age.

The highest thrust slices in the Barru and Bantimala complexes are ophiolite fragments (Fig. 8) that are interpreted as upper plate-derived, likely representing an oceanic forearc adjacent to the eastern Greater Paternoster Mega-Unit. These comprise ultramafic rocks, predominantly serpentinized peridotites with podiform chromite lenses (Maulana et al., 2015, 2010; Wakita et al., 1996) that are common in SSZ ophiolites (Arai, 1997; Zhou et al., 2014). The Barru Ophiolite is underlain by amphibolites with MORB geochemistry interpreted as a metamorphic sole (Maulana et al., 2010). The age of the ophiolite or the underlying metamorphic soles, which would provide a minimum age of subduction initiation, is unknown, but the Bantimala Ophiolite is unconformably overlain by sandstone with intercalations of chert and siliceous shale with radiolarians of upper Albian–Turonian age (Wakita et al., 1996) and is structurally underlain by high-pressure metamorphic rocks recording burial at ~137 Ma (Böhnke et al., 2019; Parkinson et al., 1998; Wakita et al., 1996, 1994b) that constrain a minimum age of the ophiolite.

The *Barru Complex* is underlain by a non-metamorphic OPS sequence (Fig. 8) that includes manganese carbonate nodules with Lower Cretaceous (Valanginian–Barremian) radiolaria (Munasri, 2013), chert interbedded with hemipelagic sedimentary rocks and breccia that contains fragments of metamorphic and ultramafic rocks (Maulana et al., 2010) that is common for oceanic core complexes (e.g., Blackman et al., 2002). Structurally below these sedimentary rocks are retrogressed amphibolites with Rb–Sr ages of 109.3 ± 0.7 Ma, 107.3 ± 0.7 Ma, and 70.7 ± 2.4 Ma (Maulana et al., 2018). Maulana et al. (2018) interpreted the first two Rb–Sr ages to record cooling or recrystallization during metamorphism, whereas the latter age is interpreted to record a later tectonic event represented by a regional unconformity between Upper Cretaceous turbidites and Cenozoic cover sediments. The lowest tectonic unit of the Barru Complex (Fig. 8) comprises pelitic quartzo-feldspathic garnet-mica schists that recorded burial to P–T conditions of 9–10 kbar and 500–560 °C (Setiawan et al., 2014) and yielded a K–Ar white mica age of 106 ± 5 Ma (Wakita et al., 1994b) that we interpreted to record the timing of exhumation. These pelitic schists yield U–Pb detrital zircon ages that indicate Early Triassic (~249–244 Ma) maximum depositional ages for their sedimentary protoliths (Hoffmann et al., 2019; Jaya et al., 2017),

and these were interpreted as trench-fill sediments (Setiawan et al., 2014). However, the lack of Early Cretaceous zircon may suggest these rocks may have originated as passive margin sediments, instead of trench-fill sediments. After its formation, the Barru Complex was overlain by porphyritic dacite with an adakite geochemical signature that yields U–Pb zircon ages of 88.1–87.1 Ma (Jaya et al., 2017; Wu et al., 2022).

Sub-ophiolitic tectonic slices in the *Bantimala Complex* comprise predominantly metamorphic rocks that have an inverted metamorphic grade. Most of the metamorphic rocks are eclogite and glaucophane-rich granofels that retrogressed to amphibolite or greenschist, and pelitic schists (Böhnke et al., 2019; Miyazaki et al., 1996; Wakita et al., 1996). A garnet-amphibole granofels yielded a cluster of U–Pb zircon ages of 204.9 ± 1.3 Ma, interpreted to record crystallization of its gabbroic protolith in oceanic lithosphere, whereas overgrowths on these zircons yielded an age of 133.0 ± 2.1 Ma, interpreted to record metamorphism during burial (Böhnke et al., 2019). Serpentinite-hosted high-pressure metamorphic rocks recorded burial to estimated *P–T* conditions of 23–27 kbar and 580–680 °C for eclogites (Miyazaki et al., 1996; Setiawan et al., 2016), and 22–25 kbar and 500–540 °C for jadeitite (Setiawan et al., 2013a). These rocks yielded K–Ar phengite ages of 137–113 Ma (Parkinson et al., 1998; Wakita et al., 1996, 1994b) and Rb–Sr ages of 130.0–120.6 Ma that were interpreted to record cooling (Böhnke et al., 2019) to retrograde *P–T* conditions of ~5 kbar and 350 °C during exhumation in a subduction channel (Miyazaki et al., 1996; Setiawan et al., 2016). Pelitic schists yielded K–Ar phengite ages of 115 ± 6 Ma and 114 ± 6 Ma that were interpreted to record the timing of exhumation (Wakita et al., 1996, 1994b). Sandstones with clasts of metamorphic rocks, interpreted as trench-fill, occur as tectonic slices between the metamorphic rocks. These sandstones were assigned an Early–Middle Jurassic age, based on unpublished descriptions of ammonites (*Fuciniceras*), gastropods and brachiopods (Sukamto and Westermann, 1992), but detrital zircons constrain their maximum depositional age to 110.9 ± 9.7 Ma (Jaya et al., 2017), consistent with the age of metamorphism of the adjacent deeper buried and exhumed rocks. The tectonic slices are separated by zones of mélange with blocks of chert, sandstone, basalt, limestone, schist, and granite in a sheared shale matrix (Jaya et al., 2017; Wakita et al., 1996). Two fragments of granite in this mélange yielded U–Pb zircon ages of 115.4 ± 0.8 Ma and 112.8 ± 0.8 Ma (Jaya et al., 2017), indicating that thrusting continued sometime after ~112 Ma.

Towards the top, the sheared schists are brecciated, and unconformably overlain by conglomerate and sandstones with fragments of mica schist, and chert that contains mid-Cretaceous (upper Albian to lower Cenomanian) radiolarians (Haile, 1974; Haile et al., 1979; Wakita et al., 1994b). This shows that the schists were exhumed to a deep-marine sea floor in mid-Cretaceous time. The upper part of the radiolarian chert sequence is intercalated with rhyolitic tuff layers and grades into siliceous shale (Wakita et al., 1996), indicating nearby explosive arc volcanism. These field and stratigraphic relations are reminiscent of the Boi, Miomaffo and Lolotoi massifs of the Timor Allochthon (Earle, 1983, 1979; Haile et al., 1979; Munasri and Harsolumakso, 2020) and we interpret both to represent forearc extension that led to ophiolite formation and core complex formation on the margin of the Greater Paternoster Mega-Unit (see Section 4.8, Fig. 8), suggesting that subduction continued at least into the early Cenomanian.

To the southeast of the Bantimala Complex, metamorphic rocks are exposed in the *Biru Complex*, where they comprises epidote-garnet-ampibolite with a K–Ar phengite age of 109.5 ± 2.4 Ma (Jaya et al., 2017). The Biru Complex is unconformably overlain by Upper Cretaceous (upper Campanian–lower Maastrichtian) turbidite sequences (van Leeuwen, 1981) and is intruded by granodiorite with a U–Pb zircon age of 50.7 ± 0.8 Ma (Jaya et al., 2017), extending the subduction-accretion history into the Paleogene (see Section 4.8).

Collectively, the data from the Bantimala Mélange Belt show that that oceanic lithosphere of at least Late Triassic age (~205 Ma) started subducting around ~137–133 Ma (Fig. 8). Ophiolite and metamorphic sole formation of unknown but presumed Early Cretaceous age is interpreted to have occurred at the eastern margin of the Greater Paternoster Mega-Unit above a trench that remained active at least into the Late Cretaceous, and forearc extension that exhumed subduction complex metamorphic rocks to the deep seafloor remained intermittently or continuously active during the Late Cretaceous (late Albian–Cenomanian). The Bantimala Mélange Belt is unconformably overlain by Upper Cretaceous (upper Campanian–lower Maastrichtian) turbidite sequences that are thought to reflect the end of subduction along the Bantimala Mélange Belt (Hasan, 1991; van Leeuwen, 1981; Wakita et al., 1996).

4.10. Celebes Sea Basin; North Sulawesi Arc; Gorontalo Bay Basin; East Sulawesi Ophiolite; SE Sulawesi accretionary complex

To the east of the Bantimala Mélange lies an accretionary system with as highest structural unit the East Sulawesi Ophiolite and underlying accretionary complex that is found across much of east and southeast Sulawesi (Figs. 7 and 9), oceanic crust overlain by a magmatic arc on the central and eastern North Arm of Sulawesi, and the oceanic Celebes Sea Basin.

The **Celebes Sea** that is located to the north of Sulawesi is underlain by ~8–10 km thick oceanic crust (Murauchi et al., 1973). Sea floor basalts recovered from ODP sites 767 and 770 in the northeastern part of the Celebes Sea are of MORB composition (Spadea et al., 1996, 1991) and are overlain by Upper Eocene (Priabonian) radiolarian cherts (Scherer, 1991a). Marine magnetic anomalies are younging southward: Beiersdorf et al. (1997) and Gaina and Müller (2007) interpreted a potential anomaly C21 (45.72 Ma) along the northern margin of the Celebes Sea, while Weissel (1980) identified ENE–WSW trending anomalies C20 (42.30 Ma), C19 (41.15 Ma) and C18 (38.63 Ma) in the western part of the Celebes Sea. Gaina and Müller (2007) also interpreted anomalies C17 (36.97 Ma) and C16 (35.71 Ma) in the southern part of the Celebes Sea, but these interpretations are compromised by the overlying accretionary prism of the North Sulawesi Trench (see below) (Kopp et al., 1999; Neben et al., 1998; Schlüter et al., 2001; Silver et al., 1983b). A former spreading ridge has not been identified.

Whereas the western part of the North Arm and the Neck of Sulawesi contain continental crust of the Greater Paternoster Mega-Unit (Section 4.8, Figs. 7 and 9), the central and eastern parts of **North Sulawesi** are underlain by oceanic lithosphere of Eocene age (Cottam et al., 2011; Elburg et al., 2003; Polvé et al., 1997; van Leeuwen and Muhardjo, 2005) – i.e. similar as the age of the Celebes Sea lithosphere to the north. This ocean floor is overlain by Middle Eocene (Bartonian) to lowermost Miocene arc-related volcanic and volcaniclastic rocks, and intercalated limestones, and intruded by Upper Eocene–Oligocene granites. A Lower Miocene (Aquitanian) regional angular unconformity separates this Paleogene arc sequence from overlying shallow marine clastic rocks, limestones, and volcanic rocks (Advokaat et al., 2017; Elburg et al., 2003; Polvé et al., 1997; Rudyawan et al., 2014; van Leeuwen and Muhardjo, 2005).

To the south of the North Arm arc, the highest structural units of eastern and southeastern Sulawesi are klippen of the **East Sulawesi Ophiolite**. This ophiolite has a SSZ geochemical signature and is interpreted to have formed by spreading above a nascent subduction zone (Monnier et al., 1995). The ophiolite comprises an almost complete – albeit dismembered – Penrose ophiolite

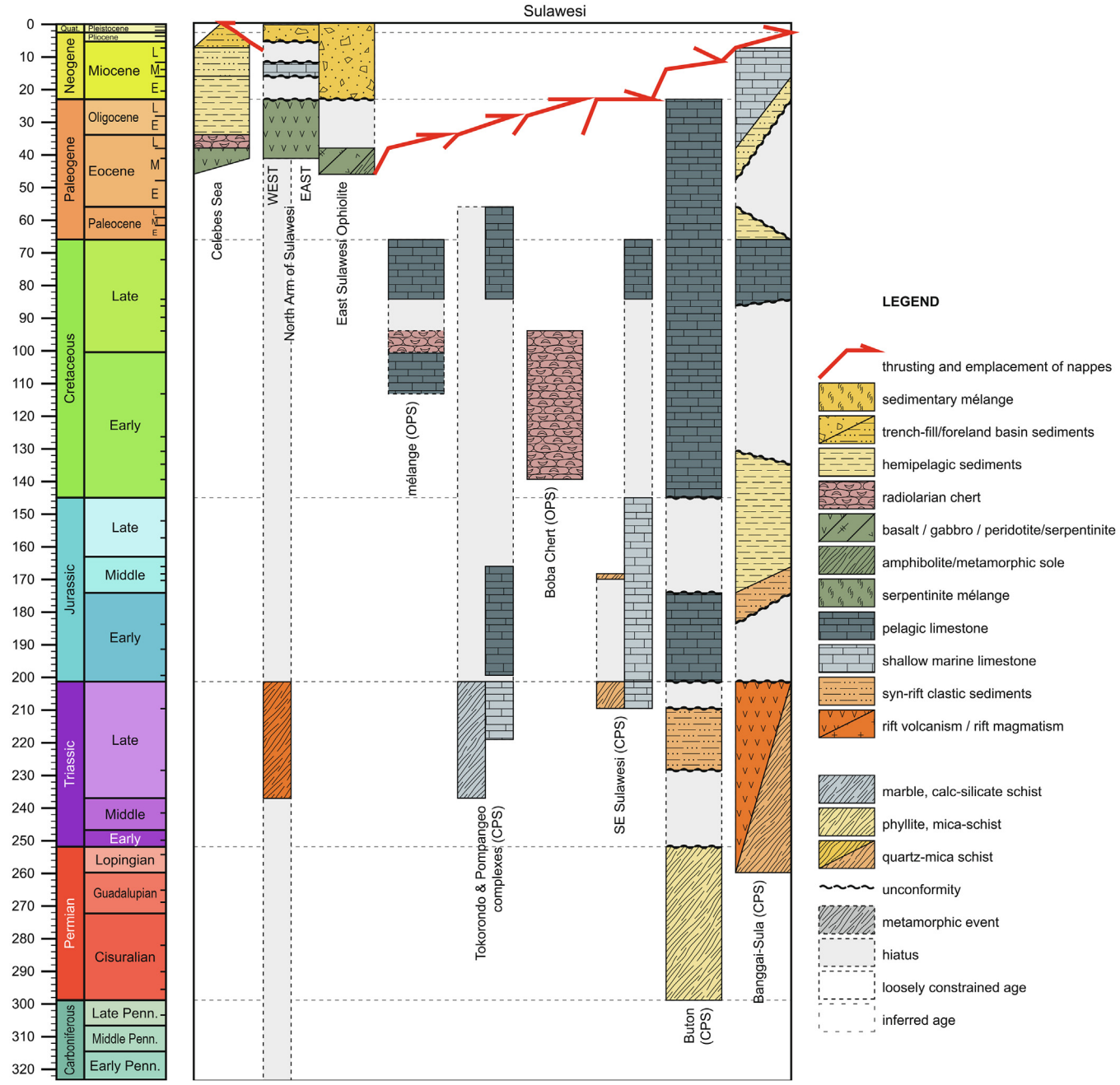

Fig. 9. Tectonostratigraphy of the Sulawesi Suture (Celebes Sea, North Arm, East Sulawesi Ophiolite, Tokorondo and Pompagneo complexes, SE Sulawesi, Buton, Banggai-Sula). Geologic Time Scale from Gradstein et al. (2012).

sequence (Kadarusman et al., 2004; Monnier et al., 1995, 1994; Parkinson, 1998b; Silver et al., 1983a), with widely dispersed K–Ar ages (between 96 and 32 Ma) for the crustal units (e.g. Mubroto et al., 1994). However, a gabbroic dyke in dunite, and a layered gabbro yielded K–Ar amphibole ages of 47.4 ± 7.1 Ma and 41.2 ± 2.3 Ma respectively that are interpreted to date the formation of the ophiolite crust, whilst a gabbroic sill yielded a K-Ar amphibole age of 37.5 ± 2.7 Ma that was interpreted to record younger hydrothermal activity (Monnier et al., 1994).

A metamorphic sole is welded to the base of the ophiolite's mantle sequence. Garnet amphibolite and hornblendite from this metamorphic sole yielded K–Ar amphibole ages of ~33 Ma, whereas epidote amphibolite yielded a K–Ar amphibole age of 26.1 ± 3.0 Ma (Parkinson, 1996). The sub-ophiolitic serpentinite-hosted mélange comprises blocks of garnet amphibolite and epidote blueschist with K–Ar amphibole ages between ~34 Ma and ~29 Ma, and greenschist facies rocks with K–Ar whole rock ages of ~28 Ma interpreted to reflect cooling during exhumation (Parkinson, 1998b, 1996).

Cooling ages of metamorphic soles are typically similar to the spreading ages of the sole, and crystallization of the sole may predate cooling and ophiolite spreading (e.g. Guilmette et al., 2018), but there are no modern Lu–Hf garnet ages to date the formation, or U–Pb and $^{40}Ar/^{39}Ar$ ages to date the inception and evolution of cooling, respectively, for the metamorphic sole of the East Sulawesi Ophiolite. The K–Ar ages from the metamorphic sole overlap with those of the underlying HP-LT metamorphic units that must postdate sole formation and we interpret these as a younger resetting,

probably associated with extensional exhumation of HP metamorphic units below the ophiolite. The ophiolite, mélange, and Oligocene HP metamorphic units are unconformably overlain by Lower Miocene (Aquitanian) to Pleistocene limestone and marine clastic sediments (Koolhoven, 1930; Nugraha et al., 2022; Nugraha and Hall, 2018; Parkinson, 1998a; van der Vlerk and Dozy, 1934). We follow Monnier et al. (1995) and reconstruct the East Sulawesi Ophiolites as formed in the forearc of a subduction zone that initiated at ~46 Ma.

Arc magmatism on the North Arm is thus coeval with HP-LT metamorphism in the accretionary complex underlying the East Sulawesi Ophiolite, and the unconformable cover of the arc has a similar age as the sedimentary rocks that unconformable cover the ophiolites and underlying accretionary complex. Monnier et al. (1995) interpreted the East Sulawesi Ophiolite as the conjugate lithosphere to the Celebes Sea crust, having formed to the south of the Celebes spreading ridge. They proposed that this spreading ridge formed above a north-dipping subduction zone since ~46 Ma and that the North Arm arc formed the associated intra-oceanic arc, an interpretation that we incorporate in our reconstruction.

Structurally below the East Sulawesi Ophiolite are accreted oceanic and continental rocks derived from the lithosphere that subducted below the East Sulawesi ophiolite. Thrust slices of accreted units related to the Sulawesi Suture (Hall and Wilson, 2000) occupy east-central Sulawesi and the SE Arm. The metamorphic grade of the accreted units ranges from non-metamorphic in the east (Cornée et al., 1999; Cornée et al., 1995) to HP-LT metamorphic in the west (Ferdian et al., 2012; Helmers et al., 1990, 1989; Kadarusman et al., 2011, 2002; Kadarusman and Parkinson, 2000; Parkinson, 1998a, 1996). This lateral trend reflects NW-SE extensional exhumation, and this extension was also responsible for the opening of the Bone Gulf Basin in the Early Miocene (Camplin and Hall, 2013; Grainge and Davies, 1985; Sudarmono, 2000; Yulihanto, 2004) (Fig. 7). The modern contact between the Cretaceous Bantimala Mélange Belt and the East Sulawesi Ophiolite and underlying nappes is thus likely extensional, but the nature of the pre-Miocene contact is not directly constrained in the field. Assuming the N-S extension in the Celebes Sea is representative for the entire oceanic system including the East Sulawesi Ophiolite, this contact was likely a subduction transform edge propagator (STEP) fault (see Govers and Wortel, 2005). We will further evaluate this in the description of the reconstruction (see Section 6.3).

In the area between the Lawanopo Fault and the Matano Fault, the accretionary complex below the East Sulawesi Ophiolite contains thrust slices of Lower Cretaceous (Albian) and Upper Cretaceous (Campanian–Maastrichtian) pelagic limestones (Cornée et al., 1995), and mélange with blocks of Upper Cretaceous (Cenomanian) radiolarian chert providing a minimum age for the subducted ocean floor (Silver et al., 1983a). Below the metamorphic and non-metamorphic OPS-derived accretionary complexes are continent-derived complexes. These are metamorphosed in the west (**Pompangeo** and eastern **Tokorondo** complexes (Figs. 7 and 9) (Parkinson, 1998a)), and non-metamorphosed in the east (Cornée et al., 1999, 1995). The Pompangeo and eastern Tokorondo complexes expose continent-derived Upper Triassic metasedimentary schists (Ferdian et al., 2012; Parkinson, 1998a, 1996). Locally, fault-bounded blocks expose unmetamorphosed Upper Triassic (upper Norian–Rhaetian) reefal limestones (Cornée et al., 1994; Martini et al., 1997), Lower–Middle Jurassic (Sinemurian–Bathonian) pelagic limestones, Lower Cretaceous (Valanginian–lower Cenomanian) cherts and calcilutites (e.g. Mubroto et al., 1994), and Upper Cretaceous (Campanian–Maastrichtian) to Paleocene pelagic limestones (Cornée et al., 1999, 1995). This sequence recorded an earliest Jurassic (Hettangian) phase of rapid deepening towards sub-CCD paleo-depths (Cornée et al., 1999).

A minimum age for burial of these continental units follows from K–Ar phengite ages of schists from the eastern Pompangeo Complex of 28.1 ± 1.8 Ma and 27.6 ± 1.6 Ma (Parkinson, 1998b, 1996). To the west, eclogites felsic and mafic granulites were found alongside garnet lherzolites, both as xenoliths in Pliocene granites, as well as exposed in fault-bounded lenses of the Palu-Koro Fault, a major Pliocene strike-slip fault (Fig. 7; see below) (Helmers et al., 1990; Kadarusman et al., 2011, 2002; Kadarusman and Parkinson, 2000; van Leeuwen et al., 2016). These high-pressure metamorphic rocks were subducted below West Sulawesi, and buried to pressures of at least 20 kbar, also in Oligocene time, as revealed by a Sm–Nd garnet core age of 27.6 ± 1.13 Ma. A Sm–Nd garnet rim age of 20.0 ± 0.26 Ma recorded retrograde conditions during exhumation (Kadarusman et al., 2011, 2002; Kadarusman and Parkinson, 2000). Final exhumation from upper crustal levels was facilitated by entrainment in Pliocene granites and by Pliocene transtension in the Palu-Koro Fault (Hennig et al., 2017b; Kadarusman and Parkinson, 2000). Collectively, these oldest accreted continental rocks were interpreted to represent the leading edge of a continental fragment of Australian affinity, that underwent major Jurassic extension and that was subducted and accreted below the East Sulawesi Ophiolite at or shortly before ~28 Ma (Cornée et al., 1999, 1995, 1994; Kadarusman et al., 2011, 2002; Kadarusman and Parkinson, 2000).

In the southern part of the SE Arm, nappes below the ophiolite expose a similar, but more shallow marine continent-derived stratigraphy (Fig. 9), with Upper Triassic (Rhaetian) deltaic sandstones and limestones of Australian affinity (Decker et al., 2017; Ferdian et al., 2012; Surono and Bachri, 2002), Jurassic shallow marine limestone, and Upper Cretaceous (Campanian–Maastrichtian) pelagic limestones (Cornée et al., 1995, 1994). In the Mendoke and Rumbia Mountains in the southwestern part of the SE Arm, near the shore of Bone Bay, blueschist-facies metasedimentary rocks are exposed (Helmers et al., 1989) from which detrital zircons with a maximum depositional age of ~170 Ma were obtained (Ferdian et al., 2012). Glaucophane schists, chlorite schists and mica schist from the Rumbia Mountains yielded $^{40}Ar/^{39}Ar$ age spectra with plateaus clustering at 23–17 Ma, interpreted as (re-) crystallization ages (Mawaleda et al., 2018), showing ongoing exhumation in the Early Miocene.

Accretion below the SE Sulawesi continent-derived blueschists continued in the Middle Miocene, although the direction of underthrusting changes from north to west as recorded by the east-verging fold-thrust belt on the island of **Buton**, immediately southeast of the SE arm of Sulawesi (Figs. 7 and 9). Thrust slices repeat CPS of sheared greenschist-facies Permian–Lower Triassic micaceous sandstone, siltstone and phyllitic slates, unconformably overlying Upper Triassic (Norian) turbidites and Lower Jurassic pelagic limestones and shales, unconformably overlying Upper Jurassic (Kimmeridgian) interbedded calcilutites and red chert, manganese-bearing siliceous mudstones, and limestones, unconformably overlying Lower Cretaceous (Berriasian) to Oligocene micritic limestones with internal Lower–Upper Cretaceous unconformities (Hetzel, 1936; Smith and Silver, 1991; Davidson, 1991). The CPS of Buton is interpreted to have formed a contiguous Australian promontory conceptually known as the Sula Spur (Klompe, 1954) that was once contiguous with Banggai Sula and the Bird's Head of New Guinea (Figs. 1 and 2). The Buton (meta)sedimentary CPS units are overthrust by peridotites, minor gabbro, and metabasites and metacherts of greenschist and amphibolite facies interpreted as an ophiolitic metamorphic sole (Smith and Silver, 1991) that likely form the southernmost exposures of the East Sulawesi Ophiolite but remain undated. The fold-thrust belt and the ophiolite are unconformably covered by an Upper Miocene–Pleistocene sequence of shallow marine, coarse-grained clastic sedimentary rocks with fragments of ophiolitic debris and reworked Creta-

ceous–Oligocene coccoliths (Smith and Silver, 1991). A rapid deepening is reflected by Lower Pliocene pelagic sedimentary rocks with occasional tephra intercalations (Fortuin et al., 1990; Smith and Silver, 1991) and subsequent uplift is constrained by Quaternary reefal limestones uplifted in terraces up to 650 m above sea level, which record uplift since 3.8 ± 0.6 Ma (Pedoja et al., 2018). Balanced cross sections through the Buton fold-thrust belt suggest 28 km of shortening during the Middle Miocene (Serravallian), i.e. after the accretion of the SE Sulawesi blueschists, and 2.5–3 km shortening during the Late Miocene (Chamberlain et al., 1990 in Davidson, 1991) (Table S1). Paleomagnetic studies on the Upper Miocene–Lower Pliocene sequence revealed that local block rotations are related to thin-skinned thrusting and northward sinistral strike-slip faulting (Ali et al., 1996) during accretion of the Tukang-Besi Block at the end of the Early Pliocene (Davidson, 1991; Fortuin et al., 1990; Milsom and Ali, 1999) (see Section 4.11).

The orogenic architecture from the Celebes Sea to southeast Sulawesi is thus summarized as an upper oceanic plate that underwent late Eocene spreading, below which oceanic and continental crust subducted, accreted, and exhumed in the Late Oligocene and Early Miocene (Fig. 9). In the Middle Miocene, extension also started to affect North and Central Sulawesi, culminating in the formation of metamorphic core complexes. For instance, the ~25 km wide N-S extensional Malino Metamorphic Complex formed in the western part of the North Arm between 17.1 Ma and 13.8 Ma (Advokaat, 2016; Advokaat et al., 2017). In the Late Miocene a tectonic reorganization affected North Sulawesi and a south-dipping back-thrust developed to the north of the North Arm that evolved into the North Sulawesi subduction zone accommodating southward subduction of Celebes Sea oceanic lithosphere (Bellier et al., 2006; Silver et al., 1983b; Socquet et al., 2006; Walpersdorf et al., 1998a). The age of inception of the North Sulawesi trench is inferred from sedimentary rocks in the in the northern Celebes Sea. There, at ODP sites 767 and 770 (Figs. 7 and 9), the oceanic crust is overlain by Upper Eocene (Priabonian) radiolarian chert (Scherer, 1991a), Oligocene to lower Miocene brown claystone and Middle–Upper Miocene nannofossil-rich claystone (Smith, 1991). From the Middle Miocene onwards, quartz-bearing turbiditic deposits become increasingly abundant, until a sudden cessation at ~8.5 Ma (Smith, 1991). This sudden cessation of turbidite deposition was interpreted as diversion of the turbidites into the North Sulawesi Trench, marking the onset of subduction in the southern Celebes Sea (Nichols and Hall, 1999; Smith et al., 1990). This is further confirmed by seismic reflection profiles showing an increasing thickness of the Upper Miocene–Holocene sequence towards the North Sulawesi Trench (Schlüter et al., 2001).

In the west, the North Sulawesi Trench connects to the transform Palu-Koro Fault Zone (Advokaat et al., 2017; Katili, 1970; Tjia, 1973). In the Neck of Sulawesi, the Palu Metamorphic Complex is bounded by faults subparallel to the Palu-Koro Fault. The Palu Metamorphic Complex was intruded by Upper Miocene–Lower Pliocene granites and recorded rapid cooling since 5.3 Ma, inferred to result from motion along these bouding faults (Hennig et al., 2017b, 2016; van Leeuwen et al., 2016). Displacement estimates for the Palu-Koro Faut are widely varying. Silver et al. (1983b) assumed a total sinistral displacement of 250 km since the Pliocene, based on correlation of outcrop patterns of the East Sulawesi Ophiolite, implying a long term displacement rate of ~50 mm/yr. Surmont et al. (1994) assumed a 20–25° counterclockwise rotation of the North Arm around a pole in the eastern end of the North Arm, based on paleomagnetic data from Eocene-Pliocene sedimentary rocks and igneous rocks, resulting in a 150 km total sinistral displacement along the Palu-Koro Fault since the Pliocene, implying a long term displacement rate of ~30 mm/yr. Sinistral displacement rates derived from GPS data vary between 30 and 50 mm/yr (Socquet et al., 2006; Vigny et al., 2002; Walpersdorf et al., 1998b, 1998a), but estimates derived from geomorphic indicators converge towards 30–35 mm/yr (Bellier et al., 2001), which led us to adopt the smaller total sinistral displacement estimate of 150 km since the Pliocene. This displacement decreases southward along the Palu-Koro Fault (Watkinson and Hall, 2011), and is kinematically accommodated by N-S extension in and along the southern margin of the **Gorontalo Bay Basin** (Fig. 7). where the N-S extensional Tokorondo and Pompangeo complexes that exhumed accretionary complex rocks from below the East Sulawesi Ophilite (Kartaadiputra et al., 1982; Pezzati et al., 2014) appear on SRTM imagery as two corrugated landforms (Spencer, 2011, 2010). North to NNW plunging stretching lineations in these metamorphic complexes are parallel to these corrugations (Parkinson, 1998a). Pliocene clastic sedimentary rocks and reefal limestones that directly overlie the schist in the valley between the Pompangeo Complex and the Tokorondo Complex constrain the minimum age of exhumation (Nugraha et al., 2022; Parkinson, 1998a). Spencer (2011, 2010) interpreted the Tokorondo Complex and Pompangeo Complex as footwalls of N–NNW dipping extensional detachment faults that experienced respectively 25 km and 67 km extension during exhumation in the Pliocene-Quaternary (Table S1). Lower Pliocene reefal limestones are also exposed on the North Arm as terraces uplifted to ~400 m (Advokaat et al., 2017), whilst drowned pinnacle reefs assumed to be of similar age are found in Gorontalo Bay at ~1.8 km waterdepth (Pholbud et al., 2012), indicating rapid uplift and subsidence respectively since the Pliocene (Hennig et al., 2014), consistent with a link to the Palu-Koro fault, in the upper plate of the North Sulawesi subduction zone. The amount of subduction in the North Sulawesi trench, extension in the Gorontalo Bay basin, and strike-slip displacement on the Palu-Koro transform fault appear more or less balanced.

The SE Arm and Bone Bay were also affected by Early Miocene to recent extension. Multibeam data and seismic sections through Bone Bay show several sub-basins and highs separated by N-S striking normal faults and NW-SE striking sinistral strike-slip faults (Camplin and Hall, 2014), including the offshore continuation of the Kolaka Fault. Undeformed dacite intrusions in strands of the Kolaka Fault yielded U–Pb zircon ages of 4.4 ± 0.2 Ma, indicating that strike-slip terminated before empacement of these dacites (White et al., 2014) (Table S1). The sinistral Lawanopo Fault has been active in the Neogene–Middle Pleistocene (Bellier et al., 2006; Hamilton, 1979; Natawidjaja and Daryono, 2015) and may still be active (Yeats, 2012). Its estimated displacement is about 100–120 km (Silver et al., 1983a) (Table S1). The sinistral Matano Fault has been active since the Neogene and has displaced peridotitic units at least 15–25 km (Bellier et al., 2006; Hamilton, 1979) (Table S1, Fig. 7).

4.11. Sula Spur fragments; Banda basins

To the east of Sulawesi are continental fragments that underwent Neogene extension, in places associated with (ultra-)high temperature metamorphism and mantle exhumation and became separated from each other by Neogene oceanic basins. These continental fragments are thought to have derived from an Australian continental promontory conceptually known as the Sula Spur that was once contiguous with the Bird's Head peninsula of western New Guinea (Fig. 1) (Klompe, 1954). The continental rocks of SE Sulawesi and the Buton fold-thrust belt that underthrusted and accreted to the East Sulawesi Ophiolite in the Late Oligocene and Middle Miocene respectively (see Section 4.10), are the westernmost units thought to have derived from the Sula Spur. In Pliocene to recent time, the Tukang-Besi and Banggai-Sula blocks (two continental fragments of the Sula Spur, see Fig. 10) accreted below the

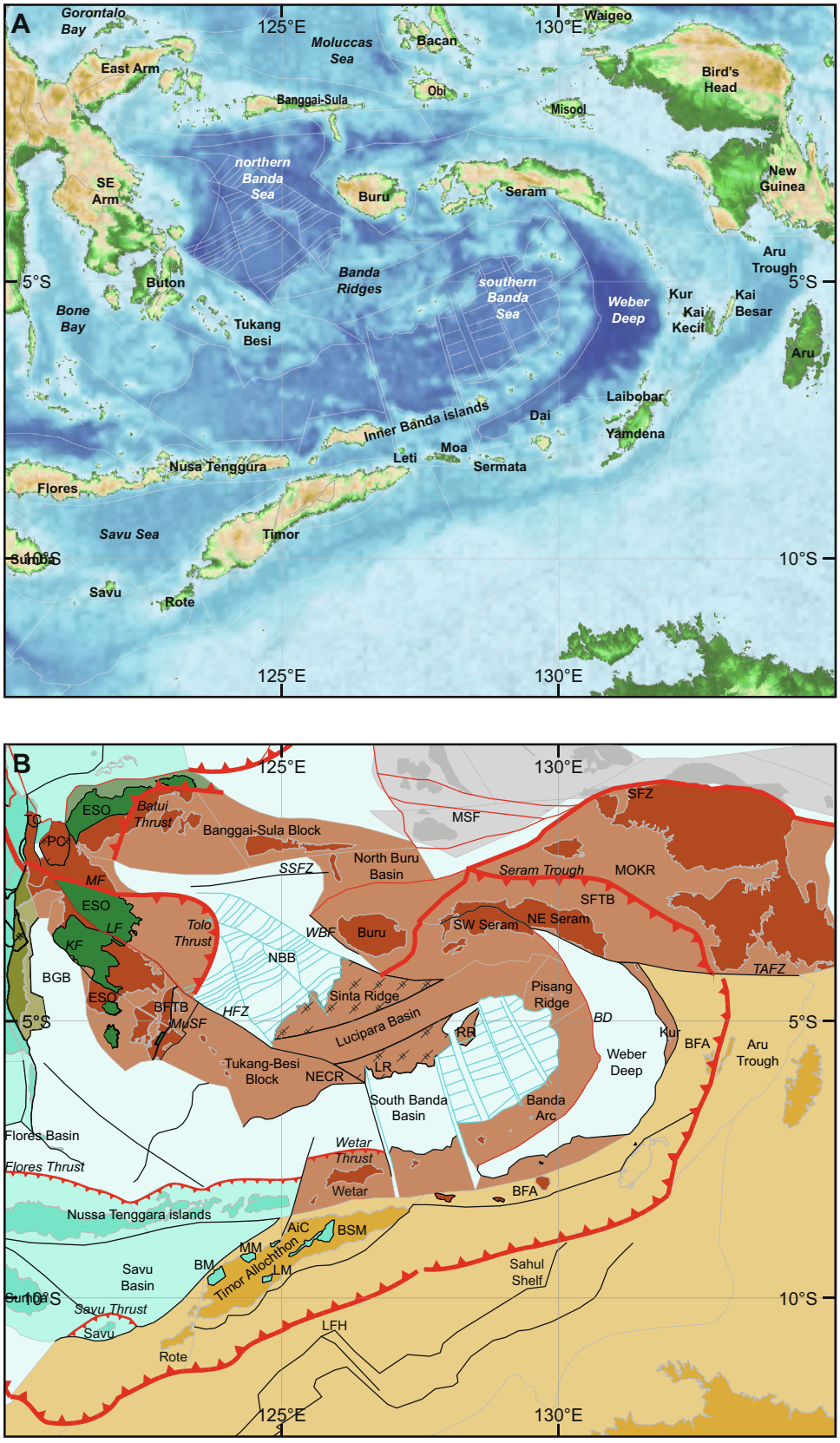

Fig. 10. A. Geographic map of the Banda Arc region. See Fig. 1 for location. B. Tectonic map of the Banda Arc region. See Fig. 2 for location. Abbreviations: AiC, Aileu Complex; BD, Banda Detachment; BFA, Banda forearc; BFTB, Buton Fold-Thrust Belt; BM, Boi Massif; BSM, Bebe Susu Massif; ESO, East Sulawesi Ophiolite; HFZ, Hamilton Fracture Zone; KF, Kolaka Fault; LF, Lawanopo Fault; LFH, Laminaria/Flamingo High; LM, Lolotoi Massif; MF, Matano Fault; LR, Lucipara Ridge; MM, Miomaffo Massif; MOKR, Misool-Onin-Kumawa Ridge; MSF, Molucca-Sorong Fault; MuSF, Muna Straits Fault; NECR, Nieuwerkerk-Emperor of China Ridge; NBB, North Banda Basin; PC, Pompangoe Complex; SFZ, Sorong Fault Zone; SSFZ, South Sulu Fault Zone; RR, Rama Ridge; TAFZ, Tarera-Arduna Fault Zone; TC, Tokorondo Complex;

East Sulawesi Ophiolite, while the intervening North Banda Basin is thrusted below SE Sulawesi.

To the east of Buton lies the **Tukang-Besi Block**. The Tukang Besi Block is separated from the Buton fold-thrust belt by the sinistral, NNE-SSW striking Muna Straits Fault that forms a graben system filled by Pliocene-Pleistocene sediments (Davidson, 1991; Milsom and Ali, 1999). The Tukang-Besi Block is covered by Upper Neogene and Quaternary limestone (Silver et al., 1985; Smith and Silver, 1991) occuring in the east as coral reefs uplifted to ~270 m above sea level, and in the west as atolls signaling recent subsidence (Verstappen, 2010), that may either be related with accretion to Buton at the end of the Early Pliocene (see Section 4.10) (Davidson, 1991; Fortuin et al., 1990), or by NE-SW directed extensional faulting as interpreted from Bougier gravity anomalies (Milsom and Ali, 1999).

To the northeast of the Tukang-Besi Block, the Hamilton Fracture Zone forms the boundary with the oceanic **North Banda Basin**. The North Banda Basin is bounded to the west by the west-dipping Tolo Trough from SE Sulawesi, to the north by the South Sula Fault Zone from the Banggai-Sula Block, to the east by West Buru Fracture Zone from Sanana and Buru, and to the south by a passive margin from the Sinta Ridge (Fig. 10). The North Banda Basin contains NE-SW striking marine magnetic anomalies 5Ar (13.03 Ma) to 3Br (7.21 Ma) (Hinschberger et al., 2000) that indicate at least 300 km of NW-SE directed oceanic spreading. Hinschberger et al. (2000) calibrated these ages with dredge samples that yield K–Ar whole rock ages of 7.33 ± 0.18 Ma near the former spreading center and 9.5–11.5 Ma near the southwestern margin of the basin (Honthaas et al., 1998; Silver et al., 1985). Thrusting at the Tolo Trough was interpreted as recent gravitational collapse of the east Sulawesi margin, whereby rocks were carried more than 100 km into the North Banda Basin (Réhault et al., 1994; Rudyawan and Hall, 2012; Silver et al., 1983a).

The North Banda Basin is separated to the north by the South Sula Fault Zone from the **Banggai-Sula Block**. The Banggai-Sula Block also comprises attenuated continental crust of the Sula Spur that underthrusted northwestward below the East Sulawesi Ophiolite and the underlying accretionary prism of Cretaceous OPS, at the Pliocene Batui Thrust (Cornée et al., 1995; Davies, 1990; Silver et al., 1983a) (Figs. 9, 10 and 11). It is overthrust from the north by mélanges that formed in the Sangihe and Halmahera trenches that together accommodated subduction of the Molucca Sea Plate during the westward advance of the Philippine Sea Plate (see Section 4.15) (Ferdian et al., 2010; Silver et al., 1983a; Watkinson et al., 2011b) (Figs. 7 and 10).

To the east and southeast of the North Banda Basin lie more Sula Spur continental fragments and intervening basins. Continental crust of the Sula Spur on the Banggai-Sula Block is attenuated with Moho depths varying between 19 km and 25 (Sardjono, 2007). This block has a Paleozoic crystalline basement that was intruded by Upper Permian–Lower Triassic granites and overlain by Upper Permian-Triassic volcanic rocks and interfingering shallow marine limestones (Ferdian et al., 2012; Garrard et al., 1988; Pigram and Supandjono, 1985). The Upper Permian–Triassic rocks are unconformably overlain by Lower Jurassic (Toarcian) to Lower Cretaceous (Hauterivian) transgressive clastic sedimentary rocks,

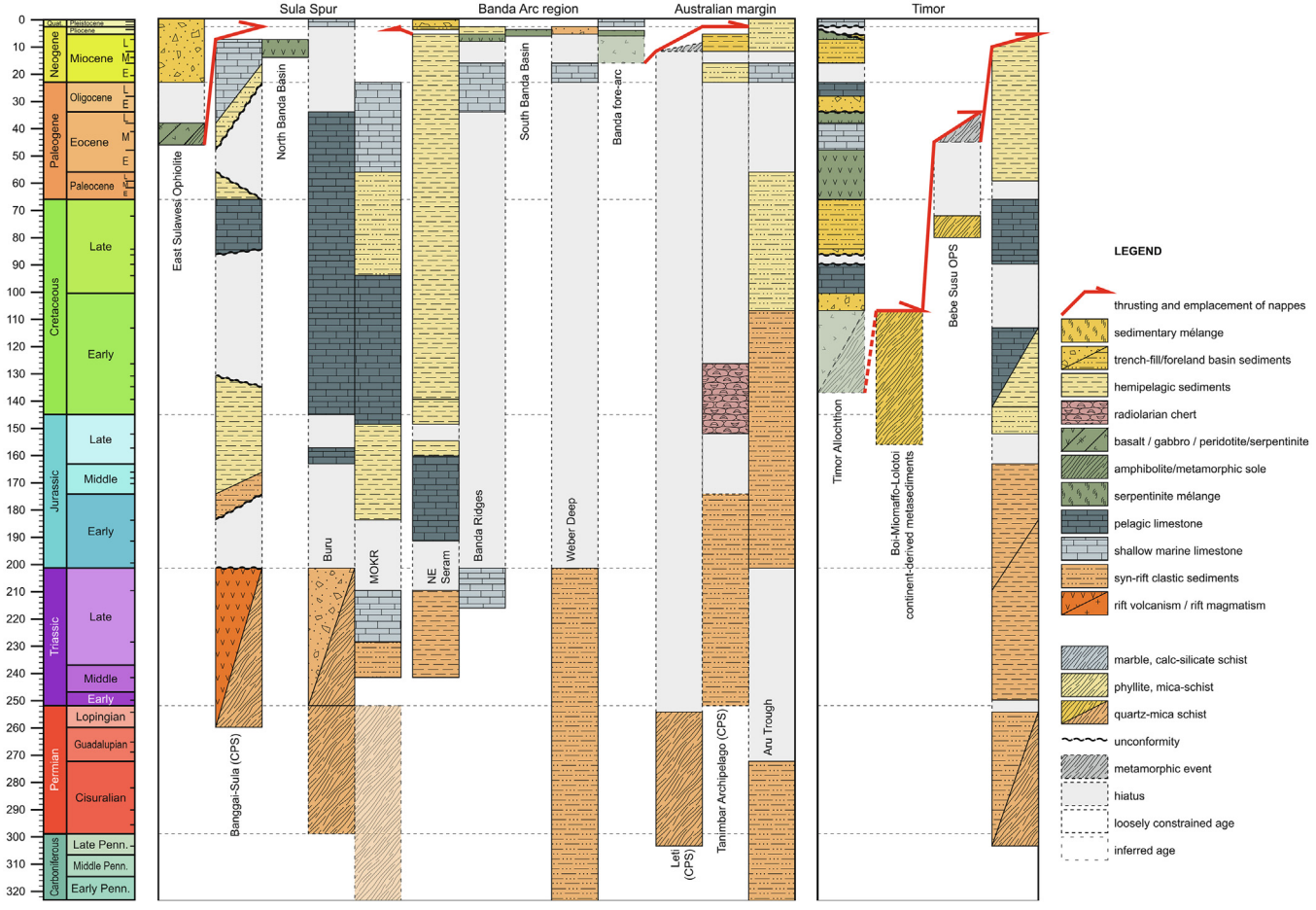

Fig. 11. Tectonostratigraphy of the Sula Spur and northern Australian margin. Geologic Time Scale from Gradstein et al. (2012).

Upper Cretaceous (Santonian–Maastrichtian) limestones, and Lower–Upper Paleocene marls (Garrard et al., 1988; Pigram and Supandjono, 1985; Sukamto and Westermann, 1992). Eocene to Middle Miocene and Quaternary limestones rest unconformaby on the older sequences (Garrard et al., 1988) (Figs. 9 and 11). On the island of **Buru**, to the southeast of the Banggai-Sula Block (Figs. 1, 10 and 11), low to medium grade metamorphic Paleozoic sedimentary rocks (Linthout et al., 1989) yield K–Ar and $^{40}Ar/^{39}Ar$ muscovite and biotite ages of 6.2–4.1 Ma, and Rb–Sr whole rock-biotite ages of 3.8–3.0 Ma (Linthout et al., 1991; Pownall et al., 2018) that likely recorded Neogene exhumation accommodated along north-dipping low-angle detachment faults (Linthout et al., 1989; Pownall et al., 2013; Watkinson and Hall, 2017). These Paleozoic sedimentary rocks are overlain by Triassic sedimentary rocks, of which the lower part is metamorphosed, whilst the upper part contains reworked metamorphic fragments derived from the Paleozoic metasedimentary rocks showing that at least part of the metamorphism and exhumation already occurred in the Triassic (Harahap and Poedjoprajitno, 2006). A hiatus separates these Triassic sedimentary rocks from basalt, tuff, and interfingering Upper Jurassic (middle Oxfordian) calcilutites and cherts, marking Jurassic extension and subsidence, and Upper Cretaceous–Eocene calcilutites and chert (Harahap and Poedjoprajitno, 2006; Sukamto and Westermann, 1992).

Also the **Misool-Onin-Kumawa Ridge,** located to the northeasteast of Buru (Figs. 10 and 11), exposes Mesozoic stratigraphy of the Sula Spur in a SE-plunging anticlinorum (Froidevaux, 1974). This ridge is contiguous with the Bird's Head peninsula of New Guinea (see Section 4.12) and exposes low-grade metamorphic rocks derived from Paleozoic sediments that are unconformably overlain by Middle–Upper Triassic (Ladinian–Carnian) turbidites. Unconformably overlying Upper Triassic (Norian) platform carbonates signal a change from deep marine to shallow marine conditions interpreted as uplift during rift initiation (Fraser et al., 1993; Pigram et al., 1982), whilst a return to deep marine conditions signals further extension and subsidence, as suggesting by the unconformably overlying sequence of Lower Jurassic (Toarcian) to Upper Jurassic (Tithonian) shales, Upper Jurassic (Tithonian) to Upper Cretaceous (Cenomanian) calcilutites, and Upper Cretaceous–Paleocene calcareous clastic sedimentary rocks. Paleocene–Oligocene shallow marine limestone forms the top of the sequence (Fraser et al., 1993; Pigram et al., 1982). These records on Banggai-Sula, Buru and the Misool-Onin-Kumawa Ridge show that the Sula Spur underwent both Triassic and Jurassic rifting, followed by passive margin sedimentation until the Neogene.

In Neogene time, the Sula Spur units described above, as well as continental fragments scattered in the Banda Sea, were deformed by thrusting, extension, and strike-slip faulting. To the east of the North Banda Basin, between Buru and the Bangai-Sula Block, is the North Buru Basin (Bowin et al., 1980), that is bounded to the east by the Buru Fracture (Letouzey et al., 1983; Malaihollo and Hall, 1996), and to the north by the Sorong Fault Zone (Patria and Hall, 2017; Rudyawan and Hall, 2012). The North Buru Basin likely formed due to sinistral transtension during opening of the North Banda Basin in the Middle–Late Miocene (Patria and Hall, 2017). During this time, the Banggai-Sula Block moved ~260 km westward relative to Buru along the ENE-WSW striking sinistral Sorong Fault Zone, whilst in Late Pliocene–Pleistocene time, Buru coupled with the Banggai-Sula Block and moved ~150 km westward relative to the Misool-Onin-Kumawa Ridge (Fig. 10) along the Sorong Fault and the Buru Fracture (Riadini et al., 2009; Saputra et al., 2014).

The island of Seram is located to the east of Buru island (Fig. 10). Seram exposes metamorphic rocks in the southwest, and a sedimentary cover sequence in the northeast. **Southwest Seram** is crosscut by multiple WNW-ESE striking, NNE-dipping low-angle extensional detachments, WNW-ESE striking sinistral strike-slip shear zones, and E-W striking high-angle normal faults (Pownall et al., 2013). The footwall of the extensional detachments comprises lherzolitic peridotites interpreted to represent subcontinental lithospheric mantle, leucogranite, granulite, and cordierite granite, whilst the hanging wall comprises hornblende granodiorite, migmatite, and upper greenschist to amphibolite facies gneiss and pelitic schist (Pownall et al., 2013). Zircon geochronology on pelitic schists from central Seram revealed they were derived from Upper Triassic sediments with a maximum depositional age of ~216 Ma (Pownall et al., 2017b). In places, these metasedimentary rocks reached upper-amphibolite facies conditions between 215 and 173 Ma, interpreted as related to Late Triassic–Middle Jurassic extension that is also recorded in the stratigraphy of the Sula Spur (see above). A second episode of kyanite-grade metamorphism between 24 and 20 Ma is interpreted as related to burial, before reaching UHT metamorphic conditions between 16.5 and 15.5 Ma that occurred simultaneously with lherzolite exhumation (Pownall, 2015; Pownall et al., 2019, 2017b, 2014). Extensive $^{40}Ar/^{39}Ar$ geochronology on various mineral phases in central and west Seram has revealed that detachment faults operated between 16.5 and 10.2 Ma, 5.8–5.6 Ma, and sinistral strike-slip shear zones were active between 4.5 and 3.5 Ma (Linthout et al., 1996; Pownall et al., 2017a). On **northeast Seram,** the non-metamorphosed sedimentary sequence of the Sula Spur is exposed (Fig. 11), which comprises at the base Middle–Upper Triassic (Ladinian–Norian) deep marine mudstone, siltstone, sandstone and conglomerate deposited in a horst and graben setting that interfinger with moderate to deep water limestone (Kemp and Mogg, 1992). These grade into shallow Lower–Upper Jurassic (Pliensbachian to lower Oxfordian) shallow marine limestones. A hiatus separates this sequence from overlying Upper Jurassic (middle Oxfordian) to Lower Cretaceous (Berriasian) shales. Within this sequence, there is a upper Kimmeridgian to mid-Tithonian hiatus (Kemp and Mogg, 1992). Lower Cretaceous (Valanginian) to Upper Miocene deep marine sedimentary rocks unconformably overlay this sequence (Kemp and Mogg, 1992; O'Sullivan et al., 1985). On the north coast of Seram, this entire sequence is deformed in the **Seram Fold-Thrust Belt,** unconformably overlain by a clay mélange with clasts of the underlying sequence. The age of this mélange is only constrained by unconformably overlying Upper Pliocene–Lower Pleistocene mudstone and siltstone, and Pleistocene fluvial sediments (De Smet et al., 1989; Kemp and Mogg, 1992; Zillman and Paten, 1975), indicating that thrusting mostly occurred in the Early Pliocene (Adlan et al., 2016). The Seram Fold-Thrust Belt continues offshore in the Seram Trough, where it overlies the Misool-Onin-Komawa Ridge in the foreland, and displays a 90° curvature changing from a E-W orientation in west Seram to an N-S orientation east of Seram (Adlan et al., 2016; Pairault et al., 2003a, 2003b; Patria and Hall, 2017). Seismic sections show that the decollement depth varies between the base of the Pliocene sequence, and the base of the Oligocene sequence, to the base of the Triassic (Pairault et al., 2003a, 2003b; Patria and Hall, 2017). Lineaments on the seafloor suggest ~80 km of WNW-ESE directed sinistral strike-slip motion (Patria and Hall, 2017; Yang et al., 2021), alongside SW-NE directed thrusting (Adlan et al., 2016). Balanced cross section restoration in the eastern Seram fold-thrust belt yields a minimum-shortening estimate of 36 km during the Early Pliocene, of which 24 km occurred between 3.8 and 3.5 Ma (Adlan et al., 2016).

To the west and south of Buru and Seram are the **Banda Ridges**, a series of highs in the Banda Sea (Fig. 10). The ~75 km wide and ~500 km long ENE-WSW striking Lucipara Basin separates the Sinta Ridge in the north from the Pisang, Lucipara, Rama, and Nieuwerkerk-Emperor of China (NEC) ridges to the south (Fig. 10). This basin opened in NW-SE direction, parallel to the

strike of the Hamilton Fault Zone. Based on the age constraints from Seram, we interpret this extension to have occurred between ~16 Ma and ~10 Ma (Table S1). Dredged samples revealed that the southern Banda Ridges expose phyllite with a K–Ar whole rock age of 22.5 ± 0.5 Ma, and amphibolite with a K–Ar whole rock age of 10.8 ± 0.1 Ma (Silver et al., 1985). The cover formations include Oligocene–Lower Miocene reefal limestones and Lower Pliocene pelagic mud (Cornée et al., 2002, 1998), basalts and andesites with K–Ar whole rock ages of 8.1–3.5 Ma, and volcaniclastic rocks with similar age ranges (Honthaas et al., 1998; Silver et al., 1985). Dregded samples from the Sinta Ridge recovered undated clastic sedimentary rocks and Upper Triassic (upper Norian–Rhaetian) shallow marine limestones consistent with those on the Sula Spur-associated islands to the north (Villeneuve et al., 1994). Based on these dredges, Cornée et al. (2002) suggested that the Banda Ridges formed one contiguous continental fragment that experienced Early–Middle Miocene high-temperature metamorphism during extension. The latest Miocene to Pliocene arc-volcanic and volcaniclastic rocks (Honthaas et al., 1998) suggest the Banda Ridges were in an upper plate position after Miocene extension and high-temperature metamorphism (Fig. 11).

To the south of the Banda Ridges is the oceanic **South Banda Basin**. Hinschberger et al. (2001) identified ENE-WSW striking marine magnetic anomalies C3Ar (6.73 Ma) to C2Ar (3.56 Ma) that constrain the timing of 215 km of oceanic spreading (Table S1). In the south and east of the South Banda Basin is the arcuate, E-W to NW-SE trending volcanic arc of the Inner Banda Islands. Volcanic activity commenced in the Pliocene, and continues to present day (Abbot and Chamalaun, 1981; Elburg et al., 2005; Ely et al., 2011; Hilton et al., 1992; Honthaas et al., 1998; Scotney et al., 2005). To the south of the Inner Banda Islands, the Outer Banda Islands of Leti and Moa expose ophiolites as highest structural unit above Australia-derived rocks on the islands of Leti and Moa (see Section 4.12) that likely represent the fore-arc of the South Banda Basin lithosphere (Ishikawa et al., 2007; Kaneko et al., 2007).

The easternmost rocks that were likely derived from the Sula Spur are exposed on the **Watubela Archipelago** and the *Kur island* in the eastern Banda Sea (Fig. 10). The Watubela islands to north and south of Kur expose serpentinite, amphibolite, radiolarite, schist, and gneiss (summarized in Bemmelen, 1949). The island of Kur itself exposes a basement of magmatic rocks (norite, hornblendite, diorite, and granodiorite) and metamorphic rocks (gneiss, mica schist, meta-greywacke, and mylonites). A sillimanite-bearing paragneiss with K–Ar feldspar and biotite ages of respectively 17.6 ± 0.4 Ma and 16.9 ± 0.4 Ma records cooling after peak temperatures of 600–700 °C. The K–Ar ages from the magmatic rocks have been (partially) reset by this event (Honthaas et al., 1997). The metamorphic rocks of Kur are unconformably overlain by fluvio-deltaic sediments that were folded during eastward thrusting over the Australian margin in the Late Pliocene (Fig. 11), and are capped by Lower Pleistocene reef terraces that signal young uplift (Honthaas et al., 1997).

Directly west of Kur is the **Weber Deep** (Fig. 10). The Weber Deep is a highly extended forearc basin that experienced ~120 km ESE-directed extension accommodated along the west-dipping Banda Detachment (Hinschberger et al., 2005; Pownall et al., 2016). Along the eastern flank of the Weber Deep, Honthaas et al. (1997) dredged samples from the footwall of the Banda Detachment in sections west and SSW of Kur. In the northern section, the lowermost dredges comprise Carboniferous–Triassic clastic sedimentary rocks (Fig. 11), followed by serpentinized peridotites, and sheared diorite and dacite with K–Ar ages of 18.08 ± 0.47 Ma and 17.53 ± 0.44 Ma. The uppermost dredges comprise Lower Pliocene breccias and conglomerates with clasts of peridotite, diorite and dacite (Honthaas et al., 1997). In the southern section, the lowermost dredges comprise strongly altered mica schist and mylonitic gneisses, followed by conglomerate and Lower Miocene limestone. The uppermost dredged sediments contain clasts of metamorphic rocks and Miocene limestone (Honthaas et al., 1997) (Fig. 11). Together with the exposures on Kur Island this suggests that the fore-arc of the South Banda Basin consists of thinned continental crust and exhumed mantle rocks that experienced extension associated with a high-temperature metamorphic event between ~18–17 Ma (Honthaas et al., 1997), similar to the record on SW Seram (Pownall, 2015; Pownall et al., 2019, 2017b, 2017a, 2014). This event was followed by post-Early Pliocene subsidence during ~150 km WNW-ESE directed hyper-extension accommodated along the Banda Detachment (Hinschberger et al., 2005; Honthaas et al., 1997; Pownall et al., 2016) that we reconstruct between 3.6 and 0 Ma (Table S1), i.e. after cessation of spreading in the South Banda Basin, and synchronous with the onset of activity of the Banda volcanic arc.

The constraints above reveal that many of the Sula Spur fragments are currently part of the upper plate of subduction zones that consumed Australian lithosphere and must thus have accreted from the downgoing to the overriding plate. The units that accreted below the East Sulawesi Ophiolite were clearly thrusted and metamorphosed under high-pressure and low-temperature conditions (Helmers et al., 1990, 1989; Kadarusman et al., 2011, 2002; Kadarusman and Parkinson, 2000), but fragments that are located to the east, such as Buru, Kur, and Seram, escaped significant thrusting, crustal thickening and burial, but experienced high temperature metamorphism (Honthaas et al., 1997; Linthout et al., 1989; Pownall, 2015; Pownall et al., 2019, 2017b, 2014). Spakman and Hall (2010) and Pownall et al. (2013) explained this as the result of lateral delamination and subsequent roll-back of mantle lithosphere (see also van de Lagemaat et al., 2021; van Hinsbergen and Schouten, 2021) from beneath the eastern Sula Spur after the western Sula Spur arrived in the trench below the East Sulawesi Ophiolite. However, in subsequent papers Pownall (2015) and Pownall et al. (2019, 2017b, 2017a, 2014) explained this as result of extensional exhumation in an upper plate setting.

4.12. Accreted Australian plate units of Timor and the Outer Banda Islands

The islands surrounding the Banda Sea, from of Savu and Rote in the west, through Timor to the Outer Banda Islands to the east and northeast (Fig. 10), expose accreted OPS and Australia-derived CPS units that accreted below the extended Greater Paternoster Mega-Unit (locally known as the Timor Allochthon, see Section 4.8) and ophiolites of South Banda Basin oceanic lithosphere (Fig. 11).

The island of Savu, on the southern margin of the Savu Basin, is underlain by thinned continental lithosphere of the Greater Paternoster Mega-Unit (see Section 4.8), whilst folded and thrusted sedimentary rocks are exposed that were accreted from the subducted distal Australian continental margin in Pliocene–Pleistocene time. These have been backthrusted northward over the extended crust of the Savu Basin during the Pleistocene (~2 Ma) (Harris et al., 2009; Rigg and Hall, 2011, 2012). We reconstruct a maximum of 130 km of shortening associated with the overthrusting of these accreted units of Savu onto the Timor Allochthon on Savu between 2 and 0 Ma (Table S1), which corresponds to the convergence of Australia relative to SE Asia during this interval.

The island of Timor contains an extensive and well-described record of Australian passive margin-derived rocks that accreted below extended Greater Paternoster Mega-Unit units, and Cretaceous ophiolites that formed at the Greater Paternoster margin (see Section 4.8, Fig. 11). The accreted rocks are duplexed between two decollements that formed along stratigraphic levels in the Australian margin stratigraphy: a basal one in Upper Carboniferous (Gzhelian) shales, and an upper one in Upper Triassic (Carnian) to

Middle Jurassic (Callovian) shales that were interpreted to represent rifting and break-up of the Australian margin (see Section 2) (Harris, 2011; Harris et al., 1998; Sawyer et al., 1993; Tate et al., 2017, 2015). The shales in which that upper decollement formed are not exposed as coherent thrust slices on the island, but are mixed with OPS fragments that formed the Bobonaro mélange, which are exposed in mud volcanoes (Harris et al., 1998). The duplexed Upper Jurassic to upper Miocene Kolbano sequence that represents the Australian passive margin sequence (see Section 2), as well as overlying klippen of the Greater Paternoster Mega-Unit, gravitationally slid southward and opened *syn*-orogenic basins floored by the Bobonaro mélange (Harris, 2011). The timing of thrusting is constrained by the youngest deposits in the Kolbano sequence, which are of late Miocene (~9.8 Ma) age in East Timor (Keep and Haig, 2010) to Early Pliocene (Zanclean) age in West Timor (Sawyer et al., 1993), as well as in the deep-marine *syn*-orogenic sediments that were deposited in basins floored by the Bobonaro mélange that started in the uppermost Miocene, with ages ranging between 5.6 Ma and 3.0 Ma on East Timor (Aben et al., 2014; Audley-Charles, 1968; Duffy et al., 2017; Haig and McCartain, 2007; Tate et al., 2014), and continuing into the Pleistocene on West Timor (De Smet et al., 1990; Tate et al., 2017). Younger *syn*-orogenic deposits include Quaternary coral terraces uplifted to elevations of ~1200 m that unconformably overlie older units (Roosmawati and Harris, 2009; Rosidi et al., 1979). Tate et al. (2017, 2015) restored three NNW-SSE striking cross sections on East and West Timor that gave minimum shortening estimates of 362 km, 326 km, and 300 km from east to west since initial underthrusting of the Australian continental margin below the allochthonous Greater Paternoster Mega-Unit on Timor. Such long-distance continental subduction of the Australian continental margin is consistent with the finding of geochemical signatures of continental contamination in Pliocene volcanoes north of Timor that overlie oceanic crust of the Flores Basin (Elburg et al., 2004) and recent seismological observations of the subducted Australian slab (Zhang and Miller, 2021).

The arrival of the Australian continental margin in the trench below the Timor Allochthon fore-arc has been estimated between 9.8 and 9.5 Ma by Keep and Haig (2010) and 7.8 Ma by Tate et al. (2015). Keep and Haig (2010) based their 9.8–9.5 Ma age on biostratigraphy of undeformed deposits that unconformably overlie folded pre-collisional strata, whereas Tate et al. (2015) based their 7.8 Ma estimate on a $^{40}Ar/^{39}Ar$ hornblende age of 7.7 ± 0.2 Ma, and $^{40}Ar/^{39}Ar$ muscovite ages of 7.13 ± 0.25 Ma and 5.36 ± 0.05 Ma for the structurally highest, paleogeographically most distal accreted unit: the high-grade metamorphic Ailieu Complex (Berry and McDougall, 1986; Tate et al., 2014). The *syn*-orogenic basins floored by the Bobonaro Mélange, the highly uplifted Quaternary reefs, and (U–Th)/He apatite ages that range between 4.5 ± 0.9 Ma in northern East Timor to 2.0 ± 0.6 Ma in southern East Timor (Tate et al., 2014) (Table S1), and GPS measurements (Nugroho et al., 2009) reveal that shortening, duplexing and uplift continued throughout the Neogene until the present-day.

The island of **Leti**, 40 km to the east of Timor (Figs. 10 and 11) exposes a non-metamorphic folded sequence of Permian clastic sedimentary rocks similar to those in the Gondwana Sequence exposed on Timor. This sequence is buried below three north-dipping fault-bounded sequences. The structurally lowest tectonic unit has top-to-SE thrust contacts and exposes greenschist to blueschist facies psammitic schists, quartzites, phyllites, and marbles with crinoid stems that reveal a Permian age (Kadarusman et al., 2010; Kaneko et al., 2007; Molengraaff, 1915). The middle tectonic unit comprises mafic and pelitic schists likely derived from OPS. In the bottom and the top of the unit these are greenschist and blueschist facies metamorphic, whereas epidote–amphibolite and amphibolite facies are recognized in the middle part of the unit (Kadarusman et al., 2010). The epidote–amphibolite and amphibolite facies rocks record *P–T* conditions of 6.3–7.6 kbar and 460–520 °C, and 9.7–10.3 kbar and 580–630 °C respectively, suggesting burial in a subduction zone. Greenschist overprinting occurred during decompression from 5.5–7 kbar to < 4 kbar at temperatures of 300–400 °C (Kadarusman et al., 2010). Within the blueschist facies unit, kyanite schist with retrograde sillimanite yields a K–Ar muscovite age of 11.0 ± 0.3 Ma that was interpreted to record the timing of exhumation (Kadarusman et al., 2010; Ota and Kaneko, 2010). Kinematic indicators in the lower part of this tectonic unit reveal a top-to-the-south sense of motion interpreted as a thrust, whereas kinematic indicators at the top of this tectonic unit suggest a top-to-the-north sense of motion, interpreted to have reflect the extensional detachment that accommodated exhumation (Kaneko et al., 2007). The highest structural unit comprises serpentinized peridotites that are interpreted as fore-arc ophiolites representing South Banda Basin ocean floor (Ishikawa et al., 2007; Kaneko et al., 2007). The island is fringed by Pleistocene reefal limestone that unconformably overlie all units and seal the fault contacts (Kadarusman et al., 2010; Kaneko et al., 2007 and references therein; Molengraaff, 1915).

To the east of Leti, the islands of **Moa** and **Sermata** expose a similar sequence of metamorphic rocks, with similar contacts between the tectonic units. On Moa, the highest tectonic unit consists of serpentinized peridotite, minor gabbro, and basalt. This unit is absent on Sermata. Conversely, the only basement unit exposed on the island of **Dai**, to the east of Moa (Fig. 10), comprises gabbro and clinopyroxenite (Ishikawa et al., 2007; Kaneko et al., 2007). All basement units on these islands are fringed by terraces of horizontal Quaternary reef limestones that are uplifted 20–250 m above sea level (Kaneko et al., 2007).

To the east of Dai, the contact between the Australian passive margin and overlying oceanic and stretched Sula Spur lithosphere of the South Banda Basin curves around to a SW-NE strike on the **Tanimbar archipelago**, where it is exposed as a NE-SW striking, SE-verging foreland propagating fold-thrust belt (Figs. 10 and 11). The southeastern island of Yamdena (Fig. 10) exposes a Triassic to Pleistocene sequence of sedimentary rocks that were deposited on the Australian continental shelf. Triassic–Lower Jurassic sandstones occur as blocks with a matrix of Lower-Middle Jurassic shales that occur in the ejecta of mud volcanoes (Charlton et al., 1991b), comparable to the Bobonaro mélange on Timor (Harris et al., 1998). The oldest in-situ strata are sandstones and intercalated Upper Jurassic (Tithonian) to Lower Cretaceous (Barremian) radiolarian cherts (Charlton et al., 1991b; Jasin and Haile, 1996) reflecting a deep marine depositional environment. These are unconformably overlain by intensely deformed Lower Miocene sandstones and Upper Miocene deep marine marls (Charlton et al., 1991b; De Smet et al., 1990). This deformed sequence is unconformably overlain by Lower Pleistocene marls and Quaternary reefs now uplifted to 200 m above sea level (Charlton et al., 1991b; De Smet et al., 1990). The northwestern islands expose predominantly mélange with a matrix of Lower Jurassic ammonite-bearing clays and blocks of Oligocene-Miocene shallow marine limestones and Miocene coal (Charlton et al., 1991b). Metamorphic rocks are only exposed on the island of **Laibobar** (Fig. 10) and comprise metapelite, metabasite and a small amount of marble and metachert that underwent amphibolite-facies metamorphic conditions, similar as on Leti and Sermata (see above). The metamorphic rocks are in normal fault contact with Quaternary limestone (Kaneko et al., 2007). Folding and thrusting of the Australian passive margin on the Tanimbar Islands, marking its arrival below the Banda forearc, started in Yamdena in the Pliocene, and in the northwestern islands in the Middle Pleistocene (1.8 Ma; Table S1) (Charlton et al., 1991b).

The contact between the Australian passive margin and the Banda forearc curves further around to a SSW-NNE strike farther

north on the Kai Islands adjacent to the Aru Trough (Fig. 10). The Aru Trough lies in the foreland of the Banda subduction zone and is a NNW-SSE striking graben bounded by normal faults. The E-W striking sinistral Tarera-Aiduna Fault Zone forms the northern boundary of the Aru Trough (Adhitama et al., 2017). Seismic sections reveal a 3–4 km thick stratigraphy (Adhitama et al., 2017) and samples dredged from the western footwall of the Aru Through (Cornée et al., 1997) comprise a pre-Carboniferous metamorphic basement, Upper Carboniferous–Lower Permian clastic sedimentary rocks, Jurassic–Lower Cretaceous sedimentary rocks that record gradual drowning of the Australian shelf, Lower Cretaceous (upper Albian) to mid-Eocene pelagic sedimentary rocks, and Middle Miocene platform carbonates that are capped by an unconformity. Above this unconformity are Upper Miocene and Pliocene–Holocene deep marine clastic sediments (Adhitama et al., 2017; Cornée et al., 1997) (Fig. 11). Balancing of seismic sections suggested that the central part of the Aru Trough has experienced ~20 km of E-W extension since the Late Miocene (Adhitama et al., 2017) (Table S1).

The island of Kai Besar is located on the Kai Arch that hosts an accretionary prism below the Banda forearc (Fig. 10). Kai Besar exposes a stratigraphy of Middle–Upper Eocene lower bathyal-upper abyssal calcilutites and marls and Upper Oligocene and Lower-Middle Miocene middle bathyal sedimentary rocks deposited in a passive margin environment (Charlton et al., 1991d; Van Marle and De Smet, 1990). Seismic sections suggest this sequence is underlain by a similar pre-Cenozoic stratigraphy as found in the Aru Trough (Adhitama et al., 2017). Seismic sections show that the stratigraphy to the west of the Kai Arch is deformed in to an east-verging fold-thrust belt that experienced up to ~30 km E-W shortening since the Pliocene (Adhitama et al., 2017; Teas et al., 2009) (Table S1). This fold-thrust belt is capped by Quaternary reef terraces at the island of Kai Kecil (Charlton et al., 1991d; Van Marle and De Smet, 1990) (Fig. 10). Interpretations of seismic sections and gravity profiles suggest the Kai Kecil is in part underlain by mélange, whereas the area further west towards the island of Kur is also underlain by fore-arc lithosphere (Honthaas et al., 1997; Milsom and Kaye, 1996) correlated to the Sula Spur (see Section 4.11).

4.13. Sulu Arc; Sulu Sea; Cagayan Arc; Palawan Accretionary Complex; Rajang-Crocker Accretionary Complex

The Sulu Arc is located to the north of the Middle Eocene Celebes Sea (Section 4.10, Fig. 12). This arc is interpreted as an Early Miocene, north-facing island arc built on continental basement (Antonio, 1972; Murauchi et al., 1973; Rangin and Silver, 1991; Tamayo et al., 2000; Yumul et al., 2004) that we correlate to the SW Borneo Mega-Unit (see Section 4.6, Fig. 13). This basement shares a passive margin with the Celebes Sea ocean basin to the south, but is separated from the oceanic Sulu Sea basin by the Sulu Trench (Fig. 12). Seismic sections show that this trench is associated with a well-developed accretionary complex (Schlüter et al., 1996). Constraints on the geological history of the Sulu Arc mostly come from correlation with the Dent and Semporna peninsulas of eastern Sabah in the west, and the Zamboanga peninsula of Mindanao in the east (Hutchison, 1992) (Fig. 12). The Dent and Semporna peninsulas expose andesitic to dacitic volcanic rocks with K–Ar ages of 18.8–2.8 Ma (Bergman et al., 2000; Rangin et al., 1990a). Sedimentary rocks intercalated with these volcanic rocks comprise tuffaceous chert, greywackes, and massive limestones of Late Oligocene to early Middle Miocene age (Rangin et al., 1990a). This sequence is folded and unconformably covered by conglomerates and shales (Haile and Wong, 1965). The northern side of the Zamboanga peninsula exposes a partly metamorphosed accretionary complex below ophiolite (Antonio, 1972; Tamayo et al., 2000; Yumul et al., 2004). The ophiolites comprise ultramafic rocks (harzburgite, dunite, and chromitite) and dismembered oceanic crustal units (gabbros, dyke swarms, basalt flows, and pillow lavas with capping red and green chert) (Yumul et al., 2004). Sub-ophiolitic clay- and serpentinite-hosted mélanges contain blocks of harzburgite, dunite, pyroxenite, slate, phyllite, low-grade schists, metasedimentary rocks, metavolcanic rocks, marble, and andesites with unknown ages (Yumul et al., 2004). The ophiolite and sub-ophiolitic OPS mélange are thrusted over a NW-dipping nappe of amphibolites that were interpreted to be derived from island arc cumulate gabbros. The underlying nappes comprise quartzo-feldspathic mica-kyanite schists were interpreted to be clastic metasediments derived from a granitic source, and meta-graywackes and epidote amphibolites that were also interpreted to be derived from island arc magmatic rocks (Tamayo et al., 2000). The meta-graywackes and epidote amphibolites record *P–T* conditions of 5–9 kbar and 550–700 °C, and the amphibolites in the highest nappe yield K–Ar amphibole ages of 24.6–21.2 Ma (Tamayo et al., 2000). The ophiolite, OPS mélange, and underlying metamorphic basement are unconformably overlain by Lower–Middle Miocene quartz-rich sandstones and interbedded limestones, siltstones and claystones, and intercalated Middle Miocene to Pleistocene andesitic volcanic rocks (Yumul et al., 2004).

The Sulu Arc itself is interpreted to be built on continental basement, overlain by (?Pliocene–Quaternary) volcanic edifices (Murauchi et al., 1973). Tawitawi island in the south exposes (ultra-)mafic plutonic rocks overlain by marine clastic rocks. The other islands expose Mesozoic metamorphic rocks, basaltic volcanic cones with fringing reefs and terrestrial and marine sediments (Geological Map of the Philippines, 1963). Hamilton (1979) reported probable mélange on the southeastern margin of the Sulu Arc. Dredge samples from the northeastern slope of the Sulu Arc include granodiorites, basaltic to dacitic volcanic rocks associated with volcanic breccias and tuffs, and limestones of Early Miocene age (Schlüter et al., 2001).

The **Sulu Sea** is an oceanic basin located to north of the Sulu Trench (Murauchi et al., 1973; Schlüter et al., 1996). The Sulu Sea is bounded to the north by the Cagayan Arc that is also constructed on continental basement (Kudrass et al., 1990; Smith, 1991; Spadea et al., 1996, 1991). Basaltic basement rocks recovered from ODP site 768 in the eastern part of the Sulu Sea (Figs. 12 and 13) are compositionally transitional between MORB and island arc tholeiite suggesting spreading in a back-arc setting (Smith, 1991; Spadea et al., 1996, 1991) and are overlain by claystones with poorly preserved late Early Miocene radiolaria (Scherer, 1991b). E-W trending magnetic anomalies C7–C5 (23.96–9.79 Ma) in the eastern part of the Sulu Sea indicate N-S spreading and southward younging directions (Roeser, 1991; Schlüter et al., 1996). The conjugate oceanic lithosphere to the south is no longer present, and is interpreted to have subducted at the Sulu Trench (Roeser, 1991; Schlüter et al., 1996). The western part of the Sula Sea is covered by a 15 km thick sequence of Lower Miocene volcaniclastic rocks, Upper Miocene–Lower Pliocene deltaic sedimentary rocks and Upper Pliocene–Pleistocene carbonates (Tamesis, 1990). Since the Late Miocene, the western part of the Sulu Sea is undergoing NE-SW directed extension accommodated by NE-dipping normal faults (Graves and Swauger, 1997; Tamesis, 1990). This extension was also accommodated at the Sulu Trench, which had very low convergence rates in the late Miocene to Pleistocene (Roeser, 1991; Silver and Rangin, 1991). We reconstruct 125 km of N-S directed half-spreading between 23.6 Ma and 9.79 Ma documented by the magnetic anomalies (Table S1). The amount of pre-drift extension between the Sulu and Cagayan arcs is not constrained, but we conservatively reconstruct ~50 km of N-S directed pre-drift extension, which was estimated to have occurred between 35 Ma and 23.96 Ma (Liu et al., 2014; Roeser, 1991).

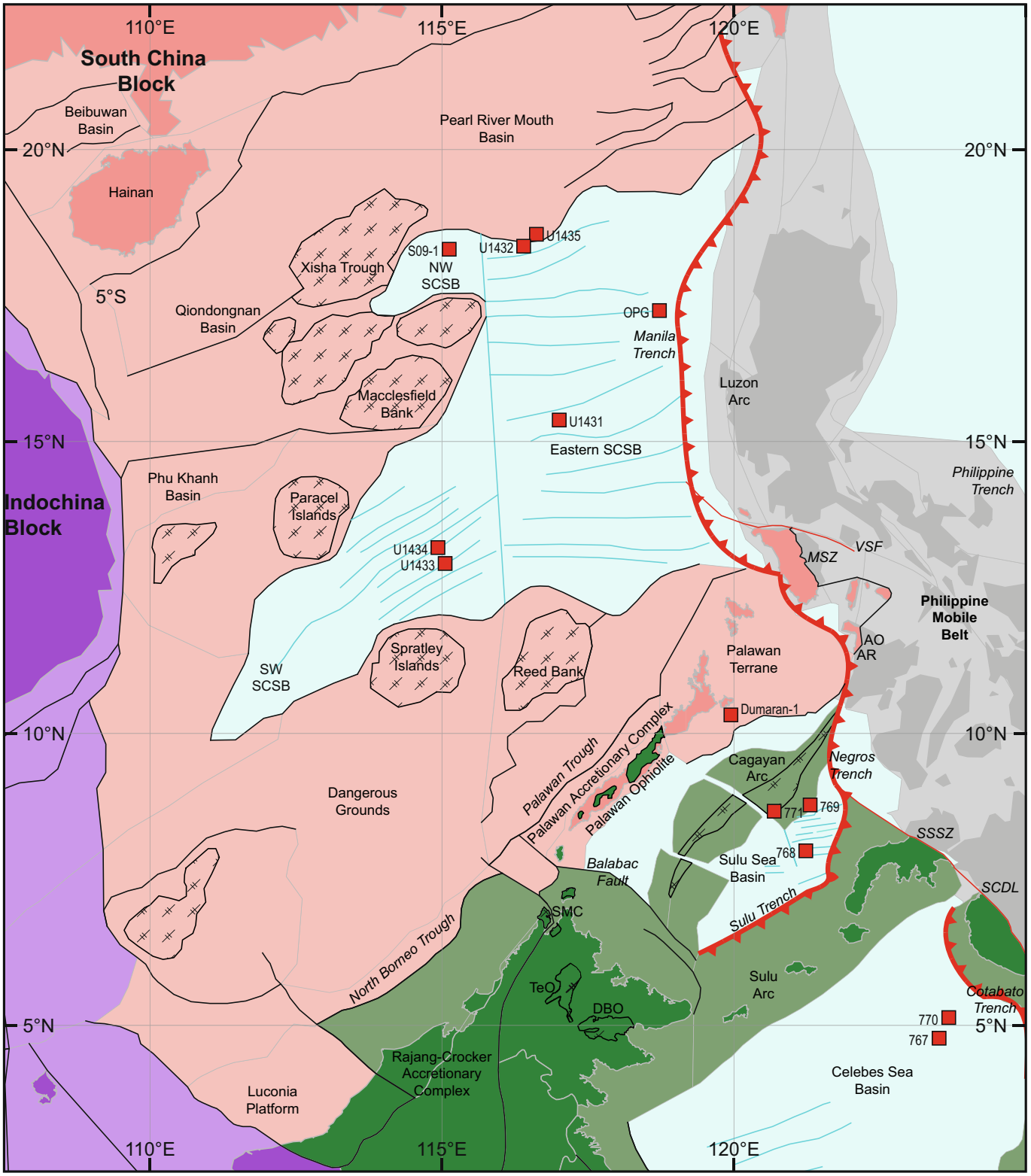

Fig. 12. Map of the Celebes and Sulu Sea, Palawan orogen, NW Borneo margin and South China Sea. See Fig. 2 for location. Abbreviations: AO, Amnay Ophiolite; AR, Antique Range; DBO, Darvel Bay Ophiolite; MSZ, Mindoro Suture Zone; TeO, Telupid Ophiolite; SCDL, Sindangan-Cotabato-Daguma Lineament; SCSB, South China Sea Basin; SMC, Sabah mélange complexes; SSSZ, Siayan-Sindangan Suture Zone; VSF, Verde Passage-Sibuyan Sea Fault.

Southeastward subduction of the Sulu Sea below the Sulu Arc must have been underway by 18.8 Ma by which time the arc was active (Bergman et al., 2000; Rangin et al., 1990a).

The **Cagayan Arc** is a submerged volcanic arc, built on a continental ribbon that shares a passive margin with oceanic lithosphere of the Sulu Sea to the south (Figs. 12 and 13). To the west, it is separated from NE Borneo along the Balabac Fault, a left-lateral transform fault that connects the Sulu Ridge and Trench to the South China Sea plate boundaries (Cullen, 2010; Schlüter et al., 1996) (Fig. 12). The Cagayan Ridge is segmented into three

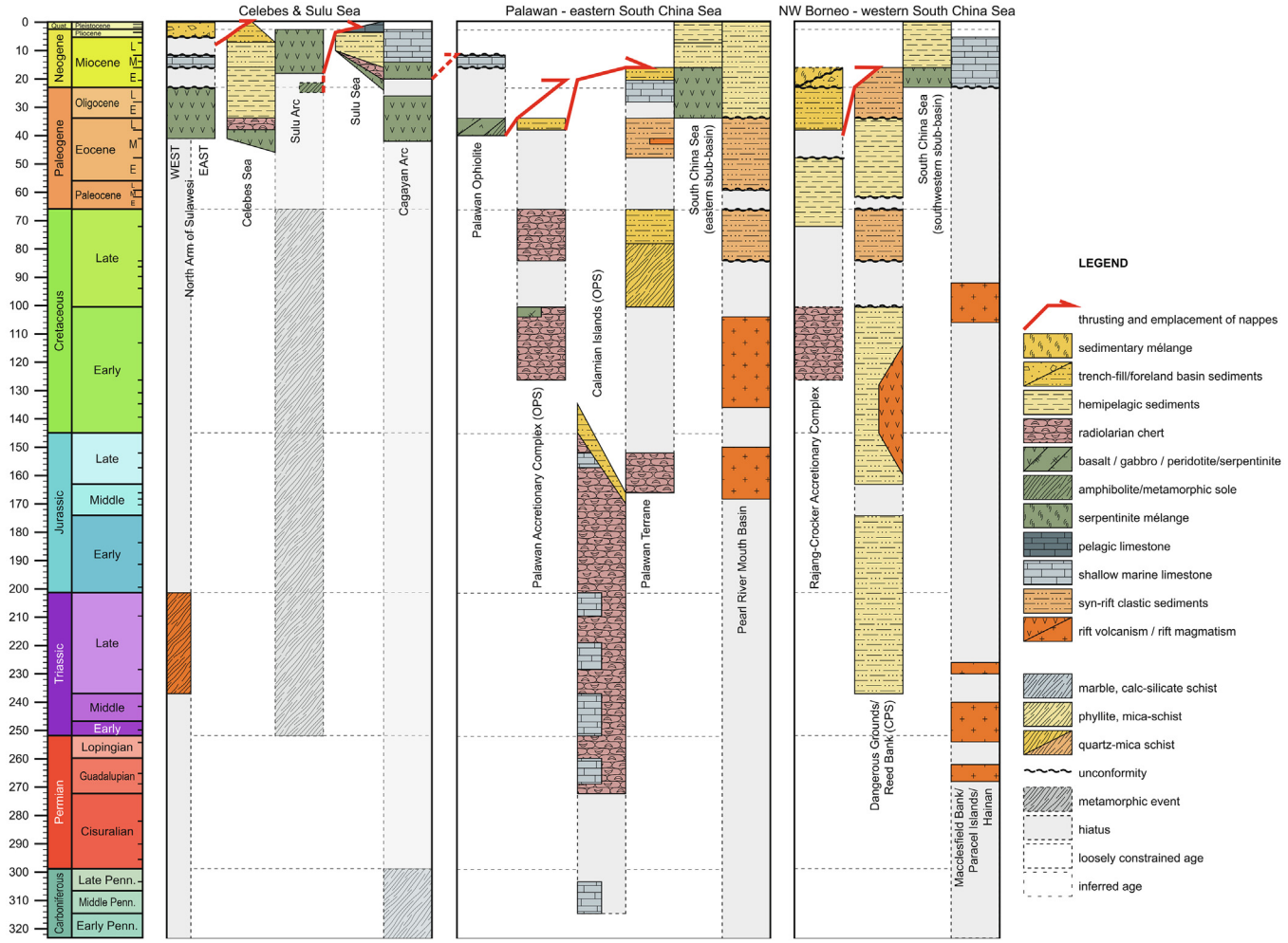

Fig. 13. Tectonostratigraphy of the Celebes and Sulu Sea, Palawan orogen, NW Borneo margin and South China Sea. Geologic Time Scale from Gradstein et al. (2012).

sections by NW-SE striking transform faults, parallel to the Balabac Fault (Schlüter et al., 1996) (Fig. 12). Basaltic and andesitic clasts recovered from the Cagayan Ridge are calc-alkaline and island arc tholeiites, and their chemical composition implies continental crust contamination (Kudrass et al., 1990; Smith, 1991; Spadea et al., 1996, 1991). Seismic reflection profiles show volcanics covering normal fault blocks at the southern flanks of the Cagayan Arc, which are interpreted to reflect break-up between the continental crust (that we tentatively correlate to the SW Borneo Mega-Unit) presently underlying the Cagayan and Sulu arcs prior to opening of the Sulu Sea Basin (Lai et al., 2021; Rangin and Silver, 1991; Schlüter et al., 1996). At ODP sites 769 and 771 (Fig. 12) the base of these covering volcanic rocks was not reached (Smith, 1991). Basalts and andesites from the southern flank of the Cagayan Arc yielded K–Ar ages of 20–14 Ma (Bellon and Rangin, 1991), whereas an andesitic tuff from the onshore continuation of the Cagayan Arc on Sabah yielded a fission track zircon age of 33.9 ± 7.7 Ma (Hutchison et al., 2000). Samples dredged from the northern and the central part of the Cagayan Arc comprise volcanic rocks with incoherent K–Ar ages, and shallow-water carbonates of Early Miocene to Pliocene age (Kudrass et al., 1990, 1986). The Cagayan Arc is interpreted to result from southward subduction to the north (see below). This arc was active since at least the Early Miocene (Bellon and Rangin, 1991; Silver and Rangin, 1991) and likely already since the Early Oligocene (Hutchison et al., 2000).

Rocks of the Cagayan Arc are thrusted over the **Central Palawan Ophiolite** (Figs. 12 and 13) to the north (Schlüter et al., 1996). This ophiolite is the structurally highest unit exposed on Palawan (Aurelio et al., 2014) and consists of a more or less coherent section of oceanic lithosphere comprising mantle harzburgite, troctolite, gabbro, plagiogranite, diabase dykes, and massive and pillowed basaltic lava (Encarnacion et al., 1995; Keenan et al., 2016). U–Pb zircon geochronology on plagiogranite in the lower crustal section of the ophiolite yield crystallisation ages of 40.0 ± 0.5 Ma and 34.1 ± 0.1 Ma (Dycoco et al., 2021; Keenan et al., 2016). A metamorphic sole composed of kyanite-muscovite-chlorite schist, quartzite, amphibolite, and garnet amphibolite is attached to the base of the Central Palawan Ophiolite and recorded P–T conditions of ~9 kbar and 700–760 °C (Encarnacion et al., 1995). Metabasite pods in the metamorphic sole yield U–Pb zircon ages of 35.9–35.3 Ma (Keenan et al., 2016). A kyanite schist yielded a $^{40}Ar/^{39}Ar$ white mica age of 34.25 ± 0.3 Ma, whereas the amphibolite and garnet amphibolite yielded $^{40}Ar/^{39}Ar$ hornblende ages of 34.2 ± 0.6 Ma and 34.2 ± 0.5 Ma respectively, interpreted to record rapid cooling below 550–400 °C during decompression to 5–6 kbar (Encarnacion et al., 1995; Keenan et al., 2016). Geochemical data indicate that the ophiolite formed as SSZ ophiolite above an active, likely juvenile subduction zone (e.g. Keenan et al., 2016). Keenan et al. (2016) interpreted the ~35 Ma zircons in the mafic pods in the ophiolite as the age of the MORB protoliths, and consequently suggested that subduction below the Palawan ophiolite started at ~35 Ma at a spreading ridge. However, in metamorphic sole rocks of Oman, which formed in Cretaceous time in lithosphere of Permian age (e.g., van Hinsbergen et al., 2019b), such melt pockets

have also been found, and they thus may also have formed during partial melting of the sole during its typical HT metamorphism preceding cooling recorded by $^{40}Ar/^{39}Ar$ ages by 10 Myr or more (Guilmette et al., 2018). The Palawan ophiolite more likely formed by forearc spreading at the continental margin of the Cagayan Arc portion of the SW Borneo Mega-Unit.

Structurally below the Central Palawan Ophiolite is the **Palawan Accretionary Complex** (Fig. 13) that comprises blocks of syenite and olivine gabbro with U–Pb zircon ages of 103.0 ± 1.1 Ma and 100.7 ± 1.1 Ma respectively (Dycoco et al., 2021), and a series of thrust slices with an OPS sequence of Lower Cretaceous (Aptian–Albian) interbedded calcareous clay and radiolarian chert (Muller, 1991), Upper Cretaceous (Campanian–Maastrichtian) radiolarian chert and pelagic sedimentary rocks intercalated with pillow basalts, and trench-fill sediments comprising Upper Eocene sandstone and conglomerate (Aurelio et al., 2014; Wolfart et al., 1986). The top of this sandstone is weakly metamorphosed where it is in thrust contact with the Central Palawan Ophiolite. These thrust slices are unconformably covered by Lower Miocene clastic sedimentary rocks (Aurelio et al., 2014).

Below the accreted OPS sequence is a composite unit referred to as the **Palawan Terrane**, which is a fragment of a Mesozoic accretionary prism (Fig. 13). The oldest stratigraphic unit is an OPS sequence comprising carbonate breccias and bioclastic limestone with Upper Carboniferous (Moscovian–Kasimovian) fusulinids that may be reworked (Kiessling and Flügel, 2000), Middle Permian–Upper Jurassic radiolarian chert, several coherent Middle Permian to Upper Jurassic limestone blocks that were deposited on seamounts, and Middle Jurassic (Bajocian) to Lower Cretaceous (Valanginian) trench-fill sedimentary rocks. These OPS sequences are exposed on the Calamian Islands in three belts that young from north to south, suggesting consecutive accretion in the Middle Jurassic, Late Jurassic and Early Cretaceous in a northwest dipping subduction zone (Zamoras and Matsuoka, 2004, 2001). A similar Middle–Upper Jurassic (Callovian–Kimmeridgian) OPS mélange is also exposed on Palawan (Faure and Ishida, 1990), where detrital zircons in the sandstone members suggest a South China continental arc provenance (Cao et al., 2021). This accretionary complex is intruded by an Upper Cretaceous granite (Padrones et al., 2017) and is overlain by Upper Cretaceous (upper Campanian–Maastrichtian) deltaic sandstone and a sequence of low-grade metasedimentary schist, phyllite and non-metamorphic turbidite sandstone. Detrital zircons in this sequence suggest a South China provenance with evidence for contemporaneous arc magmatism (Cao et al., 2021; Shao et al., 2017; Suggate et al., 2014; Suzuki et al., 2000; Walia et al., 2012). Upper Cretaceous siltstone and shale were also encountered in drill site Dumaran-1 in the northeastern Sulu Sea (Fig. 12), where they occur above serpentinized peridotite (Schlüter et al., 1996). The Mesozoic sequence is intruded by a granite with a U–Pb zircon age of 42 ± 0.5 Ma and is unconformably overlain by Eocene *syn*-rift turbidites that still have a South China provenance (Cao et al., 2021; Shao et al., 2017; Suggate et al., 2014). A ~33 Ma break-up unconformity marks the separation of the Palawan Terrane from South China (see Section 4.15). Above this break-up unconformity are Upper Oligocene–Lower Miocene limestones that were deposited during the drift of the Palawan Terrane, followed by trench-fill clastic sedimentary rocks of Early Miocene (Burdigalian) age that date its arrival in the Palawan Trench below the Central Palawan Ophiolite (Aurelio et al., 2014; Ilao et al., 2018; Steuer et al., 2013). These thrusts are sealed by Middle Miocene limestone marking the end of major thrusting (Aurelio et al., 2014; Steuer et al., 2013). Minor contractional deformation of the wedge continued until ~12 Ma (Aurelio et al., 2014).

A Middle Eocene to Middle Miocene subduction complex is also present along-strike towards the southwest, in NW Borneo. There, the **Rajang-Crocker Accretionary Complex** (Figs. 12 and 13) forms a curved northwest verging foreland-propagating fold-thrust belt interpreted to have formed at a south-dipping subduction zone below North Borneo from the middle Eocene to the Middle Miocene (Hall et al., 2008; Honza et al., 2000; Van Hattum et al., 2013). The structurally highest thrust slices of the Rajang-Crocker Accretionary Complex comprise Upper Cretaceous (Maastrichtian) to Lower Eocene deep marine turbidites of the Rajang Group (Galin et al., 2017; Honza et al., 2000; Sapin et al., 2011) that were interpreted to have been deposited in either a post-collisional foreland basin or a remnant ocean basin (Moss, 1998). Structurally lower thrust slices show an unconformable relation between the Rajang Group and the overlying Upper Eocene–lowermost Miocene deep marine turbidites of the Crocker Fan (Sapin et al., 2011; Van Hattum et al., 2013). The structurally lowest thrust slices expose Crocker Fan deposits and Lower Miocene sedimentary mélanges. These mélanges incorporate blocks of ultramafic and mafic rocks and Lower Cretaceous radiolarian chert, which were likely derived from the underlying stratigraphy by mud diapirism (Aitchison, 1994; Clennell, 1991; Jasin, 2000; Sapin et al., 2011) (Fig. 13). The Crocker Fan deposits are truncated by a Lower Miocene unconformity (Van Hattum et al., 2013). Above this unconformity are Lower Miocene shallow marine clastic sedimentary rocks (Tongkul, 2006, 1994; Van Hattum et al., 2013). In the western part of the Rajang-Crocker Accretionary Complex, there is significant dextral strike-slip faulting along major ESE-WNW striking thrust faults onshore and offshore Sarawak (Blankenaauw, 2017; Mat-Zin and Swarbrick, 1997). The Rajang-Crocker Accretionary Complex is thrust northward over continental fragments in the South China Sea that are thought to have derived from the South China margin, analogous to the Palawan Terrane (Sapin et al., 2011). The thrust slices of the Rajang-Crocker Accretionary Complex are truncated by a Middle Miocene unconformity (Levell, 1987; Morley et al., 2023b, 2003; Sapin et al., 2011). The overlying Middle Miocene–Upper Pliocene fluviodeltaic and shallow marine sediments and Pleistocene–Holocene deep marine sediments onlap on continental fragments in the north Borneo Trough (Hesse et al., 2009) and host several intraformational unconformities (Hazebroek and Tan, 1993; Levell, 1987). Line-length balancing of seismic sections has revealed that minor (up to 6 km) of Late Miocene–recent extension in NW Borneo shelf is in part balanced by up to 10 km of Late Miocene-recent shortening in the deep-marine offshore section (Hesse et al., 2009) interpreted to reflect minor gravitational collapse of the NW Borneo slope since the Late Miocene (Hall, 2013) following cessation of subduction (Aurelio et al., 2014).

4.14. South China Sea Basin

North of the former trenches of the Rajang-Crocker Accretionary Complex and the Palawan Accretionary Complex lies the South China Sea, that is bounded to the west by a transform system that runs along the northeastern Sunda Shelf and the eastern Indochina margin, and that is bounded to the east by the Manila Trench. Its northern boundary is formed by the South China passive margin. The South China Sea contains hyperextended conjugate continental margins in the north and south, and an oceanic basin in the centre (Figs. 12 and 13).

The central oceanic basin comprises the eastern, northwestern, and southwestern sub-basins (Li and Song, 2012). In the eastern sub-basin, magmatic spreading started prior to ~29 Ma, as suggested by dredged plagiogranite sample OPG (Fig. 12) with a $^{40}Ar/^{39}Ar$ pyroxene age of 32.3 ± 0.5 Ma and a $^{40}Ar/^{39}Ar$ whole rock age of 28.9 ± 1.9 Ma (Zhong et al., 2018). Initially E-W striking magnetic anomalies were interpreted as C11 to C6 (30.59–18.75 Ma) (Taylor and Hayes, 1983) and C11 to C5b (30.59–14.78 Ma)

(Briais et al., 1993). Barckhausen et al. (2014) re-interpreted these anomalies as C12 to C6A1 (33.16–20.04 Ma), signalling an earlier arrest of spreading. However, deep tow magnetic surveys by Li et al. (2014) identified these marine magnetic anomalies as C12r to C5Br (33.16–15.16 Ma), which confirmed earlier studies (Briais et al., 1993; Taylor and Hayes, 1983). In the northwestern sub-basin, spreading started prior to ~24 Ma as suggested by a cored basalt sample S09-1 with $^{40}Ar/^{39}Ar$ groundmass ages of 23.80 ± 0.18 Ma and 23.29 ± 0.22 Ma (Li et al., 2015). In the southwestern sub-basin, Briais et al. (1993) identified marine magnetic anomalies C6 to C5b (20.04–14.78 Ma), which were later re-interpreted by Barckhausen and Roeser (2004) as C6C to C6A (23.96–20.04 Ma), signalling an earlier arrest of spreading. However, deep-tow magnetic surveys by Li et al. (2014) identified these anomalies as C6AAr to C5Cn.1n (21.77–15.97 Ma), confirming the earlier interpretation of Briais et al. (1993). We have adopted the above mentioned deep-tow marine magnetic anomaly interpretations of Li et al. (2014) and reconstruct 820 km N-S directed oceanic spreading in the eastern sub-basin between 31.5 and 15 Ma, and 360 km N-S directed oceanic spreading in the western sub-basin between 23.5 and 16 Ma (Table S1).

The hyperextended continental lithosphere of the southern South China Sea hosts the continental extensional allochthons of the Luconia Platform, Spratly Islands, Reed Bank and Palawan Terrane (see previous section) that are separated by intervening highly extended continental crust of the submarine Borneo Trough, Dangerous Grounds, and Palawan Trough (Fig. 12). Extensive dredging has revealed that these blocks comprise Upper Triassic–Jurassic deltaic and marine clastic sedimentary rocks, granitic rocks with U–Pb zircon ages of 159–127 Ma, Upper Jurassic–Lower Cretaceous sandstones, siltstones and shales, and metamorphic rocks with K–Ar ages recording cooling from metamorphic events between 145 and 104 Ma (Hinz and Schlüter, 1985; Kudrass et al., 1986; Yan et al., 2010). Locally, Upper Cretaceous terrestrial to shallow marine clastic rocks unconformably overlie this sequence (Schlüter et al., 1996). Middle Paleocene–Upper Eocene clastic sedimentary rocks conformably cover the Upper Cretaceous sequence and are unconformably overlain by Lower Oligocene to Lower Miocene *syn*-rift sedimentary rocks. Middle Miocene to recent post-rift sediments cover the whole sequence (Ding et al., 2013; Franke et al., 2011; Liang et al., 2019; Sales et al., 1997). The Luconia Platform, the Spratly Islands and Reed Bank are virtually undeformed, while the Dangerous Grounds is characterized by a 'Basin and Range' morphology interpreted to result from extension (Liang et al., 2019). Fault-heave analysis of the Dangerous Grounds led to a total NW-SE directed extension estimate of 66 km, of which 45 km was accomplished sometime between 66 and 33 Ma and 15 km between 33 and 23 Ma (Ding et al., 2013) (Table S1). The Palawan Trough is a necking zone with stretching factors of 2.5–3.0, corresponding to 60 km of NW-SE directed extension, sometime between 66 and 33 Ma (Franke et al., 2011; Sales et al., 1997) (Table S1).

The hyperextended northern margin of the South China Sea comprises crystalline basement blocks of the Macclesfield Bank, Paracel Islands, Hainan, and South China, and the intervening Phu Khanh Basin, Qiondongnan Basin, Beibuwan Basin, and Pearl River Mouth Basin (McIntosh et al., 2014; Savva et al., 2014; Zhang et al., 2020a) (Figs. 12 and 13). The Paracel Islands and Macclesfield Bank are built on a Precambrian metamorphic basement (Wang et al., 1979), intruded by Mesozoic arc plutons (Jiqing and Bingwei, 1987). Shallow marine limestones of Early–Late Miocene age and younger (Honggang and Huimin, 2002; Ma et al., 2018) unconformably cover this basement. The island of Hainan exposes a Precambrian–Paleozoic basement (Li et al., 2002) intruded by Permian–Triassic and Cretaceous arc granites (Li et al., 2006; Yan et al., 2017). None of the islands expose a Mesozoic accretionary prism like on the Palawan Terrane and rifting here thus migrated away from the margin further into the South China continent and arc.

Savva et al. (2014) interpreted from seismic sections that the Paracel Islands, Macclesfield Bank, and Hainan behaved as rigid blocks, in which the plutons remained virtually undeformed. Stretching of the continental margin was accommodated by intervening necking zones in the Phu Khanh Basin, the Xisha Trough, and the Qiondongnan Basin (Fig. 10). This stretching ultimately led to exhumation of mantle rocks in the Phu Kanh Basin (Savva et al., 2014, 2013). Based on crustal cross-sectional area balancing, Hayes and Nissen (2005) interpreted that ~150 km of N-S extension was accommodated in the Phu Khanh Basin (Table S1) during westward rift propagation (between ~23.5–21.5 Ma) in the southwest sub-basin of the South China Sea, and ~175 km of NNW-SSE extension was accommodated in the Qiondongnan Basin between the Middle Paleocene (Selandian: 61.6 Ma) and break-up of the South China margin at 33 Ma (Li et al., 2014; Su et al., 1989) (Table S1). Based on the interpretations of Savva et al. (2014) we also infer 30 km NNW-SSE directed extension in the Xisha Trough (Table S1) between 31.5 and 27.4 Ma to balance early extension in the eastern sub-basin of the South China Sea. In the Beibuwan Basin adjacent to Hainan (Fig. 12), continental basement is overlain by an Upper Paleocene to Middle Eocene *syn*-rift sequence and a Middle Eocene–Quaternary post rift sequence (Su et al., 1989). Backstripping analysis in the Beibuwan Basin suggested stretching factors of 1.2–1.4 corresponding to 20–30 km of extension between the Middle Paleocene (61.6 Ma) and ~43 Ma (Clift and Lin, 2001; Su et al., 1989).

The Pearl River Mouth Basin (Figs. 12 and 13) is floored by a Precambrian–Paleozoic continental metamorphic basement intruded by Upper Jurassic and Lower Cretaceous arc granites (Xu et al., 2016). This basement was extensionally exhumed in the Late Cretaceous and is locally overlain by Upper Cretaceous rift sedimentary rocks (Ye et al., 2018) and Upper Paleocene–Upper Eocene fluvio-deltaic clastic rocks (Cao et al., 2018; Chan et al., 2010; Morley, 2016b; Su et al., 1989). Lower Oligocene to Holocene shelf sediments unconformably overlie this sequence (Su et al., 1989). Crustal thicknesses below the Pearl River Mouth Basin vary between ~15–20 km near the continent-ocean-boundary with the eastern sub-basin of the south China, and ~30 km near the shore of South China. Based on cross-sectional area balancing, Hayes and Nissen (2005) inferred ~175 km NNW-SSW directed extension starting in the Late Paleocene (Su et al., 1989). Near Taiwan, Paleogene extension in the South China margin increases to ~200 km (McIntosh et al., 2014). At the southern edge of the extended South China continental margin, IODP site U1435 (Fig. 12) records an unconformity at ~33 Ma, which is interpreted as breakup unconformity marking the end of continental extension and the start of seafloor spreading (Li et al., 2014) (Table S1).

4.15. Active margins with Panthalassa/Pacific-derived plates

The SE Asian accretionary orogen that we reviewed above is bounded to the east and southeast by a system of thrust faults and trenches, from the South China Sea margin in Taiwan, along the Philippine Mobile Belt (Gervasio, 1967), to the Sorong Fault Zone on Bird's Head (Dow and Sukamto, 1984) (Fig. 14). To the east of this belt is oceanic lithosphere that was derived from the Panthalassa/Pacific realm (Hall, 2002; Yumul et al., 2003; van de Lagemaat and van Hinsbergen, 2024). In this section, we describe the nature of this boundary (Figs. 15 and 16), but we will not reconstruct the tectonic history of the lithosphere to the east of this boundary in detail here, as this is provided in van de Lagemaat and van Hinsbergen (2024).

The South China continental margin and the eastern sub-basin of the South China Sea are subducting eastwards at the **Manila Trench** below Cretaceous and Eocene oceanic lithosphere of the Philippine Sea Plate (Deschamps et al., 2000; Hilde and Chao-Shing, 1984; Yumul et al., 2003). This oceanic lithosphere is exposed on the Philippine Islands and is east of the Manila Trench overlain by the 1200 km long Luzon Arc, where the oldest volcaniclastic forearc sedimentary rocks are of Early Miocene age (Burdigalian, NN3: ~18 Ma) (Chi and Suppe, 1985) and volcanic rocks yield K–Ar whole rock ages of ~15.5 Ma and younger (e.g., Bellon and Yumul, 2000; de Boer et al., 1980; Defant et al., 1989; Florendo, 1994). In Taiwan, the oceanic Philippine Sea Plate lithosphere overthrusted the South China continental margin. The main constituents of the Taiwan orogen are Luzon arc and forearc rocks, OPS relics and accreted margin CPS (Conand et al., 2020; Huang et al., 2006; Zhang et al., 2020c). The highest unit is the Luzon Arc and mélange-hosted SSZ-ophiolitic blocks interpreted to be part of the Luzon forearc (Huang et al., 2018). Gabbro and plagiogranite blocks yielded U–Pb zircon ages of 17.8–17.2 Ma (Huang et al., 2018; Lo et al., 2020), similar in age to the oldest volcaniclastic forearc sediments from the northern Luzon Arc (Chi and Suppe, 1985), whereas basalt blocks and volcanic zircons in chert yielded U–Pb zircon ages of 14.1 ± 0.4 Ma and 14.7 ± 0.2 Ma respectively (Hsieh et al., 2017; Lo et al., 2020), i.e. younger than the fossil spreading ridge of the South China Sea (Li et al., 2014). Below, metamorphic OPS mélange consists of mafic blueschist facies tectonic blocks with U–Pb zircon crystallization ages of 16.0–15.0 Ma, similar to the fossil spreading ridge of the South China Sea (Chen et al., 2017; Lo et al., 2020), and $^{40}Ar/^{39}Ar$ amphibole and white mica ages of 12.2–9.0 Ma (Lo and Yui, 1996; Lo et al., 2020) that likely recorded cooling during exhumation. The structurally highest, most distal, South China margin CPS unit comprises metasedimentary blueschists with a Lu–Hf garnet-whole rock age of 5.1 ± 1.7 Ma (Sandmann et al., 2015) recording peak metamorphic conditions of 10–14 kbar and 550 ± 40 °C (Baziotis et al., 2017; Beyssac et al., 2008; Tsai et al., 2013). The units below are upper greenschist facies Permian marbles and Cretaceous metapelites and metagranitoids, which are thrusted over greenschist facies Upper Eocene–Lower Miocene slates (Chen et al., 2017; Conand et al., 2020; Zhang et al., 2020c). The lowest unit is a fold-thrust belt comprising Paleocene–Upper Miocene neritic clastic sedimentary rocks, that is unconformably overlain by a deformed foreland basin with Upper Miocene–Pleistocene neritic clastic sedimentary rocks and Holocene alluvial sediments (Conand et al., 2020; Huang et al., 2006; Lin et al., 2003; Yue et al., 2005; Zhang et al., 2020c). This suggests the South China continental margin arrived in the Manila Trench below the Philippine Sea Plate-derived Luzon Arc around 6.5 Ma (Lin et al., 2003). Balanced cross section restoration indicates at least 120 km of E-W shortening of the South China continental margin since the latest Miocene due to westward overthrusting (Suppe, 1980). Seismic tomographic images of the Manila slab below the Luzon Arc suggest that 400–500 km of lithosphere may have subducted in total (Koulakov et al., 2014; Lallemand et al., 2001; Rangin et al., 1999; Van der Meer et al., 2018; Wu et al., 2016; Zhao and Ohtani, 2009; Zheng et al., 2013), suggesting that subduction initiated ~300–400 km outboard of the South China margin east of Taiwan at ~18 Ma.

Towards the south, continental crust is also accreted below the southern Luzon forearc (Arfai et al., 2011), where the Manila Trench links up with the E-W striking Verde Passage and the NW-SE striking **Mindoro Suture Zone** (Marchadier and Rangin, 1990; Rangin et al., 1985; Sarewitz and Karig, 1986) on the island of Mindoro. The Mindoro Suture Zone continues to the east on the Romblon Islands (Dimalanta et al., 2009) and continues further south into the Antique Range on the island of Panay (Yumul et al., 2013; Zamoras et al., 2008) (Fig. 14). The Mindoro Suture Zone separates the accretionary complex of the Palawan Terrane and the continental and arc lithosphere of the Cagayan Arc in the west and southwest respectively from the overlying oceanic lithosphere exposed in the Phillipine Mobile Belt in the east and northeast (Sarewitz and Karig, 1986). Southwest Mindoro exposes a southwest verging accretionary complex of three tectonic units (Canto et al., 2012; Marchadier and Rangin, 1990; Rangin et al., 1985) (Fig. 15). The highest tectonic unit comprises a heterogenous metamorphic basement that comprises Paleozoic (likely Upper Carboniferous: Bashkirian–Kasimovian) marbles (Knittel and Daniels, 1987) intruded by a meta-granodiorite with a U–Pb zircon age of 251 ± 3 Ma (Knittel et al., 2010) and meta-rhyolite with a U–Pb zircon age of 83 ± 1 Ma (Knittel, 2011). These crystalline rocks also host sheared ophiolitic blocks of serpentinized harzburgites, gabbro, dolerite dykes and basaltic pillow lavas (Concepcion et al., 2012). The sequence is unconformably overlain by Upper Eocene–Lower Oligocene clastic sedimentary rocks that are interpreted as derived from a passive continental margin (Canto et al., 2012; Concepcion et al., 2012) and that were in part metamorphosed during burial below the ophiolitic blocks (Knittel et al., 2017). We tentatively correlate this unit with the basement of the Cagayan Arc. The middle tectonic unit is formed by the Amnay Ophiolite that comprises an upper mantle and oceanic crust sequence, with peridotites, pyroxenite, gabbro, sheeted dykes, and basaltic pillow lavas that are capped by Oligocene pelagic mudstone (Rangin et al., 1985; Yumul et al., 2009b). Rangin et al. (1985) interpreted the Amnay Ophiolite as a trapped fragment of South China Sea oceanic lithosphere, but we consider it more likely that this a continuation of the Palawan Ophiolite. The lowest tectonic unit comprises Jurassic ammonite bearing siltstones and Upper Cretaceous (Campanian–Maastrichtian) black shales that are unconformably overlain by Middle Eocene–Lower Oligocene *syn*-rift clastic sedimentary rocks. This sequence is unconformably overlain by Upper Oligocene–Lower Miocene post-rift clastic sedimentary rocks and carbonates (Marchadier and Rangin, 1990). We tentatively correlate this unit with the Palawan Terrane. The onset of shortening is recorded by Middle Miocene conglomerate that reworks all the older sequences (Marchadier and Rangin, 1990; Rangin et al., 1985). All tectonic units are unconformably covered by Lower Pliocene–Lower Pleistocene tuffaceous sandstone, siltstone, conglomerate and limestone (Canto et al., 2012; Marchadier and Rangin, 1990).

Rocks correlated to the Palawan Terrane have also been found on the Romblon Islands to the east of Mindoro (Figs. 14 and 15). These islands expose a structurally highest unit that comprises a Penrose type ophiolite underlain by an amphibolite sole (Dimalanta et al., 2009; Faure et al., 1989). A diorite in the upper crustal section of the ophiolite yielded a K–Ar whole rock age of 43.2 ± 2.5 Ma (Dimalanta et al., 2009). Below this ophiolite are accreted OPS sequences with pillow lava and Jurassic–Cretaceous radiolarian chert (Maac and Ylade, 1988) and a serpentinite-hosted mélange with clasts of peridotite, gabbro, volcanic rocks, and metasedimentary rocks (Dimalanta et al., 2009). Below, pelitic metasedimentary rocks with a maximum depositional age of ~112 Ma (Knittel et al., 2017) yield K–Ar mica ages of 12.3 ± 0.2 Ma and 12.2 ± 0.2 Ma (Dimalanta et al., 2009) that likely recorded cooling during exhumation. The lower part of the metamorphic series comprises undated gneisses derived from acid volcaniclastic rocks intruded by undated, weakly foliated granitoids (Faure et al., 1989). The entire nappe stack is overlain by an Upper Miocene (Tortonian) to Lower Pliocene arc sequence of the Luzon Arc, and Upper Pliocene–Pleistocene clastic sediments and coralline limestone (Bellon and Rangin, 1991; Dimalanta et al., 2009; Maac and Ylade, 1988; Marchadier and Rangin, 1990, 1989). We correlate these units to the Palawan fold-thrust belt, with the ophiolite as

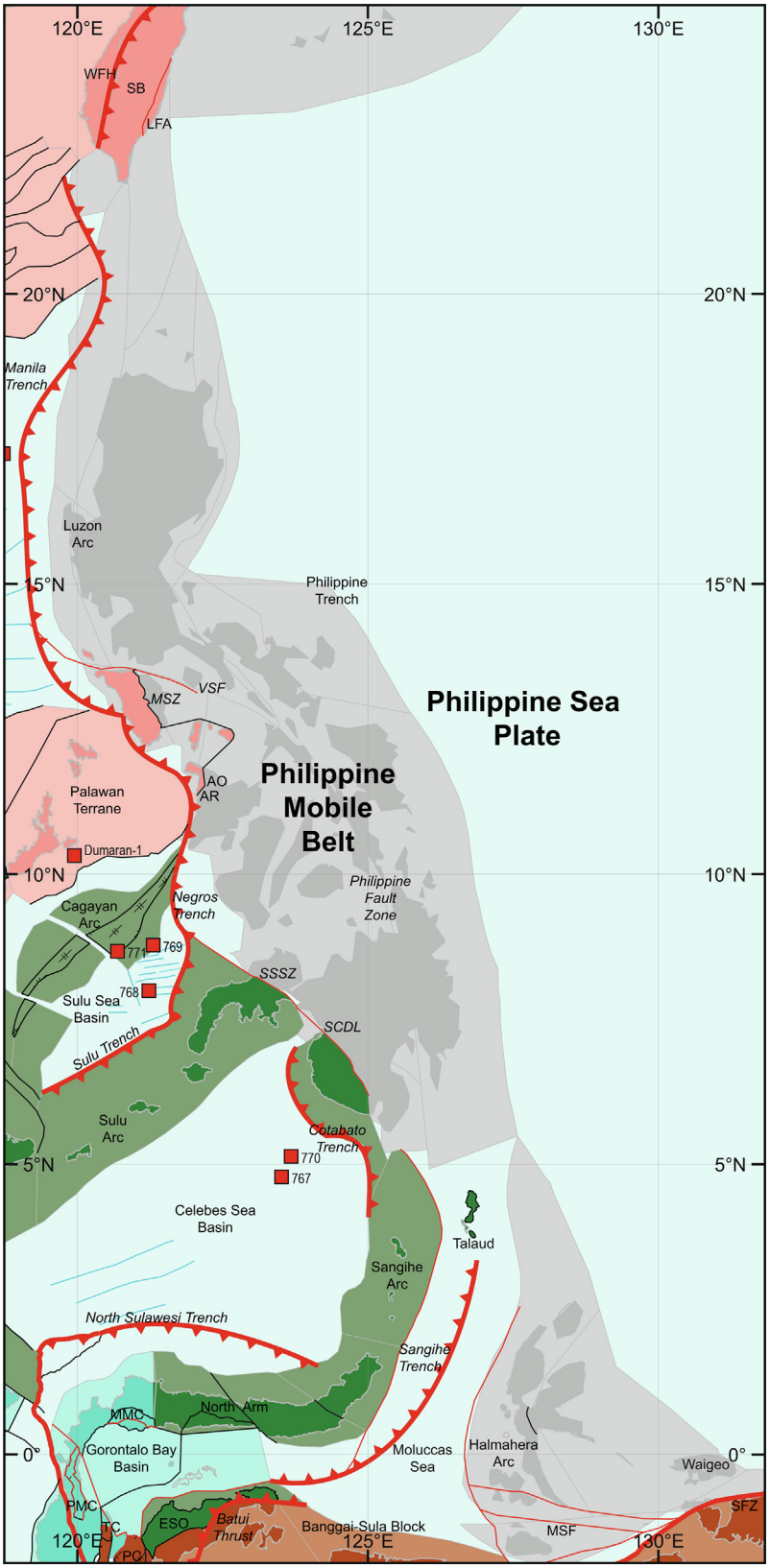

Fig. 14. Tectonic map of the western Philippines. See Fig. 2 for location. Abbreviations: AO, Amnay Ophiolite; AR, Antique Range; ESO, East Sulawesi Ophiolite; LFA, Luzon forearc; MMC, Malino Metamorphic Complex; MSF, Molucca-Sorong Fault; MSZ, Mindoro Suture Zone; PC, Pompangeo Complex; PMC, Palu Metamorphic Complex; SB, Slate Belt; SCDL, Sindangan-Cotabato-Daguma Lineament; SFZ, Sorong Fault Zone; SSSZ, Siayan-Sindangan Suture Zone; TC, Tokorondo Complex; VSF, Verde Passage-Sibuyan Sea Fault; WFH, Western Foot Hills.

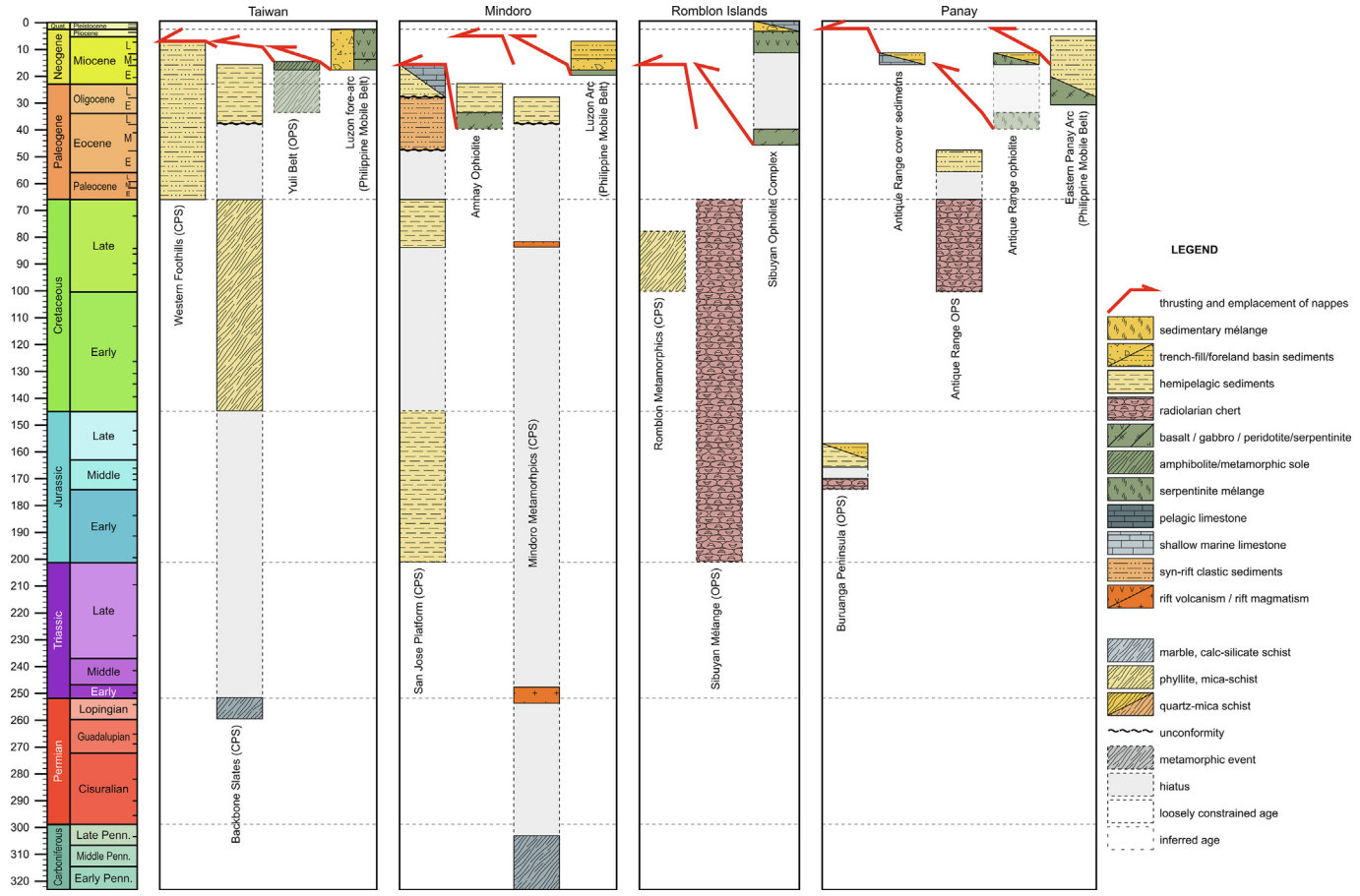

Fig. 15. Tectonostratigraphy of Taiwan, the margin of the Philippine Mobile Belt (Mindoro, Romblon, Panay). Geologic Time Scale from Gradstein et al. (2012).

Palawan Ophiolite, the OPS as Palawan Accretionary Complex, and the metamorphic rocks as the Palawan Terrane. Yumul et al. (2009a) noted that there are no rocks of the Philippine Mobile Belt exposed on the Romblon Islands, suggesting the suture is located offshore, to the east of Sibuyan.

To the south of Mindoro and to the east of the Sulu Sea, the Buruanga Pensinula on northwest Panay exposes an OPS sequence of Middle Jurassic (Aalenian) radiolarian chert, Middle–Upper Jurassic (Callovian–Oxfordian) siliceous shale and Upper Jurassic (Oxfordian) continent-derived sandstones (Zamoras et al., 2008) (Fig. 15), similar to the OPS sequences on northern Palawan and the Calamian Islands (Faure and Ishida, 1990; Zamoras and Matsuoka, 2004, 2001). The Buruanga Peninsula is overthrust to the east by a west-verging fold-thrust belt in the Antique Range (Tamayo et al., 2001) (Fig. 15). The structurally highest unit in this fold-thrust belt comprises a plutonic-volcanic basement with K–Ar ages of 31–21 Ma (Bellon and Rangin, 1991; Rangin et al., 1991) overlain by Upper Oligocene–Upper Miocene marine sedimentary rocks, which are part of the deformed western margin of the Philippine Sea Plate known as the Philippine Mobile Belt (Tamayo et al., 2001). This unit overthrusts ophiolitic lithologies (serpentinite, gabbro) that are overlain by deformed Middle Miocene volcanic and volcaniclastic rocks and undeformed Pliocene fluvio-deltaic sedimentary rocks, and fault-bounded lenses of Middle Miocene serpentinite hosted mélange (Tamayo et al., 2001). Structurally below these ophiolitic lithologies is an OPS sequence that includes Upper Cretaceous radiolarian chert and Lower Eocene calcarenite (Rangin et al., 1991). The lowest thrust slices comprise Middle Miocene limestone and tuffaceous sedimentary rocks (Tamayo et al., 2001). We correlate these lithologies to the Palawan fold-thrust belt, with the Jurassic-Cretaceous OPS units interpreted as Palawan Terrane, the ophiolites as Palawan Ophiolite, the Cretaceous-Eocene OPS as proto-South China Sea derived rocks, and the Middle Miocene limestones and tuffs as a orogenic cover. Field relations and fission track zircon and apatite ages of ~16–7 Ma suggest thrusting occurred during the Middle Miocene–Pliocene (Tamayo et al., 2001; Walia et al., 2013).

Collectively, the geologic record in Mindoro, the Romblon Islands and Panay suggest the leading edge of the pre-Middle Miocene Palawan orogen (Palawan Ophiolite, Palawan Accretionary Complex, Palawan Terrane) underthrusted the Philippine Mobile Belt in the Middle Miocene (Fig. 15). The ophiolites of the Philippines Mobile Belt were thrusted westwards since the Middle Miocene, contemporaneously with the formation of the Manila trench to the north. However, the Mindoro Suture Zone protrudes ~250 km eastwards relative to the Manila Trench, and is connected by the Verde Passage-Sibuyan Sea Fault to the Manila Trench (Rangin, 1991; Yumul et al., 2005). Hypocentres of current seismic events do not show a slab below ~50–100 km below the Mindoro Suture (Yumul et al., 2013). This appears to reflect a smaller westward displacement of the Philippine Ophiolites over the Cagayan-Palawan orogen than over the South China Sea lithosphere, and the difference is accommodated by sinistral strike slip motion on the Verde Passage-Sibuyan Sea Fault and the Philippine Fault Zone, and westwards subduction below the Philippine Trench (Yumul et al., 2005).

The Antique Range links up to the south with the NNW–SSE striking **Negros Trench** (Fig. 14) where seismic sections show a west-verging accretionary prism thrusting over the eastern Sulu Sea (Schlüter et al., 1996). Negros Island, east of the Negros Trench, exposes a basement comprising of Paleogene volcanic and

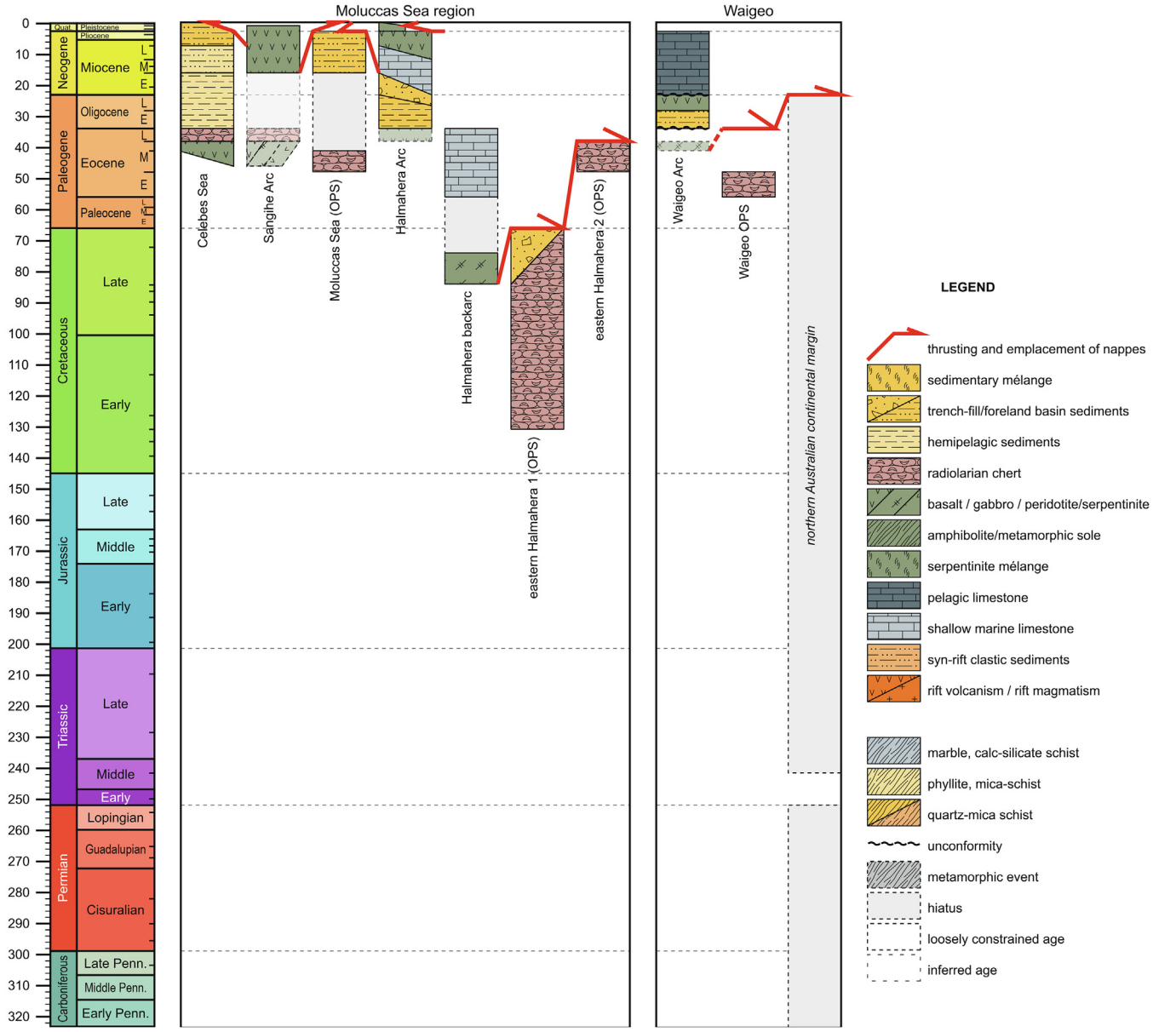

Fig. 16. Tectonostratigraphy of the Molucca Sea and Waigeo. Geologic Time Scale from Gradstein et al. (2012).

sedimentary arc sequences, intruded by an Oligocene diorite, and overlain by Miocene clastic, carbonate, and volcanic rocks, interpreted as part of the Philippine Mobile Belt. The island hosts several active stratovolcanoes, that expose basaltic-dacitic lavas with K–Ar whole rock ages of 1.97–0.28 Ma (Sajona et al., 2000). Eastward subduction of eastern Sulu Sea along the Negros Trench is interpreted to have started in the latest Miocene or Pliocene (Roeser, 1991; Silver and Rangin, 1991), coeval with the Late Miocene onset of NE-SW extension in the western Sulu Sea (Graves and Swauger, 1997; Tamesis, 1990). Current seismicity (Cardwell et al., 1980; Yumul et al., 2013) and seismic tomography of the upper mantle (Rangin et al., 1999) indicates that subduction has remained limited to ~100 km, similar to the estimated underthrusting at the Mindoro Suture Zone.

The Negros Trench links up with the NW-SE striking **Siayan-Sindangan Suture Zone** (Fig. 14) that is bounded by active strike-slip faults crosscutting the island of Mindanao (Pubellier et al., 1991; Yumul et al., 2004). At this suture the Sulu Arc continental basement underthrusts ophiolites overlain by a Middle Miocene arc exposed on northeast Mindanao (Sajona et al., 1997; Yumul et al., 2004). The suture exposes a serpentinite mélange with blocks of harzburgite with chromitite, gabbro, basalt, and chert (Yumul et al., 2004) likely derived from the upper plate oceanic lithosphere of the Philippine Mobile Belt, and a Middle Miocene shale-hosted matrix (Pubellier et al., 1991) with blocks of sandstone, andesite, metamorphic rocks, and Upper Oligocene–Lower Miocene limestone derived from the Sulu Arc (Yumul et al., 2004). The Siayan-Sindangan Suture Zone is unconformably overlain by upper Middle Miocene basaltic-andesitic flows and breccias, Upper Miocene limestone, basaltic lava and volcaniclastic rocks, and unconformably overlying Pliocene volcanic rocks (Yumul et al., 2004). After thrusting, the suture was reactivated in the Late Miocene as a sinistral strike-slip fault zone that forms the **Sindangan-Cotabato-Daguma Lineament** (Pubellier et al., 1996; Quebral et al., 1996). We interpret subduction along the Siayan-Sindangan Suture Zone between the Middle–Late Miocene, and sinistral strike-slip motion along the Sindangan-Cotabato-Daguma Lineament since the Late Miocene–Early Pliocene.

The Sindangan-Cotabato-Daguma Lineament links up to the southeast with the Sangihe backthrust and **Sangihe Arc** (Lallemand et al., 1998; Rangin et al., 1996) that forms the eastern boundary of the Celebes Sea (Figs. 14 and 16). The Sangihe Arc comprises over 25 Quaternary volcanic edifices, of which the eight currently active volcanoes are confined to the southern part of the arc (Fig. 14), and formed above a west-dipping subduction zone that is well imaged in seismic tomography to a depth of ~675 ± 50 km (Hall and Spakman, 2002; Rangin et al., 1999; Van der Meer et al., 2018; Widiyantoro and van der Hilst, 1997). The Sangihe Arc exposes andesites with K–Ar ages of 15.64–0.93 Ma (Morrice et al., 1983). The arc continues farther south onto the northeastern tip of the North Arm of Sulawesi, where volcanic rocks yielded similar K-Ar ages of 15.12–2.59 Ma (Elburg and Foden, 1998). To the east of the Sangihe Arc, its fore-arc is exposed on Talaud Island (Fig. 1) (Moore et al., 1981; Rangin et al., 1996), where it has completely consumed the oceanic lithosphere of the Molucca Sea Plate, and is thrusted over the Halmahera fore-arc (see below). The structurally highest unit of the Sangihe fore-arc is formed by a dismembered ophiolite suite with serpentinized peridotites, gabbro, basaltic pillow lava, and undated chert (Fig. 16). This ophiolite is structurally underlain by a Middle Miocene–Pleistocene sequence of marine volcaniclastic sedimentary rockss and andesitic volcanic rocks. The structurally lowest unit is a red shale mélange with blocks of ultramafics, gabbro, basalt, shale, sandstone, and Middle Eocene (Lutetian) radiolarian-bearing red chert and limestone (Moore et al., 1981) that provide a minimum age constraint for the subducted lithosphere of the Molucca Sea Plate. Pleistocene coral limestone and alluvium unconformably cover the older units (Moore et al., 1981). Based on the geologic record of the Sangihe Arc and its forearc on Talaud Island (Elburg and Foden, 1998; Moore et al., 1981; Morrice et al., 1983), we follow Hall (Hall, 2002, 2000) and interpret that subduction started at the end of the Early Miocene.

Along the northernwestern part of the Sangihe Arc, the northeastern Celebes Sea is subducting eastward below the NW-SE trending **Cotabato Trench** (Rangin et al., 1996) offshore southwest Mindanao (Figs. 1 and 14). Seismic sections through the Cotabato Trench show a west-verging accretionary prism in the lower slope, and west-dipping normal faults in the upper slope (Schlüter et al., 2001). The accretionary prism is overlain by a forearc basin comprising of sediments of assumed Late Miocene to Holocene age, while Middle Miocene sedimentary rocks are thrusted below the fore-arc (Schlüter et al., 2001). Current seismicity indicates that the slab has reached a depth of < 100 km (Cardwell et al., 1980) (Table S1), similar as towards the north. The Cotabato Trench gradually disappears southward, and its displacement is instead accommodated at the Sangihe Trench and the former Halmahera trench (Fig. 14).

The **Molucca Sea Plate** was not only consumed by westward subduction below the Sangiye Arc and forearc, but also by eastward subduction below the Halmahera Arc that is constructed on the Philippine Sea Plate. The lithosphere of the Molucca Sea Plate in entirely covered by the accretionary complexes of the Sangihe fore-arc and the Halmahera fore-arc (Mccaffrey et al., 1980; Silver and Moore, 1978). Seismic tomography images the Halmahera Slab to a depth of 760 ± 100 km (Hall and Spakman, 2015, 2003, 2002; Rangin et al., 1999; Van der Meer et al., 2018; Widiyantoro and van der Hilst, 1997; Wu et al., 2016). This restores the Molucca Sea as an oceanic basin that was at least ~1500–1600 km wide (Wu et al., 2016) prior to bivergent subduction initiation in the Middle Miocene (see below).

The **Halmahera Arc** forms the western active margin of the Philippine Sea Plate and extends from Morotai and Halmahera in the north to Bacan and Obi islands in the south, where it connects to the Sorong Fault Zone (Section 4.11) (Malaihollo and Hall, 1996). On eastern Halmahera (Fig. 16), the Halmahera Arc is underlain by a basement comprising imbricated tectonic slices of Lower–Upper Cretaceous (Barremian–Maastrichtian) and Middle Eocene pelagic radiolarian-bearing limestones, Upper Cretaceous (Campanian–M aastrichtian) proximal volcaniclastic sedimentary rocks, and Lower–Middle Eocene shallow marine limestones (Hall et al., 1988a), that we interpret as OPS sequence, trench-fill, and forearc basin deposits, respectively. This sequence is tectonically intercalated with rare metamorphic rocks (including black slate, metachert, metacarbonates, greenschist, blueschist, and amphibolite), and SSZ ophiolitic lithologies (including serpentinized peridotites, boninitic diorite with an $^{40}Ar/^{39}Ar$ hornblende age of 87.3 ± 7.0 M a and SSZ diorite with a $^{40}Ar/^{39}Ar$ hornblende age of 73.8 ± 1.5 Ma, pillow lava and basaltic tuff (Ballantyne, 1992, 1991; Hall et al., 1996, 1988a)). Hall et al. (1988a) interpreted this assemblage as a Late Cretaceous to Paleogene east-facing forearc. In contrast, southern Bacan and Obi expose an pre-Oligocene continental basement of Australian derivation that comprises a diorite with a U–Pb zircon age of 329.8 ± 2.7 Ma, micaceous sandstones with a maximum depositional age of 159 Ma, and amphibolite facies (~5 kbar, 600 °C) metasedimentary gneiss with a maximum depositional age of 87 Ma (Decker et al., 2017; Hall et al., 1988a; Malaihollo and Hall, 1996). This continental basement is juxtaposed to the forearc basement of north Bacan and Halmahera by the Molucca-Sorong Fault splay of the Sorong Fault Zone (Hall et al., 1988a; Malaihollo and Hall, 1996; Saputra et al., 2014). The forearc consists of oceanic basement that is unconformably overlain by Oligocene marl, and Upper Oligocene–Lower Miocene conglomerate with clasts of the underlying oceanic basement. The conglomerate grades into Lower–Upper Miocene shallow marine limestone with volcaniclastic detritus that locally unconformably overlies the basement. This sequence is overlain by a Upper Miocene–Lower Pliocene marls, volcaniclastic sandstones and volcanic rocks (Hall et al., 1988b; Nichols and Hall, 1991). Arc activity commenced at 11.5 ± 0.5 Ma on Obi and migrated northward to Bacan at 7.5 ± 1.0 Ma, whilst arc activity on Halmahera was synchronous with that on Bacan and was continuously active between 7.8 and 4.0 Ma (Baker and Malaihollo, 1996). Based on this earliest arc activity at ~11 Ma, Baker and Malaihollo (1996) argued that eastward subduction of the Molucca Sea Plate below the Philippine Sea Plate started around 17–15 Ma, coinciding with a thermal event at ~15 Ma recorded on Bacan (Decker et al., 2017; Malaihollo and Hall, 1996). The Oligocene–Lower Pliocene sequence is intensely folded and faulted, and is unconformably overlain by Upper Pliocene–Middle Pleistocene volcanic rocks and Quaternary coral reefs (Baker and Malaihollo, 1996; Hall et al., 1988b; Nichols and Hall, 1991). Late Pliocene–Early Pleistocene (3.0–1.8 Ma) volcanic activity shifted ~50 km westward, interpreted to be the consequence of ~60 km westward thrusting of the back-arc over the Halmahera Arc during collision of the Halmahera fore-arc with the Sangihe fore-arc in the Pliocene (Baker and Malaihollo, 1996; Hall, 2000; Nichols and Hall, 1991). The present active calc-alkaline intra-oceanic volcanic arc passing through the islands of Ternate and Tidore (Morris et al., 1983) is built on tilted fault blocks (Verstappen, 1964) located ~30 km west of Halmahera and became active in the Middle Pleistocene (Baker and Malaihollo, 1996; Hall et al., 1988b).

The Halmahera Trench connects to splays of the **Sorong Fault Zone** that bound and crosscut the islands of Bacan and Obi (Figs. 1 and 14). Quaternary volcanic activity on Bacan and Obi is concentrated along these fault splays (Baker and Malaihollo, 1996; Malaihollo and Hall, 1996; Silitonga, 1981) and the volcanic products have geochemical composition that suggests eruption through continental crust (Morris et al., 1983). The Sorong Fault Zone continues farther east, along the northern coast of Misool (Section 4.11) and the southern coast of the island of Waigeo, where

it forms the southern boundary of the Philippine Sea Plate. The island of Waigeo exposes dismembered ophiolites that are tectonically intercalated with Lower Eocene radiolarian chert (Charlton et al., 1991c; Ling et al., 1991). This assemblage is unconformably overlain by sandstone with ophiolitic detritus, Lower Oligocene volcaniclastic sandstone, Upper Oligocene calc-alkaline island arc basalt (Fig. 16). The ophiolite and the overlying sequence shows intense deformation with E-W trending tight folds, and is unconformably overlain by Lower Miocene–Pliocene deep marine limestone (Charlton et al., 1991c). Charlton et al. (1991c) interpreted that Waigeo hosted an intra-oceanic arc that collided with the passive continental margin of northern Australia in the Late Oligocene–Early Miocene, and was subsequently deformed by sinistral strike-slip motion along the Sorong Fault Zone that resulted in 20 km NE-SW shortening in the Pliocene. The Sorong Fault Zone continues farther east into the Bird's Head, where it juxtaposes an Lower–Upper Oligocene island arc to Australian continental crust, north and south of the Sorong Fault Zone respectively (Gold et al., 2014, 2017; Pieters et al., 1983). Both the island arc terrane in the north and the Australian continental crust in the south are unconformably overlain by Lower–Middle Miocene limestone and Upper Miocene deep marine fine grained siliciclastic and carbonate rocks (Gold et al., 2017) constraining the arrival of the Australian margin at the trench to the earliest Miocene (Aquitanian). Estimated sinistral displacement along the Sorong Fault was 90–150 km (Saputra et al., 2014) during the Late Pliocene and Pleistocene. However, Riadini et al. (2009) suggested that the Sorong Fault Zone also underwent a transpressional event during the Middle–Late Miocene, and Gold et al. (2014) and Webb et al. (2019) estimated sinistral displacement of 260–300 km during the Late Miocene–Early Pliocene (10.5–4.5 Ma). Collectively, these data suggest that the Sorong Fault Zone reactivated a Lower Miocene plate boundary between Australia and the Philippine Sea Plate that is found along the northern margin of the Bird's Head and the rest of New Guinea (see van de Lagemaat and van Hinsbergen, 2024).

5. Kinematic restoration tested against paleomagnetic data

5.1. Paleomagnetic database of SE Asia

To test our reconstruction against paleolatitudinal and vertical axis rotation constraints, we compiled a database of all published paleomagnetic studies in SE Asia. For this compilation, we adopted lenient criteria and only excluded poles if they (1) were not used by the original authors if the reason for exclusion is provided; (2) are characterized by<4 samples (or 4 sub-sites in cases of volcanic rocks); (3) have *K* or *k*-values (precision parameters of Fisher (1953) on poles or associated directions, respectively) below 7. In addition, we excluded sites with an *A*95 outside the $A95_{min-max}$ confidence envelope of Deenen et al. (2011).

Where available, we compiled paleomagnetic data based on the original specimen directions. Where these data were not available, we compiled the data by parametric sampling using paleomagnetism.org (Koymans et al., 2020, 2016). Where not explicitly mentioned, we assumed that paleomagnetic directions from sediments (given in green datapoints) were corrected for bedding tilt. For volcanic rocks, when tilt-correction was explicitly mentioned, we color-coded these results purple in our figures. All other igneous rocks, in which no bedding is visible, are colored orange. Paleomagnetic sites that did not pass the compilation criteria are not shown on maps or diagrams. The paleomagnetic compilation is given in Paleomagnetism.org 2.0 format (Koymans et al., 2020) as well as in a Table S2 after applying the above-mentioned criteria and is provided in Supplementary Information 2 and 3.

Ages of rocks sampled for paleomagnetism in SE Asia are often poorly constrained. Igneous rocks sampled for paleomagnetism were seldomly directly dated by the original authors, but assigned an age based on lithostratigraphic correlations or ages assigned on geological maps. Where radiometric ages are available, these are often K–Ar ages (e.g. Haile et al., 1977) or zircon fission track ages (e.g. Sasajima et al., 1980), and the errors are not always provided. Most paleomagnetic studies only reported the age of the sampled sedimentary rocks at system level for the Mesozoic or series level for the Cenozoic (e.g. Fuller et al., 1999). However, in recent years, age ranges of the sedimentary sequences have become better constrained by new biostratigraphic studies, and igneous rocks have been dated by modern radiometric methods, including the U–Pb method and the $^{40}Ar/^{39}Ar$ method. Where available, we have assigned these better-constrained ages to the paleomagnetic sampled rock units.

5.2. Paleomagnetic tests of the reconstruction

Based on the reconstruction steps outlined in Section 3, and the kinematic constraints reviewed in Section 4 and Table S1, we developed a geometrically consistent kinematic restoration, whereby we used a simplest case scenario for motions in absence of kinematic constraints (e.g., minimum shortening). We now test our reconstruction against the paleomagnetic database by rotating the GAPWaP of Vaes et al. (2023) into the coordinates of our reconstructed blocks, using Paleomagnetism.org and methods outlined in Li et al. (2017) and Koymans et al. (2020). With our paleomagnetic compilation, we were able to test for paleolatitude and large-scale vertical axis rotations of relatively undeformed parts of the West Burma Block, SW Borneo Mega-Unit, Kuching Zone, and Greater Paternoster Mega-Unit (Kutai Basin, Celebes Sea, West Sulawesi, Sumba). For intensely deformed accreted units (e.g., Woyla Arc, Sula Spur, Australian margin) we could use the paleomagnetic database only to test for paleolatitude (see Supplementary Information 1, Figs. S7–S10, S13). Below, we briefly describe the paleomagnetic tests, and the paleomagnetism-based modifications of the reconstruction (Tables 1 and 2). When paleomagnetic data clearly falsified our simplest case reconstruction, we modified the reconstruction to fit paleomagnetic data, within the compiled structural geology and marine magnetic anomaly constraints.

Our reconstruction incorporates the restoration of rotations of **Indochina** as detailed in Li et al. (2017), that restore a ~15° counterclockwise rotation of Indochina and the Thai Peninsula between 20 Ma and 30 Ma. We incorporated part of the paleomagnetic database compiled by Advokaat et al. (2018b) for **Sundaland** from Mesozoic–Cenozoic rocks. Paleomagnetic data from Mesozoic rocks in *Peninsular Malaysia* show large clockwise and counterclockwise declinations (Haile et al., 1983; Otofuji et al., 2017; Richter et al., 1999). Advokaat et al. (2018b) attributed these directions to local vertical axis rotations caused by strike-slip faulting, and we did not specifically restore these local rotations, but only the documented strike-slip displacements. Richter et al. (1999) concluded that the timing of magnetization is poorly understood, and block rotations giving rise to these directions are correspondingly weakly constrained. For this reason, we decided to discard the paleomagnetic dataset from Peninsular Malaysia.

Sites from Mesozoic–Cenozoic rocks in *Sumatra* do not show significant rotations relative to north (Fig. S2), and our restoration thus rotates western Sundaland 15° counterclockwise relative to Indochina, following Advokaat et al. (2018b). To this dataset we added six paleomagnetic sites from Permian–Triassic rocks in Sumatra (Haile, 1979; Sasajima et al., 1978). These sites show that both the West Sumatra Block and the Sibumasu Block, to the west and east of the Medial Sumatran Tectonic Zone respectively, were

Table 1
Paleomagnetic constraints on vertical axis rotations.

Region	Site Latitude (°)	Site Longitude (°)	Mean Dec (°)	dDx (°)	Mean Inc (°)	dIx (°)	n	Pole Longitude (°)	Pole Latitude (°)	A95 (°)	mean age (Ma)	minimum age (Ma)	maximum age (Ma)
West Burma													
Yaw Fm (SA)	23.243	94.263	17.4	2.7	7.1	5.3	161	230.8	64.4	2.7	38.50	37.80	38.40
Magwe Volcanics (SA)	19.939	94.103	50.8	3.0	33.1	12.6	31	174.0	42.5	8.1	64.43	64.06	64.80
Kanza Chang Batholith (SA)	24.233	95.611	65.5	7.5	0.6	9.2	45	198.1	16.4	4.6	98.50	91.00	106.00
Sumba													
Sumba Fm (SA)	−9.740	120.067	358.7	3.4	−23.6	3.9	160	322.6	87.0	2.2	9.80	3.60	16.00
Jawila Fm (SA)	−9.588	119.386	5.4	3.8	−22.2	5.5	130	231.6	83.0	3.1	37.40	31.30	43.50
Tanadoro Fm (SA)	−9.558	119.587	44.2	6.0	−22.5	6.7	64	217.8	46.8	3.8	62.85	59.20	66.50
Massu Fm (SA)	−10.000	120.100	90.1	4.7	−9.1	8.0	94	217.9	12.8	4.1	80.75	76.10	85.40
Lasipu Fm (SA)	−9.750	119.671	44.7	3.5	−25.0	4.4	147	219.5	45.8	2.5	80.95	72.10	89.80
Misool													
Fafanlap Fm (SA)	−1.986	130.326	353.8	3.5	−34.1	5.0	51	328.7	71.7	3.3	69.00	66.00	72.10
Waaf limestone (SA)	−2.135	130.196	315.0	4.0	−39.9	5.1	37	10.4	41.7	3.7	84.90	83.60	86.30
Palawan													
Espina Basalt (SA)	9.042	118.042	296.0		2.4		38	25.0	25.8	4.5	83.00	66.00	100.50

SA, sample average; n, number of samples.

Table 2
APWP of Borneo based on paleomagnetic data.

n	Pole Longitude (°)	Pole Latitude (°)	A95 (°)	Age (Ma)	mean age (Ma)
11	84.8	86.8	5.6	0	2.7
20	102.1	87.6	5.9	5	5.7
50	181.9	83.1	5.4	10	12.4
91	30.0	84.8	4.3	15	15.1
77	25.7	77.8	3.4	20	19.7
38	29.5	81.7	4.2	25	23.6
14	16.1	70.4	5.6	30	32.9
44	19.8	67.6	4.8	35	38.6
30	21.2	66.2	6.7	40	36.9
22	40.8	42.9	5.7	45	47.0

n, number of samples.

located at a paleolatitude of ~15°S in the Late Permian–Middle Triassic (Fig. S2).

Paleomagnetic data from the **West Burma Block** were derived from mid-Cretaceous granites, mid-Cretaceous volcanic rocks, undated sedimentary rocks of assumed Lower or Upper Cretaceous age, Lower Paleocene to Middle Miocene clastic and volcaniclastic sedimentary rocks and Oligocene volcanic rocks (Li et al., 2020c; Westerweel et al., 2020, 2019) and Pleistocene to recent volcanic rocks (Richter et al., 1993) in the Central Myanmar Basin. Structural geological and marine magnetic anomaly data from the Andaman Sea and eastern Myanmar show that in Oligocene time (~27.5 Ma), the West Burma block was adjacent to northern Sumatra (Curray, 2005; Morley, 2017b; Morley and Arboit, 2019), but provide no constraints before that time, other than that there are Cretaceous oceanic rocks exposed along the Sagaing Fault (Lai et al., 2018; Suzuki et al., 2020), suggesting younger suturing between the West-Burma Block and Myanmar. When attaching the West Burma Block to the Australian plate prior to 27.5 Ma, a good fit is obtained with the paleomagnetic data (Westerweel et al., 2019) (Fig. 17). In addition, the data of Westerweel et al. (2019) and Li et al. (2020) suggest that the West Burma Block underwent a major clockwise rotation of ~90° in Paleogene time. We used this rotation as input for our reconstruction and accommodated it by moving the modern northern top of the West Burma Block with the Indian plate while keeping the modern southern tip attached to the Australian plate between 66 and 44 Ma (Fig. 17). This reconstruction predicts a collision between the West-Burma Block in the downgoing Australian plate and the Andaman Ophiolites in the Sunda forearc in the Paleocene, consistent with evidence for uplift of the Andaman ophiolites and the arrival of West-Burma-derived sediments onto the Andaman ophiolites around this time (Bandopadhyay et al., 2022). Prior to this time, West Burma as part of the Australian plate would have moved from west to east at a stable paleolatitude, satisfying the paleomagnetic constraints of Westerweel et al. (2019).

The rotation of **Borneo** plays a prominent role in the tectonic evolution of SE Asia. Structural geologic constraints indicate that Borneo's convergence with the South China Sea that is required to accommodate Borneo's rotation had ceased by 16 Ma (Aurelio et al., 2014), but there are no direct structural geological constraints that demonstrate the onset of Borneo's rotation history. Here we used paleomagnetic data as input for the reconstruction, whereby we follow the paleomagnetic constraints provided by and compiled in Advokaat et al. (2018b) from Mesozoic– Cenozoic rocks in Borneo. To this dataset we added four sites that were recovered from ODP drill site 770 in the **Celebes Sea** (Shibuya et al., 1991). Shibuya et al., 1991) used the low-temperature overprint as correction for the declination of the ChRM and determined declinations of ~315–320° for the Eocene, ~335° for the Lower Oligocene and ~345° for the Upper Oligocene–Lower Miocene. These estimates are consistent with the predicted APWP for Borneo in our reconstruction (Fig. 18). Advokaat et al. (2018b) reconstructed two phases of Cenozoic counterclockwise rotation for Borneo, whereby the first ~30° counterclockwise rotation occurred between ~41 Ma and 34 Ma. In our reconstruction we modified the start of this rotation to 45.7 Ma (corresponding to marine magnetic anomaly C21). This coincides with opening of the Celebes Sea and reduces latitudinal motion of the North Arm of Sulawesi. This

is permitted by and consistent with the paleomagnetic data. Advokaat et al. (2018b) reconstructed the second phase of ~13° counterclockwise rotation between 23.0 Ma to present day. We changed the end of this rotation to 16.0 Ma, as there is no evidence for significant convergence between Borneo and the South China Sea after this time (Aurelio et al., 2014). This choice also satisfies paleomagnetic constraints (Fig. 18). The paleomagnetic data also suggest that the Kuching Zone and the SW Borneo Mega-Unit underwent a counterclockwise rotation and were located at different paleolatitudes prior to their amalgamation. To satisfy these paleomagnetic constraints, we restore a ~35° counterclockwise rotation of the SW Borneo Mega-Unit and a 60° counterclockwise rotation of the Kuching Zone during their collision (Figs. S3 and S4).

Paleomagnetic data from Cretaceous and Paleogene sites in **West Sulawesi** yielded declinations of ~335°, while Neogene sites show no significant rotations (Haile, 1978a; Kwong, 2011; Sasajima et al., 1980). These declinations are consistent with our kinematic reconstruction based on structural geological constraints. All paleomagnetic sites yielded near-equatorial southern hemisphere paleolatitudes consistent with our prediction (Fig. S5). A large paleomagnetic dataset from **Sumba** was collected from Upper Cretaceous sedimentary rocks, Upper Cretaceous–Middle Paleocene intrusions and Upper Eocene–Lower Eocene volcanic rocks (Chamalaun and Sunata, 1982; Fortuin et al., 1997; Otofuji et al., 1981b; Wensink, 1997, 1994; Wensink and van Bergen, 1995). Upper Cretaceous volcanic rocks from eastern Sumba suggest a 90° clockwise rotation (Wensink, 1994), but these were sampled in an area affected by normal faulting (Fleury et al., 2009). However, Upper Cretaceous volcaniclastic sedimentary rocks sampled all over Sumba and Upper Cretaceous–Middle Paleocene intrusions reveal a smaller 45° clockwise rotation (Wensink, 1997), which was completed by the Oligocene as suggested by paleomagnetic data from Middle Eocene–Lower Oligocene volcanic rocks (Wensink and van Bergen, 1995). This rotation does not follow from (but is permitted by) kinematic data. To restore this rotation consistent with the paleomagnetic data, we close the Savu

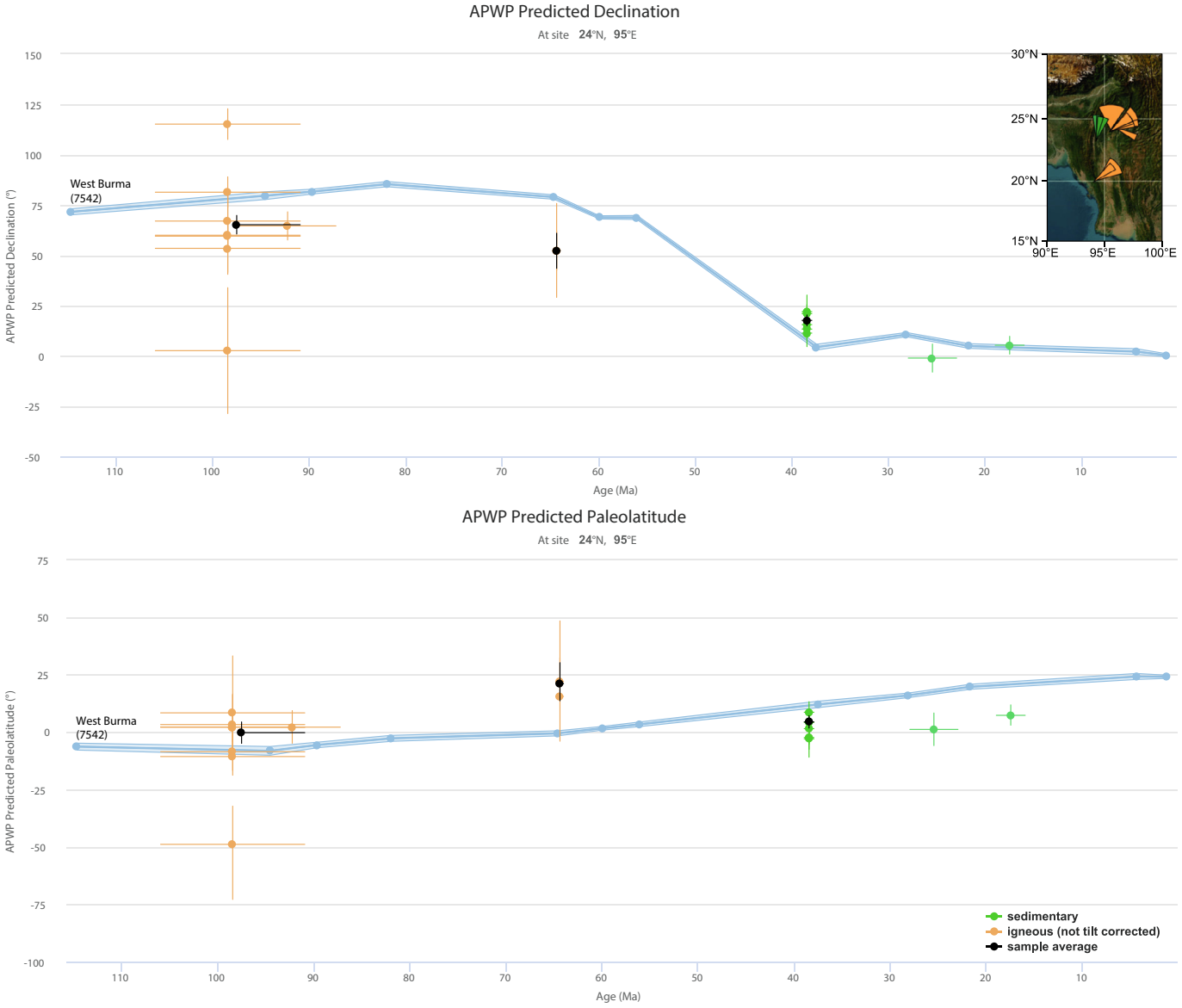

Fig. 17. Paleomagnetic data from West Burma, declination versus age diagram and paleolatitude vs age diagram. Color coding according to lithology (green: sedimentary; orange: igneous, not tilt corrected; black: sample average of sampled formation). Blue curves show the GAPWaP of Vaes et al. (2023) rotated in the coordinates of West Burma (7542).

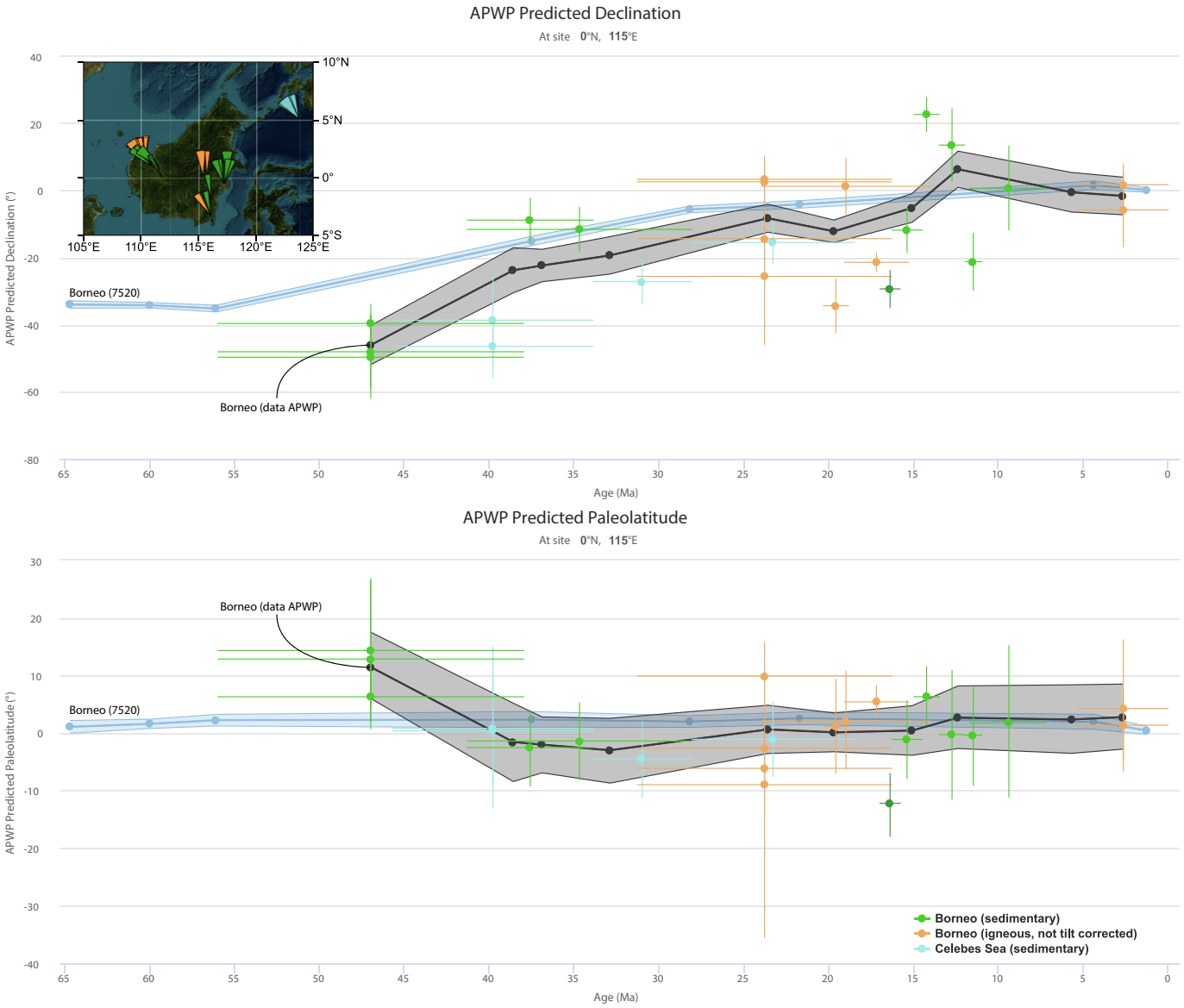

Fig. 18. Paleomagnetic data from Borneo and the Celebes Sea, declination versus age diagram and paleolatitude vs age diagram. Color coding according to lithology (green: sedimentary; orange: igneous, not tilt corrected) and provenance (turquoise: Celebes Sea, sedimentary). Dark grey curve shows the APWP of Borneo based on paleomagnetic data in a 10 Ma sliding window over 5 Ma intervals, calculated for true mean age (Table 1). Blue curve shows the GAPWaP of Vaes et al. (2023) rotated in the coordinates of Borneo (7520) (blue curve).

Basin between 2.0 Ma and 16.0 Ma along a rotation pole in the western end of the basin and close the Flores Basin along a rotation pole in the western end of the basin during the Eocene-Paleocene (33.9–66.0 Ma). This reconstruction satisfies paleolatitudes from Sumba (Fig. 19). Paleomagnetic data from the **Timor Allochthon** were sampled in Eocene Metan and Quelicai volcanics and Upper Miocene Manamas and Oecussi volcanics (Chamalaun and Sunata, 1982; Wensink and Hartosukohardjo, 1990a) that also yielded paleolatitudes consistent with our reconstruction of Sumba (Fig. S7).

Large collections of paleomagnetic data from the **North Arm of Sulawesi** were predominantly sampled in igneous lithologies that did not allow for bedding correction. Moreover, many of these sites were sampled in strike-slip fault zones (Otofuji et al., 1981a; Sasajima et al., 1980; Surmont et al., 1994) creating additional scatter in the declination (see discussion in Surmont et al., 1994). Three paleomagnetic sites in Middle Eocene–lowermost Miocene sedimentary rocks yielded equatorial paleolatitudes (Surmont et al., 1994), consistent with our reconstruction (Fig. S8).

Paleomagnetic data from the northern margin of the **Sula Spur** come from Valanginian–lower Cenomanian radiolarian cherts and Upper Cretaceous basalts in *SE Sulawesi*, that yield a paleolatitudes of 16–26°S after tilt correction (Mubroto et al., 1994), consistent with our reconstruction (Fig. S9). Upper Cretaceous (Coniacian–Santonian) shales from *Banggai Sula* yielded a paleolatitude of ~20°S (Ali and Hall, 1995), consistent with our reconstruction (Fig. S9). Upper Cretaceous (Maastrichtian) shales from *Misool* (Wensink et al., 1989) yielded paleolatitudes and declinations that are consistent with our reconstruction of the Bird's Head, whereby we reconstructed a ~10° counterclockwise rotational shortening in the Early Miocene (Fraser et al., 1993; Froidevaux, 1974; Pigram et al., 1982) that is also consistent with paleomagnetic data (Fig. S10). We note that Upper Cretaceous (Santonian) limestones (Wensink et al., 1989) sampled near the edge of the Misool-Onin-Kumawa Ridge also yielded paleolatitudes that are consistent with our reconstruction, but their declination suggests larger counterclockwise rotations (Fig. S11). We interpret this as local rotation near the deformation front of the transpressive Seram-Fold Thrust

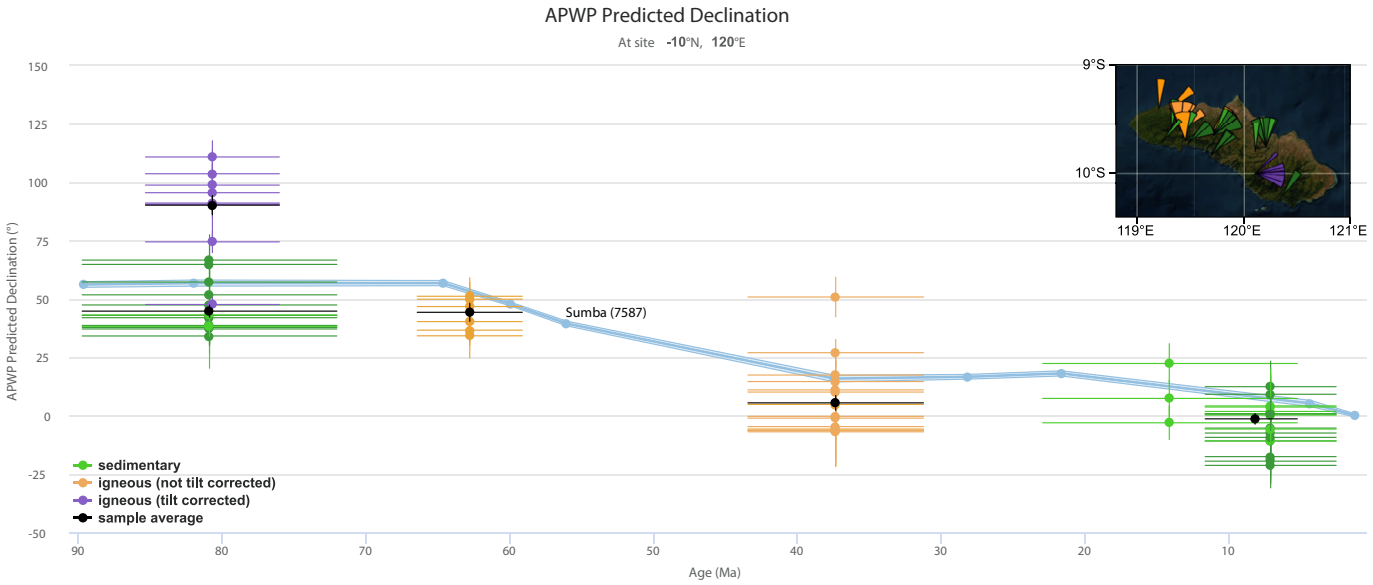

Fig. 19. Paleomagnetic data from Sumba, declination versus age diagram. Color coding according to lithology (green: sedimentary; orange: igneous, not tilt corrected, purple; igneous, tilt corrected; black: sample average of sampled formation). Blue curves show the GAPWaP of Vaes et al. (2023) rotated in the coordinates of Sumba (7587).

Belt. Paleomagnetic data from *Seram* were collected from Upper Triassic shales and Upper Miocene volcanic rocks (Haile, 1978), which yielded paleolatitudes that are consistent with our reconstruction, but both sites show declinations that significantly deviate from our prediction (Fig. S12). We interpret these as local rotations induced by the sinistral, Pliocene Kawa Shear Zone (Pownall et al., 2013, 2017a).

Paleomagnetic data from the **Australian margin units** of Timor come from the Kolbano Sequence and the Gondwana Series (Chamalaun, 1977a, 1977b; Chamalaun and Sunata, 1982; Wensink et al., 1987; Wensink and Hartosukohardjo, 1990b). Paleomagnetic data from Gondwana Series were sampled in Lower Permian (Artinskian–Kungurian) redbeds of the Cribas Formation in East Timor (Chamalaun, 1977a), Lower Permian (Sakmarian–Kungurian) limestones of the Maubisse Formation and Upper Triassic (Carnian–Norian) radiolarian calcilutites of the Aituto Formation in West Timor (Chamalaun, 1977b; Wensink and Hartosukohardjo, 1990b), while the Kolbano Sequence was sampled in intensely deformed Lower Cretaceous (Berriasian–Aptian) calcilutites of the Nakfunu Formation (Wensink et al., 1987) and Lower Cretaceous (Aptian–Albian) calcilutites of the Wai Bua Formation (Chamalaun and Sunata, 1982). All yielded paleolatitudes that cluster around or north of the predicted APWP of Australia (Fig. S13).

Finally, four lava sites from the Upper Cretaceous Espina Basalts on **Palawan** yielded reliable paleomagnetic directions, suggesting a near-equatorial paleolatitude (Almasco et al., 2000), south of the reconstructed position of Palawan Terrane and overlapping with Cagayan Arc (Fig. S14). This suggests that these basalts were formed in the proto-South China Sea close to the Palawan Ophiolite and became accreted to the base of the Palawan Ophiolite shortly after subduction initiation, consistent with the geologic record in the Palawan Accretionary Complex (Section 4.13, Fig. 13).

6. Stepwise reconstruction of SE Asia: Finding Argoland

We present our reconstruction of the SE Asian region in a series of paleo-tectonic maps starting from the present back to the Late Triassic (Figs. 20–54). We present our maps at regular time intervals of 5 million years (between present and 155 Ma), and 20 million years (between 155 Ma and 215 Ma). These maps are projected in the paleomagnetic reference frame of Vaes et al. (2023), so they can be directly used for paleoclimate studies (van Hinsbergen et al., 2015). The paleotectonic maps are also available in Supplementary Information 4, GPlates files are available in Supplementary Information 5, and animations are available in Supplementary Information 6. We show the reconstruction backward in time by describing the paleogeographic consequences of reconstructing the main events that are reconstructed at the discussed time step compared to the previous time step. We identify where our reconstruction systematically deviates from selected previously published reconstructions that we believe are representative for the various schools of thought. These include Gibbons et al. (2012), Hall (2012, 2002, 1996), Heine et al. (2004, 2002), Heine and Müller (2005), Hinschberger et al. (2005), Jablonski and Saitta (2004), Lee and Lawver (1995, 1994), Longley et al. (2002), Metcalfe (2013a, 2011a, 2011b, 1996, 1990), Rangin et al. (1990b), Spakman and Hall (2010), van Hinsbergen et al. (2011), Zahirovic et al. (2016, 2014), and Zhang et al. (2020b).

6.1. Zanclean – 5 Ma

Around 5 million years ago (Fig. 21), several tectonic events occurred that have major implications for our reconstruction farther back in time, especially in eastern Indonesia (see Sections 6.6 and 6.7). In the Banda region, the Banda arc and fore-arc, which migrated south- and eastward during N-S opening of the South Banda Basin, WNW-ESE extension in the Weber Deep, and sinistral slip along the Kawa Shear Zone in Seram, respectively, are reconstructed farther north- and westward. Between the Kay islands and Leti island, this resulted in a Banda Embayment with a reconstructed width increasing from 100 km in the east to 350 km in the west. At 5 Ma, northward subduction of the Banda Embayment below the Banda Arc was ongoing. Further to the west, ~150 km of NNW-SSE shortening in Timor is restored, resulting in Timor forming a promontory of the northern Australian continental margin. As a result, the reconstructed N-S distance between the Timor promontory and the Sula Spur promontory is only ~110 km.

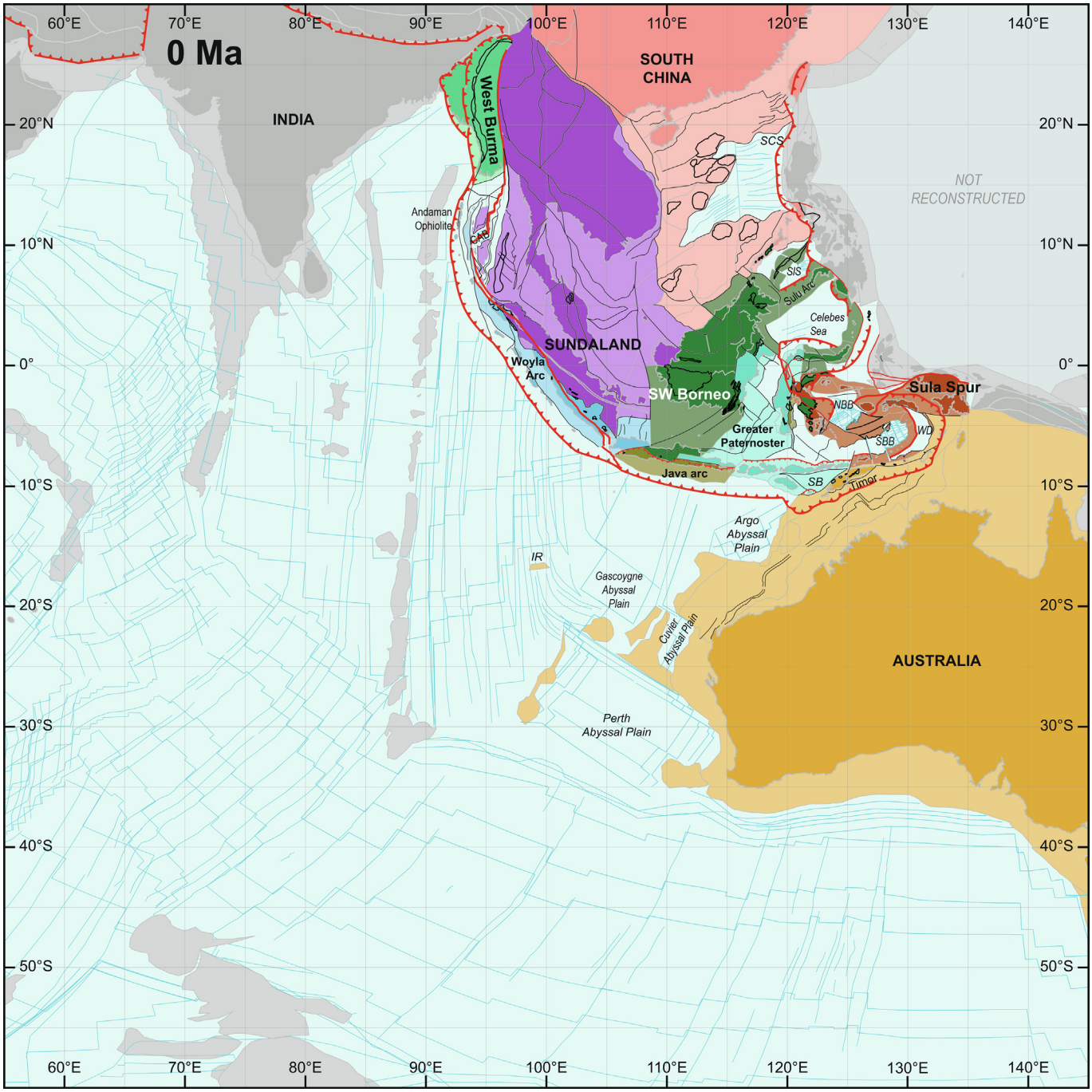

Fig. 20. Tectonic map for the Holocene (0 Ma). Abbreviations: CAB, Central Andaman Basin; IR, Investigator Ridge; SB, Savu Basin; NBB, North Banda Basin; SBB, South Banda Basin; SCS, South China Sea; SlS, Sulu Sea; WD, Weber Deep.

In Sulawesi, up to ~150 km southward subduction of the Celebes Sea is restored, which was accommodated by N-S extension in Gorontalo Bay and exhumation of the Palu, Tokorondo, and Pampangeo metamorphic complexes, dextral strike-slip faulting on the Palu-Koro Fault, and clockwise rotation of the North Arm of Sulawesi. The North Sulawesi Trench is reconstructed farther south in a position that lines up with the West Sulawesi continental margin, and is nearby the reconstructed position of the fossil spreading ridge in the Celebes Sea. This suggest the North Sulawesi Trench may have been formed by inversion of a mid-ocean ridge (see Section 7.1). At 5 Ma, the first sediments derived from the Banggai-Sula Bock entered the trench below the East Sulawesi Ophiolite. The Banggai Sula Block is restored in a position ~300 km farther to the southeast, with the continental margin close to the Batui Thrust. This westward motion of the Banggai-Sulu Block was accommodated by extension within the Banggai-Sulu Block and sinistral motion along the Sorong Fault Zone and the Buru Fracture Zone.

Along the western Sundaland margin, the West Burma Block is located 118 km farther south, by fully restoring N-S oceanic spreading in the Central Andaman Basin (Raju et al., 2004). sinistral strike-slip motion on the Sumatra Fault System. This is about half of the northward motion of India, consistent with a record of E-W convergence and dextral strike-slip motion in the Indo-Burman

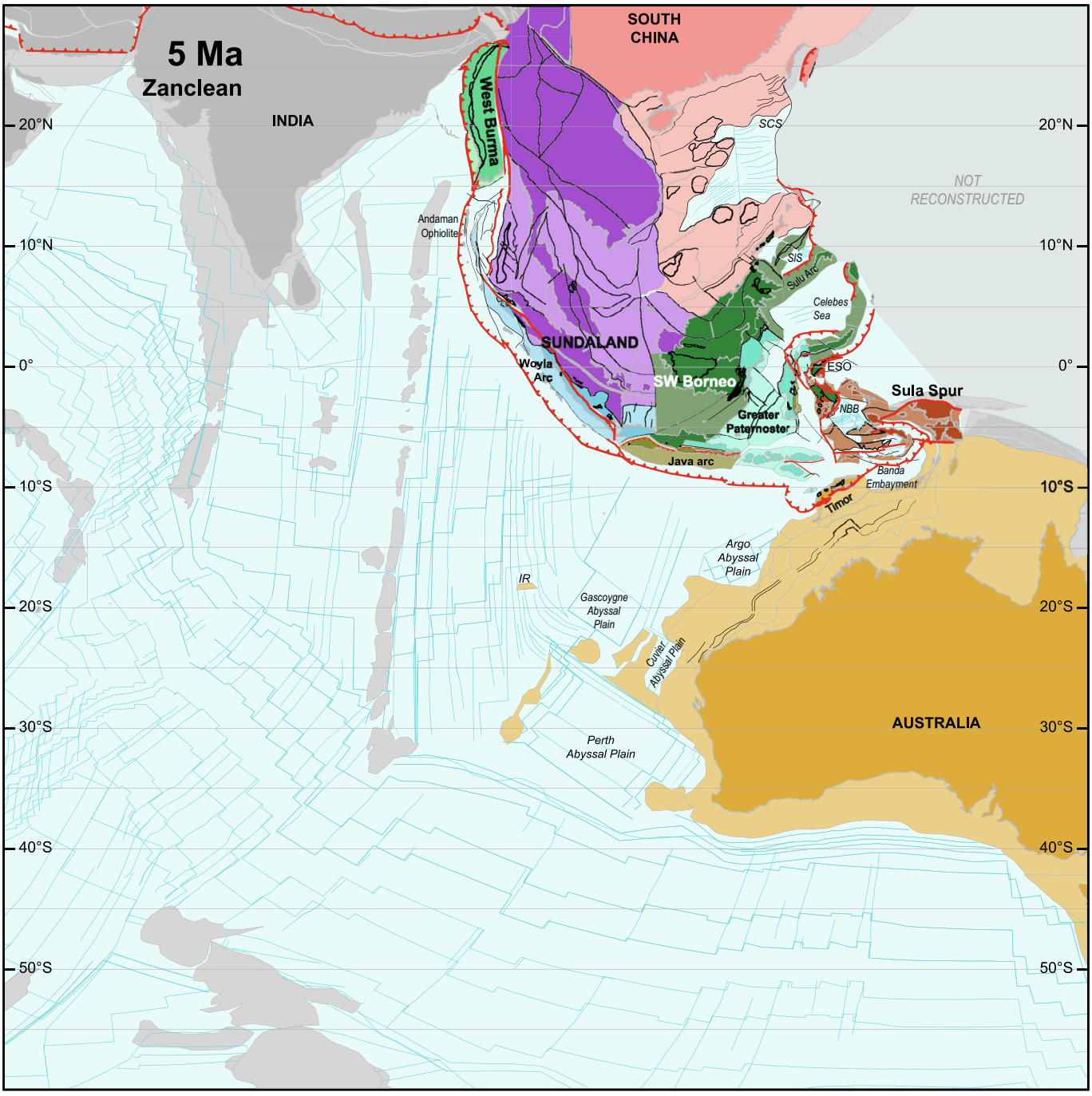

Fig. 21. Paleotectonic map for the Zanclean (5 Ma). Abbreviations: ESO, East Sulawesi Ophiolite; IR, Investigator Ridge; NBB, North Banda Basin; SCS, South China Sea; SIS, Sulu Sea.

ranges since the latest Miocene (Betka et al., 2018; Hossain et al., 2022; Maurin and Rangin, 2009; Morley et al., 2020). On Sumatra, the forearc segment southwest of the Sumatran Fault System is restored to the SW correcting for dextral strike-slip displacement.

Our reconstruction of the Banda Arc region is broadly similar to reconstructions with sufficient detail that restore subduction of one slab (Hall, 2012, 2002; Rangin et al., 1990b; Spakman and Hall, 2010), but differs with reconstructions that restore subduction by two slabs (Hall, 1996; Hinschberger et al., 2005; Lee and Lawver, 1995). However, the most prominent difference between our reconstruction and previous reconstruction is the position of Timor that we restore as promontory at the northern Australian margin following the constraints of Tate et al. (2017, 2015), similar to Keep and Haig (2010), whereas no other previous reconstruction has restored this shortening. This has implications for the age and nature of the Banda Embayment, which we will further discuss in Sections 6.6 and 6.7.

Our reconstruction of southward subduction of the Celebes Sea and rollback of the North Sulawesi Trench is similar to the reconstructions of Lee and Lawver (1995), Hall (2012, 2002) and Spakman and Hall (2010), that all show this is accommodated by upper plate extension in Gorontalo Bay, sinistral strike-slip motion on the Palu-Koro Fault and rotation of the North Arm of Sulawesi, but differs from reconstructions that show this accommodated as

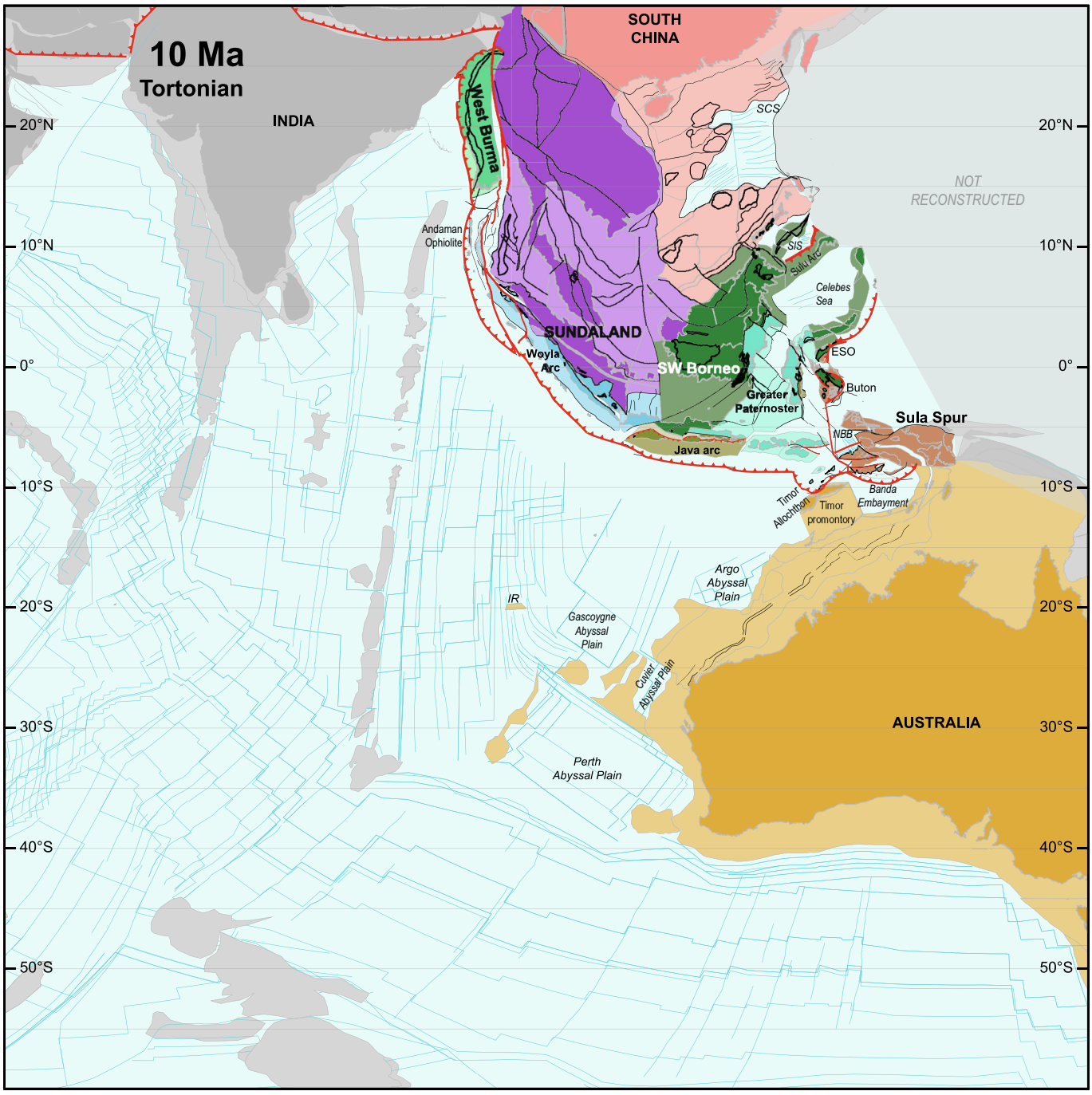

Fig. 22. Paleotectonic map for the Tortonian (10 Ma). Abbreviations: ESO, East Sulawesi Ophiolite; IR, Investigator Ridge; NBB, North Banda Basin; SCS, South China Sea; SIS, Sulu Sea.

combined rigid block rotation of the North Arm and East Sulawesi Ophiolite driven by collision of the Banggai-Sula Block (Hall, 1996; Hinschberger et al., 2005; Rangin et al., 1990b; Silver et al., 1983b; Zahirovic et al., 2016, 2014).

Our reconstruction of the Central Andaman Basin is similar to the reconstruction of Curray (2005), but differs from all other reconstructions. Reconstructions that were published prior to 2004 (Hall, 2002, 1996; Lee and Lawver, 1995) did not have access to the marine magnetic anomalies identified by Raju et al. (2004) and interpret ~460 km NW-SE directed spreading in the Central Andaman Basin since ~11 Ma, following Curray et al. (1979) that based their estimate on now outdated interpretations of magnetic anomalies and seismic sections in the Central Andaman Basin, and displacement estimates of the Sagaing Fault by Mitchell (1976). Also later reconstructions did not use the marine magnetic anomalies of Raju et al. (2004): Zahirovic (2016, 2014) adopted the rotation poles of Lee and Lawver (1995), and Hall (2012) did not update his reconstruction of the Andaman Sea region. All these reconstructions thus restore ~200 km N-S extension in the Central Andaman Basin around 5 Ma, which would result in a northward motion of the West Burma Block that is equal to the northward motion of India.

6.2. Chattian – 25 Ma

The most fundamental change in the Cenozoic paleogeography of SE Asia was the consecutive accretion of Sula Spur fragments to

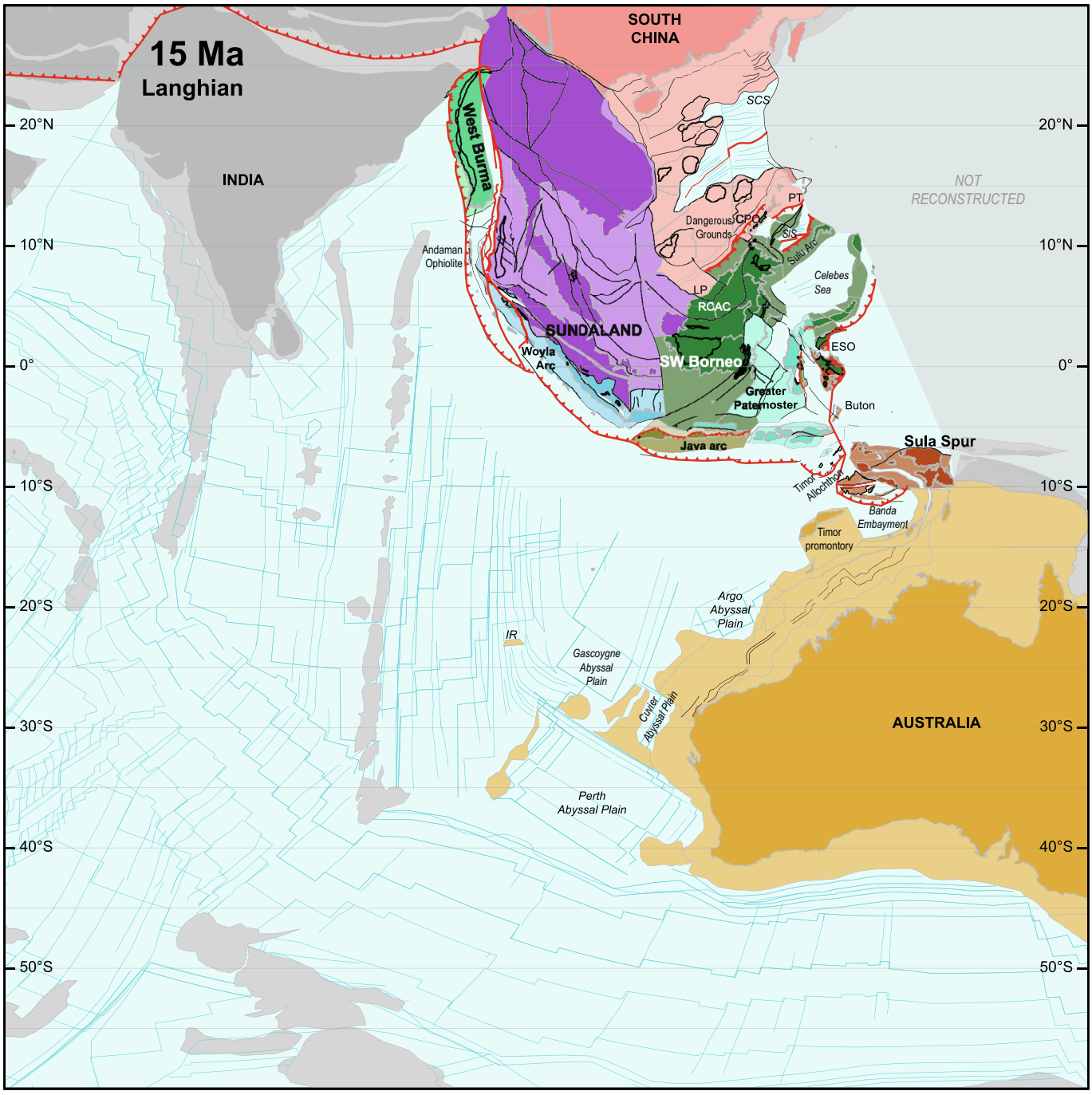

Fig. 23. Paleotectonic map for the Langhian (15 Ma). Abbreviations: CPO, Central Palwan Ophiolite; ESO, East Sulawesi Ophiolite; IR, Investigator Ridge; LP, Luconia Platform; PT, Palawan Terrane; RCAC, Rajang-Crocker Accretionary Complex; SCS, South China Sea; SIS, Sulu Sea.

SE Asia since the Late Oligocene–Early Miocene (Figs. 22–25). These events were responsible for a counterclockwise rotation, reconstructed as 13°, of eastern Sundaland in the Early Miocene, and the tectonic accretion in Sulawesi and Buton during the Early–Middle Miocene, followed by upper plate extension in Sulawesi and the Banda Sea region during the Middle Miocene to present day. At 25 Ma ago, Neogene upper plate extension accommodated by NW-SE extension in Bone Gulf, and N-S extension in Savu Basin are restored. We also further restored shortening of the Timor promontory that started in the latest Miocene, reconstructing Timor ~150 km further north compared to the map of 5 Ma. In our reconstruction, collision of the Sula Spur with Sundaland was partly accommodated by ~10° counterclockwise rotation of the Bird's Head and Sula Spur fragments during the Early Miocene. Restoring this rotation and shortening of the Timor promontory results in a ~600 km wide Banda Embayment between northern Australain margin east of Timor and the Banda Ridges, and a ~350 km wide opening between the Timor promontory and the Banda Ridges.

The consecutive accretion of Sula Spur fragments to SE Asia since the middle Oligocene is reconstructed, including the Pliocene accretion of the Banggai-Sula and Tukang-Besi Blocks, the Middle Miocene accretion of Buton, and the Early Miocene accretion of SE Sulawesi. This results in a paleogeography characterized by

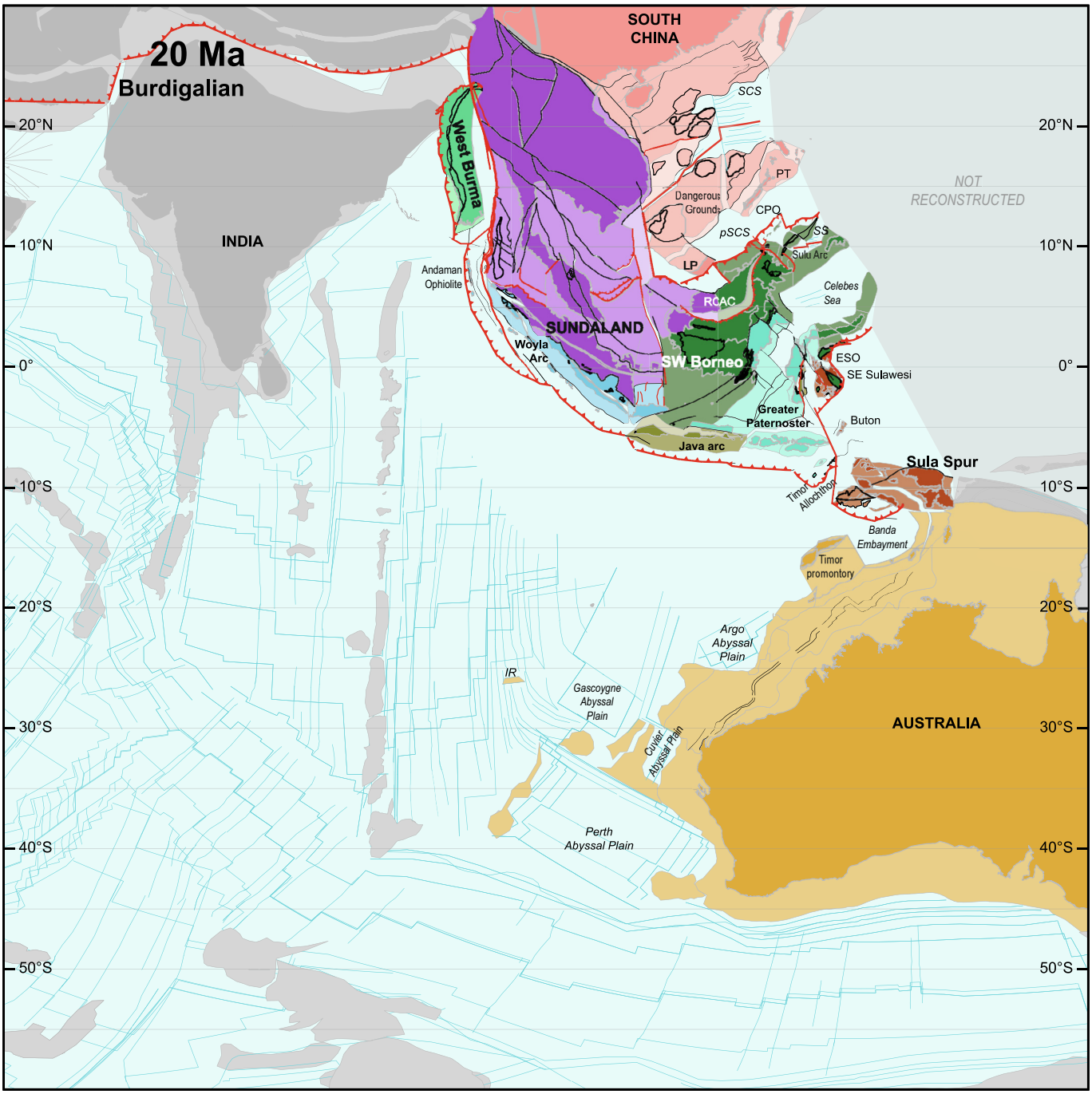

Fig. 24. Paleotectonic map for the Burdigalian (20 Ma). Abbreviations: CPO, Central Palawan Ophiolite; ESO, East Sulawesi Ophiolite; IR, Investigator Ridge; LP, Luconia Platform; pSCS, proto-South China Sea; PT, Palawan Terrane; RCAC, Rajang-Crocker Accretionary Complex; SCS, South China Sea; SIS, Sulu Sea.

two isolated continental fragments (SE Sulawesi and Buton), separated from the Sula Spur promontory by ~170 km and ~250 km wide oceanic basins, respectively (Fig. 25).

Borneo and Java are back-rotated by 13° clockwise following paleomagnetic constraints (Advokaat et al., 2018b). This rotation was accommodated in the western Java Sea, and our reconstruction restores up to 115 km of E-W extension between northwest Java and southeast Sumatra. As result, the Java segment of the Sunda Trench is restored to a WNW-ESE orientation. Along the western margin of Sundaland, ~100 km of post-Middle Miocene shortening in Java is restored bringing west-Java southward relative to Sundaland. The West Burma Block and Mount Victoria Land are reconstructed southward assuming that they follow the northward motion component of India, over a distance of ~700 km, which also restores Miocene continental extension in the Andaman Sea region. The Andaman Ophiolites are reconstructed southward together with the West-Burma Block, and lie at 25 Ma in the forearc of NW Sumatra, west of the accreted Woyla Arc (Fig. 25).

In the South China Sea region, the South China-derived continental fragments of the Luconia Block, Dangerous Grounds, Reed Bank and Palawan Terrane, which migrated southward during the South China Sea opening between the late Oligocene and middle Miocene, are reconstructed northward, closer to South China. As a result of the reconstructed counterclockwise rotation of Bor-

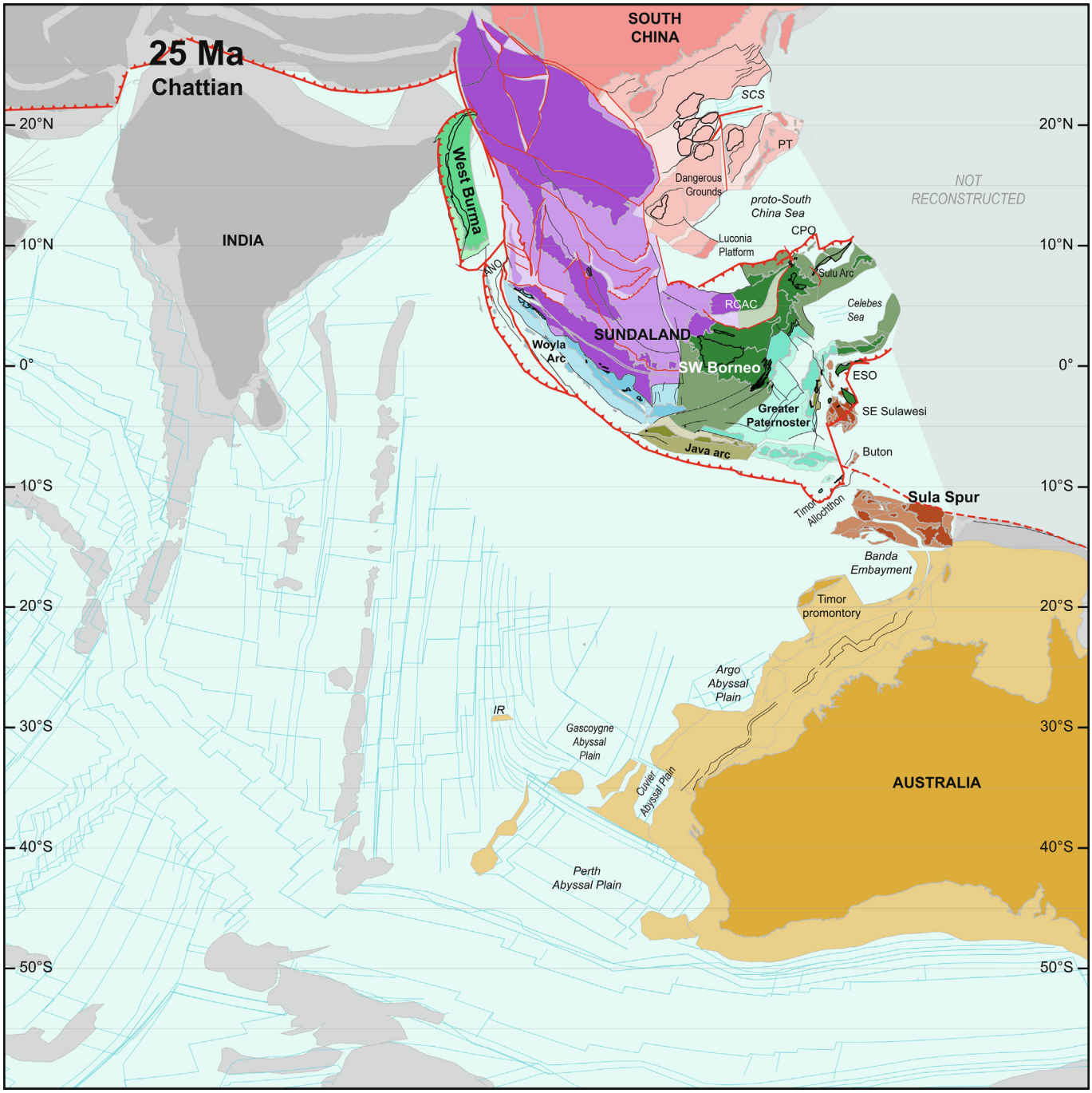

Fig. 25. Paleotectonic map for the Chattian (25 Ma). Abbreviations: ANO, Andaman-Nicobar ophiolites; CPO, Central Palawan Ophiolite; ESO, East Sulawesi Ophiolite; IR, Investigator Ridge; PT, Palawan Terrane; RCAC, Rajang-Crocker Accretionary Complex; SCS, South China Sea.

neo, the proto-South China Sea domain was wider than the modern South China Sea, increasing in width from ~450 km in the west between the Luconia Platform and the Kuching Zone, to ~900 km in the east between the Palawan Terrane and the Palawan Ophiolite. At 25 Ma, southward subduction of the proto-South China Sea below Borneo and Palawan was ongoing (Fig. 25).

The largest difference between our reconstruction at 25 Ma and previous renditions is due to the rotation of Borneo. Previous reconstruction either rotated Borneo ~40–50° counterclockwise between 25 Ma and 10 Ma (Hall, 2012, 2002, 1996; Spakman and Hall, 2010; Zahirovic et al., 2016, 2014) or did not rotate Borneo at all (Lee and Lawver, 1995; Rangin et al., 1990b). This affects the width of the reconstructed proto-South China Sea that becomes wider with a larger reconstructed rotation, the orientation of the Sunda trench, and the reconstructed width of the Sula Spur. The large-rotation estimates predict the lowest convergence rates between the Sula Spur and the Sundaland orogen, and as a result, our reconstruction shows a wider N-S distribution of the Sula Spur units than previous reconstructions. This width is also influenced by the reconstructed timing of accretion of Sula Spur units. We reconstruct progressive accretion between the Late Oligocene/Early Miocene and the Pliocene, similar in timing to Rangin et al.

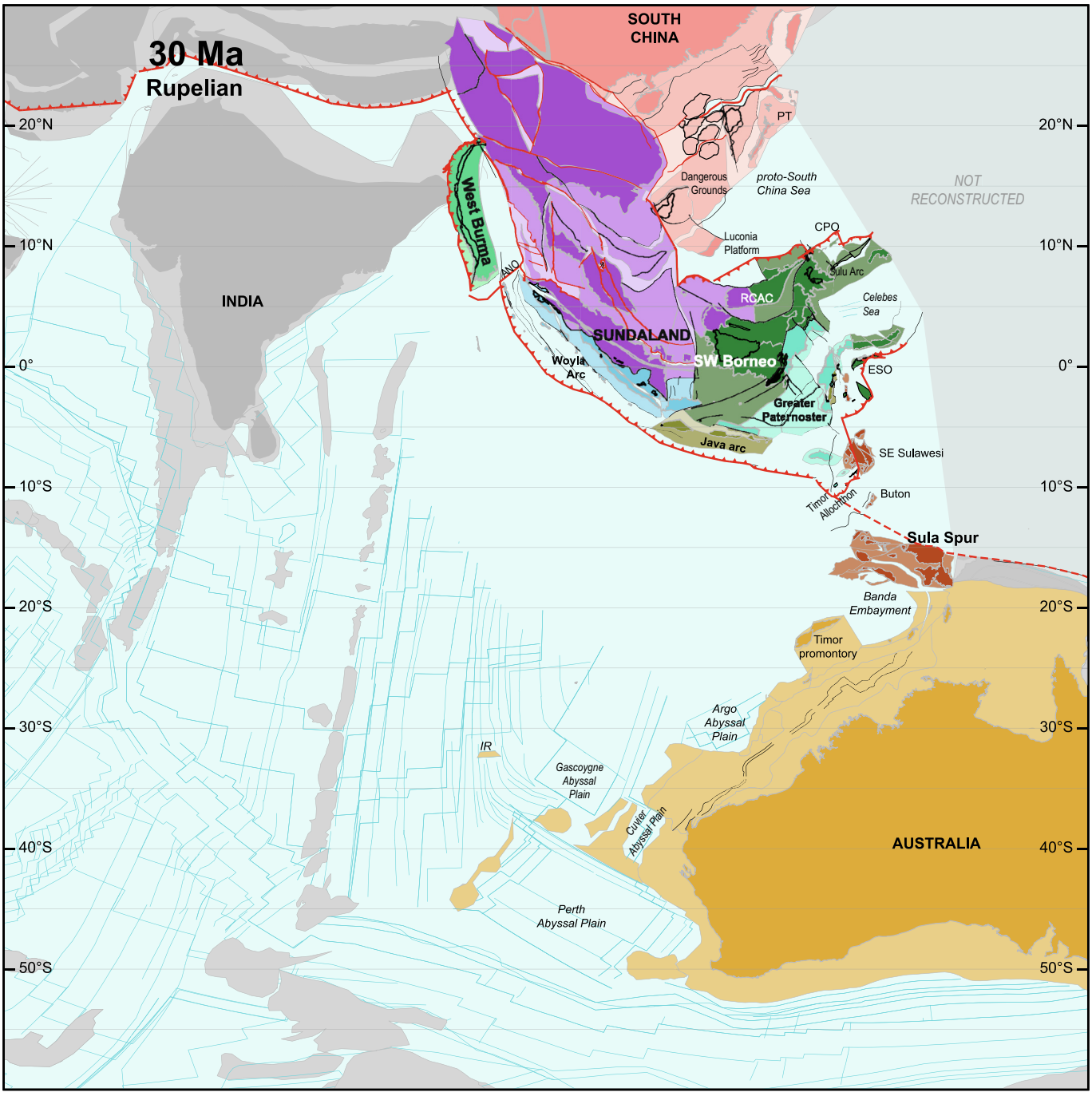

Fig. 26. Paleotectonic map for the Rupelian (30 Ma). Abbreviations: ANO, Andaman-Nicobar ophiolites; CPO, Central Palawan Ophiolite; ESO, East Sulawesi Ophiolite; IR, Investigator Ridge; PT, Palawan Terrane; RCAC, Rajang-Crocker Accretionary Complex.

(1990b), Lee and Lawver (1995), Hall (2012, 2002, 1996), Spakman and Hall (2010) and Zahirovic et al. (2016), but a much longer one than the 10–5 Ma interval of Zahirovic et al. (2014).

Previous reconstructions differ from ours in restoring the position of Sumba and extension in the Flores Basin. Zahirovic et al. (2016, 2014) restored Sumba as part of Australia, implying a suture of Pliocene-Pleistocene age in the Savu Basin, and as a result considered the Flores Basin as the forearc to which accretion occurred, in which they did not reconstruct extension. Rangin et al. (1990b) restored extension in the Flores basin since 10 Ma, whereas Hall (2012, 2002) and Spakman and Hall (2010) restored opening of the Flores Basin between 15 Ma and 3 Ma, and Lee and Lawver (1995) restored the opening of the Flores Basin between 25 Ma and 15 Ma. Because we infer that the Flores Basin is of Paleogene age (Emmet et al., 2009; Prasetyo, 1992), our reconstruction at 25 Ma still reveals the basin in its modern width.

Our reconstruction of the Andaman Sea Basin restores a similar amount of N-S extension as van Hinsbergen et al. (2011), but a larger amount than all other previous reconstructions (Hall, 2012, 2002, 1996; Lee and Lawver, 1995; Zahirovic et al., 2016, 2014) that used the constraints of Curray et al. (1979) and restored ~460 km of NW-SE extension in the Central Andaman Basin since 11 Ma. As consequence, all these reconstructions restore a similar ~460 km northward motion of West Burma, but the onset of this

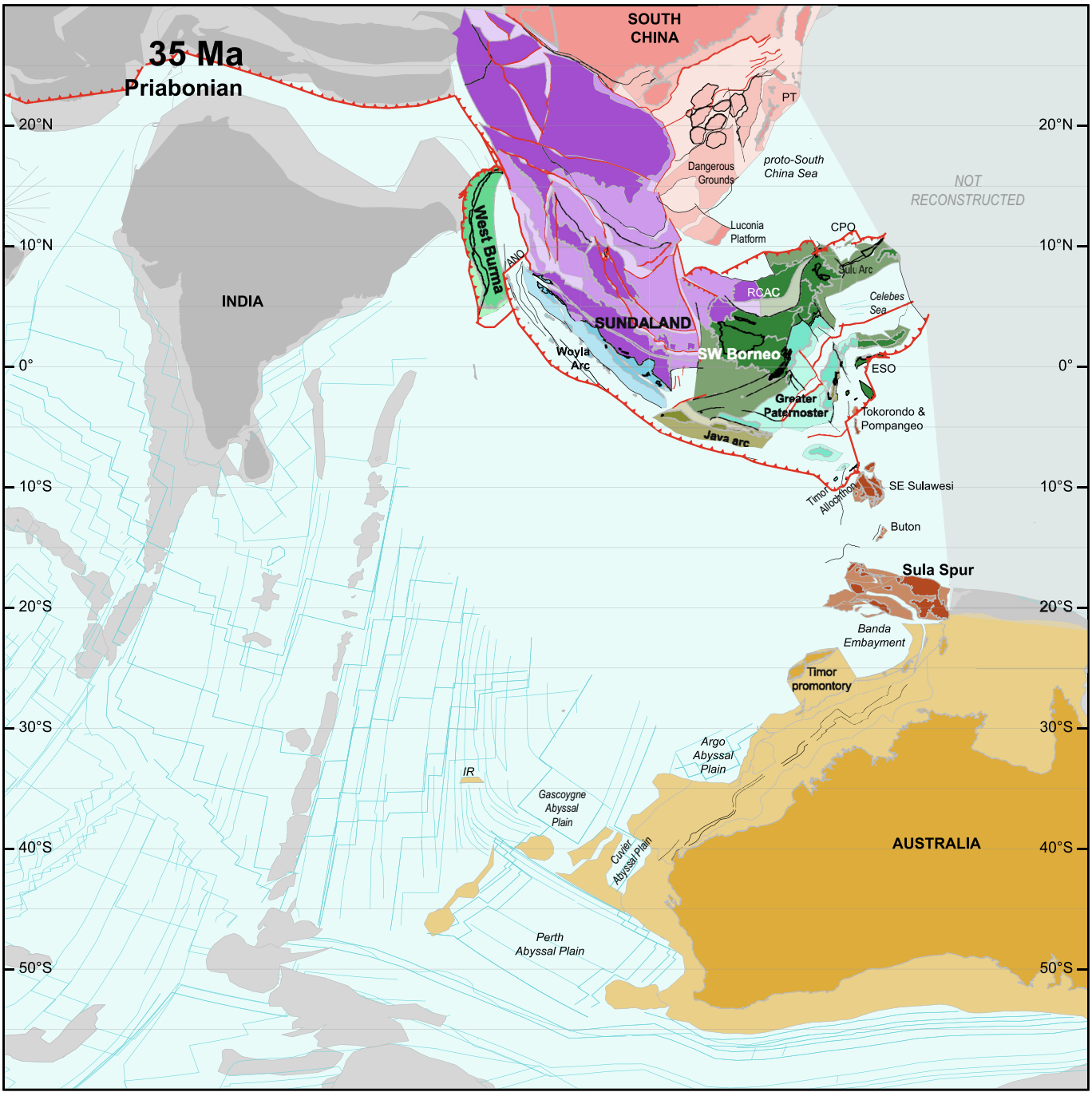

Fig. 27. Paleotectonic map for the Priabonian (35 Ma). Abbreviations: ANO, Andaman-Nicobar ophiolites; CPO, Central Palawan Ophiolite; ESO, East Sulawesi Ophiolite; IR, Investigator Ridge; PT, Palawan Terrane; RCAC, Rajang-Crocker Accretionary Complex.

motion varies between 15 Ma (Lee and Lawver, 1995), 20 Ma (Hall, 2012, 2002), or 30 Ma (Zahirovic et al., 2016, 2014).

Finally, our South China Sea region reconstruction differs only in detail from previous reconstructions. We followed reconstructions that restored the Luconia Block prior to the Middle Miocene as conjugate margin of South China (Hall, 1996; Lee and Lawver, 1995, 1994; Metcalfe, 2013a, 2011a, 2011b, 1990; Rangin et al., 1990b; Zahirovic et al., 2016, 2014), but Fyhn et al. (2010b) Hall (2012, 2002) and Spakman and Hall (2010) restored it as an allochthonous block that accreted to Sundaland in the Late Cretaceous or early Paleogene. In addition, the timing of accretion varies between reconstructions, from 10 Ma (Zahirovic et al., 2016, 2014), to 15 Ma (Lee and Lawver, 1995, 1994), or 20 Ma (Rangin et al., 1990b). Our reconstructed time of 16 Ma has as consequence that the restored position of the Luconia Block is farther south than reconstructions that restore a younger (10 Ma) accretion (Zahirovic et al., 2016, 2014) and farther north than reconstruction that restore an older (20 Ma) accretion (Rangin et al., 1990b).

6.3. Lutetian – 45 Ma

Around 45 million years ago, Australia underwent a sharp change in its plate motion relative to Eurasia, from eastward to northward. Our reconstruction at 45 Ma restores SE Asia to the

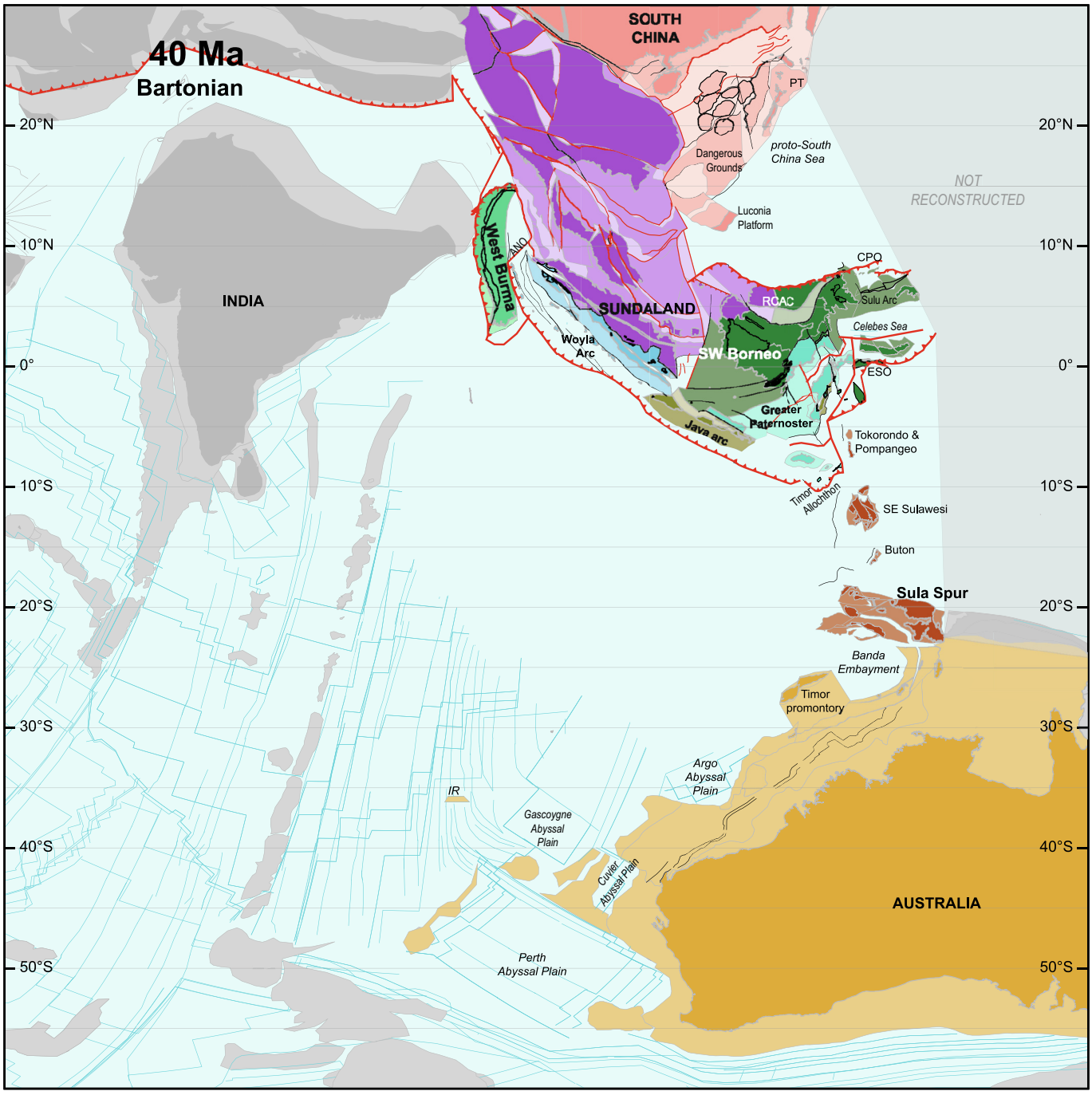

Fig. 28. Paleotectonic map for the Bartonian (40 Ma). Abbreviations: ANO, Andaman-Nicobar ophiolites; CPO, Central Palawan Ophiolite; ESO, East Sulawesi Ophiolite; IR, Investigator Ridge; PT, Palawan Terrane; RCAC, Rajang-Crocker Accretionary Complex.

moment onset of this northward motion, reconstructing all deformation that occurred since Australia started to move northward (Figs. 26–29).

In the southeast, the reconstruction back to 45 Ma restored the spreading that formed the Celebes Sea and the East Sulawesi Ophiolite. The subduction zone that was responsible for this, that eventually ended up on Timor, was at 45 Ma in its incipient stages and lies restored to the southern margin of the Sulu Ridge. This subduction zone is connected through a N-S trending transform along the Bantimala Mélange Belt with the Sunda Trench to the southwest. To the east, this trench must continue to connect with plate boundaries within the Panthalassa system that we did not restore in detail. Reconstructing the Oligocene accretion of the Tokorondo and Pompangeo complexes that form the northernmost Sula Spur units below the East Sulawesi Ophiolite, results in a paleogeography whereby these complexes form a continental sliver separated from the SE Sulawesi fragment by a ~300 km wide oceanic basin. To avoid overlap with the eastern Sundaland margin (Sumba and Nusa Tenggara), we tentatively infer 380 km westward motion of the Tokorondo Complex, Pompangeo Complex, and SE Sulawesi relative to the other Sula Spur fragments and the Australian continent during the Oligocene. We infer this motion was accommodated by sinistral strike-slip motion along the New Guinea Mobile Belt (Hill and Hall, 2003), which is an Oligocene–Early Mio-

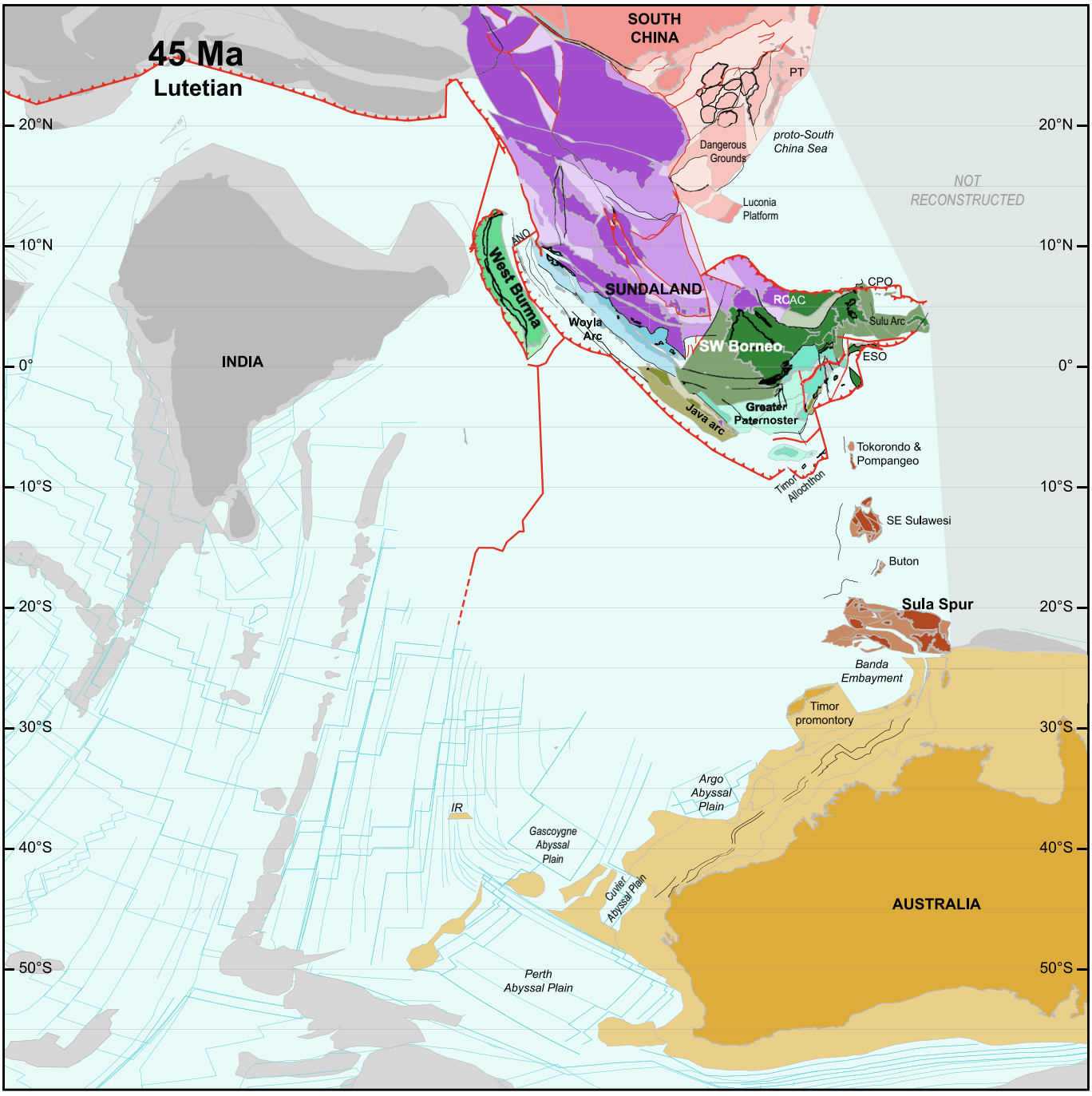

Fig. 29. Paleotectonic map for the Lutetian (45 Ma). Abbreviations: ANO, Andaman-Nicobar ophiolites; CPO, Central Palawan Ophiolite; ESO, East Sulawesi Ophiolite; IR, Investigator Ridge; PT, Palawan Terrane; RCAC, Rajang-Crocker Accretionary Complex.

cene suture zone (Hill and Raza, 1999) with evidence for significant oblique convergence and sinistral strike-slip (Carey, 1958; Hall, 2002), likely driven by westward motion of plates in the Panthalassa realm (van de Lagemaat and van Hinsbergen, 2024). Our reconstructed paleogeography of the northern Sula Spur fragments prior to accretion below the East Sulawesi Ophiolite align them along a N-S trending domain from the westernmost Bird's Head to the north. We infer that this N-S trending ridge formed a transform fault zone during break-up of Australia, and that fragments were left behind during plate boundary migrations from one transform to the next (see Sections 6.5 and 6.6), perhaps similar to the separation of the Maledives and Mauritania in the Indian Ocean (Torsvik et al., 2013).

The main regional difference between the Chattian time slice (Fig. 25) and the Lutetian time slice (Fig. 29) is the reconstruction of ~15° counterclockwise rotation of Indochina, and ~30° clockwise rotation of Borneo (both relative to the north), and by inference, of Java, and Sulawesi that we reconstruct with Borneo. In the northeast, we restored N-S directed oceanic spreading in the eastern sub-basin of the South China Sea, and pre-drift extension in its conjugate continental margins. Reconstructing the rotation of Borneo results in a triangular proto-South China Sea varying in width from ~300 km in the west to ~2400 km in the east whose post-45 Ma removal was accommodated by subduction below North Borneo and Palawan that may have been in an incipient stage around 45 Ma.

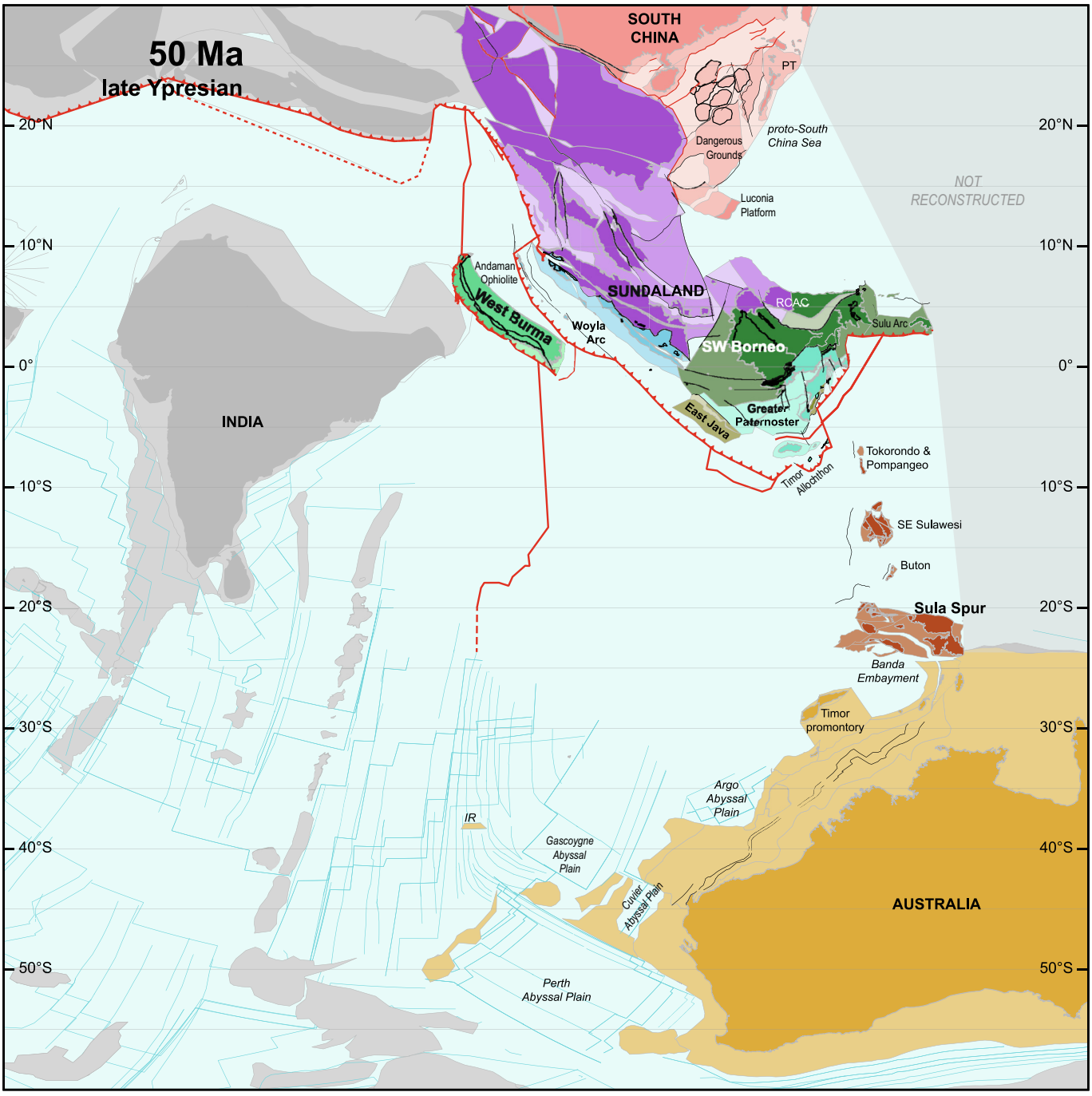

Fig. 30. Paleotectonic map for the late Ypresian (50 Ma). Abbreviations: IR, Investigator Ridge; PT, Palawan Terrane; RCAC, Rajang-Crocker Accretionary Complex.

In the west, reconstructing differential rotation between Indochina, Sundaland, and Borneo removes transpressional strike-slip faulting in the core of Sundaland (Ranong, Khlong Marui, and Songkla-Penang faults (Fig. 29, Table S1)). At the western margin, this differential rotation was associated with trench-parallel extension. The restored Sunda Trench at 45 Ma is much less curved than today and is striking NW-SW from the Banda region towards Sumatra and NNW-SSE from Sumatra to the north. The trench-parallel extension was restored by removing ~100 km NNW-SSE extension documented in the Mergui-North Sumatra Basin (Curray, 2005). To further accommodate this trench parallel extension, we also restored ~270 km E-W extension that was distributed in the southwestern Java Sea (e.g., Advokaat et al., 2018b). We restore the West Burma Block and Mount Victoria Land as part of the Australian plate. This places the West Burma Block and Mount Victoria Land in a position ~1700 km further south than their present location, adjacent to, and likely underthrust below, the Andaman Ophiolite (Bandopadhyay et al., 2022). At the (modern) western margin of the West-Burma Block is a subduction zone marking the Australia-India plate boundary with the West-Burma Block and Mount Victoria Land in an upper plate position (Fig. 29).

The difference at 45 Ma between our reconstruction and previous reconstructions that rotated Borneo ~40–50° counterclock-

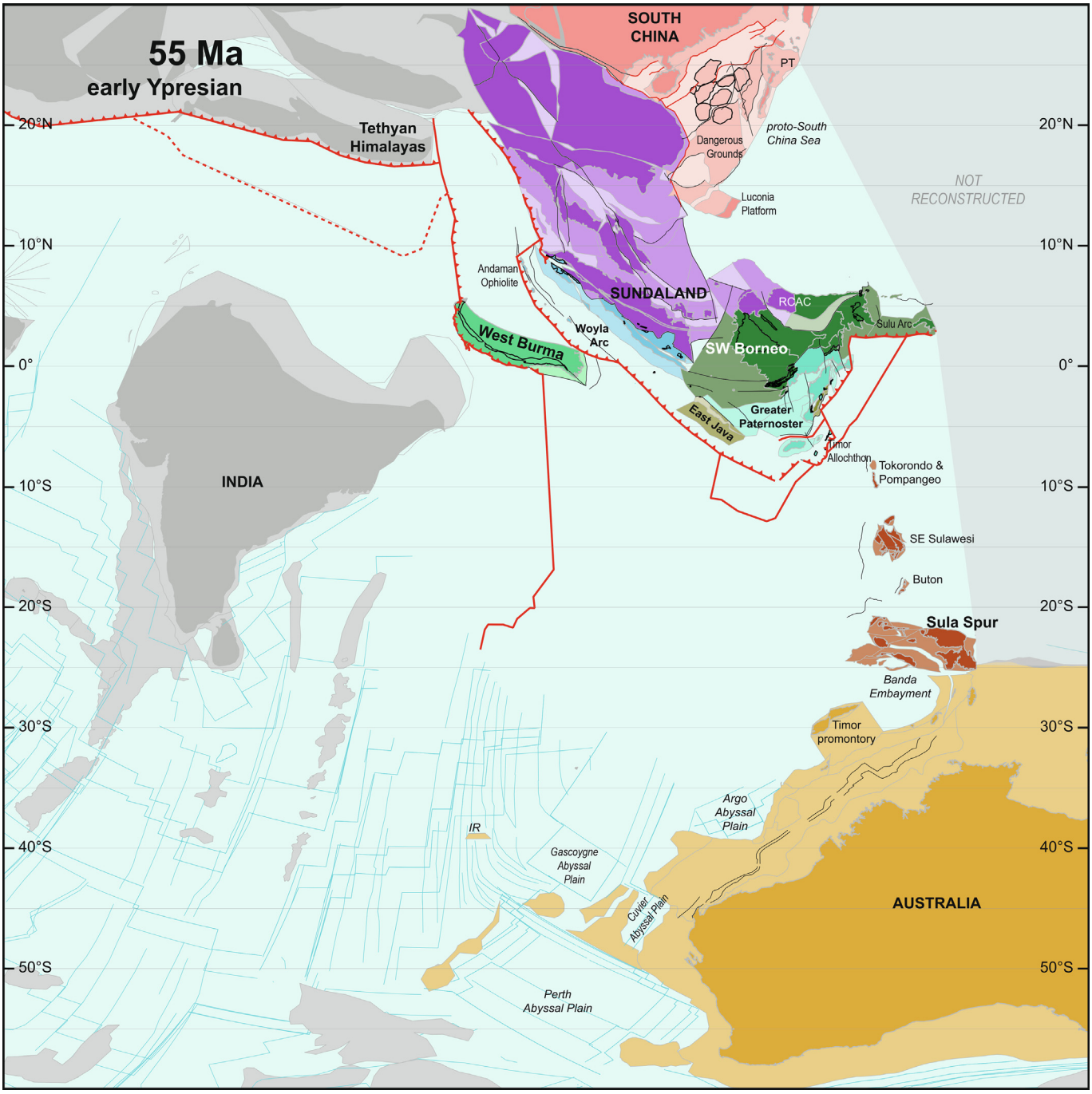

Fig. 31. Paleotectonic map for the early Ypresian (55 Ma). Abbreviations: IR, Investigator Ridge; PT, Palawan Terrane; RCAC, Rajang-Crocker Accretionary Complex.

wise between 25 Ma and 10 Ma (Hall, 2012, 2002, 1996; Spakman and Hall, 2010; Zahirovic et al., 2016, 2014) has, logically, become smaller relative to the 25 Ma time slice (Fig. 25). The difference with reconstructions that assumed no rotation of Borneo (Lee and Lawver, 1995; Rangin et al., 1990b) became larger, primarily manifested in the width of the Proto-South China Sea and the orientation of the Sunda Trench. Our reconstruction of the South China Sea and its pre-drift extension is similar to previous reconstructions (Hall, 2012, 2002, 1996; Lee and Lawver, 1995, 1994; Rangin et al., 1990b; Zahirovic et al., 2016, 2014). Rangin et al. (1990b) restored a major clockwise rotation of Indochina and western Sundaland relative to Borneo between 32 Ma and 20 Ma, which was accommodated by southward subduction of the proto-South China Sea below NW Borneo and the Palawan Ophiolite.

For the western part of the study area, our reconstruction differs from all previous reconstructions that restore West Burma and Mount Victoria Land rigidly attached to Sibumasu, around 450 km (Hall, 2012, 2002; Lee and Lawver, 1995; Zahirovic et al., 2016) or ~1100 km (van Hinsbergen et al., 2011) south of its modern position. As summarized in Sections 4.4 and 5.2, the new arguments for our reconstruction are the recent paleomagnetic

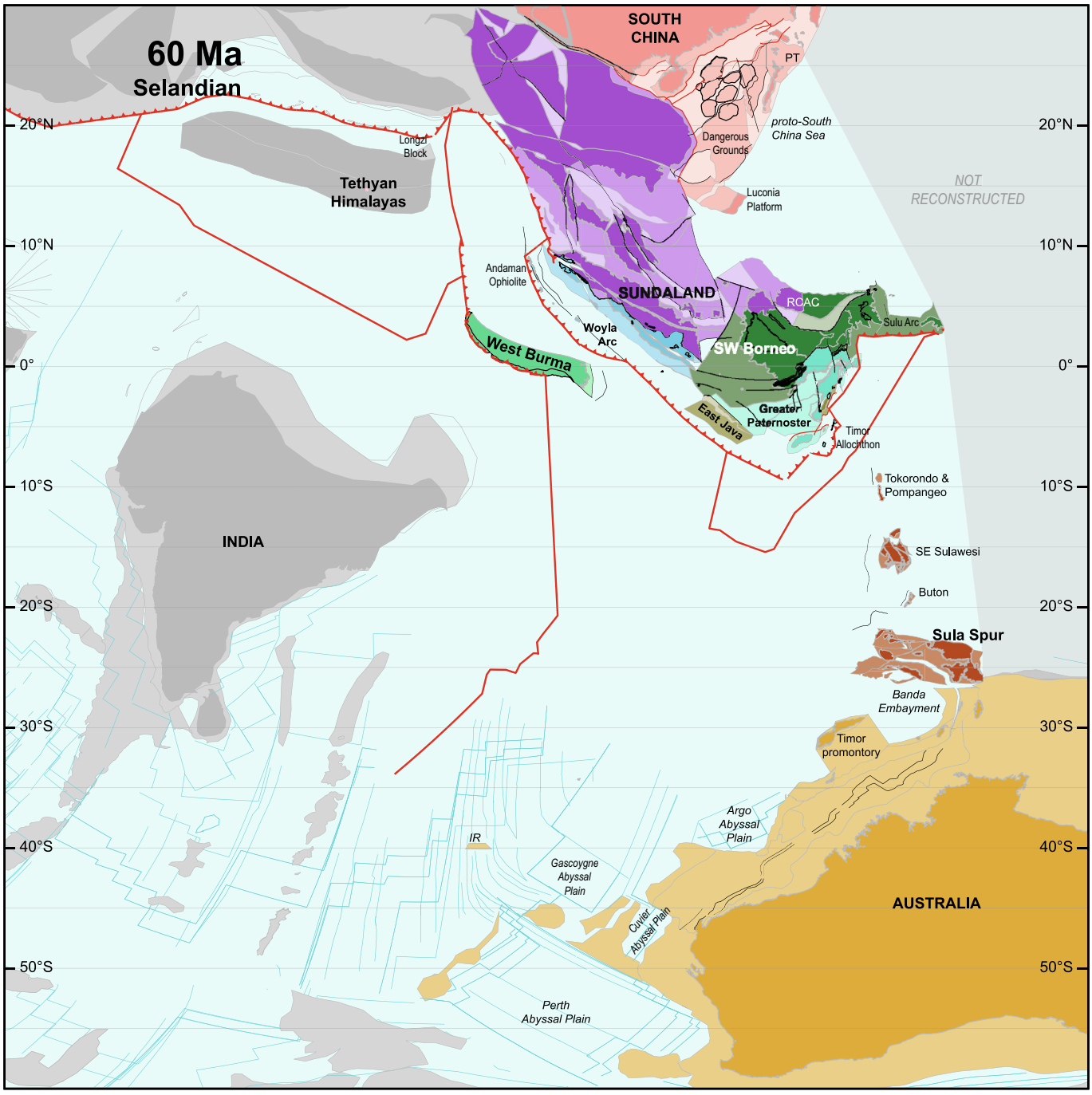

Fig. 32. Paleotectonic map for the Selandian (60 Ma). Abbreviations: IR, Investigator Ridge; PT, Palawan Terrane; RCAC, Rajang-Crocker Accretionary Complex.

data from the West-Burma Block of Westerweel et al. (2020, 2019), and the sediment provenance data from Bandopadhyay et al. (2022) that were unavailable to previous reconstructions.

In the east, the Oligocene accretion of the Tokorondo and Pompangeo complexes has not been reconstructed before. As a result, the N-S separation of fragments assigned to the Sula Spur in our reconstruction does not appear on previous maps, who instead restored the pre-Miocene paleogeography of the Sula Spur as one contiguous promontory of the Bird's Head (Hall, 2012, 2002, 1996; Metcalfe, 2013a, 2011a, 2011b, 1996, 1990; Rangin et al., 1990b; Spakman and Hall, 2010; Zahirovic et al., 2016, 2014). Our reconstruction of the extension of the East Sulawesi Ophiolite as conjugate plate from the Celebes Sea is similar to Monnier et al. (1995, 1994), Parkinson (1998b, 1996), Spakman and Hall (2010), and Hall (2012), but differs from reconstructions that restored the East Sulawesi Ophiolite as part of the Sula Spur (Hall, 2002, 1996; Lee and Lawver, 1995; Mubroto et al., 1994; Zahirovic et al., 2016, 2014) or the Pacific Plate (Kadarusman et al., 2004). As result, our restored trench lies further south than in this latter group of reconstructions.

6.4. Santonian – 85 Ma

The time slice of 85 Ma represents an important change in the accretionary history of SE Asia. The period between 45 and 85 Ma was tectonically relatively quiet (Clements et al., 2011; Harbury et al., 1990), dominated by slow subduction accommodated at the Sunda Trench and below the southeastern margin of

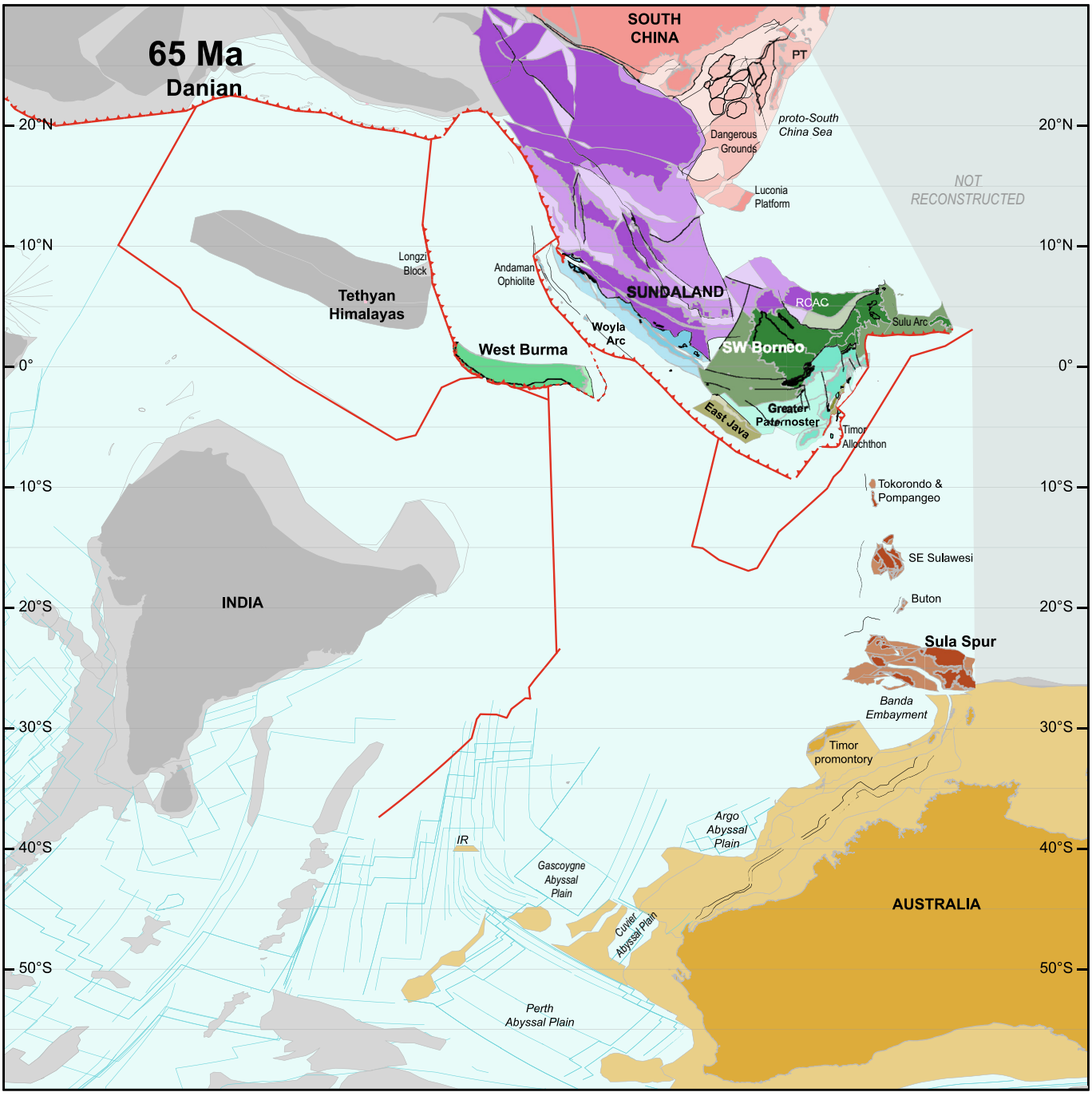

Fig. 33. Paleotectonic map for the Danian (65 Ma). Abbreviations: IR, Investigator Ridge; PT, Palawan Terrane; RCAC, Rajang-Crocker Accretionary Complex.

the Sulu Arc (Figs. 30–37). Geological records of this period of subduction are sparse, mostly concentrated on the forearc ophiolites of the Andaman Islands (Bandopadhyay et al., 2022) and Timor (Harris, 2006; Standley and Harris, 2009), likely owing to the very slow Australia-Sundaland plate motion. The Sundaland core and the accreted Gondwana-derived continental fragments of the SW Borneo Mega-Unit, the Greater Paternoster Mega-Unit, and the East Java Block underwent little deformation. Only in the southeast, we reconstructed extension in the Flores Basin starting in the Paleogene, and restored an associated Paleogene ~45° clockwise rotation of Sumba relative to West Sulawesi (Fig. 33).

In the east of SE Asia there is little evidence of deformation or magmatism during the interval 85–45 Ma. The width of the embayment of the proto-South China Sea at 85 and 45 Ma are essentially the same. Accretionary and magmatic evidence from north Borneo as well as in the Palawan Terrane suggests that subduction along the perimeter of the proto-South China Sea Embayment continued until ~75 Ma (Figs. 35 and 36). How this subduction was accommodated or why it stopped, cannot be constrained by the data that we compiled, and cannot be explained by relative Borneo-South China motion, which does not appear to have occurred or changed in this time. However, van de Lagemaat et al. (2023) suggested that subduction stopped when an oceanic plateau that occupied the proto-South China Sea entered the trenches around its perimeter.

The 85 Ma time slice marks the final accretion of the Gondwana-derived ('Argoland') fragments to Sundaland (Fig. 37). The SW Borneo Mega-Unit accreted to the east Sundaland margin,

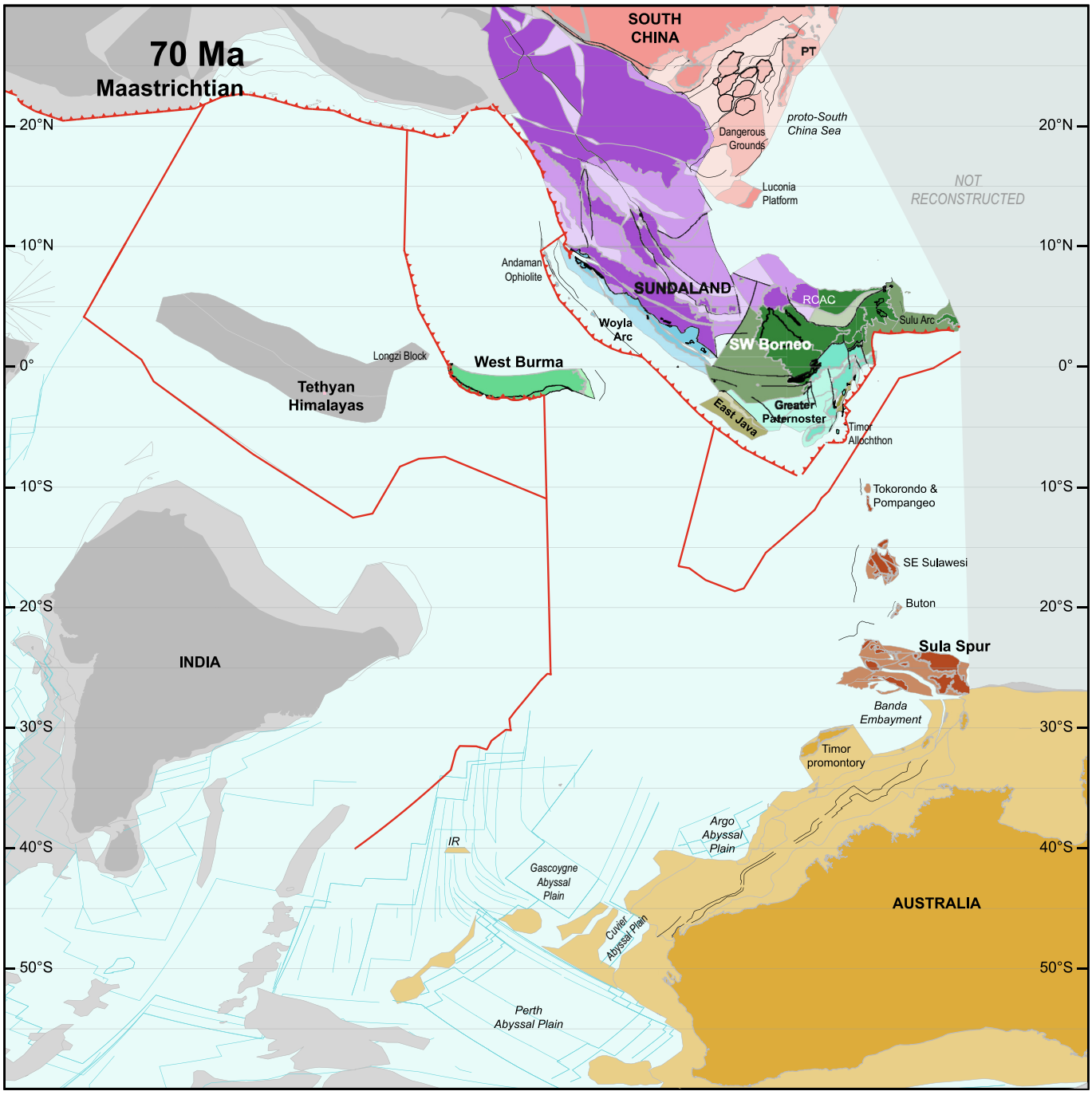

Fig. 34. Paleotectonic map for the Maastrichtian (70 Ma). Abbreviations: IR, Investigator Ridge; PT, Palawan Terrane; RCAC, Rajang-Crocker Accretionary Complex.

and the Greater Paternoster Mega-Unit and East Java Block accreted to the margins of the SW Borneo Mega-Unit. The subduction zones between these blocks came to an arrest around 85 Ma. Also the intra-oceanic Woyla Arc underwent its final suturing against the West Sumatra Block of the SW Sundaland margin, and the double subduction zones that appear to have existed between these – west-dipping below Woyla and east-dipping between West Sumatra-terminated (Advokaat et al., 2018a; Barber et al., 2005a). In contrast to the subduction zones between the Gondwana-derived fragments, convergence here continued between the Australian plate and Sundaland. This convergence became accommodated to the west of the Woyla Arc, where subduction had initiated in the back-arc region around 105 Ma, and which by 99 Ma started to produce arc magmatism (Bandyopadhyay et al., 2021; Plunder et al., 2020).

The largest difference between the 45 and 85 Ma time slices concerns the position of the West Burma and Mount Victoria Land blocks, in the Neotethyan ocean west of Sundaland. These are reconstructed in an E-W orientation following paleomagnetic constraints of Westerweel et al. (2019) prior to its interaction with the Sunda forearc (following Bandopadhyay et al., 2022), the Longzi Block (Min et al., 2022) and Indian promontory in the Paleogene. We reconstruct the West Burma Block and Mount Victoria Land as part of the Australian plate, satisfying paleolatitude esti-

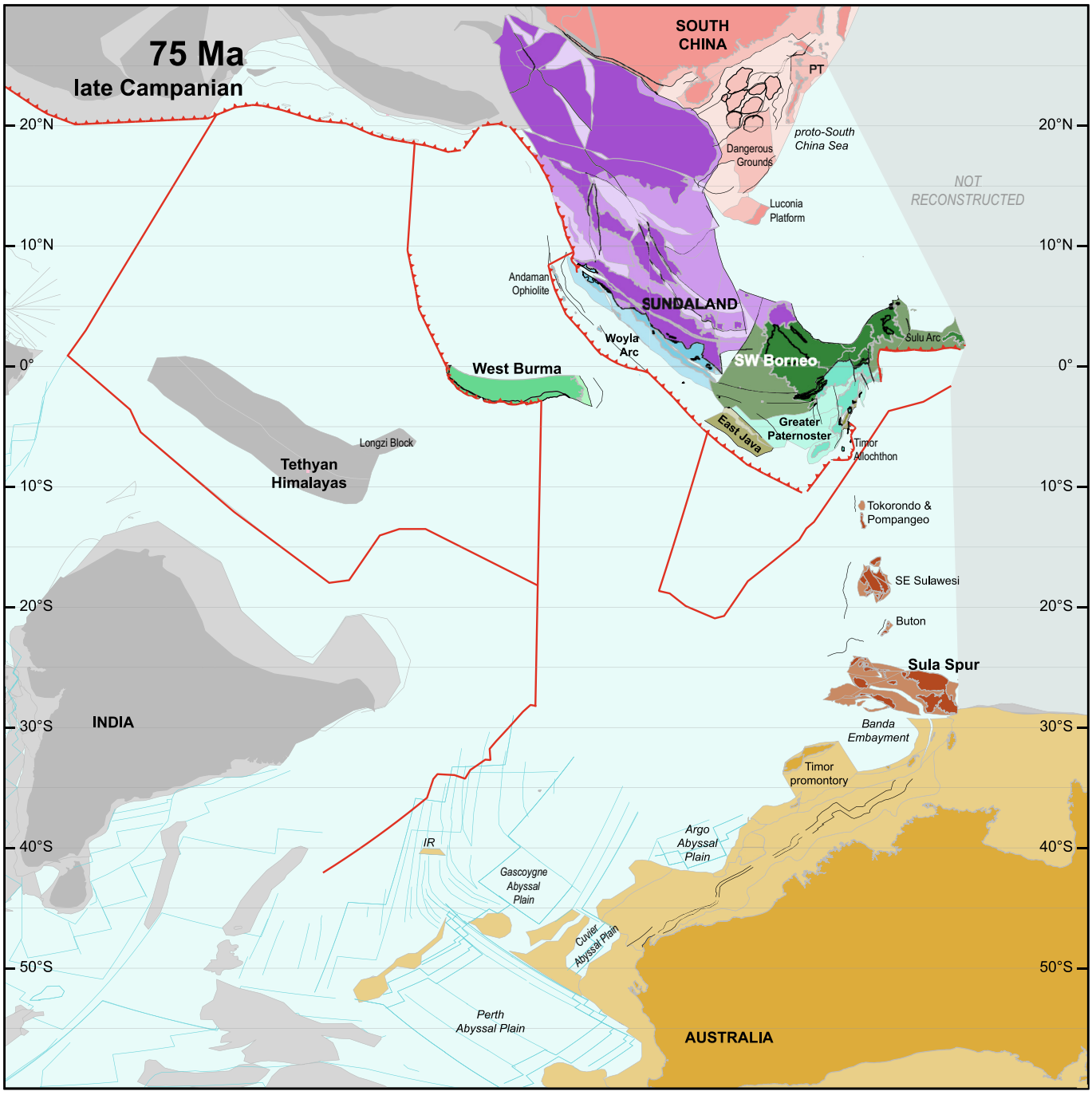

Fig. 35. Paleotectonic map for the late Campanian (75 Ma). Abbreviations: IR, Investigator Ridge; PT, Palawan Terrane.

mates of Westerweel et al. (2019). Relative motion between the Tethyan Himalayan plate, which we reconstruct as a separate plate that underwent N-S spreading relative to the India following van Hinsbergen et al. (2019a, 2012), and the Australian plate was accommodated by northward subduction below West Burma and Mount Victoria Land, and by dextral motion along the India-Australia transform. The India-Australia transform had alternatingly a divergent, convergent, and again a divergent component on an overall transform motion (Hall, 2012), whereby the convergent component occurred between 83.64 and 64.49 Ma, implying this was accommodated by subduction, most likely of the Indian plate below the Australian plate. Should we treat the Tethyan Himalayas as part of the rigid Indian plate, the same plate boundary configuration with the West Burma Block would be appropriate, only relative motion rates would be lower.

Our reconstruction broadly agrees with the reconstructions of Zahirovic et al. (2014, 2016) that also restored ongoing converge of the Indian and Australian plate relative to Sundaland during the Late Cretaceous–Paleocene, accommodated by eastward subduction below the west-Sundaland margin. In contrast, Hall (2012) interpreted that there was no subduction below Sundaland between 90 and 45 Ma, a view that was adopted by Metcalfe (2013a). Hall (2012) based this interpretation on the perceived absence of widespread magmatism in Sumatra and Java. Our main argument for continuing subduction is the evidence for relative (albeit slow) plate convergence across the reconstructed Sundaland

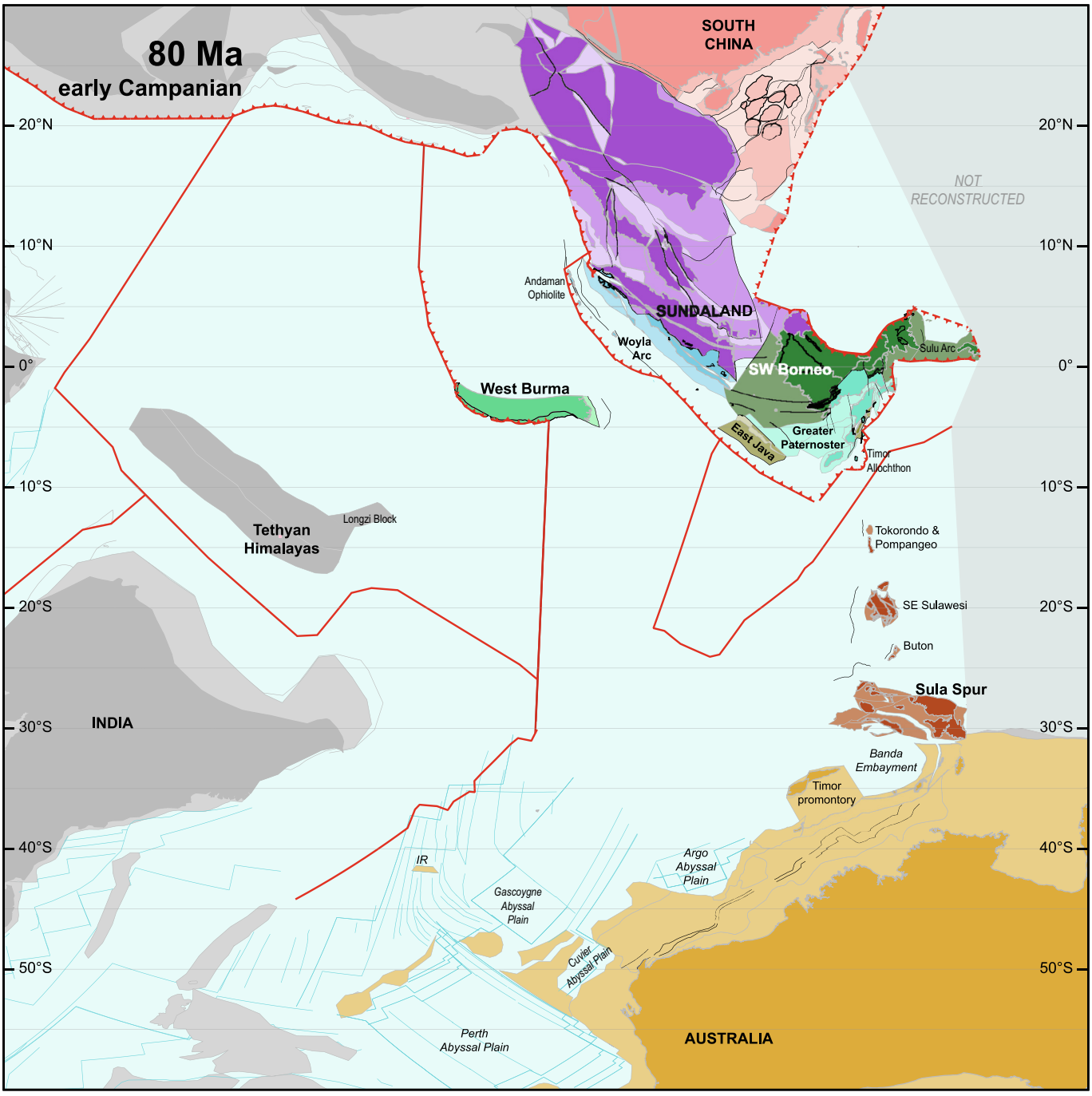

Fig. 36. Paleotectonic map for the early Campanian (80 Ma). Abbreviations: IR, Investigator Ridge.

margin, consistent with evidence for arc magmatism on Sumatra, Java, and Sumba in the 85–45 Ma interval (Abdullah et al., 2000; Bellon et al., 2004; Chamalaun and Sunata, 1982; Lai et al., 2023; McCourt et al., 1996; Schiller et al., 1991; Smyth et al., 2007; Suparka, 1988; Van Halen, 1996; Wensink, 1997; Zhang et al., 2019).

The most prominent difference between our map at 85 Ma and previous maps concerns our reconstruction of the West Burma Block (and Mount Victoria Land) as part of the Australian plate, as suggested by the recent paleomagnetic data of Westerweel et al. (2019). Many previous reconstructions kept the West Burma Block firmly welded to Sundaland since the Triassic (Hall, 2012, 2002; Metcalfe, 2013a, 2011a, 2011b; Sevastjanova et al., 2016; Zahirovic et al., 2016). Zahirovic et al. (2014) restored accretion of the Indo-Burman Ranges to West Burma at 55 Ma, after a clockwise rotation between 55 Ma and 70 Ma. Prior to this rotation, Zahirovic et al. (2014) restored the Indo-Burman Ranges as part of the Indian plate. Westerweel et al. (2019) restored a clockwise rotation of West Burma between 50 Ma and ~80 Ma, and restored West Burma on a speculated plate that would also host the Kohistan Arc and was in an upper plate position relative to India (or the Tibetan Himalaya), while subducting below Tibet, despite that the two trenches did not converge (see also Martin et al., 2020). Westerweel et al. (2019) invoked this scenario to satisfy the paleomagnetic constaints that revealed Cretaceous paleolatitudinal stability around the equator of the West Burma Block while being

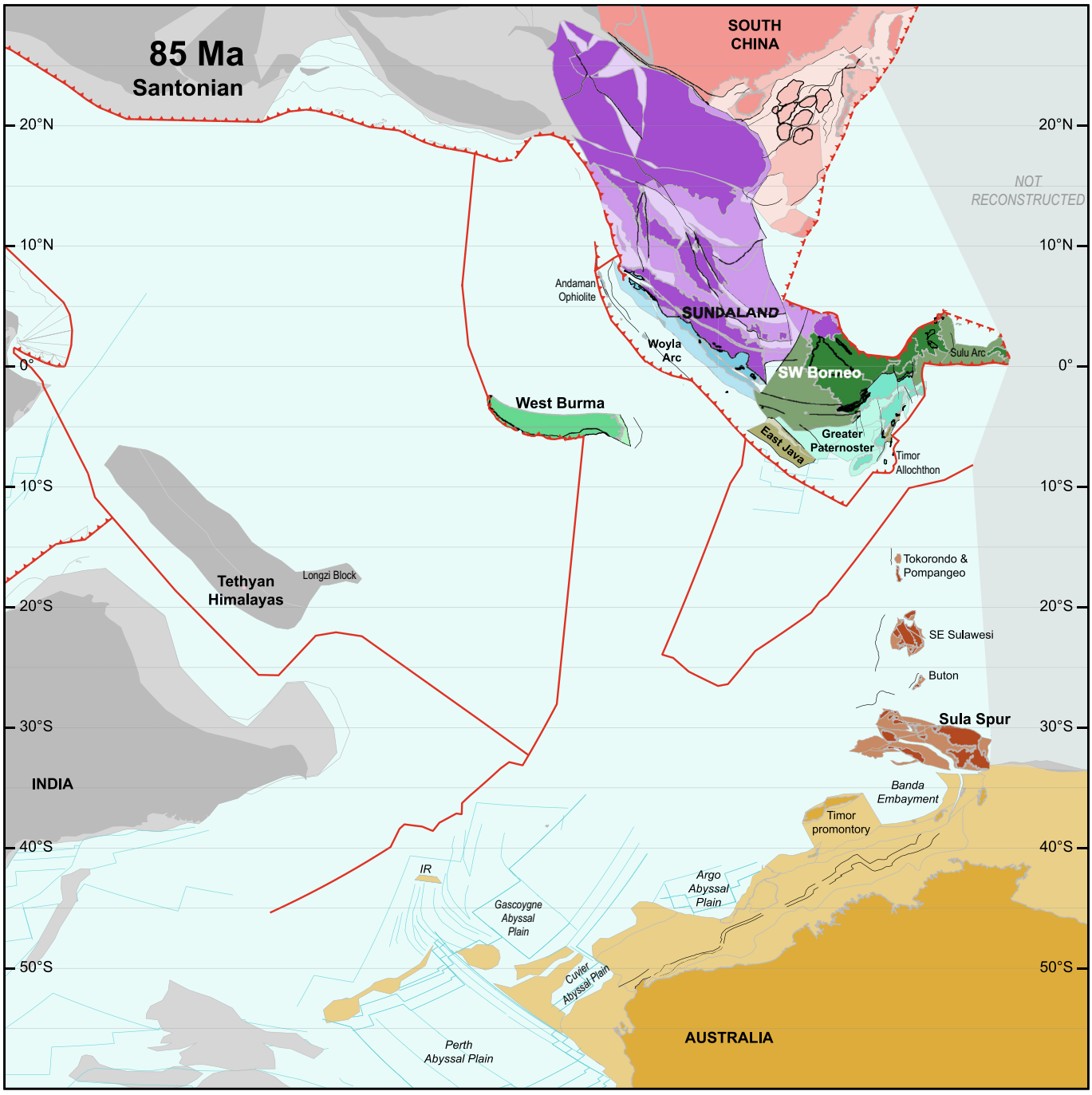

Fig. 37. Paleotectonic map for the Santonian (85 Ma). Abbreviations: IR, Investigator Ridge.

in an upper plate position above a subduction zone as required by arc magmatic and accretionary records of the West Burma Block and Inner Indo-Burman Ranges. Our reconstruction satisfies the same constraints, without requiring a speculative *trans*-Tethyan subduction zone to the Kohistan Arc.

6.5. Valanginian – 135 Ma

The interval from 85 to 135 Ma is characterized by slow relative motion between Australia and Eurasia, with only minor convergence (Figs. 38–47). However, the geological record of SE Asia shows that the ocean basins between the main Gondwana-derived mega-units and blocks all underwent subduction and closure suggesting that convergence between the Gondwana-derived units and Eurasia exceeded Australia-Eurasia motion, and that they thus diverged from Australia. The 135 Ma time slice coincides with the ophiolite ages and oldest metamorphic ages in subduction complexes along the West Burma Block, along the northern SW Borneo Mega-Unit, as well as within the Meratus Suture, and in the Bantimala Mélange. We tentatively interpret the initiation of subduction below the intra-oceanic Woyla Arc, whose oldest dated arc rocks are 122 Ma (Gafoer et al., 1992; Koning, 1985;

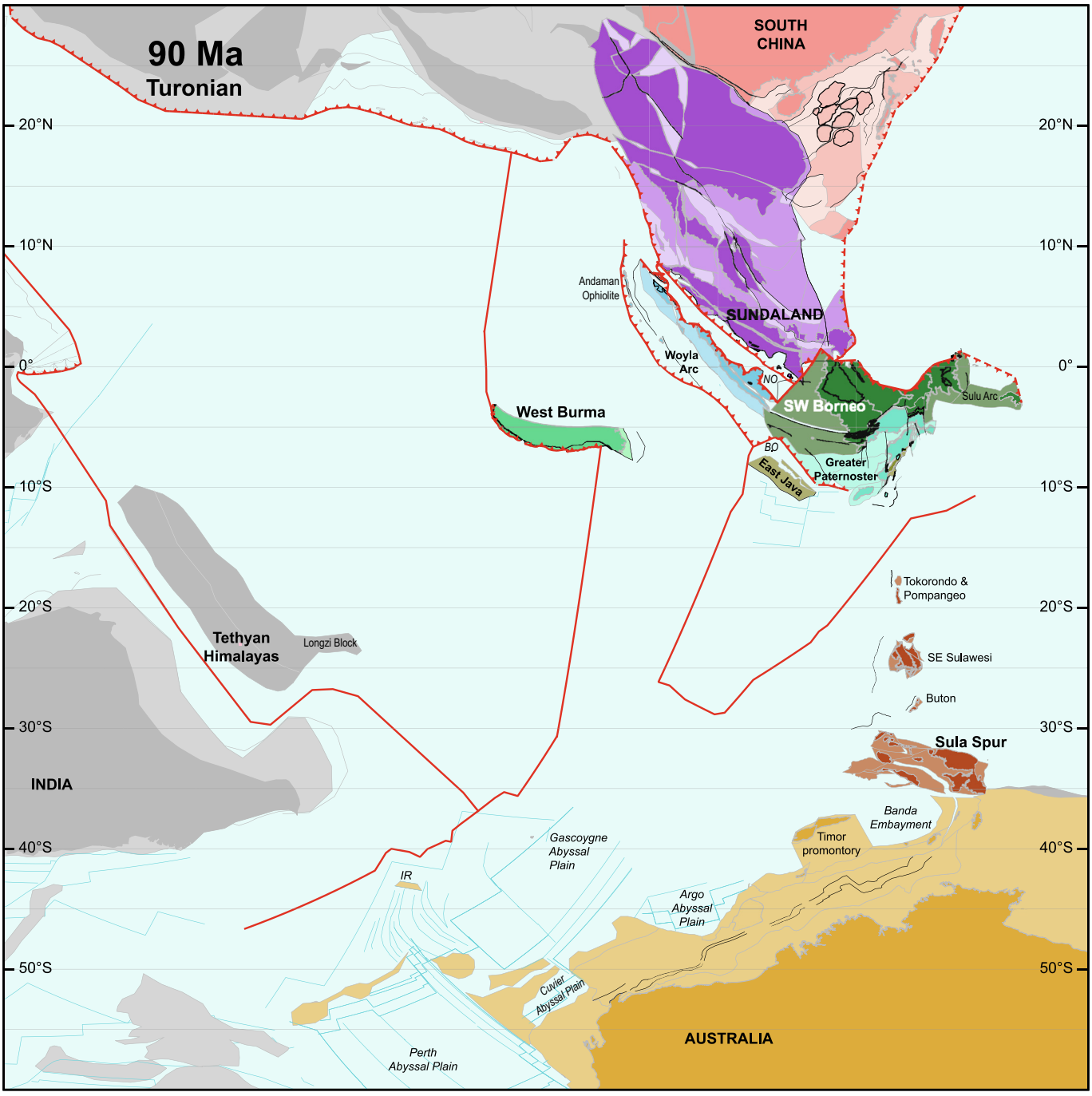

Fig. 38. Paleotectonic map for the Turonian (90 Ma). Abbreviations: BO, Bantimala Ocean; IR, Investigator Ridge; NO, Ngalau Ocean.

Pulunggono and Cameron, 1984) as also occurring around 135 Ma. It is unclear what drove the formation of these subduction zones. This time also coincides with the onset of India-Australia and India-Antarctica rifting and break-up (Gaina et al., 2007; Gibbons et al., 2013), and rifting within Greater India recorded by the Wölong Volcanics in the Tibetan Himalaya (Hu et al., 2010), and corresponds to the onset of supra-subduction zone ophiolite formation and metamorphic sole exhumation in the ophiolites that formed along the south Tibetan margin (Guilmette et al., 2009; Hébert et al., 2012; Huang et al., 2015), after initial underthrusting along the south Tibetan margin recorded by Lu–Hf garnet ages of the metamorphic soles of ~144 Ma (Guilmette et al., 2023). These larger plate motions and the initiation of subduction may be causally related.

In SE Asia, we reconstruct a NW-SE striking trench along the western margin of Sibumasu and the West Sumatra Block. The Valanginian is characterized by initiation of southward subduction below the Woyla Arc and the SW Borneo Mega-Unit, and by northward subduction of small ocean basins that existed between the different Gondwana-derived fragments. The ocean that was closed between the Woyla Arc/SW Borneo Mega-Unit and Sundaland was thus consumed by double-sided subduction, and corresponds to part of the Neotethys that was named the Ngalau Ocean by Advokaat et al. (2018a). Our reconstruction displays ~400–

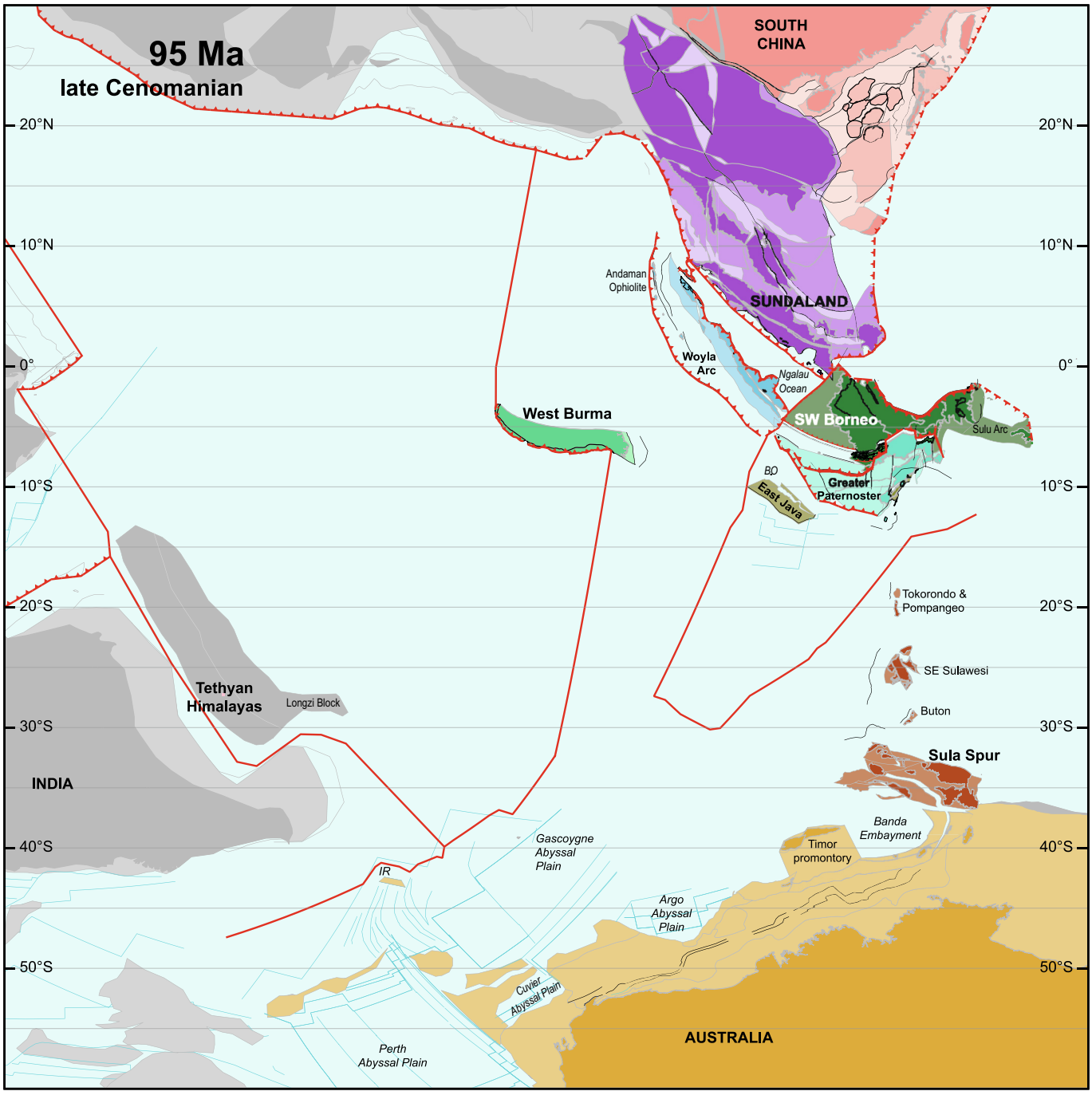

Fig. 39. Paleotectonic map for the late Cenomanian (95 Ma). Abbreviations: BO, Bantimala Ocean; IR, Investigator Ridge.

500 km wide Meratus and Bantimala oceans between the SW Borneo Mega-Unit, the Greater Paternoster Mega-Unit, and the East Java Block (Fig. 47). These widths are somewhat arbitrary, but are wide enough to sustain long-lived, slow subduction (Chenin et al., 2017), and narrow enough to remain conservative in inferring major poorly constrained plate motions. Prior to accretion of Mount Victoria Land to the West Burma Block at ~115 Ma, we reconstruct the West Burma Block on the same plate as the Greater Paternoster Mega-Unit, whilst Mount Victoria Land was located on the same plate as the East Java Block. Prior to 120 Ma, we reconstruct the Tokorondo and Pompangeo complexes of central Sulawesi also on this plate. This plate was separated by mid-oceanic spreading centers from the Australian plate and the Indian plate.

Previous reconstructions restore the accretion and drift of Gondwana-derived fragments in fundamentally different ways. Only Morley et al. (2020) restored accretion of Mount Victoria Land to the West Burma Block around 115 Ma. Hall (2012) instead assumed West Burma was already part of Sundaland in the Triassic. His reconstruction at 135 Ma of southwestward subduction below the SW Borneo Mega-Unit and the Woyla arc resembles ours. His reconstruction merged the units that we identified as the East Java and Greater Paternoster units, but their position relative to the SW Borneo Mega-Unit at 135 Ma is similar. Zahirovic et al. (2014, 2016) considered the SW Borneo Mega-Unit, and the Paternoster Terrane on Borneo as part of Sundaland since at least 155 Ma. Zahirovic et al. (2014) reconstructed only Mount Victoria

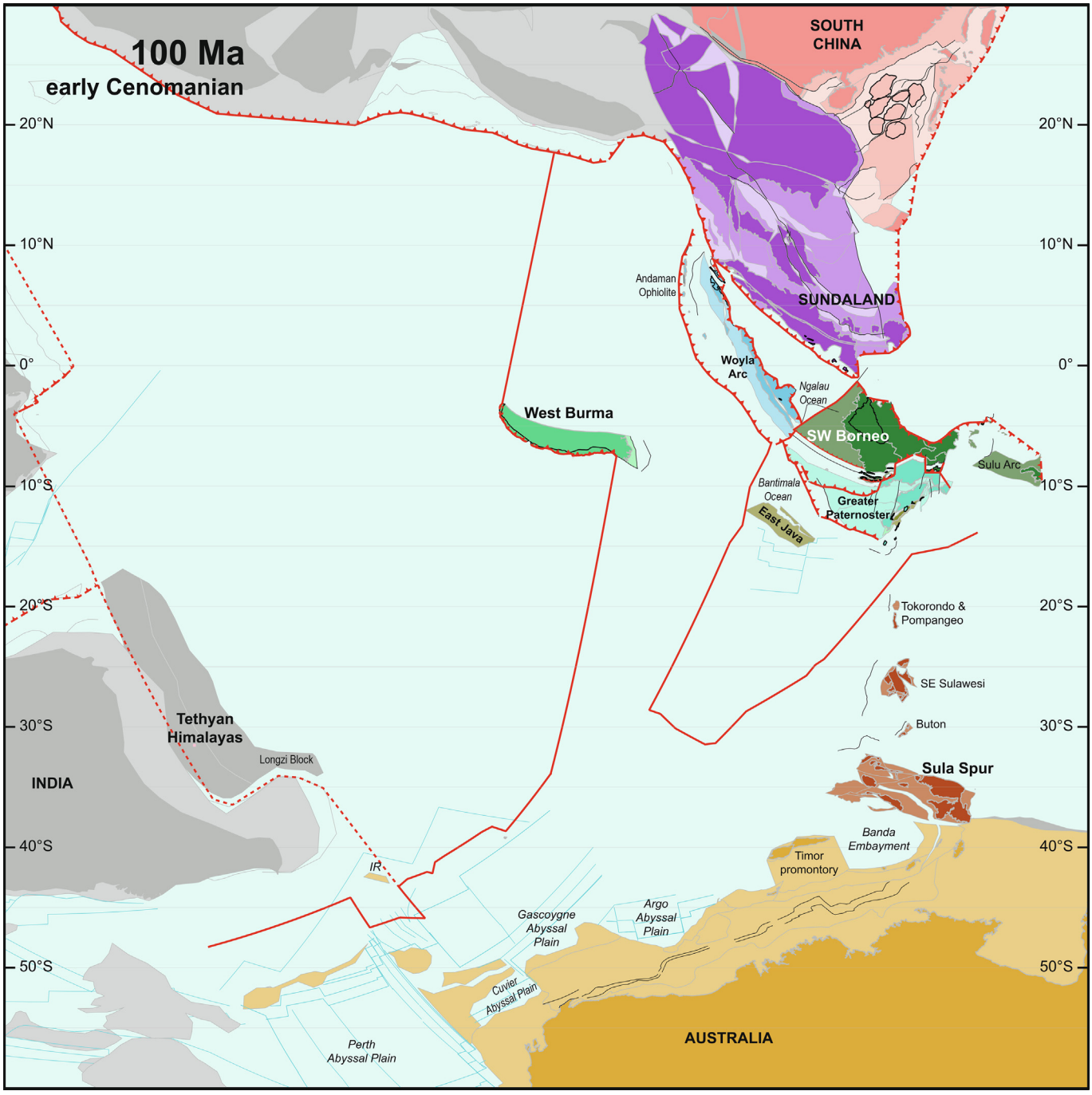

Fig. 40. Paleotectonic map for the early Cenomanian (100 Ma). Abbreviations: IR, Investigator Ridge.

Land (equivalent to their Mawgyi microcontinent), East Java, and West Sulawesi as Gondwana-derived. The position Zahirovic et al. (2014) inferred for the Mount Victoria Block in the Early Cretaceous is similar to ours, after which the block in their reconstruction underwent a motion towards the West Burma Block (where it arrives around 65 Ma) that is independent from the rest of SE Asia. Prior to Late Cretaceous accretion to Sundaland, Zahirovic et al. (2014) portrays Argoland fragments on two different plates that are separated by a mid-oceanic spreading center whereas Zahirovic et al. (2016) only restored East Java-West Sulawesi (the latter being part of our Greater Paternoster Mega-Unit) as Argoland fragments and placed them on one plate that lies far east compared to our reconstruction because they reconstruct them as derived from northern New Guinea. Zhang et al. (2022) interpreted that the Longzi Block of the NE Himalaya, which recorded Late Jurassic break-up and Early Cretaceous folding cut by ~130 Ma mafic dykes (with a plume rather than an arc-related geochemical signature) was a fragment of Argoland and that the folding related to collision with the West Burma Block. To satisfy paleomagnetic data from this block (Yuan et al., 2021), which place the Longxi terrane much farther south than predicted by Zhang et al. (2022), we instead infer that the Longzi Block was part of the Tibetan Himalayan margin of Greater India, and that the folding relates to transpression along the Wallaby Fracture zone during the breakup of (Greater) India from Australia.

Our reconstruction in general sense agrees with previous reconstructions in that the Gondwana-derived units in Early Cretaceous time must have diverged from Australia in order to accommodate

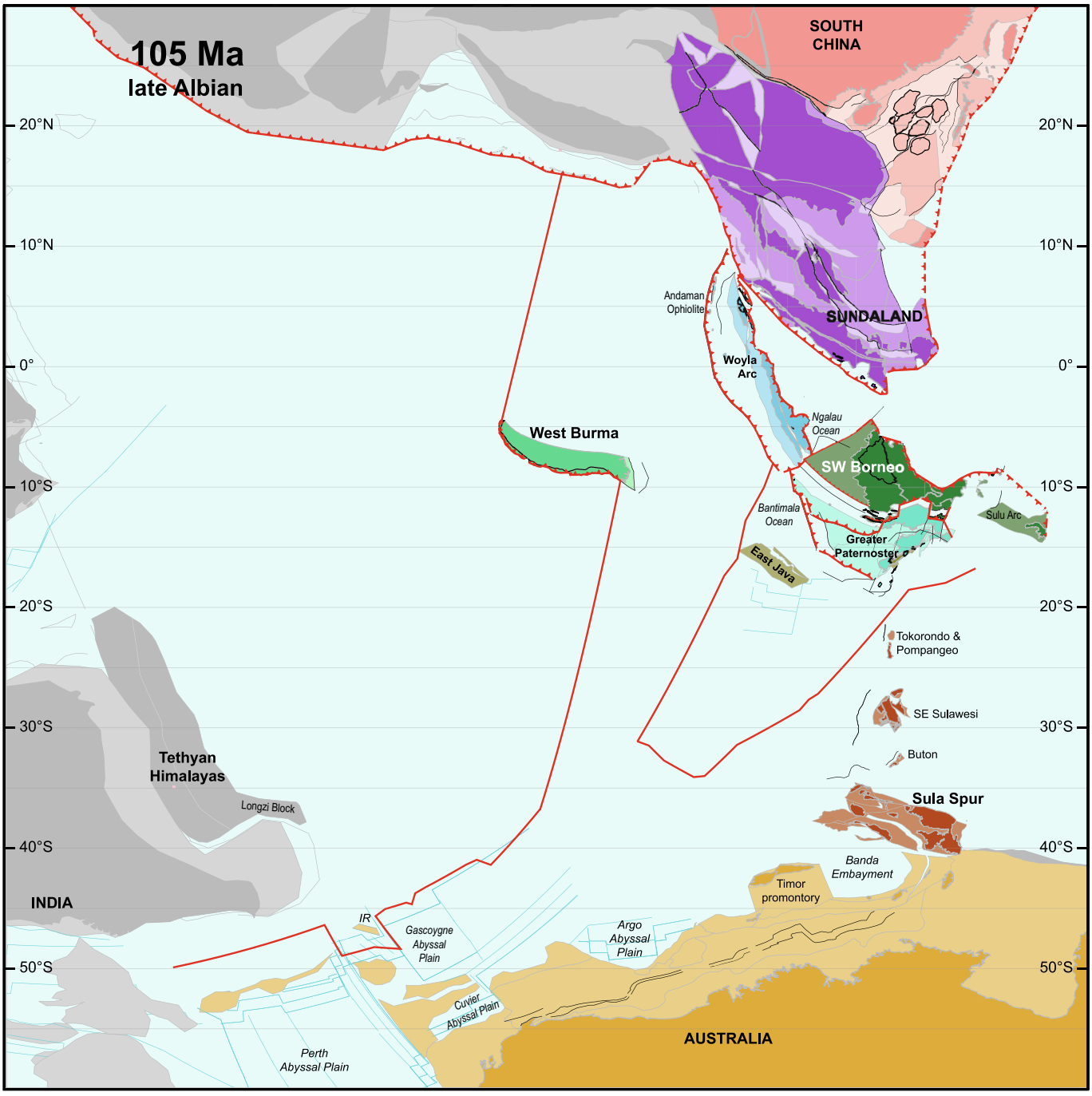

Fig. 41. Paleotectonic map for the late Albian (105 Ma). Abbreviations: IR, Investigator Ridge.

the subduction documented from the geological records found along their modern margins (Gibbons et al., 2012; Hall, 2012; Heine et al., 2004, 2002; Heine and Müller, 2005; Zahirovic et al., 2016, 2014). However, our reconstruction of the Woyla Arc differs from most previous reconstructions. Our recontruction of the Woyla Arc at 135 Ma is broadly similar to Hall (2012), but he assumed Woyla subduction started already 155 Ma ago, with the intra-oceanic Woyla Arc located along the northern Greater Indian margin. Metcalfe (2013a, 2011a, 2011b) displays a similar scenario. Conversely, Zahirovic et al. (2014) reconstructed only passive margins along the Woyla Arc fragments (Natal, Sikuleh), whereas Zahirovic et al. (2016) reconstructed that the Woyla Arc rifted off Sundaland in the Early Cretaceous (~145 Ma) above a northeast-dipping subduction zone.

6.6. Kimmeridgian – 155 Ma

The Kimmeridgian, at 155 Ma, corresponds to the continental break-up recorded in the Australian Northwest Shelf that lies at the basis of the Argoland concept. Our reconstruction shows that instead of one coherent and contiguous Argoland continent, the Kimmeridgian paleogeography consists of continental fragments

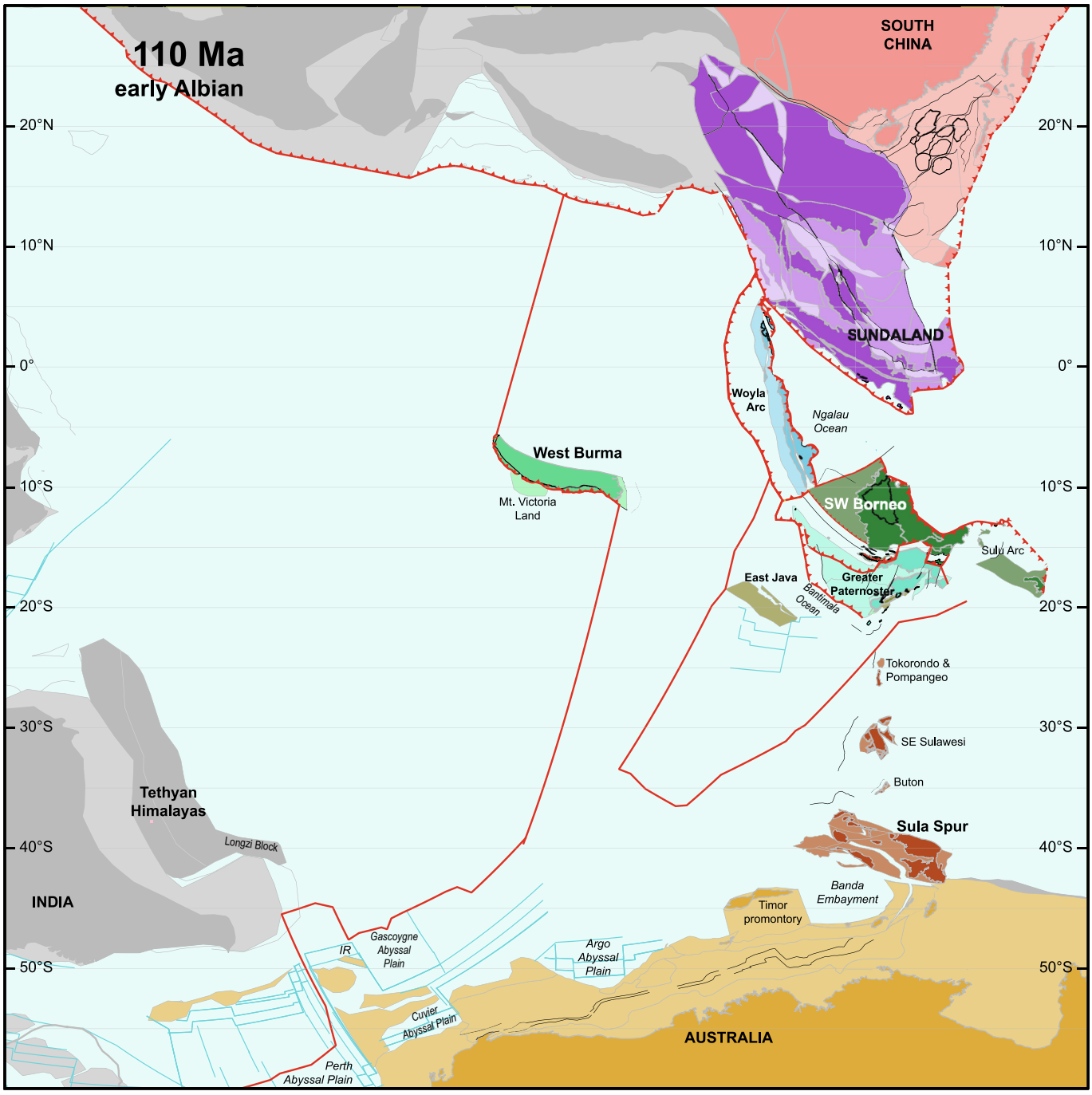

Fig. 42. Paleotectonic map for the early Albian (110 Ma). Abbreviations: IR, Investigator Ridge.

(SW Borneo Mega-Unit, Greater Paternoster Mega-Unit, East Java Block, West Burma Block, Mount Victoria Block, and the smaller blocks of the Sula Spur) that are separated by pre-Kimmeridgean oceanic basins whose relics are found in the OPS-bearing sutures of Bantimala, Meratus, and the inner Indo-Burman Ranges. Only the East Java Block and Mount Victoria Land actually rifted and broke off Australia at 155 Ma, to open the Argo Abyssal Plain and the predecessor of the Gascoygne Abyssal Plain (Figs. 48–51). The rest of the plate (or plates, we reconstructed that northwestern Australia was conjugate to two plates) already contained a series of microcontinents and oceans, but these contained no active plate boundaries anymore. Rather than Argoland, our reconstruction suggests that the tectonic configuration may be better termed 'Argopelago' at Kimmeridgian time.

At 155 Ma (Fig. 51) we reconstruct a western Argopelago plate carried the West Burma Block and Mount Victoria Land, whilst the eastern Argopelago plate carried the SW Borneo Mega-Unit, the Greater Paternoster Mega-Unit and the East Java Block. These plates are separated from each other and from Australia by ridges meeting in a triple junction that was located near the northwestern corner of the Exmouth Plateau. The Late Jurassic break-up recorded in the Longzi Block of the northeastern Tibetan Himalayas (Zhang et al., 2022b) occurred on the south side of the rift that separates the Argopelago (West Burma Block, Mount Victoria Land, and intervening basins) from Greater India. During the break-up and subsequent drift of Argopelago from the Australian margin, we reconstruct a transtensional plate boundary between eastern Argoland and the Sula Spur, along which the Sula Spur was fragmented, leaving behind SE Sula-

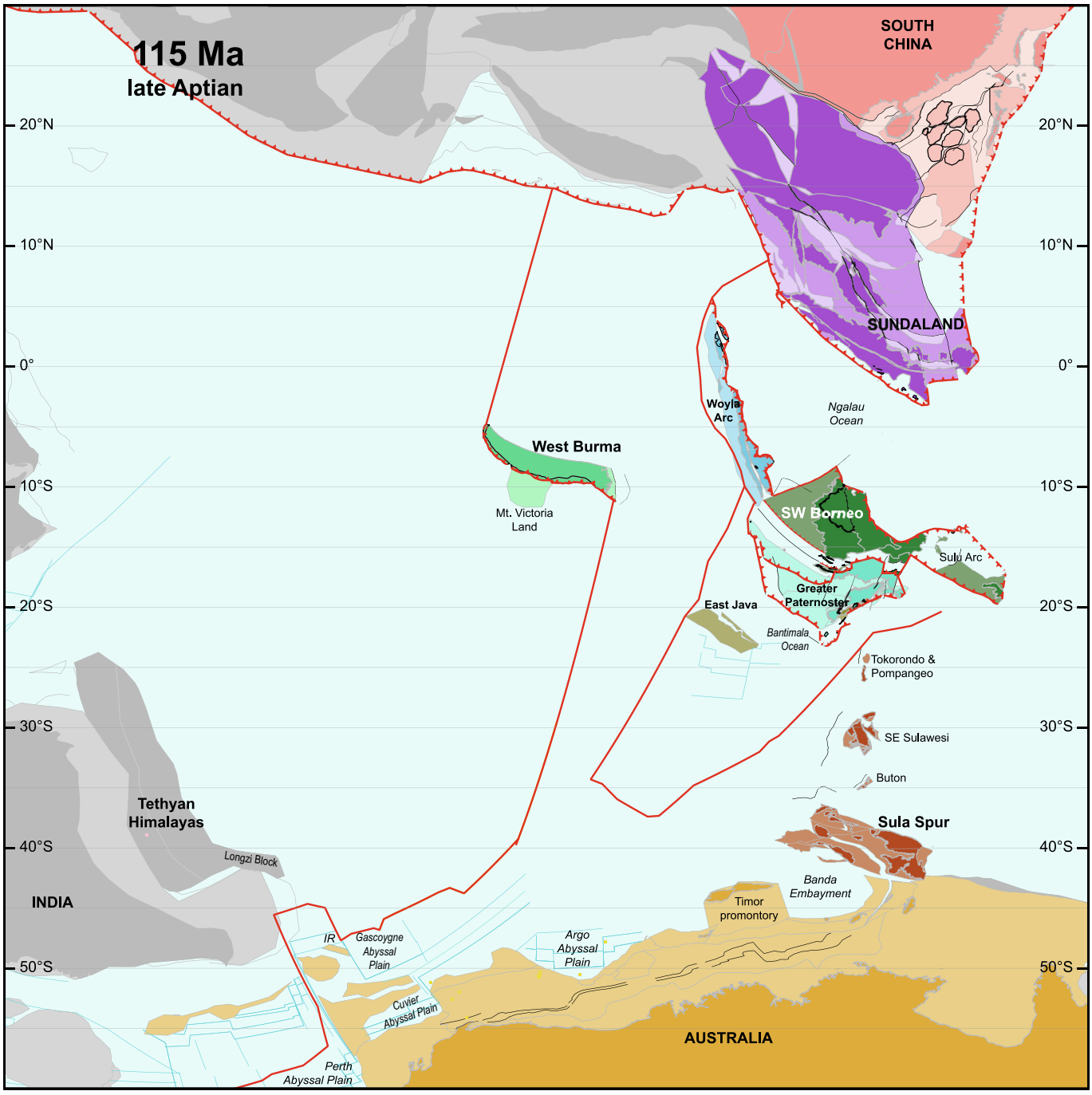

Fig. 43. Paleotectonic map for the late Aptian (115 Ma). Abbreviations: IR, Investigator Ridge.

wesi and Buton as rifted continental fragments on the Australian plate. SE Sulawesi and Buton are restored as the northern conjugate of the Bird's Head and also rifted off in the Jurassic.

Our reconstruction of Argoland as instead an 'Argopelago' reveals a paleotectonic configuration of northwestern Australia that resembles that of eastern Australia and Zealandia today (Fig. 51). Also east of Australia, continental fragments are intervened by deep, in part oceanic basins (Mortimer et al., 2019, 2017). An equivalent of the Jurassic rifting and break-up documented in the Argo Abyssal Plain would be if a rift initiated along the modern east Australian margin, and the already-deformed Zealandia basins and ranges would drift off, in ways similar as reconstructed for Greater Adria in the Triassic-Jurassic in the Mediterranean region (van Hinsbergen et al., 2020).

Our reconstruction differs from previous reconstructions, which either restored Argoland as a single continent that broke off from the northern Australian margin at 155 Ma (Gibbons et al., 2012; Heine et al., 2004, 2002; Heine and Müller, 2005; Zahirovic et al., 2016), or as multiple fragments that broke off between ~150–160 Ma (Hall, 2012; Longley et al., 2002; Metcalfe, 2013a, 2011b, 2011a, 1996, 1990; Zahirovic et al., 2014) or as early as the Early Jurassic (Hettangian; Jablonski and Saitta, 2004). Most reconstructions show the Argoland fragments surrounded by passive margins during their drift from northern Australia to Sundaland (Gibbons et al., 2012; Heine et al., 2004, 2002; Heine and Müller, 2005; Metcalfe, 1996, 1990; Zahirovic et al., 2016, 2014). In contrast, Hall (2012) reconstructed southward subduction below the Argoland fragments, a scenario adopted by Metcalfe (2013a, 2011a, 2011b).

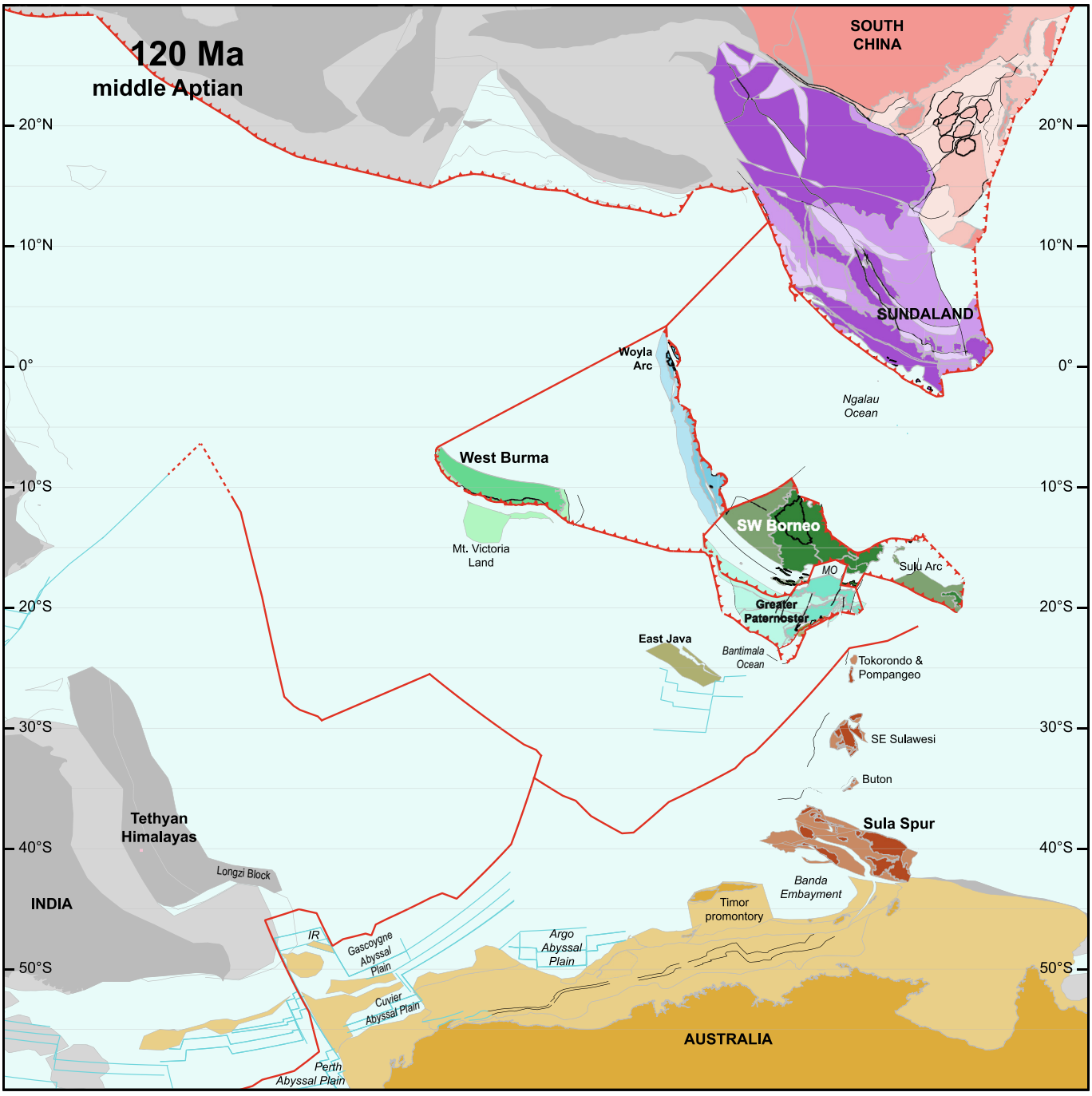

Fig. 44. Paleotectonic map for the middle Aptian (120 Ma). Abbreviations: IR, Investigator Ridge; MO, Meratus Ocean.

Another difference of our reconstruction with previous reconstructions is the restored location of the Argoland fragments. All previous reconstructions restored Argoland fragments in the Argo Abyssal Plain and north of Timor, but only Gibbons et al. (2012) and Yao et al. (2017) restored Argoland fragments west of the Exmouth Plateau, similar to our reconstruction. Similar to our reconstruction, Heine et al. (2004, 2002), Heine and Müller (2005) and Zahirovic et al. (2016), do not restore Argoland fragments within the Banda Embayment. However, many reconstructions restore Argoland fragments within the Banda Embayment (e.g., Gibbons et al., 2012; Hall, 2012; Metcalfe, 2013a, 2011a, 2011b; Zahirovic et al., 2014), which is incompatible with our restored position of the Timor promontory in front of the Banda Embayment. Similar to our reconstruction, only Zahirovic et al. (2014) restored fragments along the northern margin of the Bird's Head and Papua New Guinea.

6.7. Norian – 215 Ma

Prior to Oxfordian/Kimmeridgian break-up and formation of the Argo Abyssal Plain, most of the basins formed that broke Argoland into Argopelago (Figs. 52–54). We restored widespread NNW-SSE extension in Argopelago and the Northwest Australian Shelf since the Late Triassic that resulted in the formation of two branches of ocean basins. In the 215 Ma time slice, the opening of the Meratus Ocean has been restored, juxtaposing the SW Borneo Mega-Unit (that includes the basement underlying the Sula and Cagayan arcs) against the Greater Paternoster Mega-Unit. In addition, the

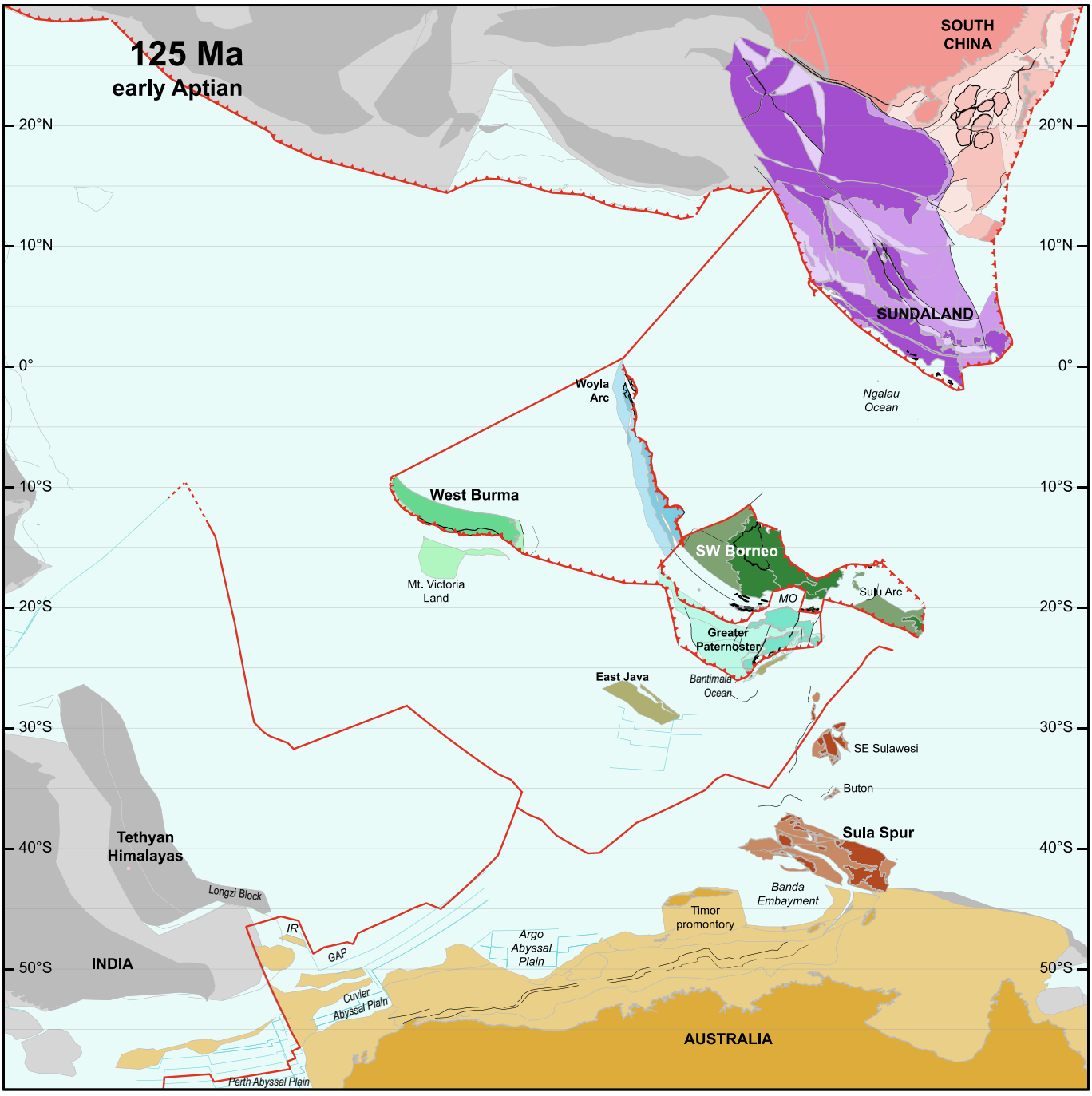

Fig. 45. Paleotectonic map for the early Aptian (125 Ma). Abbreviations: GAP, Gascoygne Abyssal Plain; IR, Investigator Ridge; MO, Meratus Ocean.

opening of Bantimala Ocean has been restored, juxtaposing the West Burma Block and Greater Paternoster Mega-Unit against the East Java Block, Mount Victoria Land, and the Australian Northwest Shelf. The Greater Paternoster Mega-Unit, and the Tokorondo and Pompangeo complexes, are juxtaposed against the reconstructed Timor margin, adjacent to the Bird's Head and Sula Spur, consistent with sediment provenance (Decker et al., 2017; Ferdian et al., 2012; Zhang et al., 2020b). From there, Argoland reaches to the Wallaby Plateau where Mount Victoria Land and the West Burma Block lie adjacent to the Tethyan Himalayas on the northern Indian margin, consistent with the similar sediment provenance of the Longxi Block of the Tibetan Himalayas and Mount Victoria Land (Aitchison et al., 2019; Cai et al., 2016; Yao et al., 2017; Zhang et al., 2022b; Zhang et al., 2020b).

We also reconstructed extension in the Banda Embayment between the Sula Spur/Bird's Head and Australia in the Late Triassic–Early Jurassic (215–175 Ma), which was interpreted based on high-temperature (granulite facies) metamorphism in central Seram (Pownall et al., 2017b). Our reconstruction places the Birds Head's and Sula Spur fragments adjacent to Timor and resulted in a ~400 km wide Banda Embayment between the Sula Spur and the northern Australian margin to the east of Timor (Fig. 54).

But even at 215 Ma, not all ocean basins that broke Argoland into Argopelago are fully restored (Fig. 54). The Banda Embayment likely accommodated N-S extension between Timor and the Sula Spur during the Late Carboniferous–Early Permian and a subsequent extension phase during the Late Permian–Middle Triassic (Charlton, 2001). In this time interval, also an ocean basin opened

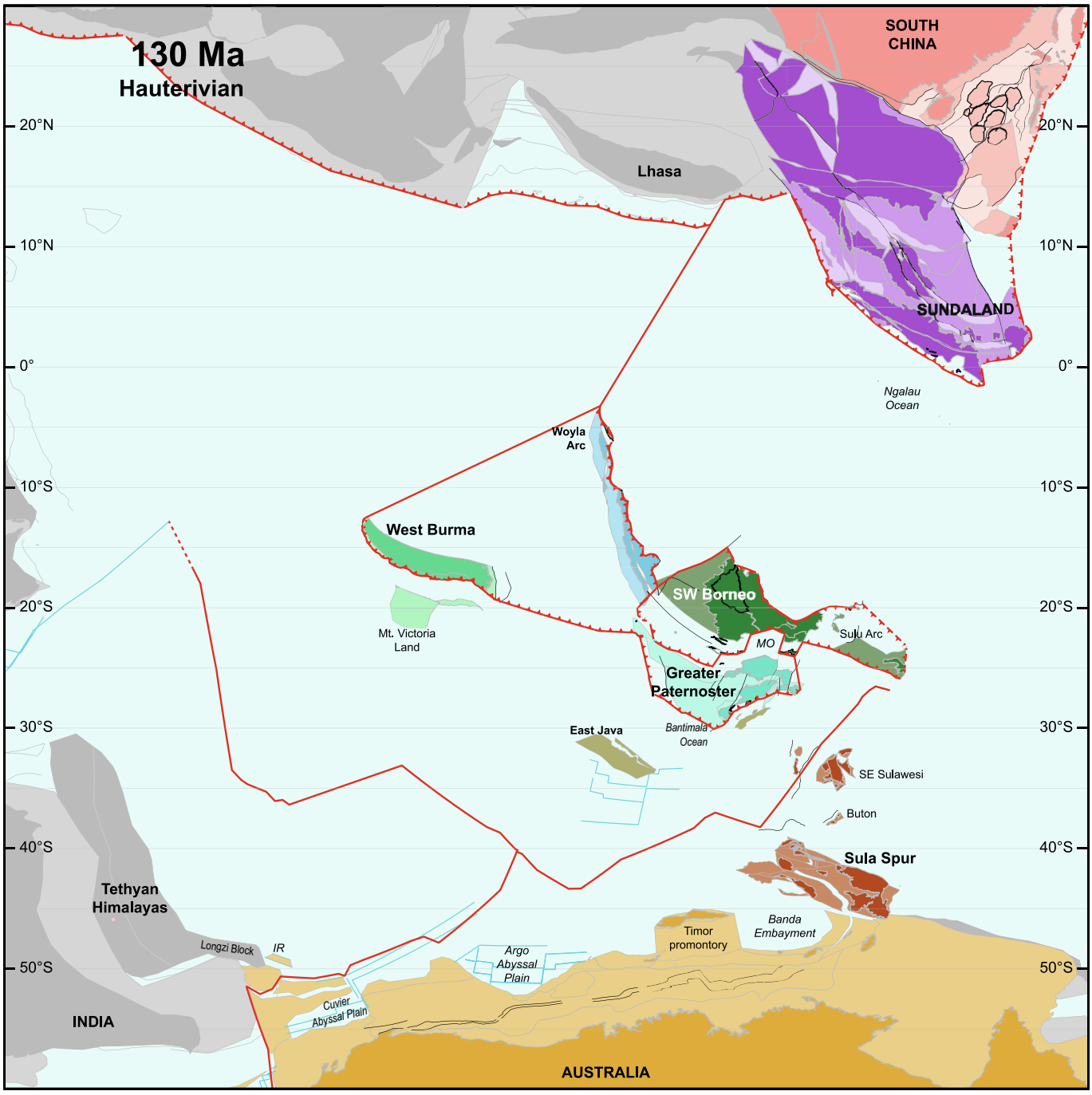

Fig. 46. Paleotectonic map for the Hauterivian (130 Ma). Abbreviations: IR, Investigator Ridge; MO, Meratus Ocean.

with a reconstructed width of ~300 km between the Greater Paternoster Mega-Unit in the north and the East Java Block in the south, consistent with zircon provenance data that suggest SW Borneo was not connected to the northwest Australian margin in the Triassic (Zhang et al., 2023). This basin likely opened associated with Late Carboniferous (Kasimovian/Gzhelian) to Early Permian (Sakmarian) rifting documented from the Northwest Australian Shelf (Gartrell et al., 2022) and may have been occupied by exhumed lower continental crust and lithospheric mantle as documented in the Australian Northwest Shelf (Bellingham and Mcdermott, 2014; Deng and McClay, 2019; Etheridge and O'Brien, 1994).

Few reconstructions restored the Late Triassic–Late Jurassic extension in Argoland and the Australian margin. Metcalfe (1996, 1990) restored the West Burma Block outboard of the Argo Abyssal Plain as part of the Australian Northwest Shelf in the Late Jurassic, and restored it on the Argo Abyssal Plain in the Late Triassic. Jablonski and Saitta (2004) show an Early Jurassic (Hettangian) break-up of their Mangkalihat fragment, and failed rifts between their Paternoster-Meratus and Sikuleh fragments and the Sahul Platform of the northern Australian margin.

The Late Triassic extension that we reconstructed in Argoland is probably linked with the break-up of the Lhasa terrane from Greater India and West Australia, as reconstructed based on geologic records of rifting (Longley et al., 2002; Metcalfe, 1996, 1990; Zhu et al., 2013) and paleomagnetic data (Li et al., 2022, 2016). Interestingly, Zhu et al. (2013) suggested that the Lhasa Terrane rifted off the Gondwana margin earlier, in the latest Carboniferous–Early Permian, together with the Qiantang Terrane, but

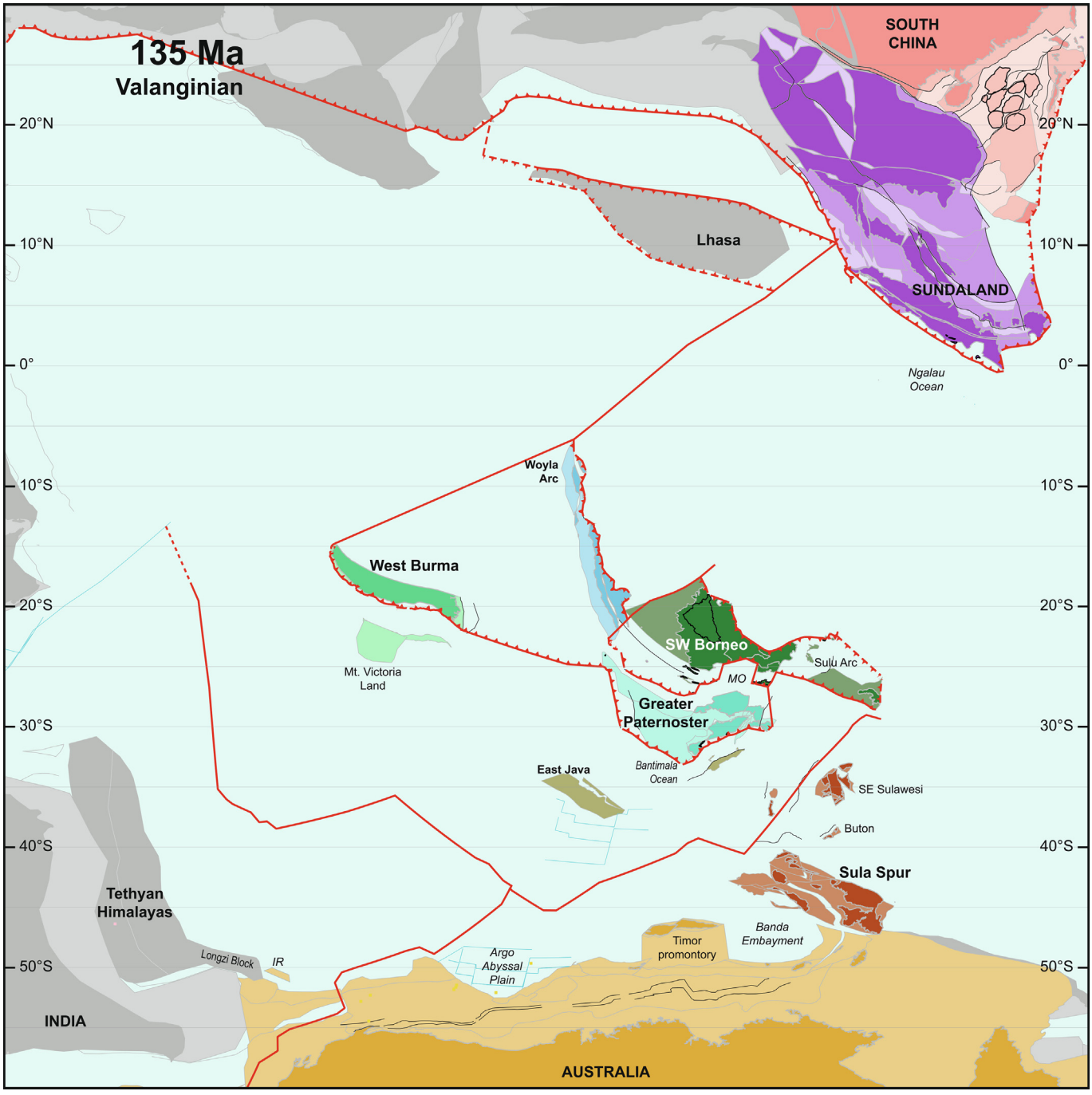

Fig. 47. Paleotectonic map for the Valanginian (135 Ma). Abbreviations: IR, Investigator Ridge; MO, Meratus Ocean.

following break-up of the Qiantang and Lhasa in the Middle Triassic (Zheng et al., 2022), converged with the Gondwana margin again and collided in the mid Triassic. Such a scenario could explain the enigmatic shortening during the Middle–Late Triassic 'Fitzroy' Movements documented from the Australian Northwest Shelf that preceded late Triassic rifting (Gartrell et al., 2022; Longley et al., 2002; Smith et al., 1999), and is consistent with sparse Permian to Triassic paleomagnetic data from the Lhasa terrane (Li et al., 2016). The Late Carboniferous–Early Permian extension documented in the NW Australian margin, within Argoland, and along the Nepal segment of the Tibetan Himalaya (e.g., Garzanti et al., 1999) may thus witness these break-up phases of the Gondwana margin.

7. Discussion

Our reconstruction of Argopelago and Argoland from the orogenic architecture of SE Asia is subject to the uncertainties that we indicated in our extensive review of SE Asian tectonic configuration. Many of the radiometric ages that we rely on are old K–Ar datings that may change with modern techniques. The dense vegetation cover and seas in the area we reconstructed complicated our correlations and they may not always be correct. Adding up these uncertainties may change the exact configurations in our reconstruction, in any case in detail (for instance the subduction polarity of the Meratus and Lok Ulo complexes (Wakita, 2000)), and if modern dating techniques drastically change the ages, these

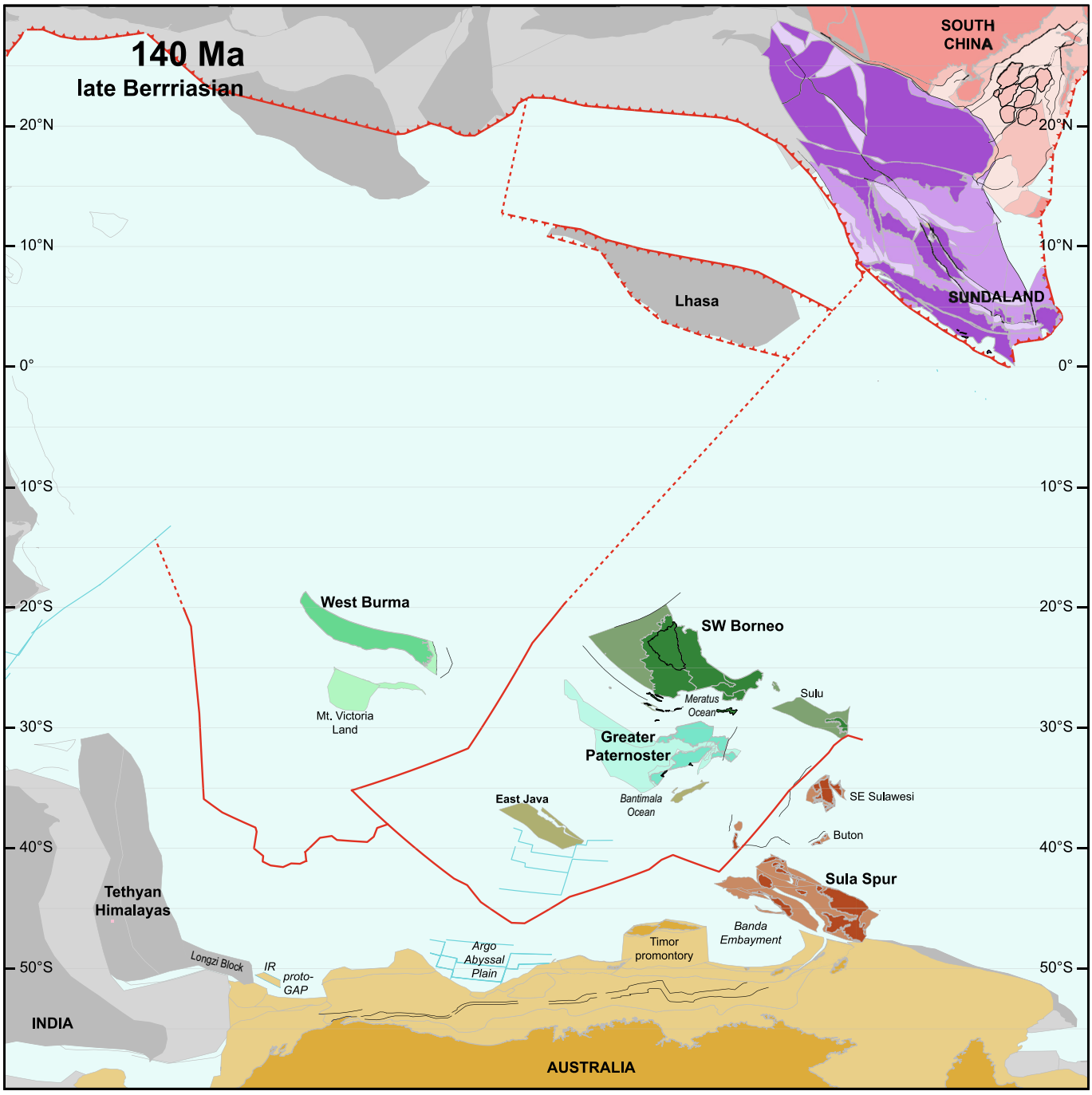

Fig. 48. Paleotectonic map for the late Berriasian (140 Ma). Abbreviations: IR, Investigator Ridge; proto-GAP, proto-Gascoygne Abyssal Plain.

will have bigger effects on our reconstruction. We hope that the comprehensive overview, and the reconstruction files, which are accessible in the Supplementary Information 5, allow to update the reconstruction if future data require so. In the discussion below, we highlight how SE Asian geology, and our reconstruction thereof, may provide opportunities for three problems that are widely discussed in the geodynamic community: subduction initiation, Greater Indian paleogeography, and continental subduction.

7.1. Argopelago destruction and subduction initiation in SE Asia

The destruction of the ocean basins within Argopelago was accommodated by subduction zones that formed along continental margins, along mid-ocean ridges, and by subduction polarity reversal following arc continent collision and ophiolite emplacement. These may be used in future studies targeting the dynamics of subduction initiation, and added to recent compilations of subduction initiation records (Crameri et al., 2020; Lallemand and Arcay, 2021).

Two subduction zones were truly intra-oceanic: the Woyla Arc that formed in the Early Cretaceous within the eastern Neotethys Ocean, perhaps along a former ridge segment (Fig. 47), and the present-day North Sulawesi Trench that formed by inversion of a back-arc basin spreading ridge in the latest Miocene (Figs. 21 and 22). Also the east-dipping subduction zone below the Philippine Sea Plate (Figs. 14 and 20), that likely formed in the Early Miocene, appears to have been intra-oceanic, but a detailed reconstruction of the Philippine Sea Plate is required to analyze in detail in which

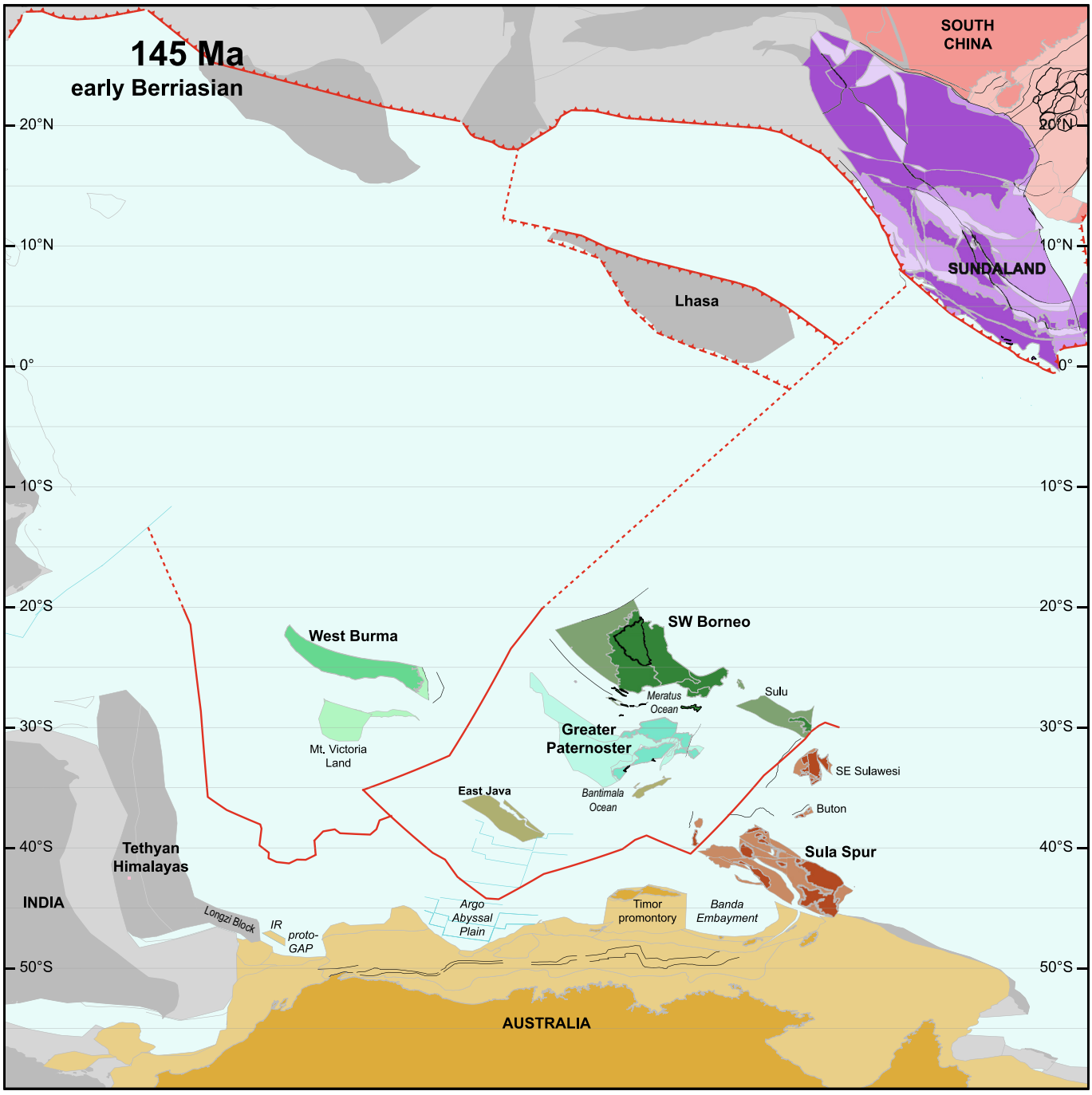

Fig. 49. Paleotectonic map for the early Berriasian (145 Ma). Abbreviations: IR, Investigator Ridge; proto-GAP, proto-Gascoygne Abyssal Plain.

context and setting this subduction started. One subduction zone formed by subduction polarity reversal, which occurred upon the collision of the Woyla Arc with the west Sundaland margin of Sumatra (Advokaat et al., 2018a; Bandyopadhyay et al., 2021; Barber et al., 2005a; Plunder et al., 2020) (Figs. 6 and 37–42). Two more polarity reversals may currently be underway in the arc-continent collision zones of Taiwan (Chemenda et al., 1997; Clift et al., 2003; Lallemand et al., 2001; Sibuet and Hsu, 2004; Suppe, 1984; Ustaszewski et al., 2012; von Hagke et al., 2016) and Timor (Harris, 2011; McCaffrey, 1996; McCaffrey and Nábělek, 1986; Silver et al., 1983c; Snyder et al., 1996; Tate et al., 2017, 2015) (Figs. 10–12, 15, 20 and 21). But all other subduction zones in our reconstruction formed along continental margins.

Geological records that are thought to be witnesses of subduction initiation are supra-subduction zone ophiolites and underlying metamorphic soles (e.g., Guilmette et al., 2018; Stern et al., 2012; Stern and Bloomer, 1992). These are thought to form upon catastrophic collapse of an incipient subduction zone, either spontaneously (Stern, 2004; Stern and Bloomer, 1992), or following a period of induced subduction (Guilmette et al., 2018) whereby the latter may be demonstrated from a time delay between the onset of formation of sub-ophiolitic metamorphic soles that record initiation of thrusting, and the formation of the ophiolites that signal upper plate extension (Guilmette et al., 2018) and onset of self-sustained subduction (Shuck et al., 2022). Several of the SE Asian subduction zones developed supra-subduction zone ophiolites. The Andaman-Nicobar Ophiolites and underlying metamorphic

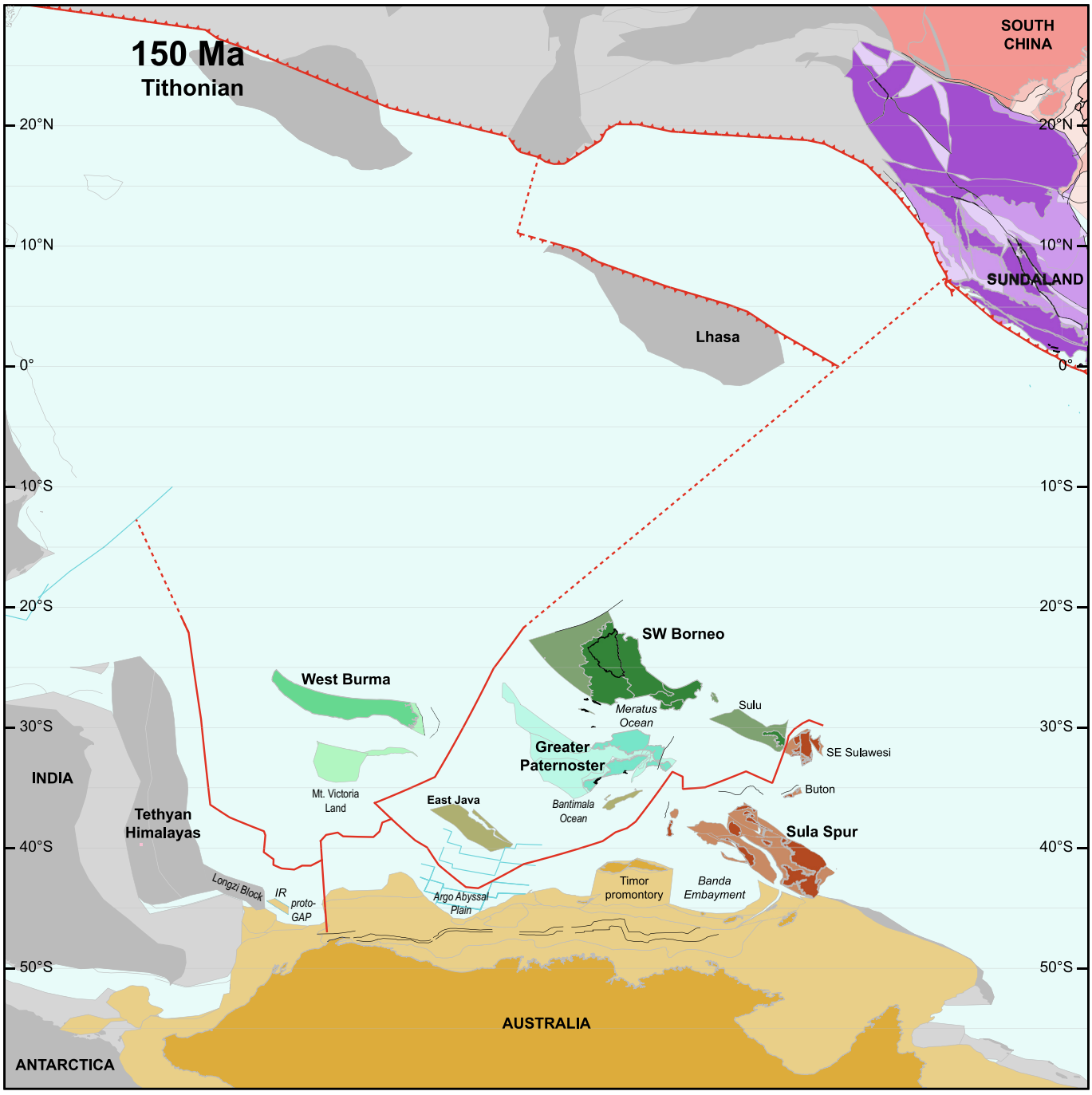

Fig. 50. Paleotectonic map for the Tithonian (150 Ma). Abbreviations: IR, Investigator Ridge; proto-GAP, proto-Gascoygne Abyssal Plain.

sole formed around 105 Ma upon the subduction polarity reversal during Woyla Arc-Sundaland collision (Plunder et al., 2020), whereby subduction likely initiated in the back-arc domain (Figs. 41–43), close to the western margin of the Woyla Arc (Bandyopadhyay et al., 2021). All other supra-subduction zone ophiolites we reconstruct have formed by forearc spreading following subduction initiation along a continental margin. Ophiolites of the Meratus Suture formed around 137 Ma close to the eastern margin of the SW Borneo Mega-Unit (Soesilo, 2012), ophiolites of the Timor Allochthon and Bantimala Mélange Belt (undated, but presumed Early Cretaceous) formed close to the eastern and southern margin of the Greater Paternoster Mega-Unit (Fig. 47), the SE Sulawesi ophiolites and the conjugate sea floor of the Celebes Sea formed upon Eocene (~45 Ma or slightly therefore) subduction initiation along the SW Borneo Mega-Unit basement underlying the Sulu Arc (Gaina and Müller, 2007; Monnier et al., 1995, 1994; Weissel, 1980), and the Palawan Ophiolites formed around 40–35 Ma following subduction initiation along the northern margin of the SW Borneo Mega-Unit (Dycoco et al., 2021; Encarnacion et al., 1995; Keenan et al., 2016) (Fig. 29). Previously, the presence of magmatic zircons of ~35 Ma in the metamorphic sole of the Palawan Ophiolites that have a similar metamorphic age were interpreted to reflect initiation at a mid-ocean ridge in the proto-South China Sea (Keenan et al., 2016). However, there is no geological record that could explain the post-35 Ma consumption of large amount of Proto-South China

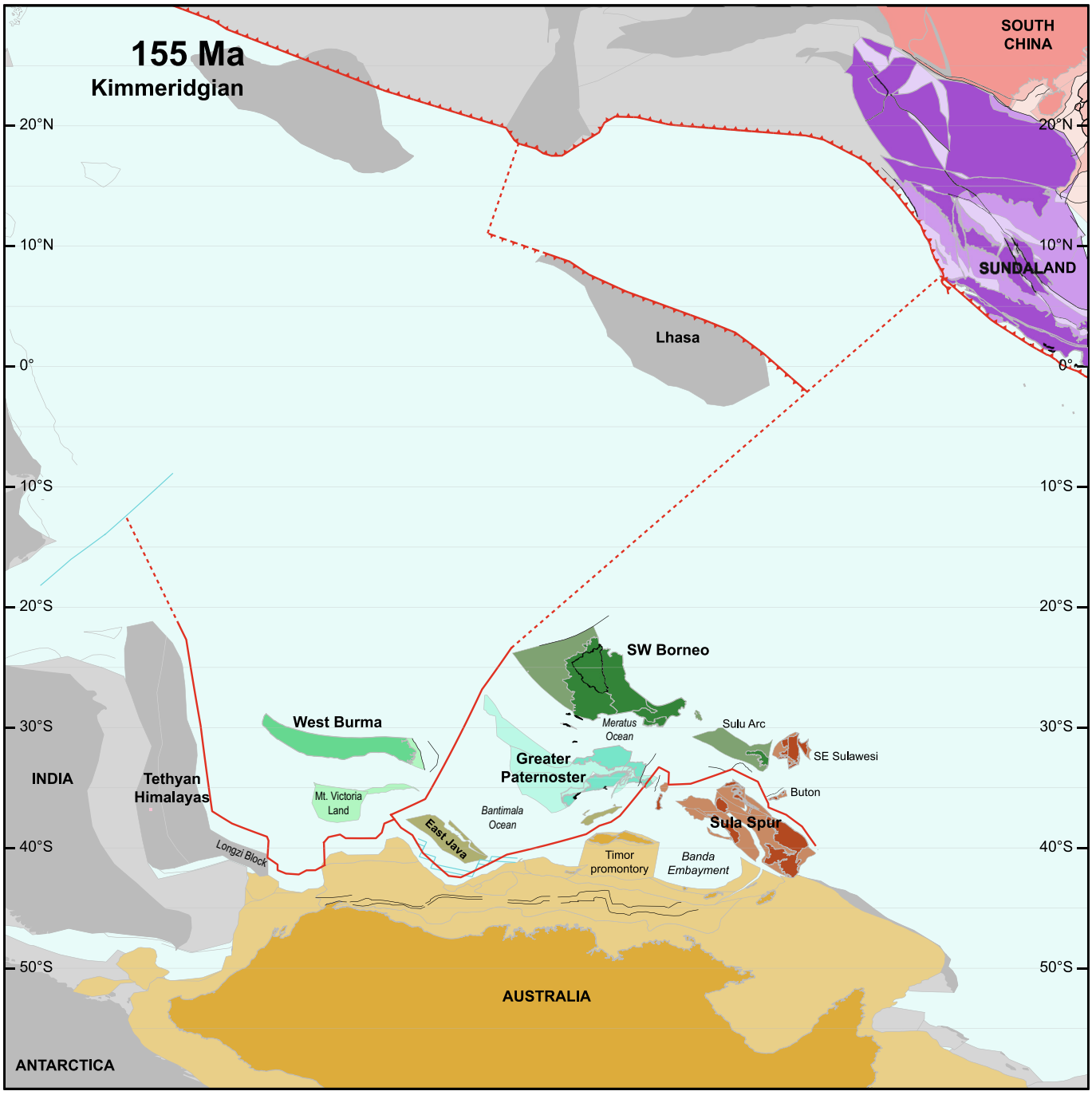

Fig. 51. Paleotectonic map for the Kimmeridgian (155 Ma).

Sea lithosphere between the Palawan Ophiolites and the Cagayan Arc to the south. We consider it more likely that the zircons found by Keenan et al. (2016) in the Palawan metamorphic sole resulted from crystallization of a partial melt during sole metamorphism, as has been documented in the sole of the Semail Ophiolite of Oman (Guilmette et al., 2018). These supra-subduction zone ophiolites of SE Asia considerably expand the database for forearc spreading following subduction initiation along continental margins, which so far comprised the Jurassic ophiolites that formed along the southern Pontide margin of Turkey (Topuz et al., 2013b, 2013a; van Hinsbergen et al., 2020), and the Lower Cretaceous ophiolites of the Indus-Yarlung suture south of the Lhasa Block of Tibet (Huang et al., 2015; Maffione et al., 2015). The SE Asian ophiolite belts may thus provide key research targets for future study of subduction initiation processes and dynamics.

7.2. Argoland and the pre-late Jurassic width of Greater India

Our reconstruction of Argoland has direct implications for the long-standing debate of the paleogeographic dimension of Greater India, and the dynamics of the India-Asia collision history. Greater India comprises the continental portion of the Indian continent that was consumed by subduction or otherwise underthrusting below the south Tibetan margin, and from which the nappes of the Himalaya were derived (e.g., Ali and Aitchison, 2005). Reconstructions of the shortening accommodated in the Himalayan

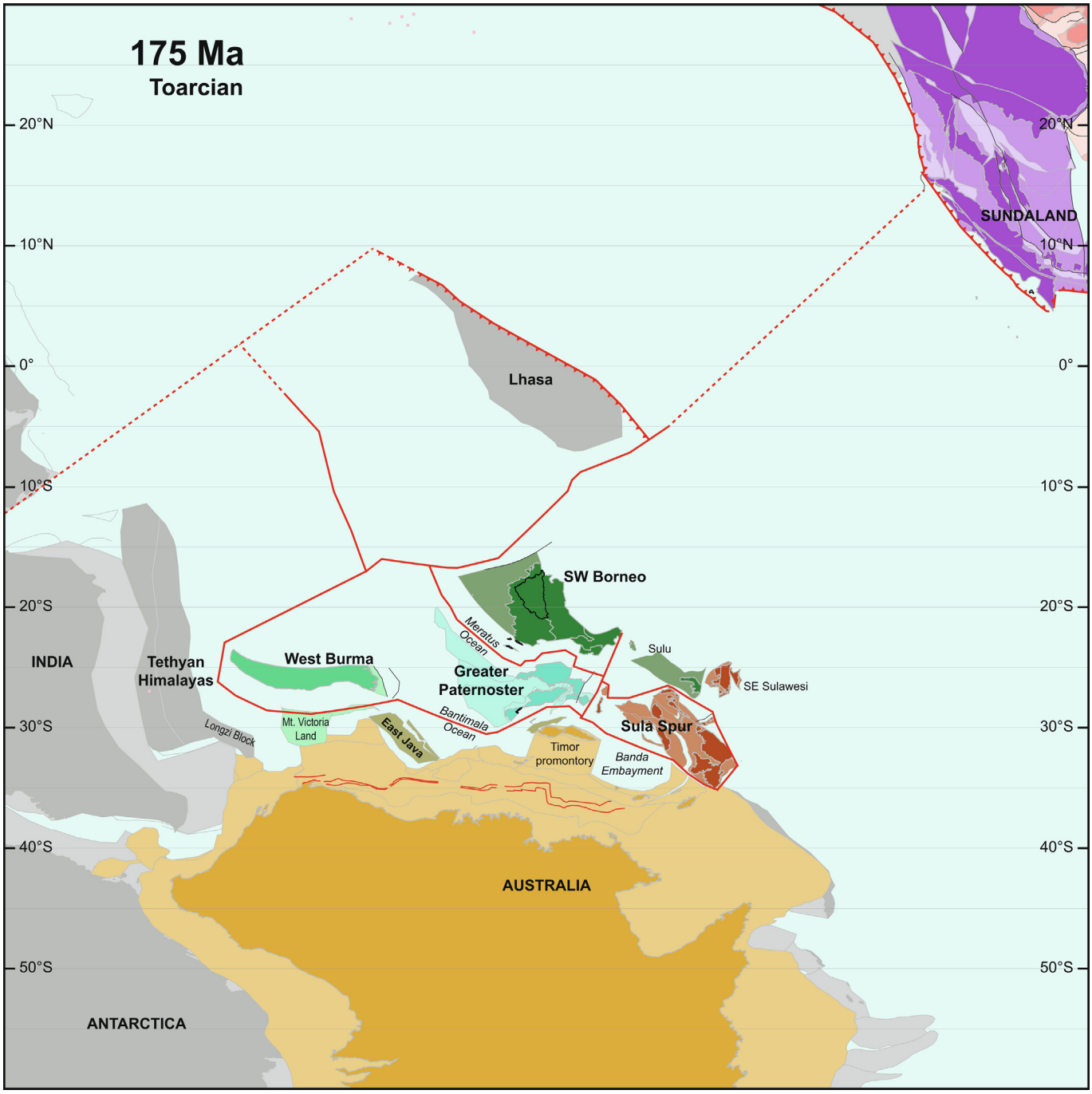

Fig. 52. Paleotectonic map for the Toarcian (175 Ma).

nappes reveals that at least 600–900 km of continental crust (measured perpendicular to the orogen) must have been present, before the onset of Himalayan thrusting around 60 Ma (Long et al., 2011). Records of metamorphism and stratigraphy in the Himalaya show that the northern two main nappe units, the Tibetan and Greater Himalayan nappes, were incorporated in the Himalayan orogen after 60 and before 50 Ma, whereas the Lesser Himalayan nappes that form the structurally deepest parts of the orogen were not incorporated in the fold-thrust belt until the Miocene, ~23 Ma or younger (van Hinsbergen, 2022, and references therein). A long-standing debate is where plate convergence was accommodated in the intervening period, during which time more than 2000 km of plate convergence was accommodated. There are three end-member scenarios. The most widely assumed scenario is that all of this entirely subducted lithosphere was continental, which would suggest that Greater India was some 3000 km wide and formed the conjugate margin of all of western Australia to at least the Argo Abyssal Plane (e.g., Ingalls et al., 2016). The second option infers that the orogenic deformation in the Tibetan and Greater Himalaya resulted from obduction of ophiolites and arcs at an equatorial position, perhaps linked to subduction records of the West Burma Block, followed by a late Eocene (40 ± 5 Ma) collision with Asia (Aitchison et al., 2007; Jagoutz et al., 2015; Kapp and DeCelles, 2019; Westerweel et al., 2019). In this case, Greater India extended to the Cape Range Fracture Zone of western Australia. The third option is that the Tibetan and Greater Himalayan rocks

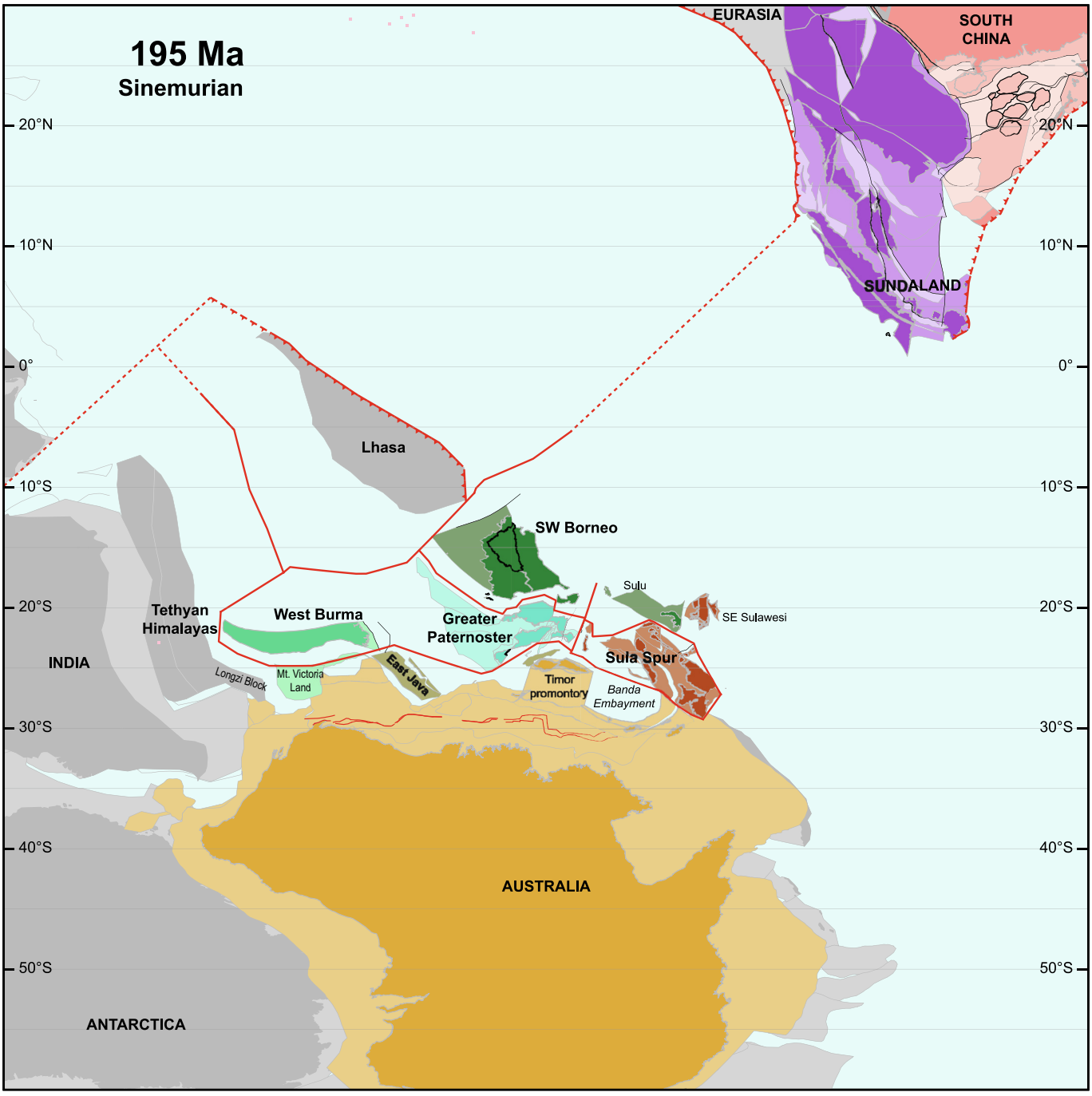

Fig. 53. Paleotectonic map for the Sinemurian (195 Ma).

were derived from a microcontinental fragment that broke off northern India in the Early Cretaceous and drifted north relative to India opening a Greater India Basin in its wake that subducted after Paleocene-early Eocene collision of the microcontinent with the southern Eurasian margin. The final India-Asia collision is reconstructed at Miocene (van Hinsbergen et al., 2012), which marks the final phase of slab break-off (Qayyum et al., 2022; Replumaz et al., 2010; Webb et al., 2017), and the transition from subduction of Indian lithosphere to the onset of horizontal underthrusting below the Tibetan Plateau as imaged by seismology (van Hinsbergen, 2022; van Hinsbergen et al., 2019a). In this scenario, Greater India would not have extended beyond the Wallaby Fracture Zone, as previously inferred based on paleomagnetic data (Ali and Aitchison, 2005), and reconstruction of magnetic anomalies that infer that Jurassic break-up continued as far south as the Wallaby Fracture zone (Gibbons et al., 2012).

Our reconstruction of Argoland now provides independent evidence that in Jurassic time, Greater India cannot have extended beyond the Wallaby Fracture Zone (Figs. 51–54). The Longzi margin of the eastern Tibetan Himalaya, where Zhang et al. (2022) documented evidence for Jurassic continental breakup, reconstructs directly west of the Wallaby Plateau to the south of Argoland, and is fully consistent with the prediction of Gibbons et al. (2012). Our reconstructed width of Argoland, which comprises the West Burma and Mount Victoria blocks adjacent to the Longzi Block (Figs. 51–54), does not extend west of the Longzi Block and is

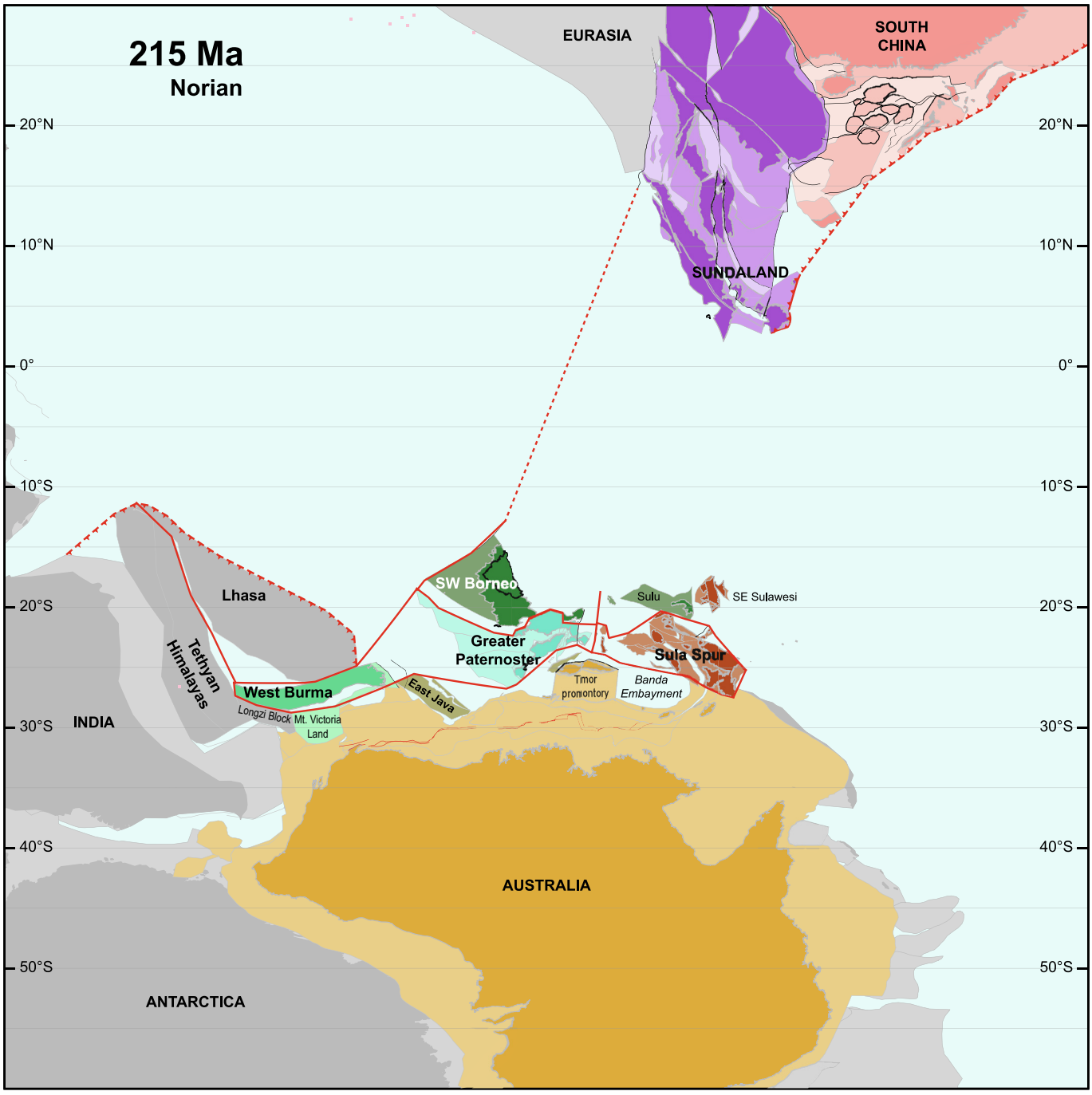

Fig. 54. Paleotectonic map for the Norian (215 Ma). Note that our reconstruction of Sundaland is simplified: we did not restore late Triassic deformation associated with the final stages of collision between Sibumasu, Indochina, and South China.

thus consistent with an older passive margin farther west where a Permian break-up unconformity was concluded from the Nepal Himalaya (Garzanti, 1999). Moreover, the Longzi Block and the Mount Victoria blocks share a Triassic clastic sedimentary stratigraphy with a west Australian provenance (Cai et al., 2016; Yao et al., 2017), which is satisfied by our reconstruction (Fig. 54).

A fully continental Greater India after Paleocene collision with Asia is thus precluded by our Argoland reconstruction. This shows that after initial collision, long-lived oceanic subduction must have been accommodated in the India-Asia collision, either to the south of a microcontinent, or to the north of an obducted margin (van Hinsbergen, 2022). The limited width of Greater India further implies that the pre-Miocene history of the Tibetan Plateau occurred above an oceanic subduction zone, perhaps intervened by a short period of continental subduction upon Paleocene-early Eocene microcontinent arrival at the trench, but also requires finding an explanation for the low volumes of arc magmatism and the lack of a conclusive accretionary record of oceanic subduction (van Hinsbergen, 2022). The India-Asia collision history thus still provides widespread opportunity to constrain geodynamic processes and the geological response thereto.

7.3. Implications of Argoland reconstruction for continental subduction

The paradigm underlying paleogeographic reconstruction, which provides a key constraint on our understanding of plate tec-

tonics and mantle dynamics, as well as paleoclimate, -biology, and - oceanography, is that continental crust does not disappear without leaving a geological record (van Hinsbergen and Schouten, 2021, and references therein). With the reconstruction of Argoland that we present in this paper, spanning the continent that was conjugate to the west and northwest Australian margin from the Wallaby Fracture Zone to the Sula Spur in the northeast, this paradigm remains intact: not only is there no necessity to invoke large-scale wholesale continental subduction below Tibet, but Argoland as reconstructed here is based on the modern area of SE Asia, corrected for documented deformation.

Arrival of continental lithosphere at trenches has two possible documented responses. On the one hand, it may lead to arrest and relocation of subduction leads to preservation of the original lithosphere in an orogen – as for instance happened upon arrival of the Indochina, Qiangtang-Sibumasu, or Lhasa Blocks at the margin of Eurasia (Kapp and DeCelles, 2019; Metcalfe, 2013a; van Hinsbergen and Schouten, 2021). On the other hand, subduction (or shallow underthrusting) may continue, and upper continental crust is offscraped from their subducting lower crustal and mantle underpinnings – as for instance happened to much of the Greater Adria or Briançonnais continents in the Mediterranean region (Handy et al., 2010; van Hinsbergen et al., 2020, 2005), or to the Himalaya (Long et al., 2011; van Hinsbergen et al., 2019a). The arrival of Argoland's lithosphere at the trenches around Sundaland was mostly associated with the former style of accretion. Much of Argoland's original lithosphere thus still exist in Indonesia (e.g., Granath et al., 2011), albeit deformed by extension during oroclinal bending of Sundaland, and by opening of back-arc basins such the Sulu Sea Basin or the Flores Basin. Continental subduction was restricted to the western Sula Spur with upper crustal nappes remaining in Sulawesi, the Australian margin with nappes remaining at Timor, Mount Victoria Land with nappes remaining in the Indo-Burman Ranges, and the relics of the South China margin preserved in the Palawan Terrane. The comparison of the different responses of the basins and ranges of Argopelago and Greater Adria, both paleogeographic domains that may be compared to Zealandia today (Mortimer et al., 2017), may form a basis for analysis of continental subduction and accretion.

8. Summary and conclusions

The geological record of the northwest Australian margin from Timor in the northeast to the Wallaby Fracture Zone in the southwest has long been argued to result from a late Jurassic continental break-up of a continent, conceptually known as Argoland. Finding Argoland proved challenging, suggesting that large parts may have subducted without leaving a representative geological record. In this paper, we reconstruct the SE Asian orogenic belt to identify whether it contains the remains of contintal crust that once covered the entire NW Australian margin.

We therefore review the architecture of the modern SE Asian orogen and NW Australian passive margin and identify continent-derived blocks and tectonic 'mega-units' that cover (parts of) multiple islands and sea floors, and surrounding suture zones, and summarize the chronological, stratigraphic, and structural constraints that quantify their deformation history. We then use this architecture in combination with a systematic reconstruction protocol for orogenic belts, cast in context of the Australia-Eurasia plate circuit, and using GPlates plate reconstruction software, to reconstruct the plate tectonic and paleogeographic evolution from continental break-up to orogenesis, covering a time from the present back to the Triassic.

We find that 'Argoland' at the time of late Jurassic break-up of the west Australian continental margin consisted of several continental fragments separated by Late Jurassic or older oceanic basins. These continents included the West Burma Block, Mount Victoria Land, the SW Borneo Mega-Unit, the Greater Paternoster Mega-Unit, the East Java Block, and fragments summarized as the Sula Spur. We find that together, these blocks covered the entire northwest Australian passive margin from Timor to the Wallaby Fracture Zone. However, during the late Jurassic break-up, Argoland was no longer one coherent and contiguous continental fragment, but was already deformed into microcontinents and intervening, narrow ocean basins that formed in Carboniferous-Permian, and late Triassic-middle Jurassic time. The paleogeography of 'Argoland', which we instead term 'Argopelago' in the late Jurassic bears similarities with that of Zealandia to the east of Australia today, and bears similarities to 'Greater Adria' reconstructed from the Mediterranean region. The Late Triassic-Early Jurassic deformation of the NW Australian margin and Argoland coincides with and may be related to the break-up of the Lhasa terrane from the Gondwana margin, whereas the late Paleozoic extension may also relate to break-up of Tibetan fragments, including the Qiangtang-Sibumasu mega-unit.

An important implication of our reconstruction of Argoland is that continental crust of Greater India in the late Jurassic did not extend beyond the Wallaby Fracture zone, limiting the paleogeographic width of Greater India to <1000 km, consistent with paleomagnetic results and Himalayan shortening records. This way, our reconstruction of Argoland reveals that the continental crust that must have existed along the passive margin of Australia in the early-mid Mesozoic, as well as from Greater India, is accounted for in the modern geological records of the Himalaya and SE Asia. There is no unequivocal demonstration of large-scale, wholesale continental subduction in the eastern Tethyan realm. meaning that the paradigm that underlies paleogeographic reconstruction – that the geography of the past may be represented by a redistribution of modern continental crust – is not challenged by eastern Neotethyan geological records.

Declaration of Competing Interest

The authors declare that they have no known competing financial interests or personal relationships that could have appeared to influence the work reported in this paper.

Acknowledgements

DJJvH acknowledges funding through NWO Vici grant 864.11.004. ELA started this reconstruction in 2016 at the Department of Earth Sciences at Utrecht University and was able to continue working part-time on this project at the Department of Physical Geography at Utrecht University for which opportunity he kindly acknowledges Martin Hendriks and Steven de Jong. ELA thanks colleagues at both departments for their inspiration and discussion. We also thank Marco Maffione (University of Birmingham, United Kingdom) for inspiration, opportunity, and discussion. We thank Wim Spakman for discussions on slab and mantle dynamics. ELA thanks Robert Hall and colleagues at SE Asia Research Group of Royal Holloway University of London for introduction to the geology of SE Asia. We acknowledge the many colleagues for stimulating discussions that helped us understand the region (where we got it right, they deserve credit. Where we did not, we are to blame). These include Shihu Li on Indochina; Ian Watkinson on the Thai Peninsula; Jorien van der Wal on Peninsular Malaysia; Christian Heine on the Sunda Shelf; Jan Westerweel, Alexis Licht, Pierrick Roperch, and Ji'en Zhang on the West Burma Block and the Indo-Burman Ranges; Anthony Barber, Michael Crow, and Mayke Bongers on the Woyla Arc; Debaditya Bandy-

opadhyay, Alexis Plunder, and the late Pinaki Bandopadhyay on the Andaman-Nicobar Islands; Sara Pena Castellnou on Java; Theo van Leeuwen, Giovanni Pezzati, Alfend Rudyawan, Juliane Hennig-Breitfeld and Abang Mansyursyah Surya Nugraha on Sulawesi; Garrett Tate, Ron Harris, and Nadine McQuarrie on Timor; Jonathan Pownall on the Banda Arc region; David Gold on the Bird's Head; Suzanna van de Lagemaat, Junaidi Asis, Alex Burton-Johnson, Licheng Cao, and John Suppe on the evolution of the western Pacific margin in South China and NE Borneo. Discussions with Thomas Schouten, Nalan Lom, and Abdul Qayyum inspired and motivated the Mesozoic part of the reconstruction. Comments by Romy Meyer helped to improve the reconstruction of the West Burma Block and Mount Victoria Land. We thank Robert Crookbain for enthusiastic and challenging questions regarding paleomagnetic data from the region. Han van Gorsel's bibliography (vangorsel-slist.com) provided many entries into literature on the geology of SE Asia. We appreciate reviews from Manuel Pubellier, Chris Morley, and Peter Cawood. Finally, we dedicate this work to our mentor, the late Reinoud Vissers, whose maternal family is Indonesian, and who taught and inspired us both. This one is for you, old man!

Appendix A. Supplementary Material

Supplementary data to this article can be found online at https://doi.org/10.1016/j.gr.2023.10.005.

References

Abbot, M.J., Chamalaun, F.H., 1981. Geochronology of some Banda Arc volcanics. Geol. Tectonics East. Indonesia, pp. 253–268.
Abdullah, C.I., Rampnoux, J.-P., Bellon, H., Maury, R.C., Soeria-Atmadja, R., 2000. The evolution of Sumba Island (Indonesia) revisited in the light of new data on the geochronology and geochemistry of the magmatic rocks. J. Asian Earth Sci. 18, 533–546.
Aben, F.M., Dekkers, M.J., Bakker, R.R., van Hinsbergen, D.J.J., Zachariasse, W.J., Tate, G.W., McQuarrie, N., Harris, R., Duffy, B., 2014. Untangling inconsistent magnetic polarity records through an integrated rock magnetic analysis: A case study on Neogene sections in East Timor. Geochem. Geophys. Geosyst. 15, 2531–2554.
Acharyya, S.K., 2015. Indo-Burma Range: a belt of accreted microcontinents, ophiolites and Mesozoic-Paleogene flyschoid sediments. Int. J. Earth Sci. 104, 1235–1251.
Acharyya, S.K., Roy, D.K., Mitra, N.D., 1986. Stratigraphy and palaeontology of the Naga Hills ophiolite belt. Mem. Geol. Surv. India 119, 64–74.
Adhitama, R., Hall, R., White, L.T., 2017. Extension in The Kumawa Block, West Papua, Indonesia. Proc. Indones. Pet. Assoc. Annu. Conv. 41, IPA17-125-G.
Adlan, Q., Kartanegara, S.M., Kesumajana, A.H.P., Syaripudin, E.A., 2016. Explanation of Seram Island's More Prolific Oil Potential Compared to Its Offshore Area Using Palinspastic and Basin Modeling Approaches. Proc. Indones. Pet. Assoc. Annu. Conv. 40, IPA16-294-G
Advokaat, E.L., 2016. Neogene Extension and Exhumation in NW Sulawesi. University of London.
Advokaat, E.L., Hall, R., White, L.T., Watkinson, I.M., Rudyawan, A., BouDagher-Fadel, M.K., 2017. Miocene to recent extension in NW Sulawesi, Indonesia. J. Asian Earth Sci. 147. https://doi.org/10.1016/j.jseaes.2017.07.023.
Advokaat, E.L., Bongers, M.L.M., Rudyawan, A., BouDagher-Fadel, M.K., Langereis, C. G., Van Hinsbergen, D.J.J., 2018a. Early Cretaceous origin of the Woyla Arc (Sumatra, Indonesia) on the Australian plate. Earth Planet. Sci. Lett. 498, 348–361.
Advokaat, E.L., Marshall, N., Li, S., Spakman, W., Krijgsman, W., van Hinsbergen, D.J. J., 2018b. Cenozoic rotation history of Borneo and Sundaland, SE Asia, revealed by paleomagnetism, mantle tomography and kinematic reconstruction. Tectonics 37, 2486–2512.
Agius, M.R., Lebedev, S., 2013. Tibetan and Indian lithospheres in the upper mantle beneath Tibet: Evidence from broadband surface-wave dispersion. Geochem. Geophys. Geosyst. 14, 4260–4281.
AGSO, North West Shelf Study Group, 1994. Deep reflections on the North West Shelf: changing perceptions of basin formation. Proc. Pet. Expl. Soc. Aust., 63–76.
Aitchison, J.C., 1994. Early Cretaceous (pre-Albian) radiolarians from blocks in Ayer Complex melange, eastern Sabah, Malaysia, with comments on their regional tectonic significance and the origins of enveloping melanges. J. SE Asian Earth Sci. 9, 255–262.
Aitchison, J.C., Ao, A., Bhowmik, S., Clarke, G.L., Ireland, T.R., Kachovich, S., Lokho, K., Stojanovic, D., Roeder, T., Truscott, N., 2019. Tectonic evolution of the western margin of the Burma microplate based on new fossil and radiometric age constraints. Tectonics 38, 1718–1741.
Aitchison, J.C., Ali, J.R., Davis, A.M., 2007. When and where did India and Asia collide? J. Geophys. Res. Solid Earth 112.
Alam, M., Alam, M.M., Curray, J.R., Chowdhury, M.L.R., Gani, M.R., 2003. An overview of the sedimentary geology of the Bengal Basin in relation to the regional tectonic framework and basin-fill history. Sed. Geol. 155, 179–208.
Alfing, J.J., Bröcker, M.M., Setiawan, N.I., 2021. Rb–Sr geochronology of metamorphic rocks from the Central Indonesian Accretionary collision complex: Additional age constraints for the Meratus and Luk Ulo complexes (South Kalimantan and Central Java). Lithos 105971.
Ali, J.R., Aitchison, J.C., 2005. Greater India. Earth-Sci. Rev. 72, 169–188.
Ali, J.R., Hall, R., 1995. Evolution of the boundary between the Philippine Sea Plate and Australia: palaeomagnetic evidence from eastern Indonesia. Tectonophysics 251, 251–275.
Ali, J.R., Milsom, J., Finch, E.M., Mubroto, B., 1996. SE Sundaland accretion: palaeomagnetic evidence of large Plio-Pleistocene thin-skin rotations in Buton. Geol. Soc. Lond. Spec. Publ. 106, 431–443.
Ali, M.A.M., Willingshofer, E., Matenco, L., Francois, T., Daanen, T.P., Ng, T.F., Taib, N. I., Shuib, M.K., 2016. Kinematics of post-orogenic extension and exhumation of the Taku Schist, NE Peninsular Malaysia. J. Asian Earth Sci. 127, 63–75.
Almasco, J.N., Rodolfo, K., Fuller, M., Frost, G., 2000. Paleomagnetism of Palawan, Philippines. J. Asian Earth Sci. 18, 369–389.
An, W., Hu, X., Garzanti, E., Wang, J., Liu, Q., 2021. New precise dating of the India-Asia collision in the Tibetan Himalaya at 61 Ma. Geophys. Res. Lett. 48.
Andi Mangga, S., Amiruddin, Suwarti, T., Gafoer, S., Sidarto, 1994. Geology of the Kotaagung Quadrangle, Sumatera (1:250,000). Geol. Res. Dev. Centre, Bandung.
Andreason, M.W., Mudford, B., Onge, J.E.S., 1997. Geologic evolution and petroleum system of the Thailand Andaman Sea basins. Proc. Pet. Syst. SE Asia Australas. Conf., 337–350.
Antonio, L.R., 1972. Preliminary report on the geology of east-central Zamboanga Peninsula, Mindanao. Unpubl. Rep. Philipp. Bur. Mines 58.
Arai, S., 1997. Origin of podiform chromitites. J. Asian Earth Sci. 15, 303–310.
Arfai, J., Franke, D., Gaedicke, C., Lutz, R., Schnabel, M., Ladage, S., Berglar, K., Aurelio, M., Montano, J., Pellejera, N., 2011. Geological evolution of the West Luzon Basin (South China Sea, Philippines). Mar. Geophys. Res. 32, 349–362.
Aribowo, S., Husson, L., Natawidjaja, D.H., Authemayou, C., Daryono, M.R., Puji, A.R., Valla, P.G., Pamumpuni, A., Wardhana, D.D., de Gelder, G., 2022. Active Back-Arc Thrust in North West Java, Indonesia. Tectonics 41, e2021TC007120.
Armandita, C., Morley, C.K., Rowell, P., 2015. Origin, structural geometry, and development of a giant coherent slide: The South Makassar Strait mass transport complex. Geosphere 11, 376–403.
Atkinson, C., Renolds, M., Clarke, A., Sampurno, S., 2004. Why Look in Deepwater When Elephants Prefer the Shallows? The Biliton Basin Revisited.
Audley-Charles, M.G., 1965. Permian palaeogeography of the northern Australia-Timor region. Palaeogeogr. Palaeoclimatol. Palaeoecol. 1, 297–305.
Audley-Charles, M.G., 1968. The geology of the Portuguese timor. Geol. Soc. Lond. Mem. 4, 1–76.
Audley-Charles, M.G., 1986. Rates of Neogene and Quaternary tectonic movements in the Southern Banda Arc based on micropalaeontology. J. Geol. Soc. Lond. 143, 161–175.
Audley-Charles, M.G., Carter, D.J., 1972. Palaeogeographical significance of some aspects of Palaeogene and early Neogene stratigraphy and tectonics of the Timor Sea region. Palaeogeogr. Palaeoclimatol. Palaeoecol. 11, 247–264.
Audley-Charles, M.G., Harris, R.A., 1990. Allochthonous terranes of the Southwest Pacific and Indonesia. Philos. Trans. R. Soc. Lond.. Ser. A Math. Phys. Sci. 331, 571–587.
Aung, A.K., Cocks, L.R.M., 2017. Cambrian-Devonian stratigraphy of the Shan Plateau, Myanmar (Burma). Geol. Soc. Lond., Mem. 48, 317–342.
Aurelio, M.A., Forbes, M.T., Taguibao, K.J.L., Savella, R.B., Bacud, J.A., Franke, D., Pubellier, M., Savva, D., Meresse, F., Steuer, S., 2014. Middle to Late Cenozoic tectonic events in south and central Palawan (Philippines) and their implications to the evolution of the south-eastern margin of South China Sea: Evidence from onshore structural and offshore seismic data. Mar. Pet. Geol. 58, 658–673.
Baker, S., Malaihollo, J., 1996. Dating of Neogene igneous rocks in the Halmahera region: arc initiation and development. Geol. Soc. Lond. Spec. Publ. 106, 499–509.
Ballantyne, P., 1991. Petrological constraints upon the provenance and genesis of the East Halmahera ophiolite. J. SE Asian Earth Sci. 6, 259–269.
Ballantyne, P., 1992. Petrology and geochemistry of the plutonic rocks of the Halmahera ophiolite, eastern Indonesia, an analogue of modern oceanic forearcs. Geol. Soc. Lond. Spec. Publ. 60, 179–202.
Bandopadhyay, P.C., 2005. Discovery of abundant pyroclasts in the Namunagarh Grit, South Andaman: evidence for arc volcanism and active subduction during the Palaeogene in the Andaman area. J. Asian Earth Sci. 25, 95–107.
Bandopadhyay, P.C., 2012. Re-interpretation of the age and environment of deposition of Paleogene turbidites in the Andaman and Nicobar Islands, Western Sunda Arc. J. Asian Earth Sci. 45, 126–137.
Bandopadhyay, P.C., Carter, A., 2018. Paleogene Tectonic and Sedimentation History of the Andaman-Nicobar Accretionary Arc, Northeast Indian Ocean. In: The Indian Paleogene. Springer, pp. 91–112.
Bandopadhyay, P.C., Carter, A., 2017a. Mithakhari deposits. Geol. Soc. Lond., Mem. 47, 111–132.
Bandopadhyay, P.C., Carter, A., 2017b. Submarine fan deposits: petrography and geochemistry of the Andaman Flysch. Geol. Soc. Lond., Mem. 47, 133–140.
Bandopadhyay, P.C., Carter, A., 2017c. The archipelago group: current understanding. Geol. Soc. Lond., Mem. 47, 153–166.

Bandopadhyay, P.C., Chakrabarti, U., Roy, A., 2009. First report of trace fossils from Palaeogene succession (Namunagarh Grit) of Andaman and Nicobar Islands. J. Geol. Soc. India 73, 261–267.
Bandopadhyay, P.C., Ghosh, B., 2015. Provenance analysis of the Oligocene turbidites (Andaman Flysch), South Andaman Island: a geochemical approach. J. Earth Syst. Sci. 124, 1019–1037.
Bandopadhyay, P.C., van Hinsbergen, D.J.J., Bandyopadhyay, D., Licht, A., Advokaat, E.L., Plunder, A., Ghosh, B., Dasgupta, A., Trabucho-Alexandre, J.P., 2022. Paleogeography of the West Burma Block and the eastern Neotethys Ocean: constraints from Cenozoic sediments shed onto the Andaman-Nicobar ophiolites. Gondw. Res. 103, 335–361.
Bandyopadhyay, D., van Hinsbergen, D.J.J., Plunder, A., Bandopadhyay, P.C., Advokaat, E., Chattopadhaya, S., Morishita, T., Ghosh, B., 2020. Andaman ophiolite: an overview. In: The Andaman Islands and Adjoining Offshore: Geology, Tectonics and Palaeoclimate. Springer, pp. 1–17.
Bandyopadhyay, D., Ghosh, B., Guilmette, C., Plunder, A., Corfu, F., Advokaat, E.L., Bandopadhyay, P.C., van Hinsbergen, D.J.J., 2021. Geochemical and geochronological record of the Andaman Ophiolite, SE Asia: From back-arc to forearc during subduction polarity reversal?. Lithos 380, 105853.
Bannert, D., Sang Lyen, A., Htay, T., 2012. The geology of the Indoburman Ranges in Myanmar.
Barber, A.J., 2000. The origin of the Woyla Terranes in Sumatra and the Late Mesozoic evolution of the Sundaland margin. J. Asian Earth Sci. 18, 713–738.
Barber, A.J., Crow, M.J., 2003. An evaluation of plate tectonic models for the development of Sumatra. Gondw. Res. 6, 1–28.
Barber, A.J., Crow, M.J., 2005. Structure and structural history. Geol. Soc. Lond., Mem. 31, 175–233.
Barber, A.J., Crow, M.J., De Smet, M.E.M., 2005a. Tectonic evolution. Geol. Soc. Lond., Mem. 31, 234–259.
Barber, A.J., Crow, M.J., Milsom, J., 2005b. Sumatra: Geology, Resources and Tectonic Evolution. Geological Society of London.
Barber, A.J., Crow, M.J., 2009. Structure of Sumatra and its implications for the tectonic assembly of Southeast Asia and the destruction of Paleotethys. Isl. Arc 18, 3–20.
Barberi, F., Bigioggero, B., Boriani, A., Cattaneo, M., Cavallin, A., Cioni, R., Eva, C., Gelmini, R., Giorgetti, F., Iaccarino, S., 1987. The island of Sumbawa: a major structural discontinuity in the Indonesian arc. Boll. della Soc. Geol. Ital. 106, 547–620.
Barckhausen, U., Engels, M., Franke, D., Ladage, S., Pubellier, M., 2014. Evolution of the South China Sea: Revised ages for breakup and seafloor spreading. Mar. Pet. Geol. 58, 599–611.
Barckhausen, U., Roeser, H.A., 2004. Seafloor spreading anomalies in the South China Sea revisited. Cont. Interact. within East Asian Marg. seas 149, 121–125.
Bard, E., Jouannic, C., Hamelin, B., Pirazzoli, P., Arnold, M., Faure, G., Sumosusastro, P., 1996. Pleistocene sea levels and tectonic uplift based on dating of corals from Sumba Island, Indonesia. Geophys. Res. Lett. 23, 1473–1476.
Barley, M.E., Pickard, A.L., Zaw, K., Rak, P., Doyle, M.G., 2003. Jurassic to Miocene magmatism and metamorphism in the Mogok metamorphic belt and the India-Eurasia collision in Myanmar. Tectonics 22.
Batara, B., Xu, C., 2022. Evolved magmatic arcs of South Borneo: insights into Cretaceous slab subduction. Gondw 111, 142–164.
Baxter, A.T., Aitchison, J.C., Zyabrev, S.V., Ali, J.R., 2011. Upper Jurassic radiolarians from the Naga ophiolite, Nagaland, northeast India. Gondw. Res. 20, 638–644.
Baxter, K., Cooper, G.T., Hill, K.C., O'Brien, G.W., 1999. Late Jurassic subsidence and passive margin evolution in the Vulcan Sub-basin, north-west Australia: constraints from basin modelling. Basin Res. 11, 97–111.
Baziotis, I., Tsai, C., Ernst, W.G., Jahn, B., Iizuka, Y., 2017. New P-T constraints on the Tamayen glaucophane-bearing rocks, eastern Taiwan: Perple_X modelling results and geodynamic implications. J. Metam. Geol. 35, 35–54.
Beaudry, D., Moore, G.F., 1985. Seismic stratigraphy and Cenozoic evolution of West Sumatra forearc basin. Am. Assoc. Pet. Geol. Bull. 69, 742–759.
Beiersdorf, H., Bach, W., Delisle, G., Faber, E., Gerling, P., Hinz, K., 1997. Age and possible modes of formation of the Celebes Sea basement, and thermal regimes within the accretionary complexes off SW Mindanao and N Sulawesi. In: Proceedings of the International Conference on Stratigraphy and Tectonic Evolution of Southeast Asia and the South Pacific. pp. 369–387.
Bellier, O., Sébrier, M., Beaudouin, T., Villeneuve, M., Braucher, R., Bourles, D., Siame, L., Putranto, E., Pratomo, I., 2001. High slip rate for a low seismicity along the Palu-Koro active fault in central Sulawesi (Indonesia). Terra Nov. 13, 463–470.
Bellier, O., Sébrier, M., Seward, D., Beaudouin, T., Villeneuve, M., Putranto, E., 2006. Fission track and fault kinematics analyses for new insight into the Late Cenozoic tectonic regime changes in West-Central Sulawesi (Indonesia). Tectonophysics 413, 201–220.
Bellingham, P., Mcdermott, K., 2014. The Australian North West Shelf: New insights from Deep Seismic.
Bellon, H., Rangin, C., 1991. Geochemistry and isotopic dating of Cenozoic volcanic arc sequences around the Celebes and Sulu seas. Pr. ODP. Sci. Results. 124, 321–338.
Bellon, H., Maury, R.C., Soeria-Atmadja, R., Cotten, J., Polvé, M., 2004. 65 my-long magmatic activity in Sumatra (Indonesia), from Paleocene to Present. Bull. la Société géologique Fr. 175, 61–72.
Bellon, H., Yumul, G.P., 2000. Mio-Pliocene magmatism in the Baguio Mining District (Luzon, Philippines): age clues to its geodynamic setting. Comptes Rendus l'Académie des Sci. IIA-Earth Planet. Sci. 331, 295–302.
Belousov, A., Belousova, M., Zaw, K., Streck, M.J., Bindeman, I., Meffre, S., Vasconcelos, P., 2018. Holocene eruptions of Mt. Popa, Myanmar: Volcanological evidence of the ongoing subduction of Indian Plate along Arakan Trench. J. Volcanol. Geoth. Res. 360, 126–138.
Bemmelen, R.W., 1949. The Geology of Indonesia, Vol. IA: General Geology of Indonesia and Adjacent Archipelagoes. Gov. Print. Off. Hague.
Bennett, J.D., Bridge, Dm., Cameron, N.R., Djunuddin, A., Ghazali, S.A., Jeffery, D.H., Kartawa, W., Keats, W., Rock, N.M.S., Thomson, S.J., 1981. Geologic map of the Banda Aceh quadrangle, Sumatra. Geol. Res. Dev. Cent., Bandung, Indonesia.
Bergman, S.C., Coffield, D.Q., Talbot, J.P., Garrard, R.A., 1996. Tertiary tectonic and magmatic evolution of western Sulawesi and the Makassar Strait, Indonesia: evidence for a Miocene continent-continent collision. Geol. Soc. Lond. Spec. Publ. 106, 391–429.
Bergman, S.C., Hutchison, C.S., Swauger, D.A., Graves, J.E., 2000. K: Ar ages and geochemistry of the Sabah Cenozoic volcanic rocks.
Bernard, A., Munschy, M., Rotstein, Y., Sauter, D., 2005. Refined spreading history at the Southwest Indian Ridge for the last 96 Ma, with the aid of satellite gravity data. Geophys. J. Int. 162, 765–778.
Berry, R.F., McDougall, I., 1986. Interpretation of 40Ar/39Ar and K/Ar dating evidence from the Aileu formation, East Timor, Indonesia. Chem. Geol. Isot. Geosci. Sect. 59, 43–58.
Bertrand, G., Rangin, C., Maluski, H., Han, T.A., Thein, M., Myint, O., Maw, W., Lwin, S., 1999. Cenozoic metamorphism along the Shan scarp (Myanmar): evidences for ductile shear along the Sagaing fault or the northward migration of the eastern Himalayan syntaxis?. Geophys. Res. Lett. 26, 915–918.
Bertrand, G., Rangin, C., Maluski, H., Bellon, H., Party, G.S., 2001. Diachronous cooling along the Mogok Metamorphic Belt (Shan scarp, Myanmar): the trace of the northward migration of the Indian syntaxis. J. Asian Earth Sci. 19, 649–659.
Betka, P.M., Seeber, L., Thomson, S.N., Steckler, M.S., Sincavage, R., Zoramthara, C., 2018. Slip-partitioning above a shallow, weak décollement beneath the Indo-Burman accretionary prism. Earth Planet. Sci. Lett. 503, 17–28.
Beyssac, O., Negro, F., Simoes, M., Chan, Y.-C., Chen, Y.-G., 2008. High-pressure metamorphism in Taiwan: from oceanic subduction to arc-continent collision?. Terra Nov. 20, 118–125.
Bhat, G.R., Balaji, S., Iqbal, V., Balakrishna, B., Yousuf, M., 2019. Neotectonics and related crustal deformation along Carbyn thrust fault, South Andaman, India: implications of the frontal surface faulting and propagation of tectonic activity towards Andaman trench. Arab. J. Geosci. 12, 149.
Bidyananda, M., Sharma, K.A., Shukla, A.D., Kapsiotis, A., Belousova, E., 2022. Geochemical and geochronological study of rodingites from the northeast India ophiolites: Petrogenetic significance and timing of rodingitization. Geol. J. 57, 768–781.
Bird, P.R., Cook, S.E., 1991. Permo-Triassic successions of the Kekneno area, West Timor: implications for palaeogeography and basin evolution. J. SE Asian Earth Sci. 6, 359–371.
Blackman, D.K., Karson, J.A., Kelley, D.S., Cann, J.R., Früh-Green, G.L., Gee, J.S., Hurst, S.D., John, B.E., Morgan, J., Nooner, S.L., 2002. Geology of the Atlantis Massif (Mid-Atlantic Ridge, 30 N): Implications for the evolution of an ultramafic oceanic core complex. Mar. Geophys. Res. 23, 443–469.
Blankenaauw, B., 2017. Kinematic Evolution of The Rajang Group In the Sibu Zone, Sarawak, Borneo in the framework of the evolution of the South China Sea.
Boachi, A., 1856. Onderzoek naar het aanwezen van steenkolen in het terrein aan de Tjiletoekbaai, Residentie Preanger Regentschappen. Natuurkundig Tijdschr. voor Ned. Indië 11, 461–464.
Böhnke, M., Bröcker, M., Maulana, A., Klemd, R., Berndt, J., Baier, H., 2019. Geochronology and Zr-in-rutile thermometry of high-pressure/low temperature metamorphic rocks from the Bantimala complex, SW Sulawesi, Indonesia. Lithos 324, 340–355.
Bolli, H.M., 1978. Synthesis of the Leg 27 biostratigraphy and paleontology. DSDP Init. Rep. 27, 993–1000.
Bolliger, W., De Ruiter, P.A.C., 1975. Geology of the south central Java offshore area.
Booi, M., van Waveren, I.M., van Konijnenburg-Van Cittert, J.H.A., 2014. Gymnosperm permineralized wood from the Early Permian Jambi flora, Sumatra, Indonesia. IAWA J. 35, 307–331.
Boschman, L.M., van Hinsbergen, D.J.J., Torsvik, T.H., Spakman, W., Pindell, J.L., 2014. Kinematic reconstruction of the Caribbean region since the Early Jurassic. Earth-Sci. Rev. 138, 102–136.
Bothe, A.C.D., 1929. Jiwo Hills and Southern Range Excursion Guide. In: 4th Pacific Science Congress, Bandung. 1-14.
Bowin, C., Purdy, G.M., Johnston, C., Shor, G., Lawver, L., Hartono, H.M.S., Jezek, P., 1980. Arc-continent collision in Banda Sea region. Am. Assoc. Pet. Geol. Bull. 64, 868–915.
Bown, P.R., 1992. New calcareous nannofossil taxa from the Jurassic/Cretaceous boundary interval of Sites 765 and 261, Argo Abyssal Plain. Proc. OPD. Sci. Results 123, 369–380.
Bransden, P.J.E., Matthews, S.J., 1992. Structural and stratigraphic evolution of the East Java Sea, Indonesia. Proc. Indones. Pet. Assoc. Annu. Conv. 21, 417–453.
Breitfeld, H.T., Hall, R., Galin, T., Forster, M.A., BouDagher-Fadel, M.K., 2017. A Triassic to Cretaceous Sundaland-Pacific subduction margin in West Sarawak, Borneo. Tectonophysics 694, 35–56.
Breitfeld, H.T., Hall, R., Galin, T., BouDagher-Fadel, M.K., 2018. Unravelling the stratigraphy and sedimentation history of the uppermost Cretaceous to Eocene sediments of the Kuching Zone in West Sarawak (Malaysia), Borneo. J. Asian Earth Sci. 160, 200–223.
Breitfeld, H.T., Davies, L., Hall, R., Armstrong, R., Forster, M., Lister, G., Thirlwall, M., Grassineau, N., Hennig-Breitfeld, J., van Hattum, M.W.A., 2020. Mesozoic Paleo-Pacific subduction beneath SW Borneo: U-Pb geochronology of the Schwaner granitoids and the Pinoh Metamorphic Group. Front. Earth Sci. 8, 536.

Briais, A., Patriat, P., Tapponnier, P., 1993. Updated interpretation of magnetic anomalies and seafloor spreading stages in the South China Sea: Implications for the Tertiary tectonics of Southeast Asia. J. Geophys. Res. Solid Earth 98, 6299–6328.
Brown, M., Earle, M.M., 1983. Cordierite-bearing schists and gneisses from Timor, eastern Indonesia: P-T conditions of metamorphism and tectonic implications. J. Metam. Geol. 1, 183–203.
Bunopas, S., 1982. Paleogeography of Western Thailand and adjacent parts of Southeast Asia – a plate tectonics interpretation. Geol. Surv. Pap. Dep. Miner. Resour. Thail. 5, 1–810.
Burollet, P.F., Salle, C., 1982. Histoire geologique de l'Ile de Sumba (Indonesie). Bull. la Société géologique Fr. 7, 573–580.
Burton-Johnson, A., Macpherson, C.G., Millar, I.L., Whitehouse, M.J., Ottley, C.J., Nowell, G.M., 2020. A Triassic to Jurassic arc in north Borneo: Geochronology, geochemistry, and genesis of the Segama Valley Felsic Intrusions and the Sabah ophiolite. Gondw 84, 229–244.
Cai, F., Ding, L., Laskowski, A.K., Kapp, P., Wang, H., Xu, Q., Zhang, L., 2016. Late Triassic paleogeographic reconstruction along the Neo-Tethyan Ocean margins, southern Tibet. Earth Planet. Sci. Lett. 435, 105–114.
Cai, F., Ding, L., Yao, W., Laskowski, A.K., Xu, Q., Zhang, J., Sein, K., 2017. Provenance and tectonic evolution of Lower Paleozoic-Upper Mesozoic strata from Sibumasu terrane, Myanmar. Gondwana Res. 41, 325–336.
Calvert, S.J., Hall, R., 2003. The Cenozoic geology of the Lariang and Karama regions, Western Sulawesi: new insight into the evolution of the Makassar Straits region. Proc. Indones. Pet. Assoc. Annu. Conv. 29, 501–517.
Calvert, S.J., Hall, R., 2007. Cenozoic evolution of the Lariang and Karama regions, North Makassar Basin, western Sulawesi, Indonesia. Pet. Geosci. 13, 353–368.
Cameron, N.R., Clarke, M.C.G., Aldiss, D.T., Aspden, J.A., Djunuddin, A., 1980. The geological evolution of northern Sumatra. Proc. Indones. Pet. Assoc. Annu. Conv. 9, 149–187.
Camplin, D.J., Hall, R., 2013. Insights into the structural and stratigraphic development of Bone Gulf, Sulawesi. Proc. Indones. Pet. Assoc. Annu. Conv. 37, IPA13-G-079
Camplin, D.J., Hall, R., 2014. Neogene history of Bone Gulf, Sulawesi, Indonesia. Mar. Pet. Geol. 57, 88–108.
Cande, S.C., Stock, J.M., 2004. Pacific—Antarctic—Australia motion and the formation of the Macquarie Plate. Geophys. J. Int. 157, 399–414.
Cande, S.C., Patriat, P., Dyment, J., 2010. Motion between the Indian, Antarctic and African plates in the early Cenozoic. Geophys. J. Int. 183, 127–149.
Canto, A.P.B., Padrones, J.T., Concepcion, R.A.B., Perez, A.D.C., Tamayo, R.A., Dimalanta, C.B., Faustino-Eslava, D.V., Queaño, K.L., Yumul, G.P., 2012. Geology of northwestern Mindoro and its offshore islands: Implications for terrane accretion in west Central Philippines. J. Asian Earth Sci. 61, 78–87.
Cao, L., Shao, L., Qiao, P., Cui, Y., Zhang, G., Zhang, X., 2021. Formation and paleogeographic evolution of the Palawan continental terrane along the Southeast Asian margin revealed by detrital fingerprints. Geol. Soc. Am. Bull. 133, 1167–1193.
Cao, L., Shao, L., Qiao, P., Zhao, Z., van Hinsbergen, D.J.J., 2018. Early Miocene birth of modern Pearl River recorded low-relief, high-elevation surface formation of SE Tibetan Plateau. Earth Planet. Sci. Lett. 496, 120–131.
Capitanio, F.A., Morra, G., Goes, S., Weinberg, R.F., Moresi, L., 2010. India-Asia convergence driven by the subduction of the Greater Indian continent. Nat. Geosci. 3, 136.
Cardwell, R.K., Isaacks, B.L., Karig, D.E., 1980. The spatial distribution of earthquakes, focal mechanism solutions, and subducted lithosphere in the Philippine and northeastern Indonesian islands. GMS 23, 1–35.
Carey, S.W., 1958. The tectonic approach to continental drift. Continental Drift: A Symposium. University of Tasmania Hobart.
Carter, D.J., Audley-Charles, M.G., Barber, A.J., 1976. Stratigraphical analysis of island arc—continental margin collision in eastern Indonesia. J. Geol. Soc. Lond. 132, 179–198.
Caudri, C.M.B., 1934. Tertiary Deposits of Soemba. HJ Paris.
Cawood, P.A., Hawkesworth, C.J., Dhuime, B., 2013. The continental record and the generation of continental crust. Geol. Soc. Am. Bull. 125, 14–32.
Cawood, P.A., Wang, W., Zhao, T., Xu, Y., Mulder, J.A., Pisarevsky, S.A., Zhang, L., Gan, C., He, H., Liu, H., 2020. Deconstructing South China and consequences for reconstructing Nuna and Rodinia. Earth-Sci. Rev. 204, 103169.
Chamalaun, F.H., 1977a. Paleomagnetic evidence for the relative positions of Timor and Australia in the Permian. Earth Planet. Sci. Lett. 34, 107–112.
Chamalaun, F.H., 1977b. Palaeomagnetic reconnaissance result from the Maubisse Tormation, East Timor and its tectonic implication. Tectonophysics 42, T17–T26.
Chamalaun, F.H., Sunata, W., 1982. The paleomagnetism of the Western Banda Arc System–Sumba. In: Palaeomagnetic Research in Southeast and East Asia, Proc. of Workshop, Kuala Lumpur, Malaysia. pp. 162–194.
Chamalaun, F.H., Grady, A.E., Von der Borch, C.C., Hartono, H.M.S., 1981. The tectonic significance of Sumba. Bull. Geol. Res. Dev. Centre, Bandung 5, 1–20.
Chambers, J., Daley, T., 1997. A tectonic model for the onshore Kutai Basin, East Kalimantan. In: Fraser, A.J., Matthews, S.J., Murphy, R.W. (Eds.), Petroleum Geology of SE Asia. pp. 375–393.
Chamot-Rooke, N., Rangin, C., 2000. Andaman Cruise website.
Chan, L.S., Shen, W., Pubellier, M., 2010. Polyphase rifting of greater Pearl River Delta region (South China): Evidence for possible rapid changes in regional stress configuration. J. Struct. Geol. 32, 746–754.
Charlton, T.R., 1989. Stratigraphic correlation across an arc-continent collision zone: timor and the Australian northwest shelf. Aust. J. Earth Sci. 36, 263–274.
Charlton, T.R., 2001. Permo-Triassic evolution of Gondwanan eastern Indonesia, and the final Mesozoic separation of SE Asia from Australia. J. Asian Earth Sci. 19, 595–617.
Charlton, T.R., Barber, A.J., Barkham, S.T., 1991a. The structural evolution of the Timor collision complex, eastern Indonesia. J. Struct. Geol. 13, 489–500.
Charlton, T.R., De Smet, M.E.M., Samodra, H., Kaye, S.J., 1991b. The stratigraphic and structural evolution of the Tanimbar islands, eastern Indonesia. J. SE Asian Earth Sci. 6, 343–358.
Charlton, T.R., Hall, R., Partoyo, E., 1991c. The geology and tectonic evolution of Waigeo Island, NE Indonesia. J. SE Asian Earth Sci. 6, 289–297.
Charlton, T.R., Kaye, S.J., Samodra, H., 1991d. Geology of the Kai Islands: implications for the evolution of the Aru trough and Weber basin, Banda arc, Indonesia. Mar. Pet. Geol. 8, 62–69.
Charlton, T.R., Barber, A.J., Harris, R.A., Barkham, S.T., Bird, P.R., Archbold, N.W., Morris, N.J., Nicoll, R.S., Owen, H.G., Owens, R.M., 2002. The Permian of Timor: stratigraphy, palaeontology and palaeogeography. J. Asian Earth Sci. 20, 719–774.
Charlton, T.R., Barber, A.J., McGowan, A.J., Nicoll, R.S., Roniewicz, E., Cook, S.E., Barkham, S.T., Bird, P.R., 2009. The Triassic of Timor: Lithostratigraphy, chronostratigraphy and palaeogeography. J. Asian Earth Sci. 36, 341–363.
Chemenda, A.I., Yang, R.K., Hsieh, C.-H., Groholsky, A.L., 1997. Evolutionary model for the Taiwan collision based on physical modelling. Tectonophysics 274, 253–274.
Chen, W., Chung, S., Chou, H., Zugeerbai, Z., Shao, W., Lee, Y., 2017. A reinterpretation of the metamorphic Yuli belt: Evidence for a middle-late Miocene accretionary prism in eastern Taiwan. Tectonics 36, 188–206.
Chen, G., Hill, K.C., Hoffman, N., O'Brien, G.W., 2002. Geodynamic evolution of the Vulcan Sub-basin, Timor Sea, northwest Australia: a pre-compression New Guinea analogue?. Aust. J. Earth Sci. 49, 719–736.
Chenin, P., Manatschal, G., Picazo, S., Müntener, O., Karner, G., Johnson, C., Ulrich, M., 2017. Influence of the architecture of magma-poor hyperextended rifted margins on orogens produced by the closure of narrow versus wide oceans. Geosphere 13, 559–576.
Chhibber, H.L., Ramamirtham, R., 1934. The Geology of Burma. Macmillan and Company, Limited.
Chi, W.R., Suppe, J., 1985. Tectonic implications of Miocene sediments of Lan-Hsu island, northern Luzon arc. Pet. Geol. Taiwan 21, 93–106.
Chung, S.-L., Lee, T.-Y., Lo, C.-H., Wang, P.-L., Chen, C.-Y., Yem, N.T., Hoa, T.T., Genyao, W., 1997. Intraplate extension prior to continental extrusion along the Ailao Shan-Red River shear zone. Geology 25, 311–314.
Clements, B., Hall, R., Smyth, H.R., Cottam, M.A., 2009. Thrusting of a volcanic arc: a new structural model for Java. Pet. Geosci. 15, 159–174.
Clements, B., Burgess, P.M., Hall, R., Cottam, M.A., 2011. Subsidence and uplift by slab-related mantle dynamics: a driving mechanism for the Late Cretaceous and Cenozoic evolution of continental SE Asia?. Geol. Soc. Lond. Spec. Publ. 355, 37–51.
Clennell, B., 1991. The origin and tectonic significance of melanges in Eastern Sabah, Malaysia. J. Southeast Asian Earth Sci. 6, 407–429.
Clift, P., Lin, J., 2001. Preferential mantle lithospheric extension under the South China margin. Mar. Pet. Geol. 18, 929–945.
Clift, P.D., Schouten, H., Draut, A.E., 2003. A general model of arc-continent collision and subduction polarity reversal from Taiwan and the Irish Caledonides. Geol. Soc. Lond. Spec. Publ. 219, 81–98.
Cobbing, E.J., 2005. Granites. Geol. Soc. Lond., Mem. 31, 54–62.
Coffield, D.Q., Bergman, S.C., Garrard, R.A., Guritno, N., Robinson, N.M., Talbot, J., 1993. Tectonic and stratigraphic evolution of the Kalosi PSC area and associated development of a Tertiary petroleum system, South Sulawesi, Indonesia.
Coggon, J.A., Nowell, G.M., Pearson, D.G., Parman, S.W., 2011. Application of the 190Pt-186Os isotope system to dating platinum mineralization and ophiolite formation: an example from the Meratus Mountains, Borneo. Econ. Geol. 106, 93–117.
Conand, C., Mouthereau, F., Ganne, J., Lin, A.T., Lahfid, A., Daudet, M., Mesalles, L., Giletycz, S., Bonzani, M., 2020. Strain partitioning and exhumation in oblique Taiwan collision: Role of rift architecture and plate kinematics. Tectonics 39.
Concepcion, R.A.B., Dimalanta, C.B., Yumul, G.P., Faustino-Eslava, D.V., Queaño, K.L., Tamayo, R.A., Imai, A., 2012. Petrography, geochemistry, and tectonics of a rifted fragment of Mainland Asia: evidence from the Lasala Formation, Mindoro Island, Philippines. Int. J. Earth Sci. 101, 273–290.
Cornée, J.-J., Martini, R., Zaninetti, L., 1994. Une plate-forme carbonatée d'âge Rhétien au centre-est de Sulawesi (région de Kolonodale, Celèbes, Indonésie). Comptes Rendus l'Académie des Sci. IIA Earth Planet. Sci. 318, 809–8014.
Cornée, J.-J., Tronchetti, G., Villeneuve, M., Lathuilière, B., Janin, M.-C., Saint-Marc, P., Gunawan, W., Samodra, H., 1995. Cretaceous of eastern and southeastern Sulawesi (Indonesia): new micropaleontological and biostratigraphical data. J. SE Asian Earth Sci. 12, 41–52.
Cornée, J.-J., Villeneuve, M., Rehault, J.-P., Malod, J., Butterlin, J., Saint-Marc, P., Tronchetti, G., Lambert, B., Michoux, D., Burhanuddin, S., 1997. Stratigraphic succession of the Australian margin between Kai and Aru islands (Arafura Sea, eastern Indonesia) interpreted from Banda Sea II cruise dredge samples. J. Asian Earth Sci. 15, 423–434.
Cornée, J.-J., Butterlin, J., Saint-Marc, P., Réhault, J.-P., Honthaas, C., Laurenti-Ribaud, A., Chaix, C., Villeneuve, M., Anantasena, Y., 1998. An early Miocene reefal platform in the Rama Ridge (Banda Sea, Indonesia). Geo-Marine Lett. 18, 34–39.

Cornée, J.-J., Martini, R., Villeneuve, M., Zaninetti, L., Mattioli, E., Rettori, R., Atrops, F., Gunawan, W., 1999. Mise en évidence du Jurassique inférieur et moyen dans la ceinture ophiolitique de Sulawesi (Indonésie). Conséquences géodynamiques. Geobios 32, 385–394.
Cornée, J.-J., Villeneuve, M., Ferrandini, M., Hinschberger, F., Malod, J., Matsumaru, K., Ribaud-Laurenti, A., Rehault, J.-P., 2002. Oligocene reefal deposits in the Pisang Ridge and the origin of the Lucipara Block (Banda Sea, eastern Indonesia). Geo-Marine Lett. 22, 66–74.
Cottam, M.A., Hall, R., Forster, M.A., Boudagher-Fadel, M.K., 2011. Basement character and basin formation in Gorontalo Bay, Sulawesi, Indonesia: new observations from the Togian Islands. Geol. Soc. Lond. Spec. Publ. 355, 177–202.
Cottam, M.A., Hall, R., Ghani, A.A., 2013. Late Cretaceous and Cenozoic tectonics of the Malay Peninsula constrained by thermochronology. J. Asian Earth Sci. 76, 241–257.
Crameri, F., Magni, V., Domeier, M., Shephard, G.E., Chotalia, K., Cooper, G., Eakin, C. M., Grima, A.G., Gürer, D., Király, Á., 2020. A transdisciplinary and community-driven database to unravel subduction zone initiation. Nat. Commun. 11, 1–14.
Crow, M.J., Zaw, K., 2017. Appendix Geochronology in Myanmar (1964–2017). Geol. Soc. Lond., Mem. 48, 713–759.
Cullen, A.B., 2010. Transverse segmentation of the Baram-Balabac Basin, NW Borneo: refining the model of Borneo's tectonic evolution. Pet. Geosci. 16, 3–29.
Curray, J.R., 2005. Tectonics and history of the Andaman Sea region. J. Asian Earth Sci. 25, 187–232.
Curray, J.R., Moore, D.G., Lawver, L.A., Emmel, F.J., Raitt, R.W., Henry, M., Kieckhefer, R., 1979. Tectonics of the Andaman Sea and Burma: convergent margins.Am. Asoc. Pet. Geol. Mem. 29, 189–198.
Curray, J.R., Shor, G.G., Raitt, R.W., Henry, M., 1977. Seismic refraction and reflection studies of crustal structure of the eastern Sunda and western Banda arcs. J. Geophys. Res. 82, 2479–2489.
Davidson, J.W., 1991. The geology and prospectivity of Buton island, SE Sulawesi, Indonesia. Proc. Indones. Pet. Assoc. Annu. Conv. 20, 209–234.
Davies, L., Hall, R., Armstrong, R., 2014. Cretaceous crust in SW Borneo: petrological, geochemical and geochronological constraints from the Schwaner Mountains. Proc. Indones. Pet. Assoc. Annu. Conv. 38, IPA14-G-025.
Davies, I.C., 1990. Geological and exploration review of the Tomori PSC, eastern Indonesia. Proc. Indones. Pet. Assoc. Annu. Conv. 19, 41–67.
Davydov, V.I., Haig, D.W., McCartain, E., 2013. A latest Carboniferous warming spike recorded by a fusulinid-rich bioherm in Timor Leste: Implications for East Gondwana deglaciation. Palaeogeogr. Palaeoclimatol. Palaeoecol. 376, 22–38.
Davydov, V.I., Haig, D.W., McCartain, E., 2014. Latest Carboniferous (late Gzhelian) fusulinids from Timor Leste and their paleobiogeographic affinitiesLate Gzhelian Fusulinids from Timor. J. Paleo. 88, 588–605.
de Boer, P.L., Chaney, D.S., Booi, M., Iskandar, E.P.A., King, C.I., de Leeuw, J.H.V.M., 2006. Early Permian fusuline faunas of the Mengkarang and Palepat formations in the West Sumatra Block, Indonesia: Their faunal characteristics, ages, and geotectonic implications.
de Boer, J., Odom, L.A., Ragland, P.C., Snider, F.G., Tilford, N.R., 1980. The Bataan orogene: eastward subduction, tectonic rotations, and volcanism in the western Pacific (Philippines). Tectonophysics 67, 251–282.
De Genevraye, P., Samuel, L., 1972. Geology of the Kendeng Zone (Central & East Java). Proc. Indones. Pet. Assoc. Annu. Conv. 1, 17–30.
De Smet, M.E.M., Sumosusastro, P.A., Siregar, I., Van Marle, L.J., Troelstra, S.R., Fortuin, A.R., 1989. Late Cenozoic stratigraphy and tectonics of Seram, Indonesia. Geol. Mijnb. 68, 221–235.
De Smet, M.E.M., Fortuin, A.R., Troelstra, S.R., Van Marle, L.J., Karmini, M., Tjokrosapoetro, S., Hadiwasastra, S., 1990. Detection of collision-related vertical movements in the Outer Banda Arc (Timor, Indonesia), using micropaleontological data. J. SE Asian Earth Sci. 4, 337–356.
Decker, J., Ferdian, F., Morton, A., Fanning, M., White, L.T., 2017. New geochronology data from eastern Indonesia–An aid to understanding sedimentary provenance in a frontier region.
Deenen, M.H.L., Langereis, C.G., van Hinsbergen, D.J.J., Biggin, A.J., 2011. Geomagnetic secular variation and the statistics of palaeomagnetic directions. Geophys. J. Int. 186, 509–520.
Defant, M.J., Jacques, D., Maury, R.C., de Boer, J., Joron, J.-L., 1989. Geochemistry and tectonic setting of the Luzon arc, Philippines. Geol. Soc. Am. Bull. 101, 663–672.
Deighton, I., Hancock, T., Hudson, G., Tamannai, M., Conn, P., Oh, K., 2011. Infill seismic in the southeast Java Forearc Basin: implications for petroleum prospectivity. Proc. Indones. Pet. Assoc. Annu. Conv. 35, IPA11-G-068
DeMets, C., Iaffaldano, G., Merkouriev, S., 2015. High-resolution Neogene and Quaternary estimates of Nubia-Eurasia-North America Plate motion. Geophys. J. Int. 203, 416–427.
DeMets, C., Merkouriev, S., 2016. High-resolution estimates of Nubia-Somalia plate motion since 20 Ma from reconstructions of the Southwest Indian Ridge, Red Sea and Gulf of Aden. Geophys. J. Int. 207, 317–332.
Deng, H., McClay, K., 2019. Tectono-stratigraphy of the Dampier Sub-basin, North West Shelf of Australia. Geol. Soc. Lond. Spec. Publ. 476.
Deschamps, A., Monié, P., Lallemand, S., Hsu, S.-K., Yeh, K.Y., 2000. Evidence for Early Cretaceous oceanic crust trapped in the Philippine Sea Plate. Earth Planet. Sci. Lett. 179, 503–516.
Dewey, J.F., Burke, K., 1974. Hot spots and continental break-up: implications for collisional orogeny. Geology 2, 57–60.
Dimalanta, C.B., Ramos, E.G.L., Yumul, G.P., Bellon, H., 2009. New features from the Romblon Island Group: Key to understanding the arc–continent collision in Central Philippines. Tectonophysics 479, 120–129.
Ding, W., Franke, D., Li, J., Steuer, S., 2013. Seismic stratigraphy and tectonic structure from a composite multi-channel seismic profile across the entire Dangerous Grounds, South China Sea. Tectonophysics 582, 162–176.
Doust, H., Noble, R.A., 2008. Petroleum systems of Indonesia. Mar. Pet. Geol. 25, 103–129.
Dow, D.B., Sukamto, R., 1984. Western Irian Jaya: the end-product of oblique plate convergence in the late Tertiary. Tectonophysics 106, 109–139.
Drummond, B.J., Sexton, M.J., Barton, T.J., Shaw, R.D., 1991. The nature of faulting along the margins of the Fitzroy Trough, Canning Basin, and implications for the tectonic development of the trough. Explor. Geophys. 22, 111–116.
Duffy, B., Kalansky, J., Bassett, K., Harris, R., Quigley, M., van Hinsbergen, D.J.J., Strachan, L.J., Rosenthal, Y., 2017. Mélange versus forearc contributions to sedimentation and uplift, during rapid denudation of a young Banda forearc-continent collisional belt. J. Asian Earth Sci. 138, 186–210.
Dycoco, J.M.A., Payot, B.D., Valera, G.T.V., Labis, F.A.C., Pasco, J.A., Perez, A.D.C., Tani, K., 2021. Juxtaposition of Cenozoic and Mesozoic ophiolites in Palawan island, Philippines: New insights on the evolution of the Proto-South China Sea. Tectonophysics 819, 229085.
Earle, M.M., 1979. Mesozoic ophiolite and blue amphibole on Timor and the dispersal of eastern Gondwanaland. Nature 282, 375–378.
Earle, M., 1983. Continental margin origin for Cretaceous radiolarian cherts in western Timor. Nature 305, 129–130.
Elburg, M., Foden, J., 1998. Temporal changes in arc magma geochemistry, northern Sulawesi, Indonesia. Earth Planet. Sci. Lett. 163, 381–398.
Elburg, M.A., Van Bergen, M.J., Foden, J.D., 2004. Subducted upper and lower continental crust contributes to magmatism in the collision sector of the Sunda-Banda arc, Indonesia. Geology 32, 41–44.
Elburg, M.A., Foden, J.D., Van Bergen, M.J., Zulkarnain, I., 2005. Australia and Indonesia in collision: geochemical sources of magmatism. J. Volcanol. Geoth. Res. 140, 25–47.
Elburg, M., van Leeuwen, T., Foden, J., 2003. Spatial and temporal isotopic domains of contrasting igneous suites in western and northern Sulawesi, Indonesia. Chem. Geol. 199, 243–276.
Elburg, M.A., Van Leeuwen, T., Foden, J., 2002. Origin of geochemical variability by arc–continent collision in the Biru area, Southern Sulawesi (Indonesia). J. Petrol. 43, 581–606.
Ely, K.S., Sandiford, M., Hawke, M.L., Phillips, D., Quigley, M., dos Reis, J.E., 2011. Evolution of Ataúro Island: Temporal constraints on subduction processes beneath the Wetar zone, Banda Arc. J. Asian Earth Sci. 41, 477–493.
Emmet, P.A., Granath, J.W., Dinkelman, M.G., 2009. Pre-Tertiary sedimentary "keels" provide insights into tectonic assembly of basement terranes and present-day petroleum systems of the East Java Sea.
Encarnacion, J.P., Essene, E.J., Mukasa, S.B., Hall, C.H., 1995. High-pressure and-temperature subophiolitic kyanite—garnet amphibolites generated during initiation of mid-Tertiary subduction, Palawan, Philippines. J. Petrol. 36, 1481–1503.
Endang Thayyib, S., Said, E.L., Siswoyo, S.P., 1977. The Status of the Melange Complex in Ciletuh Area, South–West Java. Proc. Indones. Pet. Assoc. Annu. Conv. 6, 241–253.
Etheridge, M.A., O'Brien, G.W., 1994. Structural and tectonic evolution of the Western Australian margin basin system. Pet. Explor. Soc. Aust. J. 22, 45–63.
Faure, M., Ishida, K., 1990. The Mid-Upper Jurassic olistostrome of the west Philippines: a distinctive key-marker for the North Palawan block. J. SE Asian Earth Sci. 4, 61–67.
Faure, M., Marchadier, Y., Rangin, C., 1989. Pre-Eocene synmetamorphic structure in the Mindoro-Romblon-Palawan area, West Philippines, and implications for the history of southeast Asia. Tectonics 8, 963–979.
Ferdian, F., Hall, R., Watkinson, I., 2010. A structural re-evaluation of the north Banggai-Sula area, eastern Indonesia. Proc. Indones. Pet. Assoc. Annu. Conv. 34, IPA10-G-009.
Ferdian, F., Decker, J., Morton, A., Fanning, M., 2012. Provenance of East Sulawesi and Banggai Sula Zircons–Preliminary Result. Proc. Indones. Pet. Assoc. Annu. Conv. 36, IPA12-G-044.
Fisher, R., 1953. Dispersion on a sphere. In: Proceedings of the Royal Society of London A: Mathematical, Physical and Engineering Sciences. The Royal Society, pp. 295–305.
Fleury, J.-M., Pubellier, M., de Urreiztieta, M., 2009. Structural expression of forearc crust uplift due to subducting asperity. Lithos 113, 318–330.
Florendo, F.F., 1994. Tertiary arc rifting in northern Luzon, Philippines. Tectonics 13, 623–640.
Fortuin, A.R., De Smet, M.E.M., Hadiwasastra, S., Van Marle, L.J., Troelstra, S.R., Tjokrosapoetro, S., 1990. Late Cenozoic sedimentary and tectonic history of south Buton, Indonesia. J. Southeast Asian Earth Sci. 4, 107–124.
Fortuin, A.R., Roep, T.B., Sumosusastro, P.A., Van Weering, T.C.E., Van der Werff, W., 1992. Slumping and sliding in Miocene and Recent developing arc basins, onshore and offshore Sumba (Indonesia). Mar. Geol. 108, 345–363.
Fortuin, A.R., Van der Werff, W., Wensink, H., 1997. Neogene basin history and paleomagnetism of a rifted and inverted forearc region, on-and offshore Sumba, Eastern Indonesia. J. Asian Earth Sci. 15, 61–88.
François, T., Ali, M.A.M., Matenco, L., Willingshofer, E., Ng, T.F., Taib, N.I., Shuib, M.K., 2017. Late Cretaceous extension and exhumation of the Stong and Taku magmatic and metamorphic complexes, NE Peninsular Malaysia. J. Asian Earth Sci. 143, 296–314.
Franke, D., Barckhausen, U., Baristeas, N., Engels, M., Ladage, S., Lutz, R., Montano, J., Pellejera, N., Ramos, E.G., Schnabel, M., 2011. The continent-ocean transition at the southeastern margin of the South China Sea. Mar. Pet. Geol. 28, 1187–1204.

Fraser, T.H., Bon, J., Samuel, L., 1993. A new dynamic Mesozoic stratigraphy for the West Irian micro-continent Indonesia and its implications. Proc. Indones. Pet. Assoc. Annu. Conv. 22, 707–761.
Froidevaux, C.M., 1974. Geology of Misool Island (Irian Jaya).
Fuller, M., Ali, J.R., Moss, S.J., Frost, G.M., Richter, B., Mahfi, A., 1999. Paleomagnetism of Borneo. J. Asian Earth Sci. 17, 3–24.
Fullerton, L.G., Sager, W.W., Handschumacher, D.W., 1989. Late Jurassic-Early Cretaceous evolution of the eastern Indian Ocean adjacent to northwest Australia. J. Geophys. Res. Solid Earth 94, 2937–2953.
Fyhn, M.B.W., Boldreel, L.O., Nielsen, L.H., 2009. Geological development of the Central and South Vietnamese margin: Implications for the establishment of the South China Sea, Indochinese escape tectonics and Cenozoic volcanism. Tectonophysics 478, 184–214.
Fyhn, M.B.W., Boldreel, L.O., Nielsen, L.H., 2010a. Escape tectonism in the Gulf of Thailand: Paleogene left-lateral pull-apart rifting in the Vietnamese part of the Malay Basin. Tectonophysics 483, 365–376.
Fyhn, M.B.W., Pedersen, S.A.S., Boldreel, L.O., Nielsen, L.H., Green, P.F., Dien, P.T., Huyen, L.T., Frei, D., 2010b. Palaeocene–early Eocene inversion of the Phuquoc-Kampot Som Basin: SE Asian deformation associated with the suturing of Luconia. J. Geol. Soc. Lond. 167, 281–295.
Gafoer, S., Amin, T.C., Pardede, R., 1992. Geology of the Bengkulu Quadrangle, Sumatera. Geol. Res. Dev. Cent. Indonesia.
Gaina, C., Müller, R.D., Brown, B., Ishihara, T., Ivanov, S., 2007. Breakup and early seafloor spreading between India and Antarctica. Geophys. J. Int. 170, 151–169.
Gaina, C., Müller, D., 2007. Cenozoic tectonic and depth/age evolution of the Indonesian gateway and associated back-arc basins. Earth-Sci. Rev. 83, 177–203.
Gaina, C., Van Hinsbergen, D.J.J., Spakman, W., 2015. Tectonic interactions between India and Arabia since the Jurassic reconstructed from marine geophysics, ophiolite geology, and seismic tomography. Tectonics 34, 875–906.
Galin, T., Breitfeld, H.T., Hall, R., Sevastjanova, I., 2017. Provenance of the Cretaceous-Eocene Rajang Group submarine fan, Sarawak, Malaysia from light and heavy mineral assemblages and U-Pb zircon geochronology. Gondw. Res. 51, 209–233.
Gan, C., Qian, X., Wang, Y., Feng, Q., Zhang, Y., Asis, J.B., 2022. Late Cretaceous Granitoids along the Northern Kuching Zone: Implications for the Paleo-Pacific Subduction in Borneo. Lithosphere 2022, 3310613.
Gardiner, N.J., Robb, L.J., Morley, C.K., Searle, M.P., Cawood, P.A., Whitehouse, M.J., Kirkland, C.L., Roberts, N.M.W., Myint, T.A., 2016. The tectonic and metallogenic framework of Myanmar: A Tethyan mineral system. Ore Geol. Rev. 79, 26–45.
Gardiner, N.J., Hawkesworth, C.J., Robb, L.J., Whitehouse, M.J., Roberts, N.M.W., Kirkland, C.L., Evans, N.J., 2017. Contrasting granite metallogeny through the zircon record: a case study from Myanmar. Sci. Rep. 7, 1–9.
Gardiner, N.J., Searle, M.P., Morley, C.K., Robb, L.J., Whitehouse, M.J., Roberts, N.M.W., Kirkland, C.L., Spencer, C.J., 2018. The crustal architecture of Myanmar imaged through zircon U-Pb, Lu-Hf and O isotopes: Tectonic and metallogenic implications. Gondw. Res. 62, 27–60.
Garrard, R.A., Supandjono, J., Surono, 1988. The geology of the Banggai-Sula microcontinent, eastern Indonesia. Proc. Indones. Pet. Assoc. Annu. Conv. 17, 23–52.
Gartrell, A., Torres, J., Dixon, M., Keep, M., 2016. Mesozoic rift onset and its impact on the sequence stratigraphic architecture of the Northern Carnarvon Basin. APPEA J. 56, 143–158.
Gartrell, A., Keep, M., van der Riet, C., Paterniti, L., Ban, S., Lang, S., 2022. Hyperextension and polyphase rifting: Impact on inversion tectonics and stratigraphic architecture of the North West Shelf, Australia. Mar. Pet. Geol. 139, 105594.
Garzanti, E., 1999. Stratigraphy and sedimentary history of the Nepal Tethys Himalaya passive margin. J. Asian Earth Sci. 17, 805–827.
Garzanti, E., Le Fort, P., Sciunnach, D., 1999. First report of Lower Permian basalts in South Tibet: tholeiitic magmatism during break-up and incipient opening of Neotethys. J. Asian Earth Sci. 17, 533–546.
Gatinsky, Y.G., Hutchison, C.S., 1986. Cathaysia, Gondwanaland, and the Paleotethys in the evolution of continental Southeast Asia. Bull. Geol. Soc. Malaysia 19, 179–199.
Gee, J.S., Kent, D. V, 2007. Source of oceanic magnetic anomalies and the geomagnetic polarity time scale.
Geological Map of the Philippines, 1963. Geological Map of the Philippines, scale 1:1,000,000, 9 sheets. Manila.
Gervasio, F.C., 1967. Age and nature of orogenesis of the Philippines. Tectonophysics 4, 379–402.
Ghosh, B., Bandyopadhyay, D., Morishita, T., 2017. Andaman-Nicobar Ophiolites, India: origin, evolution and emplacement. Geol. Soc. Lond., Mem. 47, 95–110.
Gibbons, A.D., Barckhausen, U., den Bogaard, P., Hoernle, K., Werner, R., Whittaker, J. M., Müller, R.D., 2012. Constraining the Jurassic extent of Greater India: Tectonic evolution of the West Australian margin. Geochem. Geophys. Geosyst. 13.
Gibbons, A.D., Whittaker, J.M., Müller, R.D., 2013. The breakup of East Gondwana: Assimilating constraints from Cretaceous ocean basins around India into a best-fit tectonic model. J. Geophys. Res. Solid Earth 118, 808–822.
Ginger, D.C., Ardjakusumah, W.O., Hedley, R.J., Pothecary, J., 1993. Inversion history of the West Natuna basin: examples from the Cumi-Cumi PSC.
Gold, D.P., Burgess, P.M., BouDagher-Fadel, M.K., 2017. Carbonate drowning successions of the Bird's Head, Indonesia. Facies 63, 1–22.
Gold, D., Hall, R., Burgess, P., BouDagher-Fadel, M., 2014. The Biak Basin and its setting in the Bird's Head region of West Papua. Proc. Indones. Pet. Assoc. Annu. Conv. 38, IPA14-G-298.
Govers, R., Wortel, M.J.R., 2005. Lithosphere tearing at STEP faults: Response to edges of subduction zones. Earth Planet. Sci. Lett. 236, 505–523.
Gradstein, F.M., Ogg, J.G., Schmitz, M., Ogg, G., 2012. The Geologic Time Scale 2012. Elsevier.
Gradstein, F.M., 1992. 43. Legs 122 and 123, northwestern Australian margin—a stratigraphic and paleogeographic summary. Proc. ODP Sci. Results 123, 801–816.
Grainge, A.M., Davies, K.G., 1985. Reef exploration in the east Sengkang basin, Sulawesi, Indonesia. Mar. Pet. Geol. 2, 142–155.
Granath, J.W., Christ, J.M., Emmet, P.A., Dinkelman, M.G., 2011. Pre-Cenozoic sedimentary section and structure as reflected in the JavaSPANTM crustal-scale PSDM seismic survey, and its implications regarding the basement terranes in the East Java Sea. Geol. Soc. Lond. Spec. Publ. 355, 53–74.
Granath, J.W., Emmet, P.A., Dinkelman, M.G., 2009. Crustal architecture of the East Java Sea-Makassar Strait region from long-offset crustal-scale 2D seismic reflection imaging. Proc. Indones. Pet. Assoc. Annu. Conv. 33, IPA09-G-047.
Graves, J.E., Swauger, D.A., 1997. Petroleum systems of the Sandakan basin, Philippines. Proc. Pet. Syst. SE Asia Australas. Conf., 799–813.
Graves, J.E., Hutchison, C.S., Bergman, S.C., Swauger, D.A., 2000. Age and MORB geochemistry of the Sabah ophiolite basement. Bull. Geol. Soc. Malaysia 44, 151–158.
Guilmette, C., van Hinsbergen, D., Smit, M., Godet, A., Fournier-Roy, F., Butler, J., Maffione, M., Li, S., Hodges, K., 2023. Formation of the Xigaze Metamorphic Sole under Tibetan continental lithosphere reveals generic characteristics of subduction initiation. Comm. Earth & Envi. 4, 339.
Guilmette, C., Hébert, R., Wang, C., Villeneuve, M., 2009. Geochemistry and geochronology of the metamorphic sole underlying the Xigaze ophiolite, Yarlung Zangbo Suture Zone, south Tibet. Lithos 112, 149–162.
Guilmette, C., Smit, M.A., van Hinsbergen, D.J.J., Gürer, D., Corfu, F., Charette, B., Maffione, M., Rabeau, O., Savard, D., 2018. Forced subduction initiation recorded in the sole and crust of the Semail Ophiolite of Oman. Nat. Geosci. 11, 688–695.
Gupta, A.B. Das, Biswas, A.K., 2000. Geology of Assam. GSI Publ. 2.
Haig, D.W., Foster, C.B., Howe, R.W., Mantle, D., Backhouse, J., Peyrot, D., Vitacca, J., 2018. Fossil protists (algae and testate protozoans) in the marine Phanerozoic o f Western Australia: a review through latitudinal change, climate extremes an d breakup of a supercontinent. JR Soc. West. Aust. 101, 44–67.
Gürer, D., Granot, R., van Hinsbergen, D.J.J., 2022. Plate tectonic chain reaction revealed by noise in the Cretaceous quiet zone. Nat. Geosci. 15, 233–239.
Haig, D.W., Dillinger, A., Playford, G., Riera, R., Sadekov, A., Skrzypek, G., Håkansson, E., Mory, A.J., Peyrot, D., Thomas, C., 2022. Methane seeps following Early Permian (Sakmarian) deglaciation, interior East Gondwana, Western Australia: Multiphase carbonate cements, distinct carbon-isotope signatures, extraordinary biota. Palaeogeogr. Palaeoclimatol. Palaeoecol. 591, 110862.
Haig, D.W., McCartain, E., 2007. Carbonate pelagites in the post-Gondwana succession (Cretaceous–Neogene) of East Timor. Aust. J. Earth Sci. 54, 875–897.
Haig, D.W., McCartain, E., 2010. Triassic organic-cemented siliceous agglutinated foraminifera from Timor Leste: conservative development in shallow-marine environments. J. Foramin. Res. 40, 366–392.
Haig, D.W., McCartain, E., Mory, A.J., Borges, G., Davydov, V.I., Dixon, M., Ernst, A., Groflin, S., Håkansson, E., Keep, M., 2014. Postglacial Early Permian (late Sakmarian–early Artinskian) shallow-marine carbonate deposition along a 2000 km transect from Timor to west Australia. Palaeogeogr. Palaeoclimatol. Palaeoecol. 409, 180–204.
Haig, D.W., Mory, A.J., McCartain, E., Backhouse, J., Håkansson, E., Ernst, A., Nicoll, R. S., Shi, G.R., Bevan, J.C., Davydov, V.I., 2017. Late Artinskian-Early Kungurian (Early Permian) warming and maximum marine flooding in the East Gondwana interior rift, Timor and Western Australia, and comparisons across East Gondwana. Palaeogeogr. Palaeoclimatol. Palaeoecol. 468, 88–121.
Haile, N.S., 1974. An unusual unconformity of radiolarian chert on schist and gneiss east of Pangkajene, southwest arm, Sulawesi. Geol. Soc Malaysia Newsl 52, 21–22.
Haile, N.S., 1978a. Reconnaissance palaeomagnetic results from Sulawesi, Indonesia, and their bearing on palaeogeographic reconstructions. Tectonophysics 46, 77–85.
Haile, N.S., 1979. Palaeomagnetic evidence for rotation and northward drift of Sumatra. J. Geol. Soc. Lond. 136, 541–546.
Haile, N., Wong, N., 1965. The Geology and Mineral Resources of the Dent Peninsula, Sabah, Malaysia: Borneo Reg. Malaysia Geol. Surv. Mem 16.
Haile, N.S., Beckinsale, R.D., Chakraborty, K.R., Hussein, A.H., Hardjono, T., 1983. Palaeomagnetism, Geochronology and Petrology of the Dolerite Dykes and Basaltic Lavas from Kuantan, West Malaysia. Bull. Geol. Soc. Malays. 16, 71–85.
Haile, N.S., McElhinny, M.W., McDougall, I., 1977. Palaeomagnetic data and radiometric ages from the Cretaceous of West Kalimantan (Borneo), and their significance in interpreting regional structure. J. Geol. Soc. Lond. 133, 133–144.
Haile, N.S., Barber, A.J., Carter, D.J., 1979. Mesozoic cherts on crystalline schists in Sulawesi and Timor. J. Geol. Soc. Lond. 136, 65–70.
Haile, N.S., 1978b. Palaeomagnetic evidence for the rotation of Seram, Indonesia. J. Phys. Earth 26, S191–S198.
Haile, N.S., 1996. Note on the Engkilili Formation and the age of the Lubok Antu Mélange, West Sarawak, Malaysia. Newsl. Geol. Soc. Malaysia 22, 67–70.

Hakim, A.Y. Al, Melcher, F., Prochaska, W., Meisel, T.C., 2022. Magmatic and metamorphic evolution of the Latimojong Metamorphic Complex, Indonesia. J. Asian Earth Sci. 105095.
Hakim, A.Y.A., Melcher, F., Prochaska, W., Bakker, R., Rantitsch, G., 2018. Formation of epizonal gold mineralization within the Latimojong Metamorphic Complex, Sulawesi, Indonesia: Evidence from mineralogy, fluid inclusions and Raman spectroscopy. Ore Geol. Rev. 97, 88–108. https://doi.org/10.1016/j.oregeorev.2018.05.001.
Hall, R., 1996. Reconstructing Cenozoic SE Asia. Geol. Soc. Lond. Spec. Publ. 106, 153–184.
Hall, R., 2002. Cenozoic geological and plate tectonic evolution of SE Asia and the SW Pacific: computer-based reconstructions, model and animations. J. Asian Earth Sci. 20, 353–431. https://doi.org/10.1016/S1367-9120(01)00069-4.
Hall, R., 2009. The Eurasian SE Asian margin as a modern example of an accretionary orogen. Geol. Soc. Lond. Spec. Publ. 318, 351–372.
Hall, R., 2012. Late Jurassic-Cenozoic reconstructions of the Indonesian region and the Indian Ocean. Tectonophysics 570–571, 1–41. https://doi.org/10.1016/j.tecto.2012.04.021.
Hall, R., 2013. Contraction and extension in northern Borneo driven by subduction rollback. J. Asian Earth Sci. 76, 399–411.
Hall, R., Audley-Charles, M.G., Banner, F.T., Hidayat, S., Tobing, S.L., 1988a. Basement rocks of the Halmahera region, eastern Indonesia: a Late Cretaceous–early Tertiary arc and fore-arc. J. Geol. Soc. Lond. 145, 65–84.
Hall, R., Audley-Charles, M.G., Banner, F.T., Hidayat, S., Tobing, S.L., 1988b. Late Palaeogene-Quaternary geology of Halmahera, Eastern Indonesia: initiation of a volcanic island arc. J. Geol. Soc. Lond. 145, 577–590.
Hall, R., Ballantyne, P.D., Hakim, A.S., Nichols, G.J., 1996. Basement rocks of Halmahera, eastern Indonesia: implications for the early history of the Philippine Sea. In: G.P. & A.C. Salisbury (eds.) Trans. 5th Circum- Pacific Energy and Mineral Resources Conference, 301–317.
Hall, R., Clements, B., Smyth, H.R., Cottam, M.A., 2007. A new interpretation of Java's structure. Proc. Indones. Pet. Assoc. Annu. Conv. 31, IPA07-G-035.
Hall, R., Clements, B., Smyth, H.R., 2009a. Sundaland: basement character, structure and plate tectonic development.
Hall, R., Cloke, I.R., Nur'aini, S., Puspita, S.D., Calvert, S.J., Elders, C.F., 2009b. The North Makassar Straits: what lies beneath? Pet. Geosci. 15, 147–158.
Hall, R., Sevastjanova, I., 2012. Australian crust in Indonesia. Aust. J. Earth Sci. 59, 827–844.
Hall, R., Spakman, W., 2002. Subducted slabs beneath the eastern Indonesia-Tonga region: insights from tomography. Earth Planet. Sci. Lett. 201, 321–336.
Hall, R., Spakman, W., 2003. Mantle structure and tectonic evolution of the region north and east of Australia. Spec. Pap. Soc. Am., 361–382.
Hall, R., Spakman, W., 2015. Mantle structure and tectonic history of SE Asia. Tectonophysics 658, 14–45. https://doi.org/10.1016/j.tecto.2015.07.003.
Hall, R., Wilson, M.E.J., 2000. Neogene sutures in eastern Indonesia. J. Asian Earth Sci. 18, 781–808.
Hall, R., van Hattum, M.W.A., Spakman, W., 2008. Impact of India-Asia collision on SE Asia: the record in Borneo. Tectonophysics 451, 366–389.
Hall, R., 2000. Neogene history of collision in the Halmahera region, Indonesia.
Hamilton, W.B., 1979. Tectonics of the Indonesian region. US Govt. Print. Off.
Handy, M.R., Schmid, S.M., Bousquet, R., Kissling, E., Bernoulli, D., 2010. Reconciling plate-tectonic reconstructions of Alpine Tethys with the geological–geophysical record of spreading and subduction in the Alps. Earth-Sci. Rev. 102, 121–158.
Harahap, B.H., Poedjoprajitno, S., 2006. The Stratigraphy and Lithology of the Kuma River area Buru Island, Maluku. J. Geol. dan Sumberd. Miner. 16, 62–74.
Harbury, N.A., Jones, M.E., Audley-Charles, M.G., Metcalfe, I., Mohamed, K.R., 1990. Structural evolution of Mesozoic peninsular Malaysia. J. Geol. Soc. Lond. 147, 11–26.
Harris, R.A., 1992. Peri-collisional extension and the formation of Oman-type ophiolites in the Banda Arc and Brooks Range. Geol. Soc. Lond. Spec. Publ. 60, 301–325.
Harris, R., 2006. Rise and fall of the Eastern Great Indonesian arc recorded by the assembly, dispersion and accretion of the Banda Terrane. Timor. Gondwana Res. 10, 207–231.
Harris, R., 2011. The nature of the Banda Arc–continent collision in the Timor region. Arc-Continent Collision. Springer, 163–211.
Harris, R., Long, T., 2000. The Timor ophiolite, Indonesia: model or myth?. Geol. Soc. Am. Paper 349, 321–330.
Harris, R.A., Sawyer, R.K., Audley-Charles, M.G., 1998. Collisional melange development: Geologic associations of active melange-forming processes with exhumed melange facies in the western Banda orogen, Indonesia. Tectonics 17, 458–479.
Harris, R., Vorkink, M.W., Prasetyadi, C., Zobell, E., Roosmawati, N., Apthorpe, M., 2009. Transition from subduction to arc-continent collision: Geologic and neotectonic evolution of Savu Island, Indonesia. Geosphere 5, 152–171.
Harun, Z., 2002. Late mesozoic-early tertiary faults of Peninsular Malaysia. Geol. Soc. Malaysia Bull. 45, 117–120.
Hasan, K., 1991. The Upper Cretaceous flysch succession of the Balangbaru Formation, Southwest-Sulawesi. Proc. Indones. Pet. Assoc. Annu. Conv. 20, 183–208.
Hassan, M.H.A., Aung, A.-K., Becker, R.T., Rahman, N.A.A., Ng, T.F., Ghani, A.A., Shuib, M.K., 2014. Stratigraphy and palaeoenvironmental evolution of the mid-to upper Palaeozoic succession in Northwest Peninsular Malaysia. J. Asian Earth Sci. 83, 60–79.
Hawkesworth, C., Cawood, P.A., Dhuime, B., 2019. Rates of generation and growth of the continental crust. Geosci. Front. 10, 165–173.
Hayes, D.E., Nissen, S.S., 2005. The South China sea margins: Implications for rifting contrasts. Earth Planet. Sci. Lett. 237, 601–616.
Hazebroek, H.P., Tan, D.N.K., 1993. Tertiary tectonic evolution of the NW Sabah continental margin. Bull. Geol. Soc. Malaysia 33, 195–210.
Hébert, R., Bezard, R., Guilmette, C., Dostal, J., Wang, C.S., Liu, Z.F., 2012. The Indus-Yarlung Zangbo ophiolites from Nanga Parbat to Namche Barwa syntaxes, southern Tibet: First synthesis of petrology, geochemistry, and geochronology with incidences on geodynamic reconstructions of Neo-Tethys. Gondw. Res. 22, 377–397.
Heezen, B.C., Tharp, M., 1965. Physiographic Diagram of the Indian Ocean (With Descriptive Sheet). Geol. Soc. Am., New York.
Heine, C., Müller, R.D., Norvick, M., 2002. Revised tectonic evolution of the Northwest Shelf of Australia and adjacent abyssal plains. In: Keep, M., Moss, S. (Eds.), pp. 955–957.
Heine, C., Müller, R.D., 2005. Late Jurassic rifting along the Australian North West Shelf: margin geometry and spreading ridge configuration. Aust. J. Earth Sci. 52, 27–39.
Heine, C., Müller, R.D., Gaina, C., Clift, P., 2004. Reconstructing the lost eastern Tethys ocean basin: convergence history of the SE Asian margin and marine gateways. Cont. Interact. Within East Asian Marg. Seas. Geophys. Monogr. Ser. 149, 37–54.
Helmers, H., Maaskant, P., Hartel, T.H.D., 1990. Garnet peridotite and associated high-grade rocks from Sulawesi, Indonesia. Lithos 25, 171–188.
Helmers, H., Sopaheluwakan, J., Nila, E.S., Tjokrosapoetro, S., 1989. Blueschist evolution is Southeast Sulawesi, Indonesia. Netherlands J. Sea Res. 24, 373–381.
Hendaryono, A., 1998. Etude géologique de l'ile de Flores.
Hennig, J., Advokaat, E., Rudyawan, A., Hall, R., 2014. Large sediment accumulations and major subsidence offshore; rapid uplift on land: consequences of extension of Gorontalo Bay and Northern Sulawesi. Proc. Indones. Pet. Assoc. Annu. Conv. 38, IPA14-G-304.
Hennig, J., Breitfeld, H.T., Hall, R., Nugraha, A.M.S., 2017a. The Mesozoic tectono-magmatic evolution at the Paleo-Pacific subduction zone in West Borneo. Gondwana Res. 48, 292–310.
Hennig, J., Hall, R., Armstrong, R.A., 2016. U-Pb zircon geochronology of rocks from west Central Sulawesi, Indonesia: Extension-related metamorphism and magmatism during the early stages of mountain building. Gondw. Res. 32, 41–63.
Hennig, J., Hall, R., Forster, M.A., Kohn, B.P., Lister, G.S., 2017b. Rapid cooling and exhumation as a consequence of extension and crustal thinning: Inferences from the Late Miocene to Pliocene Palu Metamorphic Complex, Sulawesi, Indonesia. Tectonophysics 712, 600–622.
Hesse, S., Back, S., Franke, D., 2009. The deep-water fold-and-thrust belt offshore NW Borneo: Gravity-driven versus basement-driven shortening. Geol. Soc. Am. Bull. 121, 939–953.
Hetzel, W.H., 1936. Verslag van het onderzoek naar het voorkomen van asfaltgesteenten op het eiland Boeton. Landsdrukkerij.
Hilde, T.W.C., Chao-Shing, L., 1984. Origin and evolution of the West Philippine Basin: a new interpretation. Tectonophysics 102, 85–104.
Hill, K.C., Hall, R., 2003. Mesozoic-Cenozoic evolution of Australia's New Guinea. Evol. Dyn. Aust. Plate 372, 265.
Hill, K.C., Raza, A., 1999. Arc-continent collision in Papua Guinea: Constraints from fission track thermochronology. Tectonics 18, 950–966.
Hilton, D.R., Hoogewerff, J.A., Van Bergen, M.J., Hammerschmidt, K., 1992. Mapping magma sources in the east Sunda-Banda arcs, Indonesia: constraints from helium isotopes. Geochim. Cosmochim. Acta 56, 851–859.
Hinschberger, F., Malod, J.-A., Réhault, J.-P., Dyment, J., Honthaas, C., Villeneuve, M., Burhanuddin, S., 2000. Origine et evolution du bassin Nord-Banda (Indonesie): apport des donnees magnetiques. Comptes Rendus l'Académie des Sci. IIA-Earth Planet. Sci. 331, 507–514.
Hinschberger, F., Malod, J.-A., Dyment, J., Honthaas, C., Réhault, J.-P., Burhanuddin, S., 2001. Magnetic lineations constraints for the back-arc opening of the Late Neogene South Banda Basin (eastern Indonesia). Tectonophysics 333, 47–59.
Hinschberger, F., Malod, J.-A., Réhault, J.-P., Villeneuve, M., Royer, J.-Y., Burhanuddin, S., 2005. Late Cenozoic geodynamic evolution of eastern Indonesia. Tectonophysics 404, 91–118.
Hinz, K., Schlüter, H.U., 1985. Geology of the Dangerous Grounds, South China Sea, and the continental margin off southwest Palawan: Results of SONNE cruises SO-23 and SO-27. Energy 10, 297–315.
Hodges, K.V., 2000. Tectonics of the Himalaya and southern Tibet from two perspectives. Geol. Soc. Am. Bull. 112, 324–350.
Hoffmann, J., Bröcker, M., Setiawan, N.I., Klemd, R., Berndt, J., Maulana, A., Baier, H., 2019. Age constraints on high-pressure/low-temperature metamorphism and sedimentation in the Luk Ulo Complex (Java, Indonesia). Lithos 324, 747–762.
Honggang, L.B.X.G.W., Huimin, Z., 2002. Sea floor spreading recorded by drowning events of cenozoic carbonate platforms in the South China Sea. Sci. Geol. Sin. 4.
Honthaas, C., Villeneuve, M., Réhault, J.-P., Bellon, H., Cornée, J.-J., Saint-Marc, P., Butterlin, J., Gravelle, M., Burhanuddin, S., 1997. L'île de Kur: géologie du flanc oriental du bassin de Weber (Indonésie orientale). Comptes Rendus l'Académie des Sci. IIA-Earth Planet. Sci. 325, 883–890.
Honthaas, C., Réhault, J.-P., Maury, R.C., Bellon, H., Hémond, C., Malod, J.-A., Cornée, J.-J., Villeneuve, M., Cotten, J., Burhanuddin, S., 1998. A Neogene back-arc origin for the Banda Sea basins: geochemical and geochronological constraints from the Banda ridges (East Indonesia). Tectonophysics 298, 297–317.
Honza, E., John, J., Banda, R.M., 2000. An imbrication model for the Rajang accretionary complex in Sarawak, Borneo. J. Asian Earth Sci. 18, 751–759.

Hossain, M.S., Ao, S., Mondal, T.K., Sain, A., Khan, M.S.H., Xiao, W., Zhang, P., 2022. Understanding the Deformation Structures and Tectonics of the Active Orogenic Fold-Thrust Belt: Insights from the Outer Indo-Burman Ranges. Lithosphere 2022, 6058346.
Hsieh, R.-B.-J., Shellnutt, J.G., Yeh, M.-W., 2017. Age and tectonic setting of the East Taiwan Ophiolite: implications for the growth and development of the South China Sea. Geol. Mag. 154, 441–455.
Hu, X., Jansa, L., Chen, L., Griffin, W.L., O'Reilly, S.Y., Wang, J., 2010. Provenance of Lower Cretaceous Wölong volcaniclastics in the Tibetan Tethyan Himalaya: Implications for the final breakup of eastern Gondwana. Sed. Geol. 223, 193–205.
Huang, C.-Y., Yuan, P.B., Tsao, S.-J., 2006. Temporal and spatial records of active arc-continent collision in Taiwan: A synthesis. Geol. Soc. Am. Bull. 118, 274–288.
Huang, C.-Y., Chen, W.-H., Wang, M.-H., Lin, C.-T., Yang, S., Li, X., Yu, M., Zhao, X., Yang, K.-M., Liu, C.-S., 2018. Juxtaposed sequence stratigraphy, temporal-spatial variations of sedimentation and development of modern-forming forearc Lichi Mélange in North Luzon Trough forearc basin onshore and offshore eastern Taiwan: An overview. Earth-Sci. Rev. 182, 102–140.
Huang, W., Van Hinsbergen, D.J.J., Maffione, M., Orme, D.A., Dupont-Nivet, G., Guilmette, C., Ding, L., Guo, Z., Kapp, P., 2015. Lower Cretaceous Xigaze ophiolites formed in the Gangdese forearc: Evidence from paleomagnetism, sediment provenance, and stratigraphy. Earth Planet. Sci. Lett. 415, 142–153.
Huchon, P., Le Pichon, X., 1984. Sunda Strait and central Sumatra fault. Geology 12, 668–672.
Hutchison, C.S., 1989a. The palaeo-Tethyan realm and Indosinian orogenic system of Southeast Asia. In: Tectonic Evolution of the Tethyan Region. Springer, pp. 585–643.
Hutchison, C.S., 1989b. Geological Evolution of South-east Asia. Clarendon Press, Oxford.
Hutchison, C.S., 1994. Gondwana and Cathaysian blocks, Palaeotethys sutures and Cenozoic tectonics in South-east Asia. In: Active Continental Margins—Present and Past. Springer, pp. 388–405.
Hutchison, C.S., Bergman, S.C., Swauger, D.A., Graves, J.E., 2000. A Miocene collisional belt in north Borneo: uplift mechanism and isostatic adjustment quantified by thermochronology. J. Geol. Soc. Lond. 157, 783–793.
Hutchison, Charle.S., 1986. Formation of marginal seas by rifting of the Chinese and Australian continental margins and implications for the Borneo region. Geol. Soc. Malays. Bull 20, 201–220.
Hutchison, C.S., 1992. The Southeast Sulu Sea, a Neogene marginal basin with outcropping extensions in Sabah. Bull. Geol. Soc. Malaysia 32, 89–108.
Idrus, A., Zaccarini, F., Garuti, G., Wijaya, I.G.N.K., Swamidharma, Y.C.A., Bauer, C., 2022. Origin of Podiform Chromitites in the Sebuku Island Ophiolite (South Kalimantan, Indonesia): Constraints from Chromite Composition and PGE Mineralogy. Minerals 12, 974.
Ikhram, R., Syafri, I., Rosana, M.F., 2019. Petrological Characteristic and Whole Rock Geochemistry of Metamorphic Rocks in Melangè Complex of Ciletuh Area, West Java, Indonesia.
Ilao, K.A., Morley, C.K., Aurelio, M.A., 2018. 3D seismic investigation of the structural and stratigraphic characteristics of the Pagasa Wedge, Southwest Palawan Basin, Philippines, and their tectonic implications. J. Asian Earth Sci. 154, 213–237.
Ingalls, M., Rowley, D.B., Currie, B., Colman, A.S., 2016. Large-scale subduction of continental crust implied by India-Asia mass-balance calculation. Nat. Geosci. 9, 848–853.
Ishikawa, A., Kaneko, Y., Kadarusman, A., Ota, T., 2007. Multiple generations of forearc mafic–ultramafic rocks in the Timor-Tanimbar ophiolite, eastern Indonesia. Gondw. Res. 11, 200–217.
Ismail, W.N.W., Tahir, S.H., Jasin, B., 2014. Barremian-Aptian Radiolaria from Chert-Spilite Formation, Kudat, Sabah.
Isozaki, Y., Maruyama, S., Furuoka, F., 1990. Accreted oceanic materials in Japan. Tectonophysics 181, 179–205.
Isyqi, Ansori, C., 2021. Petrography and geochemistry preliminary study of Pucangan Serpentinite Geosite Karangsambung–Karangbolong Geopark Central Java, Indonesia. In: IOP Conference Series: Earth and Environmental Science. IOP Publishing, pp. 12027.
Jablonski, D., Saitta, A.J., 2004. Permian to Lower Cretaceous plate tectonics and its impact on the tectono-stratigraphic development of the Western Australian margin. APPEA J. 44, 287–328.
Jadoul, F., Berra, F., Garzanti, E., 1998. The Tethys Himalayan passive margin from Late Triassic to Early Cretaceous (South Tibet). J. Asian Earth Sci. 16, 173–194.
Jafri, S.H., Balaram, V., Govil, P.K., 1993. Depositional environments of Cretaceous radiolarian cherts from Andaman-Nicobar islands, northeastern Indian Ocean. Mar. Geol. 112, 291–301.
Jafri, S.H., Charan, S.N., Govil, P.K., 1995. Plagiogranite from the Andaman ophiolite belt, Bay of Bengal, India. J. Geol. Soc. Lond.. 152, 681–687.
Jagger, L.J., McClay, K.R., 2018. Analogue modelling of inverted domino-style basement fault systems. Basin Res. 30, 363–381.
Jagoutz, O., Royden, L., Holt, A.F., Becker, T.W., 2015. Anomalously fast convergence of India and Eurasia caused by double subduction. Nat. Geosci. 8, 475–478.
Jasin, B., 1992. Significance of radiolarian chert from the chert-Spilite Formation, Telupid, Sabah. Bull. Geol. Soc. Malaysia 31, 67–84.
Jasin, B., 1996. Late Jurassic to Early Cretaceous radiolaria from chert blocks in the Lubok Antu mélange, Sarawak, Malaysia. J. Southeast Asian Earth Sci. 13, 1–11.
Jasin, B., Haile, N.S., 1993. Some radiolaria from the chert block of Lubok Antu Mélange. Sarawak. Newsl. Geol. Soc. Malaysia 19, 205–209.
Jasin, B., Madun, A., 1996. Some Lower Cretaceous radiolaria from the Serabang complex, Sarawak. Newsl. Geol. Soc. Malaysia 22, 61–65.
Jasin, B., Said, U., 1999a. Significance of Early Jurassic Radiolaria from West Sarawak, Malaysia.
Jasin, B., Said, U., 1999b. Some Late Jurassic-Early Cretaceous radiolarian faunas from the Pedawan Formation, Sarawak.
Jasin, B., Tahir, S., Samsuddin, A.R.H., 1985. Lower Cretaceous Radiolaria from the Chert-Spilite Formation, Kudat. Sabah. Newsl. Geol. Soc. Malaysia 11, 161–162.
Jasin, B., Said, U., Woei, A.D., 1996. Discovery of Early Jurassic Radiolaria from the tuff sequence, near Piching, west Sarawak. Newsl. Geol. Soc. Malaysia 22, 343–347.
Jasin, B., Haile, N., 1996. Uppermost Jurassic-Lower Cretaceous radiolarian chert from the Tanimbar Islands (Banda Arc), Indonesia. J. Southeast Asian Earth Sci. 14, 91–100.
Jasin, B., Tongkul, F., 2013. Cretaceous radiolarians from Baliojong ophiolite sequence, Sabah, Malaysia. J. Asian Earth Sci. 76, 258–265.
Jasin, B., 2000. Geological significance of radiolarian chert in Sabah. Bull. Geol. Soc. Malaysia 44, 35–43.
Jaya, A., Nishikawa, O., Hayasaka, Y., 2017. LA-ICP-MS zircon U-Pb and muscovite K–Ar ages of basement rocks from the south arm of Sulawesi, Indonesia. Lithos 292, 96–110.
Jena, S.K., Acharyya, S.K., 1986. Geological map around Phokphur, Tuensang district, Nagaland (Type section Phokphur Formation). Geol. Nagaland, Geol Surv. India Mem 119.
Jiang, H., Li, W.-Q., Jiang, S.-Y., Wang, H., Wei, X.-P., 2017. Geochronological, geochemical and Sr-Nd-Hf isotopic constraints on the petrogenesis of Late Cretaceous A-type granites from the Sibumasu Block, Southern Myanmar, SE Asia. Lithos 268, 32–47.
Jingsui, Y., Zhiqin, X., Xiangdong, D., Jing, L., FaHui, X., Zhao, L., ZhiHui, C., HuaQi, L., 2012. Discovery of a Jurassic SSZ ophiolite in the Myitkyina region of Myanmar. Acta Petrol. Sin. 28, 1710–1730.
Jiqing, H., Bingwei, C., 1987. Evolution of Tethys Sea in China and Adjacent Area. Beijing Geol. Publ. House 73.
Johnson, S.Y., Nur Alam, A.B.U.M.D., 1991. Sedimentation and tectonics of the Sylhet trough, Bangladesh. Geol. Soc. Am. Bull. 103, 1513–1527.
Jolivet, L., Brun, J.-P., 2010. Cenozoic geodynamic evolution of the Aegean. Int. J. Earth Sci. 99, 109–138.
Jouannic, C., Hoang, C.-T., Hantoro, W.S., Delinom, R.M., 1988. Uplift rate of coral reef terraces in the area of Kupang, West Timor: Preliminary results. Palaeogeogr. Palaeoclimatol. Palaeoecol. 68, 259–272.
Kadarusman, A., Sopaheluwakan, J., van Leeuwen, T., 2002. Eclogite, peridotite, granulite and associated high-grade rocks from Palu-Koro region, Central Sulawesi, Indonesia: An example for mantle and crust interactions in young orogenic belt. In: AGU Fall Meeting Abstracts.
Kadarusman, A., Massonne, H.-J., van Roermund, H., Permana, H., Munasri, 2007. PT evolution of eclogites and blueschists from the Luk Ulo Complex of central Java, Indonesia. Int. Geol. Rev. 49, 329–356.
Kadarusman, A., van Leeuwen, T., Sopaheluwakan, J., 2011. Eclogite, peridotite, granulite and associated high-grade rocks from the Palu region, Central Sulawesi, Indonesia: an example of mantle and crust interaction in a young orogenic belt. In: Proc. Jt. 36th HAGI 40th IAGI Ann. Conv., Makassar 10.
Kadarusman, A., Maruyama, S., Kaneko, Y., Ota, T., Ishikawa, A., Sopaheluwakan, J., Omori, S., 2010. World's youngest blueschist belt from Leti Island in the non-volcanic Banda outer arc of Eastern Indonesia. Gondw. Res. 18, 189–204.
Kadarusman, A., Parkinson, C.D., 2000. Petrology and PT evolution of garnet peridotites from central Sulawesi, Indonesia. J. Metamorph. Geol. 18, 193–210.
Kadarusman, A., Miyashita, S., Maruyama, S., Parkinson, C.D., Ishikawa, A., 2004. Petrology, geochemistry and paleogeographic reconstruction of the East Sulawesi Ophiolite, Indonesia. Tectonophysics 392, 55–83.
Kaewkor, C., Watkinson, I., 2017. Stretching factors in Cenozoic multi-rift basins, western Gulf of Thailand. In: EGU General Assembly Conference Abstracts, pp. 19244.
Kakizaki, Y., Weissert, H., Hasegawa, T., Ishikawa, T., Matsuoka, J., Kano, A., 2013. Strontium and carbon isotope stratigraphy of the Late Jurassic shallow marine limestone in western Palaeo-Pacific, northwest Borneo. J. Asian Earth Sci. 73, 57–67.
Kallagher, H.J., 1990. The Structural and Stratigraphic Evolution of the Sunda Forearc Basin, North Sumatra, Indonesia.
Kamili, Z.A., Kingston, J., Achmad, Z., Wahab, A., Sosromihardjd, S., Crausaz, C.U., 1976. Contribution to the Pre–Baong Stratigraphy of North Sumatra.
Kaminski, M.A., Gradstein, F.M., Geroch, S., 1992. Uppermost Jurassic to Lower Cretaceous deep-water benthic foraminiferal assemblages from Site 765 on the Argo Abyssal Plain. In: Proceedings of the Ocean Drilling Program: Scientific Results, pp. 239–269.
Kanao, N., 1971. Summary Report on the Survey of Sumatra, Block 5, Japanese Overseas Mineral Development Company Limited. Unpubl. Manuscr.
Kaneko, Y., Maruyama, S., Kadarusman, A., Ota, T., Ishikawa, M., Tsujimori, T., Ishikawa, A., Okamoto, K., 2007. On-going orogeny in the outer-arc of the Timor-Tanimbar region, eastern Indonesia. Gondw. Res. 11, 218–233.
Kanjanapayont, P., Grasemann, B., Edwards, M.A., Fritz, H., 2012a. Quantitative kinematic analysis within the Khlong Marui shear zone, southern Thailand. J. Struct. Geol. 35, 17–27.
Kanjanapayont, P., Klötzli, U., Thöni, M., Grasemann, B., Edwards, M.A., 2012b. Rb–Sr, Sm–Nd, and U-Pb geochronology of the rocks within the Khlong Marui shear zone, southern Thailand. J. Asian Earth Sci. 56, 263–275.

Kapp, P., DeCelles, P.G., 2019. Mesozoic-Cenozoic geological evolution of the Himalayan-Tibetan orogen and working tectonic hypotheses. Am. J. Sci. 319, 159–254.
Kartaadiputra, L.W., Ahmad, Z., Reymond, A., 1982. Deep-sea basins in Indonesia. Proc. Indones. Pet. Assoc. Annu. Conv. 11, 53–81.
Katili, J.A., 1970. Large transcurrent faults in Southeast Asia with special reference to Indonesia. Geol. Rundschau 59, 581–600.
Keenan, T.E., Encarnación, J., Buchwaldt, R., Fernandez, D., Mattinson, J., Rasoazanamparany, C., Luetkemeyer, P.B., 2016. Rapid conversion of an oceanic spreading center to a subduction zone inferred from high-precision geochronology. Proc. Natl. Acad. Sci. 113, E7359–E7366.
Keep, M., Haig, D.W., 2010. Deformation and exhumation in Timor: Distinct stages of a young orogeny. Tectonophysics 483, 93–111.
Kelley, S., 2002. Excess argon in K-Ar and Ar–Ar geochronology. Chem. Geol. 188, 1–22.
Kemp, G., Mogg, W., 1992. A re-appraisal of the geology, tectonics, and prospectivity of Seram island, eastern Indonesia. Proc. Indones. Pet. Assoc. Annu. Conv. 21, 499–520.
Ketner, K.B., Modjo, S., Naeser, C.W., Obradovich, J.D., Robinson, K., Suptandar, T., 1976. Pre-Eocene rocks of Java, Indonesia. J. Res. U.S. Geol. Surv. 4, 605–614.
Kiessling, W., Flügel, E., 2000. Late Paleozoic and Late Triassic limestones from North Palawan block (Philippines): microfacies and paleogeographical implications. Facies 43, 39–77.
Kirk, H.J.C., 1968. The igneous rocks of the Sarawak and Sabah. Geol. Surv. Borneo Reg. Malaysia, Bull 5, 201.
Klompe, T.H.F., 1954. The structural importance of the Sula Spur (Indonesia). Indones. J. Nat. Sci. 110, 21–40.
Knittel, U., 2011. 83 Ma rhyolite from Mindoro–evidence for Late Yanshanian magmatism in the Palawan Continental Terrane (Philippines). Isl. Arc 20, 138–146.
Knittel, U., Daniels, U., 1987. Sr-isotopic composition of marbles from the Puerto Galera area (Mindoro, Philippines): Additional evidence for a Paleozoic age of a metamorphic complex in the Philippine island arc. Geology 15, 136–138.
Knittel, U., Hung, C.-H., Yang, T.F., Iizuka, Y., 2010. Permian arc magmatism in Mindoro, the Philippines: An early Indosinian event in the Palawan Continental Terrane. Tectonophysics 493, 113–117.
Knittel, U., Walia, M., Suzuki, S., Dimalanta, C.B., Tamayo, R., Yang, T.F., Yumul, G.P., 2017. Diverse protolith ages for the Mindoro and Romblon Metamorphics (Philippines): Evidence from single zircon U-Pb dating. Isl. Arc 26, e12160.
Koning, T., 1985. Petroleum geology of the Ombilin intermontane basin, West Sumatra. Proc. Indones. Pet. Assoc. Annu. Conv. 14, 117–137.
Koolhoven, W.C.B., 1930. Verslag over een verkenningstocht in den Oostarm van Celebes en den Banggai-Archipel. Jaarb. Mijnwez. Ned. Indie 58, 187–228.
Kopp, C., Flueh, E.R., Neben, S., 1999. Rupture and accretion of the Celebes Sea crustrelated to the North-Sulawesi subduction: combinedinterpretation of reflection and refraction seismicmeasurements. J. Geodyn. 27, 309–325.
Koulakov, I., Wu, Y.-M., Huang, H.-H., Dobretsov, N., Jakovlev, A., Zabelina, I., Jaxybulatov, K., Chervov, V., 2014. Slab interactions in the Taiwan region based on the P-and S-velocity distributions in the upper mantle. J. Asian Earth Sci. 79, 53–64.
Koymans, M.R., Langereis, C.G., Pastor-Galán, D., van Hinsbergen, D.J.J., 2016. Paleomagnetism. org: An online multi-platform open source environment for paleomagnetic data analysis. Comput. Geosci. 127–137, 93.
Koymans, M.R., van Hinsbergen, D.J.J., Pastor-Galan, D., Vaes, B., Langereis, C.G., 2020. Towards FAIR paleomagnetic data management through Paleomagnetism. org 2.0. Geochem. Geophys. Geosyst. 21.
Krähenbuhl, R., 1991. Magmatism, tin mineralization and tectonics of the Main Range, Malaysian Peninsula: Consequences for the plate tectonic model of Southeast Asia based on Rb–Sr, K-Ar and fission track data. Bull. Geol. Soc. Malays. 29, 1–100.
Kudrass, H.R., Muller, P., Kreuzer, H., Weiss, W., 1990. Volcanic rocks and tertiary carbonates dredged from the Cagayan Ridge and the Southwest Sulu Sea, Philippines. Proc. ODP, Init. Reports 124, 93–100.
Kudrass, H.R., Wiedicke, M., Cepek, P., Kreuzer, H., Müller, P., 1986. Mesozoic and Cainozoic rocks dredged from the South China Sea (Reed Bank area) and Sulu Sea and their significance for plate-tectonic reconstructions. Mar. Pet. Geol. 3, 19–30.
Kwong, H., 2011. Paleomagnetic investigation of the Balangbaru formation, SW Sulawesi, Indonesia. 香港大學學位論文 0–1.
Labails, C., Olivet, J.-L., Aslanian, D., Roest, W.R., 2010. An alternative early opening scenario for the Central Atlantic Ocean. Earth Planet. Sci. Lett. 297, 355–368.
Lai, Y.-M., Liu, P.-P., Chung, S.-L., Ghani, A.A., Lee, H.-Y., Quek, L.X., Li, S., Roselee, M. H., Murtadha, S., Lintjewas, L., 2023. Zircon U-Pb geochronology and Hf isotopic compositions of igneous rocks from Sumatra: implications for the Cenozoic magmatic evolution of the western Sunda Arc. Geol. Soc. Lond. Spec. Publ. 537.
Lai, C., Xia, X., Hall, R., Meffre, S., Tsikouras, B., Rosana Balangue-Tarriela, M.I., Idrus, A., Ifandi, E., Norazme, N., 2021. Cenozoic Evolution of the Sulu Sea Arc-Basin System: An Overview. Tectonics 40.
Lai, C.-K., Zaw, K., Meffre, S., 2018. Multiphase magmatism of the Neotethyan Central Ophiolite Belt in Myanmar: Zircon U-Pb age and whole-rock geochemical constraints from the Sagaing-Minwun ophiolite. EGUGA 3587.
Lallemand, S., Arcay, D., 2021. Subduction initiation from the earliest stages to self-sustained subduction: Insights from the analysis of 70 Cenozoic sites. Earth-Sci. Rev. 221, 103779.
Lallemand, S., Font, Y., Bijwaard, H., Kao, H., 2001. New insights on 3-D plates interaction near Taiwan from tomography and tectonic implications. Tectonophysics 335, 229–253.
Lallemand, S.E., Popoff, M., Cadet, J., Bader, A., Pubellier, M., Rangin, C., Deffontaines, B., 1998. Genetic relations between the central and southern Philippine Trench and the Sangihe Trench. J. Geophys. Res. Solid Earth 103, 933–950.
Lamont, T.N., Searle, M.P., Hacker, B.R., Htun, K., Htun, K.M., Morley, C.K., Waters, D. J., White, R.W., 2021. Late Eocene-Oligocene granulite facies garnet-sillimanite migmatites from the Mogok Metamorphic belt, Myanmar, and implications for timing of slip along the Sagaing Fault. Lithos 386, 106027.
Lassal, O., Huchon, P., Harjono, H., 1989. crustal stretching in Sunda Strait (Indonesia) from seismic-reflection data (Krakatau cruise). Comptes Rendus L Acad. Des. Sci. Ser. II 309, 205–212.
Laufer, F., Kraeff, A., 1957. The Geology and Hydrology of West-and Central-Sumba and Their Relationship to the Water-supply and the Rural Economy. Republik Indonesia, Kementerian Perekonomian, Pusat Djawatan Geologi.
Lee, C.P., 2009. Palaeozoic stratigraphy. Geol. Penins. Malaysia, 55–86.
Lee, H.-Y., Chung, S.-L., Yang, H.-M., 2016. Late Cenozoic volcanism in central Myanmar: Geochemical characteristics and geodynamic significance. Lithos 245, 174–190.
Lee, T.-Y., Lawver, L.A., 1994. Cenozoic plate reconstruction of the South China Sea region. Tectonophysics 235, 149–180.
Lee, T.-Y., Lawver, L.A., 1995. Cenozoic plate reconstruction of Southeast Asia. Tectonophysics 251, 85–138.
Lelgemann, H., Gutscher, M., Bialas, J., Flueh, E.R., Weinrebe, W., Reichert, C., 2000. Transtensional basins in the western Sunda Strait. Geophys. Res. Lett. 27, 3545–3548.
Leloup, P.H., Lacassin, R., Tapponnier, P., Schärer, U., Zhong, D., Liu, X., Zhang, L., Ji, S., Trinh, P.T., 1995. The Ailao Shan-Red river shear zone (Yunnan, China), tertiary transform boundary of Indochina. Tectonophysics 251, 3–84.
Leong, K.M., 1974. The geology and mineral resources of Upper Segama valley and Darvel Bay, Sabah, Malaysia. Geol. Surv. Borneo Reg. Mem. 354.
Letouzey, J., de Clarens, P., Guignard, J., Berthon, J.-L., 1983. Structure of the North Banda-Molucca area from multichannel seismic reflection data. Proc. Indones. Pet. Assoc. Annu. Conv. 12, 143–156.
Levell, B.K., 1987. The Nature and Significance of Regional Unconformities in the Hydrocarbon–Bearing Neogene Sequence Offshore West Sabah. Bull. Geol. Soc. Malaysia 18, 1–29.
Li, S., Advokaat, E.L., van Hinsbergen, D.J.J., Koymans, M., Deng, C., Zhu, R., 2017. Paleomagnetic constraints on the Mesozoic-Cenozoic paleolatitudinal and rotational history of Indochina and South China: Review and updated kinematic reconstruction. Earth-Sci. Rev. 171, 58–77. https://doi.org/10.1016/j.earscirev.2017.05.007.
Li, S., Chung, S.-L., Lai, Y.-M., Ghani, A.A., Lee, H.-Y., Murtadha, S., 2020b. Mesozoic juvenile crustal formation in the easternmost Tethys: Zircon Hf isotopic evidence from Sumatran granitoids, Indonesia. Geology.
Li, Z., Ding, L., Lippert, P.C., Song, P., Yue, Y., van Hinsbergen, D.J.J., 2016. Paleomagnetic constraints on the Mesozoic drift of the Lhasa terrane (Tibet) from Gondwana to Eurasia. Geology 44, 727–730.
Li, Z., Ding, L., Zaw, T., Wang, H., Cai, F., Yao, W., Xiong, Z., Sein, K., Yue, Y., 2020c. Kinematic evolution of the West Burma block during and after India-Asia collision revealed by paleomagnetism. J. Geodyn. 134, 101690.
Li, Z., Ding, L., van Hinsbergen, D.J.J., Lippert, P.C., Yue, Y., Xie, J., Chen, Y., Guo, X., Zhang, D., Zhao, T., 2022. Jurassic true polar wander recorded by the Lhasa terrane on its northward journey from Gondwana to Eurasia. Earth Planet. Sci. Lett. 592, 117609.
Li, J.-X., Fan, W.-M., Zhang, L.-Y., Evans, N.J., Sun, Y.-L., Ding, L., Guan, Q.-Y., Peng, T.-P., Cai, F.-L., Sein, K., 2019. Geochronology, geochemistry and Sr–Nd–Hf isotopic compositions of Late Cretaceous-Eocene granites in southern Myanmar: Petrogenetic, tectonic and metallogenic implications. Ore Geol. Rev. 112, 103031.
Li, J.-X., Fan, W.-M., Zhang, L.-Y., Peng, T.-P., Sun, Y.-L., Ding, L., Cai, F.-L., Sein, K., 2020a. Prolonged Neo-Tethyan magmatic arc in Myanmar: evidence from geochemistry and Sr–Nd–Hf isotopes of Cretaceous mafic–felsic intrusions in the Banmauk-Kawlin area. Int. J. Earth Sci. 109, 649–668.
Li, X.-H., Li, Z.-X., Li, W.-X., Wang, Y., 2006. Initiation of the Indosinian Orogeny in South China: evidence for a Permian magmatic arc on Hainan Island. J. Geol. 114, 341–353.
Li, X., Li, J., Yu, X., Wang, C., Jourdan, F., 2015. 40Ar/39Ar ages of seamount trachytes from the South China Sea and implications for the evolution of the northwestern sub-basin. Geosci. Front. 6, 571–577.
Li, C., Song, T., 2012. Magnetic recording of the Cenozoic oceanic crustal accretion and evolution of the South China Sea basin. Chin. Sci. Bull. 57, 3165–3181.
Li, S., van Hinsbergen, D.J.J., Deng, C., Advokaat, E.L., Zhu, R., 2018. Paleomagnetic Constraints From the Baoshan Area on the Deformation of the Qiangtang-Sibumasu Terrane Around the Eastern Himalayan Syntaxis. J. Geophys. Res. Solid Earth. https://doi.org/10.1002/2017JB015112.
Li, C., Xu, X., Lin, J., Sun, Z., Zhu, J., Yao, Y., Zhao, X., Liu, Q., Kulhanek, D.K., Wang, J., 2014. Ages and magnetic structures of the South China Sea constrained by deep tow magnetic surveys and IODP Expedition 349. Geochem. Geophys. Geosyst. 15, 4958–4983.
Li, X., Zhou, H., Chung, S., Ding, S., Liu, Y., Lee, C., Ge, W., Zhang, Y., Zhang, R., 2002. Geochemical and Sm–Nd isotopic characteristics of metabasites from central Hainan Island, South China and their tectonic significance. Isl. Arc 11, 193–205.
Liang, Y., Delescluse, M., Qiu, Y., Pubellier, M., Chamot-Rooke, N., Wang, J., Nie, X., Watremez, L., Chang, S., Pichot, T., 2019. Décollements, detachments, and rafts

in the extended crust of Dangerous Ground, South China Sea: The role of inherited contacts. Tectonics 38, 1863–1883.
Licht, A., Dupont-Nivet, G., Win, Z., Swe, H.H., Kaythi, M., Roperch, P., Ugrai, T., Littell, V., Park, D., Westerweel, J., 2019. Paleogene evolution of the Burmese forearc basin and implications for the history of India-Asia convergence. Geol. Soc. Am. Bull. 131, 730–748.
Licht, A., Win, Z., Westerweel, J., Cogné, N., Morley, C., Chantraprasert, S., Poblete, F., Ugrai, T., Nelson, B., Aung, D.W., 2020. Magmatic history of central Myanmar and implications for the evolution of the Burma Terrane. Gondw 87, 303–319.
Liew, T.C., McCulloch, M.T., 1985. Genesis of granitoid batholiths of Peninsular Malaysia and implications for models of crustal evolution: Evidence from a Nd Sr isotopic and U Pb zircon study. Geochim. Cosmochim. Acta 49, 587–600.
Limonta, M., Resentini, A., Carter, A., Bandopadhyay, P.C., Garzanti, E., 2017. Provenance of Oligocene Andaman sandstones (Andaman–Nicobar Islands): Ganga-Brahmaputra or Irrawaddy derived?. Geol Soc. Lond., Mem. 47, 141–152.
Lin, T.-H., Lo, C.-H., Chung, S.-L., Hsu, F.-J., Yeh, M.-W., Lee, T.-Y., Ji, J.-Q., Wang, Y.-Z., Liu, D., 2009. 40Ar/39Ar dating of the Jiali and Gaoligong shear zones: Implications for crustal deformation around the Eastern Himalayan Syntaxis. J. Asian Earth Sci. 34, 674–685.
Lin, A.T., Watts, A.B., Hesselbo, S.P., 2003. Cenozoic stratigraphy and subsidence history of the South China Sea margin in the Taiwan region. Basin Res. 15, 453–478.
Ling, H.Y., Hall, R., Nichols, G.J., 1991. Early Eocene Radiolaria from Waigeo Island, Eastern Indonesia. J. SE Asian Earth Sci. 6, 299–305.
Ling, H.Y., Chandra, R., Karkare, S.G., 1996. Tectonic significance of Eocene and Cretaceous radiolaria from South Andaman Island, northeast Indian Ocean. Isl. Arc 5, 166–179.
Ling, H.Y., Srinivasan, M.S., 1993. Significance of Eocene radiolaria from port Blair group of south Andaman island, India. J. Paheontological Soc. India 38, 1–5.
Linthout, K., Helmers, H., Sopaheluwakan, J., Nila, E.S., 1989. Metamorphic complexes in Buru and Seram, northern Banda arc. Netherlands J. Sea Res. 24, 345–356.
Linthout, K., Helmers, H., Andriessen, P.A.M., 1991. Dextral strike-slip in Central Seram and 3–4.5 Ma Rb/Sr ages in pre-Triassic metamorphics related to Early Pliocene counterclockwise rotation of the Buru-Seram microplate (E. Indonesia). J. SE Asian Earth Sci. 6, 335–342.
Linthout, K., Helmers, H., Wijbrans, J.R., Van Wees, J.D.A.M., 1996. 40Ar/39Ar constraints on obduction of the Seram ultramafic complex: consequences for the evolution of the southern Banda Sea. Geol. Soc. Lond. Spec. Publ. 106, 455–464.
Liu, C.-Z., Chung, S.-L., Wu, F.-Y., Zhang, C., Xu, Y., Wang, J.-G., Chen, Y., Guo, S., 2016a. Tethyan suturing in Southeast Asia: Zircon U-Pb and Hf-O isotopic constraints from Myanmar ophiolites. Geology 44, 311–314.
Liu, W.-N., Li, C.-F., Li, J., Fairhead, D., Zhou, Z., 2014. Deep structures of the Palawan and Sulu Sea and their implications for opening of the South China Sea. Mar. Pet. Geol. 58, 721–735.
Liu, C.-Z., Zhang, C., Xu, Y., Wang, J.-G., Chen, Y., Guo, S., Wu, F.-Y., Sein, K., 2016b. Petrology and geochemistry of mantle peridotites from the Kalaymyo and Myitkyina ophiolites (Myanmar): Implications for tectonic settings. Lithos 264, 495–508.
Lo, Y.-C., Chen, C.-T., Lo, C.-H., Chung, S.-L., 2020. Ages of ophiolitic rocks along plate suture in Taiwan orogen: Fate of the South China Sea from subduction to collision. Terr. Atmos. Ocean. Sci. 31, 383–402.
Lo, C.-H., Yui, T.-F., 1996. $^{40}Ar/^{39}Ar$ dating of high-pressure rocks in the Tananao Basement Complex, Taiwan. J.-Geol. Soc. China-Taiwan 39, 13–30.
Lokho, K., Tewari, V.C., 2011. Biostratigraphy, sedimentation and chemostratigraphy of the Tertiary Neotethys sediments from the NE Himalaya, India. In: STROMATOLITES: Interaction of Microbes with Sediments. Springer, pp. 607–630.
Lokho, K., Venkatachalapathy, R., Raju, D.S.N., 2004. Uvigerinids and associated foraminifera, their value as direct evidence for shelf and deep marine paleoenvironments during Upper Disang of Nagaland, Eastern Himalaya and its implications in hydrocarbon exploration. Indian J. Pet. Geol 13, 1–7.
Long, S., McQuarrie, N., Tobgay, T., Hawthorne, J., 2011. Quantifying internal strain and deformation temperature in the eastern Himalaya, Bhutan: Implications for the evolution of strain in thrust sheets. J. Struct. Geol. 33, 579–608.
Longley, I.M., Buessenschuett, C., Clydsdale, L., Cubitt, C.J., Davis, R.C., Johnson, M.K., Marshall, N.M., Murray, A.P., Somerville, R., Spry, T.B., 2002. The North West Shelf of Australia–a Woodside perspective. Sediment. basins West. Aust. 3, 27–88.
Ludden, J., 1992. Radiometric age determinations for basement from Sites 765 and 766, Argo Abyssal Plain and northwestern Australian margin. Proc. ODP Sci. Results 123, 557–562.
Lunt, P., 2003. Biogeography of some Eocene larger foraminifera, and their application in distinguishing geological plates. Palaeontol. Electron. 6, 22.
Ma, Z.-L., Li, Q.-Y., Liu, X.-Y., Luo, W., Zhang, D.-J., Zhu, Y.-H., 2018. Palaeoenvironmental significance of Miocene larger benthic foraminifera from the Xisha Islands, South China Sea. Palaeoworld 27, 145–157.
Maac, Y.O., Ylade, E.D., 1988. Stratigraphic and paleontologic studies of Tablas, Romblon. Rep. Res. Dev. Coop. ITIT Proj., 44–67.
Madon, M.B.H., 1997. The kinematics of extension and inversion in the Malay Basin, offshore Peninsular Malaysia.
Maffione, M., Van Hinsbergen, D.J.J., Koornneef, L.M.T., Guilmette, C., Hodges, K., Borneman, N., Huang, W., Ding, L., Kapp, P., 2015. Forearc hyperextension dismembered the south Tibetan ophiolites. Geology 43, 475–478.
Mahattanachai, T., Morley, C.K., Charusiri, P., Kanjanapayont, P., 2021. The Andaman Basin Central Fault Zone, Andaman Sea: Characteristics of a major deepwater strike-slip fault system in a polyphase rift. Mar. Pet. Geol. 128, 104997.
Malaihollo, J.F.A., Hall, R., 1996. The geology and tectonic evolution of the Bacan region, east Indonesia. Geol. Soc. Lond. Spec. Publ. 106, 483–497.
Mansor, M.Y., Rahman, A.H.A., Menier, D., Pubellier, M., 2014. Structural evolution of Malay Basin, its link to Sunda Block tectonics. Mar. Pet. Geol. 58, 736–748.
Manur, H., Jacques, J.M., 2014. Deformational Characteristics of the West Natuna Basin with Regards to its Remaining Exploration Potential. Proc. Indones. Pet. Assoc. Annu. Conv. 38, IPA14-G-193.
Marchadier, Y., Rangin, C., 1989. Passage subduction-collision et tectoniques superposées à l'extrémité méridionale de la fosse de Manille (Mindoro-Tablas: Philippines). Comptes rendus l'Académie des Sci. Série 2, Mécanique, Phys. Chim. Sci. l'univers. Sci. la Terre 308, 1715–1720.
Marchadier, Y., Rangin, C., 1990. Polyphase tectonics at the southern tip of the Manila trench, Mindoro-Tablas Islands, Philippines. Tectonophysics 183, 273–287.
Marliyani, G.I., Arrowsmith, J.R., Whipple, K.X., 2016. Characterization of slow slip rate faults in humid areas: Cimandiri fault zone, Indonesia. J. Geophys. Res. Earth Surf. 121, 2287–2308.
Martin, C.R., Jagoutz, O., Upadhyay, R., Royden, L.H., Eddy, M.P., Bailey, E., Nichols, C. I.O., Weiss, B.P., 2020. Paleocene latitude of the Kohistan-Ladakh arc indicates multistage India-Eurasia collision. Proc. Natl. Acad. Sci. 117, 29487–29494.
Martini, R., Vachard, D., Zaninetti, L., Cirilli, S., Cornée, J.-J., Lathuilière, B., Villeneuve, M., 1997. Sedimentology, stratigraphy, and micropalaeontology of the Upper Triassic reefal series in Eastern Sulawesi (Indonesia). Palaeogeogr. Palaeoclimatol. Palaeoecol. 128, 157–174.
Matthews, S.J., Bransden, P.J.E., 1995. Late cretaceous and cenozoic tectono-stratigraphic development of the East Java Sea Basin, Indonesia. Mar. Pet. Geol. 12, 499–510.
Mat-Zin, I.C., Swarbrick, R.E., 1997. The tectonic evolution and associated sedimentation history of Sarawak Basin, eastern Malaysia: a guide for future hydrocarbon exploration. Geol. Soc. Lond. Spec. Publ. 126, 237–245.
Maulana, A., Christy, A.G., Ellis, D.J., 2015. Petrology, geochemistry and tectonic significance of serpentinized ultramafic rocks from the South Arm of Sulawesi, Indonesia. Geochemistry 75, 73–87.
Maulana, A., Christy, A.G., Ellis, D.J., Bröcker, M., 2018. The distinctive tectonic and metamorphic history of the Barru Block, South Sulawesi, Indonesia: petrological, geochemical and geochronological evidence. J. Asian Earth Sci..
Maulana, A., Ellis, D.J., Christy, A.G., 2010. Petrology, geochemistry and tectonic evolution of the south Sulawesi basement rocks, Indonesia. Proc. Indones. Pet. Assoc. Annu. Conv. 34, IPA10-G-192.
Maung, M., Aung, N.T., Suzuki, H., 2014. Latest Jurassic radiolarian fauna from the Chinghkran area, Myitkyina township, Kachin state, northern Myanmar. In: Regional Congress on Mineral and Energy Resources of Southeast Asia. GEOSEA, pp. 38–39.
Maurin, T., Rangin, C., 2009. Impact of the 90 E ridge at the Indo-Burmese subduction zone imaged from deep seismic reflection data. Mar. Geol. 266, 143–155.
Maury, R.C., Pubellier, M., Rangin, C., Wulput, L., Cotten, J., Socquet, A., Bellon, H., Guillaud, J.-P., Htun, H.M., 2004. Quaternary calc-alkaline and alkaline volcanism in an hyper-oblique convergence setting, central Myanmar and western Yunnan. Bull. la Société Géologique Fr. 175, 461–472.
Mawaleda, M., Husain, J.R., Forster, M., Suparka, E., Abdullah, C.I., Basuki, N.I., Hutabarat, J., 2018. Miocene tectonic of the Southeast Arm of Sulawesi, Indonesia: Based on petrology data, geochemistry, and 40Ar/39Ar geochronology of metamorphic rocks from Rumbia Complex. In: IOP Conference Series: Earth and Environmental Science. IOP Publishing, pp. 12043.
McCaffrey, R., 1996. Slip partitioning at convergent plate boundaries of SE Asia. Geol. Soc. Lond. Spec. Publ. 106, 3–18.
Mccaffrey, R., Silver, E.A., Raitt, R.W., 1980. Crustal structure of the Molucca Sea collision zone, Indonesia. In: The Tectonic and Geologic Evolution of Southeast Asian Seas and Islands. AGU Washington, DC, pp. 161–177.
McCaffrey, R., Nábělek, J., 1986. Seismological evidence for shallow thrusting north of the Timor trough. Geophys. J. Int. 85, 365–381.
McCaffrey, R., Nabelek, J., 1987. Earthquakes, gravity, and the origin of the Bali Basin: An example of a nascent continental fold-and-thrust belt. J. Geophys. Res. Solid Earth 92, 441–460.
McCarthy, A.J., Elders, C.F., 1997. Cenozoic deformation in Sumatra: oblique subduction and the development of the Sumatran Fault System. Geol. Soc. Lond. Spec. Publ. 126, 355–363.
McCarthy, A.J., Jasin, B., Haile, N.S., 2001. Middle Jurassic radiolarian chert, Indarung, Padang District, and its implications for the tectonic evolution of western Sumatra, Indonesia. J. Asian Earth Sci. 19, 31–44.
McClay, K., Dooley, T., Ferguson, A., Poblet, J., 2000. Tectonic Evolution of the Sanga Sanga Block, Mahakam Delta, Kalimantan, Indonesia. Am. Assoc. Pet. Geol. Bull. 84, 765–786.
McCourt, W.J., Crow, M.J., Cobbing, E.J., Amin, T.C., 1996. Mesozoic and Cenozoic plutonic evolution of SE Asia: evidence from Sumatra, Indonesia. Geol. Soc. Lond. Spec. Publ. 106, 321–335.
McIntosh, K., Lavier, L., van Avendonk, H., Lester, R., Eakin, D., Liu, C.-S., 2014. Crustal structure and inferred rifting processes in the northeast South China Sea. Mar. Pet. Geol. 58, 612–626.

Merkouriev, S., DeMets, C., 2006. Constraints on Indian plate motion since 20 Ma from dense Russian magnetic data: Implications for Indian plate dynamics. Geochem. Geophys. Geosyst. 7.
Metcalfe, I., 1984. Stratigraphy, palaeontology and palaeogeography of the Carboniferous of Southeast Asia. Mem. la Soc. Geol. Fr. 147, 107–118.
Metcalfe, I., 1990. Allochthonous terrane processes in Southeast Asia [and discussion]. Philos. Trans. R Soc. Lond. A Math. Phys. Eng. Sci. 331, 625–640.
Metcalfe, I., 1996. Pre-Cretaceous evolution of SE Asian terranes. Geol. Soc. Lond. Spec. Publ. 106, 97–122.
Metcalfe, I., 2000. The Bentong-Raub Suture Zone. J. Asian Earth Sci. 18, 691–712.
Metcalfe, I., 2011a. Palaeozoic-Mesozoic history of SE Asia. Geol. Soc. Lond. Spec. Publ. 355, 7–35.
Metcalfe, I., 2011b. Tectonic framework and Phanerozoic evolution of Sundaland. Gondw. Res. 19, 3–21.
Metcalfe, I., 2013a. Gondwana dispersion and Asian accretion: Tectonic and palaeogeographic evolution of eastern Tethys. J. Asian Earth Sci. 66, 1–33. https://doi.org/10.1016/j.jseaes.2012.12.020.
Metcalfe, I., 2013b. Tectonic evolution of the Malay Peninsula. J. Asian Earth Sci. 76, 195–213.
Metcalfe, I., 1985. Lower Permian conodonts from the Terbat formation, Sarawak. Newsl. Geol. Soc. Malaysia 11, 1–4.
Midtkandal, I., Svensen, H.H., Planke, S., Corfu, F., Polteau, S., Torsvik, T.H., Faleide, J. I., Grundvåg, S.-A., Selnes, H., Kürschner, W., 2016. The Aptian (Early Cretaceous) oceanic anoxic event (OAE1a) in Svalbard, Barents Sea, and the absolute age of the Barremian-Aptian boundary. Palaeogeogr. Palaeoclimatol. Palaeoecol. 463, 126–135.
Milsom, J., Ali, J., 1999. Structure and collision history of the Buton continental fragment, eastern Indonesia. Am. Assoc. Pet. Geol. Bull. 83, 1320–1336.
Milsom, J., Kaye, S., 1996. Extension, collision and curvature in the eastern Banda arc. Geol. Soc. Lond. Spec. Publ. 106, 85–94.
Milsom, J., Dipowirjo, S., Sain, B., Sipahutar, J., 1990. Gravity surveys in the north Sumatra forearc. Sci. Contrib. Oil Gas 13, 112–122.
Min, M., Ratschbacher, L., Franz, L., Hacker, B.R., Enkelmann, E., Toreno, E.Y., Härtel, B., Schurr, B., Tichomirowa, M., Pfänder, J.A., 2022. India (Tethyan Himalaya Series) in Central Myanmar: Implications for the Evolution of the Eastern Himalayan Syntaxis and the Sagaing Transform-Fault System. Geophys. Res. Lett. 49, e2022GL099140.
Mitchell, A.H.G., 1976. Southeast Asian tin granites: magmatism and mineralization in subduction and collision-related settings. CCOP Newsl. 3, 10–14.
Mitchell, A., 2017. Geological Belts, Plate Boundaries, and Mineral Deposits in Myanmar. Elsevier.
Mitchell, A., Chung, S.-L., Oo, T., Lin, T.-H., Hung, C.-H., 2012. Zircon U-Pb ages in Myanmar: Magmatic–metamorphic events and the closure of a neo-Tethys ocean?. J. Asian Earth Sci. 56, 1–23.
Mitchell, A.H.G., Htay, M.T., Htun, K.M., Win, M.N., Oo, T., Hlaing, T., 2007. Rock relationships in the Mogok metamorphic belt, Tatkon to Mandalay, central Myanmar. J. Asian Earth Sci. 29, 891–910.
Sardjono, Mirnanda, E., 2007. Gravity Field and Structure of the Crust Beneath the East Arm of Sulawesi and the Banggai Archipelago. Proc. Indones. Pet. Assoc. Annu. Conv. 31, IPA07-G-024
Mitchell, A.H.G., 1986. Mesozoic and Cenozoic regional tectonics and metallogenesis in Mainland SE Asia. Bull. Geol. Soc. Malaysia 20, 221–239.
Miyazaki, K., Zulkarnain, I., Sopaheluwakan, J., Wakita, K., 1996. Pressure–temperature conditions and retrograde paths of eclogites, garnet–glaucophane rocks and schists from South Sulawesi, Indonesia. J. Metamorph. Geol. 14, 549–563.
Miyazaki, K., Sopaheluwakan, J., Zulkarnain, I., Wakita, K., 1998. A jadeite–quartz–glaucophane rock from Karangsambung, central Java, Indonesia. Isl. Arc 7, 223–230.
Moeremans, R., Singh, S.C., Mukti, M., McArdle, J., Johansen, K., 2014. Seismic images of structural variations along the deformation front of the Andaman-Sumatra subduction zone: implications for rupture propagation and tsunamigenesis. Earth Planet. Sci. Lett. 386, 75–85.
Molengraaff, G.A.F., 1915. De geologie van het eiland Letti: Naar onderzoekingen te velde verricht door HA Brouwer en GAF Molengraaff beschreven door GAF Molengraaff. Met medewerking van F. Broili, HA Brouwer, BG Escher, CA Haniel, RJ Schubert. Martinus Nijhoff.
Molnar, P., Pardo-Casas, F., Stock, J., 1988. The Cenozoic and Late Cretaceous evolution of the Indian Ocean Basin: Uncertainties in the reconstructed positions of the Indian, African and Antarctic plates. Basin Res. 1, 23–40.
Monnier, C., Bellon, H., Girardeau, G., 1994. Data 40K–40Ar de l'ophiolite de lile de Sulawesi (Indonesie), CR. Acad. Sci. Paris 319(II), 349–356.
Monnier, C., Girardeau, J., Maury, R.C., Cotten, J., 1995. Back-arc basin origin for the East Sulawesi ophiolite (eastern Indonesia). Geology 23, 851–854.
Monnier, C., Polvé, M., Girardeau, J., Pubellier, M., Maury, R., Bellon, H., Permana, H., 1999. Extensional to compressive Mesozoic magmatism at the SE Eurasia margin as recorded from the Meratus ophiolite (SE Borneo, Indonesia). Geodin. Acta 12, 43–55.
Moore, G.F., Karig, D.E., 1980. Structural geology of Nias Island, Indonesia: Implications for subduction zone tectonics. Am. J. Sci. 280, 193–223.
Moore, G.F., Kadarisman, D., Evans, C.A., Hawkins, J.W., 1981. Geology of the Talaud islands, Molucca sea collision zone, northeast Indonesia. J. Struct. Geol. 3, 467–475.
Morishita, T., Soe, H.M., Htay, H., Lwin, T.H., Guotana, J.M., Tamura, A., Mizukami, T., Zaw, K., 2023. Origin and Evolution of Ultramafic Rocks along the Sagaing Fault, Myanmar. J. Earth Sci. 34, 122–132.
Morley, C.K., 2001. Combined escape tectonics and subduction rollback–back arc extension: a model for the evolution of Tertiary rift basins in Thailand, Malaysia and Laos. J. Geol. Soc. Lond. 158, 461–474.
Morley, C.K., 2007. Variations in late Cenozoic-Recent strike-slip and oblique-extensional geometries, within Indochina: the influence of pre-existing fabrics. J. Struct. Geol. 29, 36–58.
Morley, C.K., 2012. Late Cretaceous–early Palaeogene tectonic development of SE Asia. Earth-Sci. Rev. 115, 37–75.
Morley, C.K., 2016a. Cenozoic structural evolution of the Andaman Sea: evolution from an extensional to a sheared margin. Geol. Soc. Lond. Spec. Publ. 431, 39–61.
Morley, C.K., 2016b. Major unconformities/termination of extension events and associated surfaces in the South China Seas: Review and implications for tectonic development. J. Asian Earth Sci. 120, 62–86.
Morley, C.K., 2017a. Cenozoic rifting, passive margin development and strike-slip faulting in the Andaman Sea: a discussion of established v. new tectonic models. Geol. Soc. Lond., Mem. 47, 27–50.
Morley, C.K., 2017b. Syn-kinematic sedimentation at a releasing splay in the northern Minwun Ranges, Sagaing Fault zone, Myanmar: significance for fault timing and displacement. Basin Res. 29, 684–700.
Morley, C.K., Alvey, A., 2015. Is spreading prolonged, episodic or incipient in the Andaman Sea? Evidence from deepwater sedimentation. J. Asian Earth Sci. 98, 446–456.
Morley, C.K., Arboit, F., 2019. Dating the onset of motion on the Sagaing fault: Evidence from detrital zircon and titanite U-Pb geochronology from the North Minwun Basin, Myanmar. Geology 47, 581–585.
Morley, C.K., Back, S., Van Rensbergen, P., Crevello, P., Lambiase, J.J., 2003. Characteristics of repeated, detached, Miocene-Pliocene tectonic inversion events, in a large delta province on an active margin, Brunei Darussalam, Borneo. J. Struct. Geol. 25, 1147–1169.
Morley, C.K., Charusiri, P., Watkinson, I.M., 2011. In: Ridd, M.F., Barber, A.J., Crow, M.J. (Eds.), Structural geology of Thailand during the Cenozoic. The Geology of Thailand, Geol. Soc, London, pp. 273–334.
Morley, C.K., Naing, T.T., Searle, M., Robinson, S.A., 2020. Structural and tectonic development of the Indo-Burma ranges. Earth-Sci. Rev. 200, 102992.
Morley, C.K., Chantraprasert, S., Chenoll, K., Sootlek, P., Jitmahantakul, S., 2023a. Interaction of thin-skinned detached faults and basement-involved strike-slip faults on a transform margin: the Moattama Basin, Myanmar. Geol. Soc. London, Spec. Publ. 524. SP524-2021.
Morley, C.K., Promrak, W., Apuanram, W., Chaiyo, P., Chantraprasert, S., Ong, D., Suphawajruksakul, A., Thaemsiri, N., Tingay, M., 2023b. A major Miocene deepwater mud canopy system: The North Sabah-Pagasa Wedge, northwestern Borneo. Geosphere 19, 291–334.
Morrice, M.G., Jezek, P.A., Gill, J.B., Whitford, D.J., Monoarfa, M., 1983. An introduction to the Sangihe arc: Volcanism accompanying arc—arc collision in the Molucca Sea, Indonesia. J. Volcanol. Geotherm. Res. 19, 135–165.
Morris, J.D., Jezek, P.A., Hart, S.R., Hill, J.B., 1983. The Halmahera island arc, Molucca Sea collision zone, Indonesia: a geochemical survey. Washingt. DC Am. Geophys. Union Geophys. Monogr. Ser. 27, 373–387.
Mortimer, N., Campbell, H.J., Tulloch, A.J., King, P.R., Stagpoole, V.M., Wood, R.A., Rattenbury, M.S., Sutherland, R., Adams, C.J., Collot, J., 2017. Zealandia: Earth's hidden continent. GSA Today 27, 27–35.
Mortimer, N., van den Bogaard, P., Hoernle, K., Timm, C., Gans, P.B., Werner, R., Riefstahl, F., 2019. Late Cretaceous oceanic plate reorganization and the breakup of Zealandia and Gondwana. Gondw. Res. 65, 31–42.
Moss, S.J., 1998. Embaluh Group turbidites in Kalimantan: evolution of a remnant oceanic basin in Borneo during the Late Cretaceous to Palaeogene. J. Geol. Soc. Lond. 155, 509–524.
Moss, S.J., Chambers, J., Cloke, I., Satria, D., Ali, J.R., Baker, S., Milsom, J., Carter, A., 1997. New observations on the sedimentary and tectonic evolution of the Tertiary Kutai Basin, East Kalimantan. Geol. Soc. Lond. Spec. Publ. 126, 395–416.
Mubroto, B., Briden, J.C., McClelland, E., Hall, R., 1994. Palaeomagnetism of the Balantak ophiolite, Sulawesi. Earth Planet. Sci. Lett. 125, 193–209.
Mueller, C.O., Jokat, W., 2019. The initial Gondwana break-up: a synthesis based on new potential field data of the Africa-Antarctica Corridor. Tectonophysics 750, 301–328.
Müller, R.D., Roest, W.R., Royer, J., Gahagan, L.M., Sclater, J.G., 1997. Digital isochrons of the world's ocean floor. J. Geophys. Res. Solid Earth 102, 3211–3214.
Müller, R.D., Cannon, J., Qin, X., Watson, R.J., Gurnis, M., Williams, S., Pfaffelmoser, T., Seton, M., Russell, S.H.J., Zahirovic, S., 2018. GPlates: building a virtual Earth through deep time. Geochem. Geophys. Geosyst. 19, 2243–2261.
Müller, R.D., Zahirovic, S., Williams, S.E., Cannon, J., Seton, M., Bower, D.J., Tetley, M. G., Heine, C., Le Breton, E., Liu, S., 2019. A global plate model including lithospheric deformation along major rifts and orogens since the Triassic. Tectonics 38, 1884–1907.
Muller, C., 1991. 9. Biostratigraphy and geological evolution of the Sulu Sea and surrounding area. Proc.ODP, Sci. Results 124, 121–131.
Munasri, Putra, A.M., 2019. First evidence of Middle to Late Triassic radiolarians in the Garba mountains, South Sumatra, Indonesia. Isl. Arc 28, e12298.
Munasri, Sashida, K., 2018. Tethyan and non-Tethyan Early Cretaceous radiolarian faunas from West Timor, Indonesia: Paleogeographic and tectonic significance. Earth Evol. Sci. 3–12.
Munasri, M., Harsolumakso, A.H., 2020. Late Cretaceous Radiolarians from the Noni Formation, West Timor, Indonesia. Ber. Sedimentol. 45, 5–18.
Munasri, 2013. Early Cretaceous radiolarians in manganese carbonate nodule from the Barru Area, South Sulawesi, Indonesia. Ris. Geol. dan Pertamb. 23, 79–88.

Muraoka, H., Nasution, A., Urai, M., Takahashi, M., Takashima, I., Simanjuntak, J., Sundhoro, H., Aswin, D., Nanlohy, F., Sitorus, K., Takahashi, H., Koseki, T., 2002. Tectonic. volcanic and stratigraphic geology of the Bajawa geothermal field, central Flores, Indonesia. Bull. Geol. Surv. Japan 53, 109–138.
Murauchi, S., Ludwig, W.J., Den, N., Hotta, H., Asanuma, T., Yoshii, T., Kubotera, A., Hagiwara, K., 1973. Structure of the Sulu Sea and the Celebes Sea. J. Geophys. Res. 78, 3437–3447.
Naing, T.T., Robinson, S.A., Searle, M.P., Morley, C.K., Millar, I., Green, O.R., Bown, P. R., Danelian, T., Petrizzo, M.R., Henderson, G.M., 2023. Age, depositional history and tectonics of the Indo-Myanmar Ranges, Myanmar. J. Geol. Soc. Lond. 180, jgs2022–091.
Natawidjaja, D.H., Daryono, M.R., 2015. The Lawanopo Fault, Central Sulawesi, East Indonesia. In: AIP Conference Proceedings. AIP Publishing LLC, pp. 30001.
Neben, S., Hinz, K., Beiersdorf, H., 1998. Reflection characteristics, depth and geographical distribution of bottom simulating reflectors within the accretionary wedge of Sulawesi. Geol. Soc. Lond. Spec. Publ. 137, 255–265.
Nelson, G., Hughes, M., Przeslawski, R., Nichol, S., Lewis, B., Rawsthorn, K., 2009. Revealing the Wallaby Plateau: Recent survey delivers geophysical, geological and biophysical data. AusGeo News 94.
Nexer, M., Authemayou, C., Schildgen, T., Hantoro, W.S., Molliex, S., Delcaillau, B., Pedoja, K., Husson, L., Regard, V., 2015. Evaluation of morphometric proxies for uplift on sequences of coral reef terraces: a case study from Sumba Island (Indonesia). Geomorphology 241, 145–159.
Nichols, G.J., Hall, R., 1991. Basin formation and Neogene sedimentation in a backarc setting, Halmahera, eastern Indonesia. Mar. Pet. Geol. 8, 50–61.
Nichols, G., Hall, R., 1999. History of the Celebes Sea Basin based on its stratigraphic and sedimentological record. J. Asian Earth Sci. 17, 47–59.
Nishimura, S., Otofuji, Y., Ikeda, T., Abe, E., Yokoyama, T., Kobayashi, Y., Hadiwisatra, S., Sopohaluwakan, J., Hehuwat, F., Barber, A.J., 1981. Physical geology of the Sumba, Sumbawa and Flores islands. Geol. Tectonics East. Indones. Res. Dev. Cent. Bandung. Spec. Publ 2, 105–113.
Noble, R.A., Pratomo, K.H., Nugrahanto, K., Ibrahim, A.M.T., Prasetya, I., Mujahidin, N., Wu, C.H., Howes, J.V.C., 1997. Petroleum systems of northwest Java, Indonesia. Proc. Pet. Syst. SE Asia Australas. Conf., 585–600.
Norvick, M.S., Smith, M.A., Power, M.R., 2001. The plate tectonic evolution of eastern Australasia guided by the stratigraphy of the Gippsland Basin. In: Petroleum Expl. Soc. Australia, (PESA). Eastern Australian Basins Symposium, Melbourne, pp. 15–23.
Nugraha, A.M.S., Hall, R., 2012. Cenozoic History of the East Java Forearc. Proc. Indones. Pet. Assoc. Annu. Conv. 36, IPA12-G-028.
Nugraha, A.M.S., Hall, R., 2018. Late Cenozoic History of Sulawesi. Palaeogeog. Palaeoclim. Palaeoecol. 490, 191–209.
Nugraha, A.M.S., Hall, R., BouDagher-Fadel, M., 2022. The Celebes Molasse: A revised Neogene stratigraphy for Sulawesi, Indonesia. J. Asian Earth Sci. 105140.
Nugroho, H., Harris, R., Lestariya, A.W., Maruf, B., 2009. Plate boundary reorganization in the active Banda Arc–continent collision: Insights from new GPS measurements. Tectonophysics 479, 52–65.
Nyunt, T.T., Massonne, H.-J., Sun, T.T., 2017. Jadeitite and other high-pressure metamorphic rocks from the Jade Mines Belt, Tawmaw area, Kachin State, northern Myanmar. Geol. Soc. Lond., Mem. 48, 295–315.
O'Sullivan, T., Pegum, D., Tarigan, J., 1985. Seram oil search, past discoveries and future oil potential. Proc. Indones. Pet. Assoc. Annu. Conv. 14, 3–20.
Okamoto, S., Kojima, S., Suparka, S., Supriyanto, J., 1994. Campanian (upper Cretaceous) radiolarians from a shale clast in the Paleogene of central Java, Indonesia. J. Southeast Asian Earth Sci. 9, 45–50.
Omang, S.A.K.S., Mohamed, W.A.W., Tahir, S.H., Rahim, S.A., 1992. The Darvel Bay Ophiolite Complex, SE Sabah. Malaysia–Preliminary Interpretations. Newsl. Geol. Soc. Malaysia 18, 81–88.
Omang, S.A.K., Faisal, M.M., Tahir, S.H., 1994. The Kudat Ophiolite Complex, Northern Sabah, Malaysia—Field Description and Discussion. Newsl. Geol. Soc. Malaysia 20, 337–346.
Omang, S.A.K., 1995. Petrology and geochemistry of the mantle-sequence peridotite of the Darvel Bay ophiolite, Sabah, Malaysia. Bull. Geol. Soc. Malaysia 38, 31–48.
Oo, T., Hlaing, T., Htay, N., 2002. Permian of Myanmar. J. Asian Earth Sci. 20, 683–689.
Ota, T., Kaneko, Y., 2010. Blueschists, eclogites, and subduction zone tectonics: Insights from a review of Late Miocene blueschists and eclogites, and related young high-pressure metamorphic rocks. Gondw. Res. 18, 167–188.
Otofuji, Y., Moriyama, Y.T., Arita, M.P., Miyazaki, M., Tsumura, K., Yoshimura, Y., Shuib, M.K., Sone, M., Miki, M., Uno, K., 2017. Tectonic evolution of the Malay Peninsula inferred from Jurassic to Cretaceous paleomagnetic results. J. Asian Earth Sci. 134, 130–149.
Otofuji, Y.-I., Sasajima, S., Nishimura, S., Dharma, A., Hehuwat, F., 1981a. Paleomagnetic evidence for clockwise rotation of the northern arm of Sulawesi, Indonesia. Earth Planet. Sci. Lett. 54, 272–280.
Otofuji, Y.-I., Sasajima, S., Nishimura, S., Yokoyama, T., Hadiwisastra, S., Hehuwat, F., 1981b. Paleomagnetic evidence for the paleoposition of Sumba Island, Indonesia. Earth Planet. Sci. Lett. 52, 93–100.
Padrones, J.T., Tani, K., Tsutsumi, Y., Imai, A., 2017. Imprints of late Mesozoic tectono-magmatic events on Palawan Continental Block in northern Palawan, Philippines. J. Asian Earth Sci. 142, 56–76.
Pairault, A.A., Hall, R., Elders, C.F., 2003a. Tectonic evolution of the Seram trough, Indonesia.
Pairault, A.A., Hall, R., Elders, C.F., 2003b. Structural styles and tectonic evolution of the Seram Trough, Indonesia. Mar. Pet. Geol. 20, 1141–1160.
Pal, T., 2011. Petrology and geochemistry of the Andaman ophiolite: melt–rock interaction in a suprasubduction-zone setting. J. Geol. Soc. Lond. 168, 1031–1045.
Parkinson, C.D., 1996. The origin and significance of metamorphosed tectonic blocks in mélanges: evidence from Sulawesi, Indonesia. Terra Nov. 8, 312–323.
Parkinson, C., 1998a. An outline of the petrology, structure and age of the Pompangeo Schist Complex of central Sulawesi, Indonesia. Isl. Arc 7, 231–245.
Parkinson, C., 1998b. Emplacement of the East Sulawesi Ophiolite: evidence from subophiolite metamorphic rocks. J. Asian Earth Sci. 16, 13–28.
Parkinson, C.D., Miyazaki, K., Wakita, K., Barber, A.J., Carswell, D.A., 1998. An overview and tectonic synthesis of the pre-Tertiary very-high-pressure metamorphic and associated rocks of Java, Sulawesi and Kalimantan, Indonesia. Isl. Arc 7, 184–200.
Patonah, A., Permana, H., 2010. Petrologi amfibolit komplek melange Ciletuh, Sukabumi, Jawa Barat. Bull. Sci. Contrib. Geol. 8, 69–77.
Patria, A., Hall, R., 2017. The origin and significance of the Seram trough, Indonesia. Proc. Indones. Pet. Assoc. Annu. Conv. 41, IPA17-19-G.
Pedersen, R.B., Searle, M.P., Carter, A., Bandopadhyay, P.C., 2010. U-Pb zircon age of the Andaman ophiolite: implications for the beginning of subduction beneath the Andaman-Sumatra arc. J. Geol. Soc. Lond. 167, 1105–1112.
Pedoja, K., Husson, L., Bezos, A., Pastier, A.-M., Imran, A.M., Arias-Ruiz, C., Sarr, A.-C., Elliot, M., Pons-Branchu, E., Nexer, M., 2018. On the long-lasting sequences of coral reef terraces from SE Sulawesi (Indonesia): Distribution, formation, and global significance. Quat. Sci. Rev. 188, 37–57.
Peltzer, G., Tapponnier, P., 1988. Formation and evolution of strike-slip faults, rifts, and basins during the India-Asia collision: An experimental approach. J. Geophys. Res. Solid Earth 93, 15085–15117.
Pena-Castellnou, S., Indah Marliyani, G., Reicherter, K., 2019. Preliminary Tectonic Geomorphology of the Opak Fault System, Java (Indonesia). EGUGA 12307.
Peterson, C., Duncan, R., Scheidegger, K.F., 1986. Sequence and longevity of basalt alteration at Deep-Sea Drilling Project Site-597. DSDP Init. Rep. 92, 505–515.
Pezzati, G., Hall, R., Burgess, P., Perez-Gussinye, M., 2014. The Poso Basin in Gorontalo Bay, Sulawesi: extension related to core complex formation on land. Proc. Indones. Pet. Assoc. Annu. Conv. 38, IPA14-G-297.
Phillips, T.L., Noble, R.A., Sinartio, F.F., 1991. Origin of hydrocarbons, Kangean Block northern platform, offshore NE Java Sea. Proc. Indones. Pet. Assoc. Annu. Conv. 20, 637–662.
Pholbud, P., Hall, R., Advokaat, E., Burgess, P., Rudyawan, A., 2012. A new interpretation of Gorontalo Bay, Sulawesi. Proc. Indones. Pet. Assoc. Annu. Conv. 36, IPA12-G-029.
Pieters, P.E., Pigram, C.J., Trail, D.S., Dow, D.B., Ratman, N., Sukamto, R., 1983. The stratigraphy of western Irian Jaya. Proc. Indones. Pet. Assoc. Annu. Conv. 12, 229–261.
Pigram, C.J., Challinor, A.B., Hasibuan, F., Rusmana, E., Hartono, U., 1982. Lithostratigraphy of the Misool Archipelago. Irian Jaya, Indonesia. Geol. Mijnb. 61, 265–279.
Pigram, C.J., Supandjono, S.J.B., 1985. Origin of the Sula platform, eastern Indonesia. Geology 13, 246–248.
Pirazzoli, P.A., Radtke, U., Hantoro, W.S., Jouannic, C., Hoang, C.T., Causse, C., Best, M. B., 1993. A one million-year-long sequence of marine terraces on Sumba Island, Indonesia. Mar. Geol. 109, 221–236.
Pivnik, D.A., Nahm, J., Tucker, R.S., Smith, G.O., Nyein, K., Nyunt, M., Maung, P.H., 1998. Polyphase deformation in a fore-arc/back-arc basin, Salin subbasin, Myanmar (Burma). Am. Assoc. Pet. Geol. Bull. 82, 1837–1856.
Planke, S., Symonds, P.A., Berndt, C., 2002. Volcanic rifted margin structure and development: A comparison between the NE Atlantic and western Australian continental margins. In: AAPG Hedberg Conference, Stavanger, Norway, pp. 8–11.
Plunder, A., Bandyopadhyay, D., Ganerød, M., Advokaat, E.L., Ghosh, B., Bandopadhyay, P., van Hinsbergen, D.J.J., 2020. History of subduction polarity reversal during arc-continent collision: Constraints from the Andaman ophiolite and its metamorphic sole. Tectonics 39, e2019TC005762.
Polachan, S., Racey, A., 1994. Stratigraphy of the Mergui Basin, Andaman Sea: implications for petroleum exploration. J. Pet. Geol 17, 373–406.
Polvé, M., Maury, R.C., Bellon, H., Rangin, C., Priadi, B., Yuwono, S., Joron, J.L., Atmadja, R.S., 1997. Magmatic evolution of Sulawesi (Indonesia): constraints on the Cenozoic geodynamic history of the Sundaland active margin. Tectonophysics 272, 69–92.
Polvé, M., Maury, R.C., Vidal, P., Priadi, B., Bellon, H., Soeria-Atmadja, R., Joron, J.-L., Cotten, J., 2001. Melting of lower continental crust in a young post-collision setting; a geochemical study of Plio-Quaternary acidic magmatism from central Sulawesi (Indonesia). Bull. la Société Géologique Fr. 172, 333–342.
Pownall, J.M., 2015. UHT metamorphism on Seram, eastern Indonesia: reaction microstructures and P-T evolution of spinel-bearing garnet–sillimanite granulites from the Kobipoto Complex. J. Metam. Geol. 33, 909–935.
Pownall, J., Hall, R., Watkinson, I.M., 2013. Extreme extension across Seram and Ambon, eastern Indonesia: evidence for Banda slab rollback.Solid. Earth 4, 277–314.
Pownall, J.M., Hall, R., Armstrong, R.A., Forster, M.A., 2014. Earth's youngest known ultrahigh-temperature granulites discovered on Seram, eastern Indonesia. Geology 42, 279–282.
Pownall, J.M., Hall, R., Lister, G.S., 2016. Rolling open Earth's deepest forearc basin. Geology 44, 947–950.

Pownall, J.M., Forster, M.A., Hall, R., Watkinson, I.M., 2017a. Tectonometamorphic evolution of Seram and Ambon, eastern Indonesia: Insights from 40Ar/39Ar geochronology. Gondw. Res. 44, 35–53.
Pownall, J.M., Hall, R., Armstrong, R.A., 2017b. Hot lherzolite exhumation, UHT migmatite formation, and acid volcanism driven by Miocene rollback of the Banda Arc, eastern Indonesia. Gondw. Res. 51, 92–117.
Pownall, J.M., Hall, R., Forster, M., & Lister, G., 2018. Insights from easternmost Tethys: Slab rollback, mantle exhumation, and UHT metamorphism in Eastern Indonesia. 2018EGUGA..20.4916P.
Pownall, J.M., Armstrong, R.A., Williams, I.S., Thirlwall, M.F., Manning, C.J., Hall, R., 2019. Miocene UHT granulites from Seram, eastern Indonesia: a geochronological–REE study of zircon, monazite and garnet. Geol. Soc. Lond. Spec. Publ. 478, 167–196.
Prasetyadi, C.T., Harris, R.A., 1996. Hinterland structure of the active Banda arc-continent collision, Indonesia: constraints from the Aileu complex of East Timor. Proc. 25th Conv. Indones. Assoc. Geol., pp. 144–173.
Prasetyadi, C., 2007. Evolusi tektonik Paleogen Jawa bagian timur. Desertasi, Progr. Dr. Tek. Geol. Inst. Teknol. Bandung.
Prasetyo, H., 1992. The Bali-Flores basin: geological transition from extensional to subsequent compressional deformation. Proc. Indones. Pet. Assoc. Annu. Conv. 21, 455–478.
Priadi, B., Polvé, M., Maury, R.C., Bellon, H., Soeria-Atmadja, R., Joron, J.L., Cotten, J., 1994. Tertiary and Quaternary magmatism in Central Sulawesi: chronological and petrological constraints. J. SE Asian Earth Sci. 9, 81–93.
Priadi, B., 1993. Geodynamic implications of Neogene potassic calc-alkaline magmatism in Central Sulawesi: geochemical and isotopic constraints. In: Proceedings of the 22nd Annual Convention of the Indonesian Association of Geologists, 1993, pp. 59–81.
Priem, H., Boelrijk, N., Bon, E., Hebeda, E., Verdurmen, E., Verschure, R., 1975. Isotope geochronology in the Indonesian tin belt. Geol. Mijnb 54, 61–70.
Priyomarsono, S., 1985. Contribution a l'etude geologique du Sud-est de Borneo, Indonesia: geologie structurale de la partie meridionale de la chaine des Meratus. Université de Savoie.
Pubellier, M., Morley, C.K., 2014. The basins of Sundaland (SE Asia): Evolution and boundary conditions. Mar. Pet. Geol. 58, 555–578.
Pubellier, M., Quebral, R., Rangin, C., Deffontaines, B., Muller, C., Butterlin, J., Manzano, J., 1991. The Mindanao collision zone: a soft collision event within a continuous Neogene strike-slip setting. J. SE Asian Earth Sci. 6, 239–248.
Pubellier, M., Rangin, C., Cadet, J.P., Tjashuri, I., 1992. L'île de Nias, un édifice polyphasé sur la bordure interne de la fosse de la Sonde (Archipel des Mentawai Indonésie). Comptes Rendus l'Academie des Sci. Paris 315, 1019–1026.
Pubellier, M., Quebral, R., Rangin, C., 1996. Docking and post-docking escape tectonics in the southern Philippines. Geol. Soc. Lond. Spec. Publ. 106, 511–523.
Pubellier, M., Girardeau, J., Tjashuri, I., 1999. Accretion history of Borneo inferred from the polyphase structural features in the Meratus Mountains. Gondwana Dispers. Asian Accretion—Final Results IGCP 321, 141–160.
Pulunggono, A., Cameron, N.R., 1984. Sumatran microplates, their characteristics and their role in the evolution of the Central and South Sumatra Basins. Proc. Indones. Pet. Assoc. Annu. Conv. 13, 121–143.
Qayyum, A., Lom, N., Advokaat, E.L., Spakman, W., van der Meer, D.G., van Hinsbergen, D.J.J., 2022. Subduction and slab detachment under moving trenches during ongoing India-Asia convergence. Geochem. Geophys. Geosyst. 23, e2022GC010336.
Qi, M., Xiang, H., Zhong, Z.-Q., Qiu, H.-N., Wang, H., Sun, X.-L., Xu, B., 2013. 40Ar/39Ar geochronology constraints on the formation age of Myanmar jadeitite. Lithos 162, 107–114.
Qian, X., Yu, Y., Wang, Y., Gan, C., Zhang, Y., Asis, J.B., 2022. Late Cretaceous Nature of SW Borneo and Paleo-Pacific Subduction: New Insights from the Granitoids in the Schwaner Mountains. Lithosphere 2022, 8483732.
Qiu, Z., Wu, F., Yang, S., Zhu, M., Sun, J., Yang, P., 2009. Age and genesis of the Myanmar jadeite: constraints from U-Pb ages and Hf isotopes of zircon inclusions. Chin. Sci. Bull. 54, 658–668.
Quebral, R.D., Pubellier, M., Rangin, C., 1996. The onset of movement on the Philippine Fault in eastern Mindanao: A transition from a collision to a strike-slip environment. Tectonics 15, 713–726.
Quek, L.X., Li, S., Morley, C.K., Ghani, A.A., Zhu, J., Roselee, M.H., Murthadha, S., Rahmat, R., Lai, Y.-M., Lintjewas, L., 2023. Southwest Borneo, an autochthonous Pangea-Eurasia assembly proxy: Insights from detrital zircon record. Geology 51, 785–790.
Rahim, A.R., Konjing, Z., Asis, J., Jalil, N.A., Muhamad, A.J., Ibrahim, N., Koraini, A.M., Kob, R.C., Mazlan, H., Tjia, H.D., 2017. Tectonostratigraphic terranes of Kudat Peninsula. Sabah. Bull. Geol. Soc. Malaysia 64, 123–139.
Rajkakati, M., Bhowmik, S.K., Ao, A., Ireland, T.R., Avila, J., Clarke, G.L., Bhandari, A., Aitchison, J.C., 2019. Thermal history of Early Jurassic eclogite facies metamorphism in the Nagaland Ophiolite Complex, NE India: New insights into pre-Cretaceous subduction channel tectonics within the Neo-Tethys. Lithos 346, 105166.
Raju, K.A.K., Ramprasad, T., Rao, P.S., Rao, B.R., Varghese, J., 2004. New insights into the tectonic evolution of the Andaman basin, northeast Indian Ocean. Earth Planet. Sci. Lett. 221, 145–162.
Rangin, C., 1991. The Philippine Mobile Belt: a complex plate boundary. J. SE Asian Earth Sci. 6, 209–220.
Rangin, C., Silver, E.A., 1991. Neogene tectonic evolution of the Celebes-Sulu basins: new insights from Leg 124 drilling. Proc. ODP Sci. Results 124, 51–63.
Rangin, C., Stephan, J.F., Muller, C., 1985. Middle Oligocene oceanic crust of South China Sea jammed into Mindoro collision zone (Philippines). Geology 13, 425–428.
Rangin, C., Bellon, H., Benard, F., Letouzey, J., Muller, C., Sanudin, T., 1990a. Neogene arc-continent collision in Sabah, northern Borneo (Malaysia). Tectonophysics 183, 305–319.
Rangin, C., Jolivet, L., Pubellier, M., 1990b. A simple model for the tectonic evolution of Southeast Asia and Indonesia region for the past 43 m.y. Bull. la Société Géologique Fr. VI, 889–905. https://doi.org/10.2113/gssgfbull.vi.6.889.
Rangin, C., Dahrin, D., Quebral, R., 1996. Collision and strike-slip faulting in the northern Molucca Sea (Philippines and Indonesia): preliminary results of a morphotectonic study. Geol. Soc. Lond. Spec. Publ. 106, 29–46.
Rangin, C., Spakman, W., Pubellier, M., Bijwaard, H., 1999. Tomographic and geological constraints on subduction along the eastern Sundaland continental margin (South-East Asia). Bull. la Société géologique Fr. 170, 775–788.
Rangin, C., Stephan, Je.-F., Butterlin, Jj., Bellon, H., Muller, C., Chorowicz, J., Baladad, D., 1991. Collision néogène d'arcs volcaniques dans le centre des Philippines: stratigraphie et structure de la chaîne d'Antique (île de Panay). Bull. la Société géologique Fr. 162, 465–477.
Ray, J.S., Pande, K., Bhutani, R., 2015. 40 Ar/39 Ar geochronology of subaerial lava flows of Barren Island volcano and the deep crust beneath the Andaman Island Arc, Burma Microplate. Bull. Volcanol. 77, 57.
Reed, D.L., 1985. Structure and Stratigraphy of the Eastern Sunda Forearc, Indonesia: Geologic Consequences of Arc-continent Collision. University of California, San Diego.
Réhault, J.-P., Maury, R.C., Bellon, H., Sarmili, L., Burhanuddin, S., 1994. La Mer de Banda Nord (Indonésie): un bassin arrière-arc du Miocène supérieur. Comptes rendus l'Académie des Sci. Série 2 Sci. la terre des planètes 318, 969–976.
Ren, J., Niu, B., Wang, J., Jin, X., Zhao, L., Liu, R., 2013. Advances in research of Asian geology—A summary of 1: 5M International Geological Map of Asia project. J. Asian Earth Sci. 72, 3–11.
Replumaz, A., Tapponnier, P., 2003. Reconstruction of the deformed collision zone between India and Asia by backward motion of lithospheric blocks. J. Geophys. Res. Solid Earth 108.
Replumaz, A., Lacassin, R., Tapponnier, P., Leloup, P.H., 2001. Large river offsets and Plio-Quaternary dextral slip rate on the Red River fault (Yunnan, China). J. Geophys. Res. Solid Earth 106, 819–836.
Replumaz, A., Negredo, A.M., Villasenor, A., Guillot, S., 2010. Indian continental subduction and slab break-off during Tertiary collision. Terra Nov. 22, 290–296.
Riadini, P., Adyagharini, A.C., Nugraha, A.M.S., Sapiie, B., Teas, P.A., 2009. Palinspatic reconstruction of the Bird Head Pop-Up structure as a new mechanism of the Sorong fault. Proc. Indones. Pet. Assoc. Annu. Conv. 33, IPA09-SG-067.
Richter, B., Fuller, M., Schmidtke, E., Myint, U.T., Win, U.M., Bunopas, S., 1993. Paleomagnetic results from Thailand and Myanmar: implications for the interpretation of tectonic rotations in Southeast Asia. J. SE Asian Earth Sci. 8, 247–255.
Richter, B., Schmidtke, E., Fuller, M., Harbury, N., Samsudin, A.R., 1999. Paleomagnetism of peninsular Malaysia. J. Asian Earth Sci. 17, 477–519.
Rigg, J.W.D., Hall, R., 2011. Structural and stratigraphic evolution of the Savu Basin, Indonesia. Geol. Soc. Lond. Spec. Publ. 355, 225–240.
Rigg, J.W.D., Hall, R., 2012. Neogene development of the Savu forearc basin, Indonesia. Mar. Pet. Geol. 32, 76–94.
Robb, M.S., Taylor, B., Goodliffe, A.M., 2005. Re-examination of the magnetic lineations of the Gascoyne and Cuvier Abyssal Plains, off NW Australia. Geophys. J. Int. 163, 42–55.
Rock, N.M.S., Aldiss, D.T., Aspden, J.A., Clarke, M.C.G., Djunuddin, A., Miswar, W.K., Thompson, S.J., Whandoyo, R., 1983. The Geology of the Lubuksikaping Quadrangle, Sumatra. Geol. Res. Dev. Cent., Bandung, Indones.
Rodolfo, K.S., 1969. Bathymetry and marine geology of the Andaman Basin, and tectonic implications for Southeast Asia. Geol. Soc. Am. Bull. 80, 1203–1230.
Roeser, H.A., 1991. Age of the crust of the southeast Sulu Sea basin based on magnetic anomalies and age determined at site 768. Proc. OPD, Sci. Results 124, 339–343.
Roosmawati, N., Harris, R., 2009. Surface uplift history of the incipient Banda arc-continent collision: Geology and synorogenic foraminifera of Rote and Savu Islands, Indonesia. Tectonophysics 479, 95–110.
Rose, R., Hartono, P., 1978. Geological Evolution of the Tertiary Kutei-Melawi Basin, Kalimantan Indonesia. Proc. Indones. Pet. Assoc. Annu. Conv. 7, 225–252.
Rosidi, H.M.O., Suwitopiroyo, K., Tjokrosapoetro, S., 1979. Geological map Kupang-Atambua Quadrangle, Timor 1: 250.000. Geol. Res. Dev. Centre, Bandung, Indones.
Rowley, D.B., 2019a. Comparing Paleomagnetic Study Means With Apparent Wander Paths: A Case Study and Paleomagnetic Test of the Greater India Versus Greater Indian Basin Hypotheses. Tectonics 38, 722–740.
Rowley, D.B., 2019b. Reply to Comment on 'Comparing Paleomagnetic Study Means with Apparent Wander Paths: A Case Study and Paleomagnetic Test of the Greater India versus Greater Indian Basin Hypotheses'. Tectonics.
Rowley, D., Ingalls, M., 2017. Reply to 'Unfeasible subduction?'. Nat. Geosci. 10, 879.
Roy, S.K., 1992. Accretionary prism in Andaman forearc. Geol. Surv. India Spec. Publ. 29, 273–278.
Roy, T.K., Chopra, N.N., 1987. Wrench faulting in Andaman forearc basin, India. In: Offshore Technology Conference. Offshore Technology Conference.
Royer, J., Chang, T., 1991. Evidence for relative motions between the Indian and Australian plates during the last 20 my from plate tectonic reconstructions: Implications for the deformation of the Indo-Australian plate. J. Geophys. Res. Solid Earth 96, 11779–11802.

Rudyawan, A., Hall, R., 2012. Structural reassessment of the south Banggai-Sula area: no Sorong fault zone. Proc. Indones. Pet. Assoc. Annu. Conv. 36, IPA12-G-030.
Rudyawan, A., Hall, R., White, L., 2014. Neogene extension of the central north Arm of Sulawesi, Indonesia. In: AGU Fall Meeting December, T43A-4681.
Rutten, M.G., 1940. On Devonian limestones with Clathrodictyon cf. spatiosum and Heliolites porosus from eastern Borneo. Proc. K. Ned. Akad. van Wet. Amsterdam 43, 1061–1064.
Sager, W.W., Fullerton, L.G., Buffler, R.T., Handschumacher, D.W., 1992. 36. Argo abyssal plain magnetic lineations revisited: implications for the onset of seafloor spreading and tectonic evolution of the Eastern Indian Ocean. Proc. ODP Sci. Results 123, 659-669.
Sajona, F.G., Bellon, H., Maury, R.C., Pubellier, M., Quebral, R.D., Cotten, J., Bayon, F.E., Pagado, E., Pamatian, P., 1997. Tertiary and quaternary magmatism in Mindanao andLeyte (Philippines): geochronology, geochemistry and tectonic setting. J. Asian Earth Sci. 15, 121–153.
Sajona, F.G., Maury, R.C., Prouteau, G., Cotten, J., Schiano, P., Bellon, H., Fontaine, L., 2000. Slab melt as metasomatic agent in island arc magma mantle sources, Negros and Batan (Philippines). Isl. Arc 9, 472–486.
Sales, A.O., Jacobsen, E.C., Morado Jr, A.A., Benavidez, J.J., Navarro, F.A., Lim, A.E., 1997. The petroleum potential of deep-water northwestPalawan Block GSEC 66. J. Asian Earth Sci. 15, 217–240.
Salmanfarsi, A.F., Shuib, M.K., Fatt, N.T., Zulkifley, M.T.M., 2018. Kinematics and timing of brittle-ductile shearing of Mylonites along the Bok Bak fault, Peninsular Malaysia. Curr. Sci. 114.
Samuel, L., Muchsin, S., 1975. Stratigraphy and sedimentation in the Kutai Basin, Kalimantan. Proc. Indones. Pet. Assoc. Annu. Conv. 4, 27–39.
Samuel, M.A., Harbury, N.A., Jones, M.E., Matthews, S.J., 1995. Inversion-controlled uplift of an outer-arc ridge: Nias Island, offshore Sumatra. Geol. Soc. Lond. Spec. Publ. 88, 473–492.
Samuel, M.A., Harbury, N.A., Bakri, A., Banner, F.T., Hartono, L., 1997. A new stratigraphy for the islands of the Sumatran Forearc, Indonesia. J. Asian Earth Sci. 15, 339–380.
Sandmann, S., Nagel, T.J., Froitzheim, N., Ustaszewski, K., Münker, C., 2015. Late Miocene to Early Pliocene blueschist from Taiwan and its exhumation via forearc extraction. Terra Nov. 27, 285–291.
Sapin, F., Pubellier, M., Lahfid, A., Janots, D., Aubourg, C., Ringenbach, J., 2011. Onshore record of the subduction of a crustal salient: example of the NW Borneo Wedge. Terra Nov. 23, 232–240.
Saputra, A., Hall, R., White, L.T., 2014. Development of the Sorong Fault Zone North of Misool, Eastern Indonesia. Proc. Indones. Pet. Assoc. Annu. Conv. 38, IPA14-G-086.
Sarewitz, D.R., Karig, D.E., 1986. Processes of allochthonous terrane evolution, Mindoro Island, Philippines. Tectonics 5, 525–552.
Sarma, D.S., Jafri, S.H., Fletcher, I.R., McNaughton, N.J., 2010. Constraints on the tectonic setting of the Andaman ophiolites, Bay of Bengal, India, from SHRIMP U-Pb zircon geochronology of plagiogranite. J. Geol. 118, 691–697.
Sasajima, S., Otofuji, Y., Hirooka, K., Suparka, S., Hehuwat, F., 1978. Palaeomagnetic studies on Sumatra Island and the possibility of Sumatra being part of Gondwanaland. Rock Magn. Paleogeophysics 5, 104–110.
Sasajima, S., Nishimura, S., Hirooka, K., Otofuji, Y., Van Leeuwen, T., Hehuwat, F., 1980. Paleomagnetic studies combined with fission-track datings on the western arc of Sulawesi, East Indonesia. Tectonophysics 64, 163–172.
Satyana, A.H., Prasetyo, A., Rosana, M.F., 2021. Ciletuh subduction, Southwest Java–new findings: nature, age, and regional implications. Proc. Indones. Pet. Assoc. Annu. Conv. 45, IPA21-G-29.
Satyana, A.H., 2015. Rifting history of the Makassar Straits: new constraints from wells penetrating the Basement and oils discovered in Eocene section-implications for further exploration of West Sulawesi Offshore. Proc. Indones. Pet. Assoc. Annu. Conv. 39, IPA15-G-104.
Sautter, B., Pubellier, M., Schlögl, S.K., Matenco, L., Andriessen, P., Mathew, M., 2019. Exhumation of west Sundaland: A record of the path of India?. Earth-Sci. Rev. 198, 102933.
Savva, D., Meresse, F., Pubellier, M., Chamot-Rooke, N., Lavier, L., Po, K.W., Franke, D., Steuer, S., Sapin, F., Auxietre, J.L., 2013. Seismic evidence of hyper-stretched crust and mantle exhumation offshore Vietnam. Tectonophysics 608, 72–83.
Savva, D., Pubellier, M., Franke, D., Chamot-Rooke, N., Meresse, F., Steuer, S., Auxietre, J.L., 2014. Different expressions of rifting on the South China Sea margins. Mar. Pet. Geol. 58, 579–598.
Sawyer, R.K., Sani, K., Brown, S., 1993. The stratigraphy and sedimentology of West Timor, Indonesia. Proc. Indones. Pet. Assoc. Annu. Conv. 22, 533–574.
Schairer, G., Zeiss, A., 1992. First record of Callovian ammonites from West Kalimantan (Middle Jurassic, Kalimantan Barat, Borneo, Indonesia). BMR J. Aust. Geol. Geophys. 13, 229–236.
Scherer, R.P., 1991a. Radiolarians of the Celebes sea, leg 124, sites 767 and 7701. ilver, EA, Rangin, C., von Breymann, MT, al., Proc. ODP. Sci. Results 124, 345–357.
Scherer, R.P., 1991b. 26. Miocene radiolarians of the Sulu Sea, Leg 124. Proc. ODP. Sci. Results 124, 359–368.
Schiller, D.M., Garrard, R.A., Prasetyo, L., 1991. Eocene submarine fan sedimentation in southwest Java. Proc. Indones. Pet. Assoc. Annu. Conv. 20, 125–181.
Schlüter, H.U., Block, M., Hinz, K., Neben, S., Seidel, D., Djajadihardja, Y., 2001. Neogene sediment thickness and Miocene basin-floor fan systems of the Celebes Sea. Mar. Pet. Geol. 18, 849–861.
Schlüter, H.U., Hinz, K., Block, M., 1996. Tectono-stratigraphic terranes and detachment faulting of the South China Sea and Sulu Sea. Mar. Geol. 130, 39–78.
Schmid, S.M., Bernoulli, D., Fügenschuh, B., Matenco, L., Schefer, S., Schuster, R., Tischler, M., Ustaszewski, K., 2008. The Alpine-Carpathian-Dinaridic orogenic system: correlation and evolution of tectonic units. Swiss J. Geosci. 101, 139–183.
Schmid, S.M., Fügenschuh, B., Kounov, A., Maţenco, L., Nievergelt, P., Oberhänsli, R., Pleuger, J., Schefer, S., Schuster, R., Tomljenović, B., 2020. Tectonic units of the Alpine collision zone between Eastern Alps and western Turkey. Gondw. Res. 78, 308–374.
Schmidtke, E.A., Fuller, M.D., Haston, R.B., 1990. Paleomagnetic data from Sarawak, Malaysian Borneo, and the late Mesozoic and Cenozoic tectonics of Sundaland. Tectonics 9, 123–140.
Schoenbohm, L.M., Burchfiel, B.C., Liangzhong, C., Jiyun, Y., 2006. Miocene to present activity along the Red River fault, China, in the context of continental extrusion, upper-crustal rotation, and lower-crustal flow. Geol. Soc. Am. Bull. 118, 672–688.
Scholl, D.W., von Huene, R., 2009. Implications of estimated magmatic additions and recycling losses at the subduction zones of accretionary (non-collisional) and collisional (suturing) orogens. Geol. Soc. Lond. Spec. Publ. 318, 105–125.
Scotney, P.M., Roberts, S., Herrington, R.J., Boyce, A.J., Burgess, R., 2005. The development of volcanic hosted massive sulfide and barite–gold orebodies on Wetar Island, Indonesia. Miner. Depos. 40, 76–99.
Searle, M.P., Noble, S.R., Cottle, J.M., Waters, D.J., Mitchell, A.H.G., Hlaing, T., Horstwood, M.S.A., 2007. Tectonic evolution of the Mogok metamorphic belt, Burma (Myanmar) constrained by U-Th-Pb dating of metamorphic and magmatic rocks. Tectonics 26.
Searle, M.P., Yeh, M.-W., Lin, T.-H., Chung, S.-L., 2010. Structural constraints on the timing of left-lateral shear along the Red River shear zone in the Ailao Shan and Diancang Shan Ranges, Yunnan, SW China. Geosphere 6, 316–338.
Searle, M.P., Morley, C.K., Waters, D.J., Gardiner, N.J., Htun, U.K., Nu, T.T., Robb, L.J., 2017. Tectonic and metamorphic evolution of the Mogok Metamorphic and Jade Mines belts and ophiolitic terranes of Burma (Myanmar). Geol. Soc. Lond., Mem. 48, 261–293.
Searle, M.P., Garber, J.M., Hacker, B.R., Htun, K., Gardiner, N.J., Waters, D.J., Robb, L.J., 2020. Timing of Syenite-Charnockite Magmatism and Ruby and Sapphire Metamorphism in the Mogok Valley Region, Myanmar. Tectonics 39, e2019TC005998.
Şengör, A.M.C., Altıner, D., Cin, A., Ustaömer, T., Hsü, K.J., 1988. Origin and assembly of the Tethyside orogenic collage at the expense of Gondwana Land. Geol. Soc. Lond. Spec. Publ. 37, 119–181.
Setiawan, N.I., Osanai, Y., Prasetyadi, C., 2013c. A preliminary view and importance of metamorphic geology from Jiwo Hills in Central Java. In: Prosiding Seminar Nasional Kebumian Ke-6, Teknik Geologi Universitas Gadjah Mada, pp. 12–24.
Setiawan, N.I., Osanai, Y., Nakano, N., Adachi, T., 2014. Metamorphic evolution of garnet-biotite-muscovite schist from Barru Complex in South Sulawesi, Indonesia. J. Appl. Geol. 6.
Setiawan, N.I., Osanai, Y., Nakano, N., Adachi, T., Asy'ari, A., 2015. Metamorphic evolution of garnet-bearing epidote-barroisite schist from the Meratus complex in South Kalimantan, Indonesia. Indones. J. Geosci. 2, 139–156.
Setiawan, N.I., Osanai, Y., Nakano, N., Adachi, T., 2013a. Jadeite Jade from South Sulawesi in Indonesia and its Geological Significance. In: Proceedings of International Conference on Geological Engineering, Geological Engineering Department, Engineering Faculty, pp. 40–56.
Setiawan, N.I., Osanai, Y., Nakano, N., Adachi, T., Setiadji, L.D., Wahyudiono, J., 2013b. Late Triassic metatonalite from the Schwaner Mountains in West Kalimantan and its contribution to sedimentary provenance in the Sundaland. Ber. Sedimentol. 12, 4–12.
Setiawan, N.I., Osanai, Y., Nakano, N., Adachi, T., Yonemura, K., Yoshimoto, A., 2016. Prograde and retrograde evolution of eclogites from the Bantimala Complex in South Sulawesi, Indonesia. J. Mineral. Petrol. Sci. 111, 211–225.
Setiawan, N.I., Osanai, Y., Nakano, N., Adachi, T., Hendratno, A., Sasongko, W., Ansori, C., 2020. Peak Metamorphic Conditions of Garnet Amphibolite from Luk Ulo Complex, Central Java, Indonesia: Implications for Medium-Pressure/High-Temperature Metamorphism in the Central Indonesian Accretionary Collision Complex. Indones. J. Geosci. 7, 225–239.
Sevastjanova, I., Clements, B., Hall, R., Belousova, E.A., Griffin, W.L., Pearson, N., 2011. Granitic magmatism, basement ages, and provenance indicators in the Malay Peninsula: insights from detrital zircon U-Pb and Hf-isotope data. Gondw. Res. 19, 1024–1039.
Sevastjanova, I., Hall, R., Rittner, M., Paw, S.M.T.L., Naing, T.T., Alderton, D.H., Comfort, G., 2016. Myanmar and Asia united, Australia left behind long ago. Gondw. Res. 32, 24–40.
Shao, L., Cao, L., Ojao, P., Zhang, X., Li, Q., van Hinsbergen, D.J.J., 2017. Cretaceous–Eocene provenance connections between the Palawan Continental Terrane and the northern South China Sea margin. Earth Planet. Sci. Lett. 477, 97–107.
Shi, G., Cui, W., Cao, S., Jiang, N., Jian, P., Liu, D., Miao, L., Chu, B., 2008. Ion microprobe zircon U-Pb age and geochemistry of the Myanmar jadeitite. J. Geol. Soc. Lond. 165, 221–234.
Shibuya, H., Merrill, D.L., Hsu, V., 1991. Leg 124 Shipboard Scientific Party, 1991. Paleogene counterclockwise rotation of the Celebes Sea—orientation of ODP cores utilizing the secondary magnetization. Silver, EA, Rangin, C., von Breymann, MT, al., Proc. ODP. Sci. Results 124, 519–523.

Shuck, B., Gulick, S.P.S., Van Avendonk, H.J.A., Gurnis, M., Sutherland, R., Stock, J., Hightower, E., 2022. Stress transition from horizontal to vertical forces during subduction initiation. Nat. Geosci. 15, 149–155.
Sibuet, J.-C., Hsu, S.-K., 2004. How was Taiwan created?. Tectonophysics 379, 159–181.
Sieh, K., Natawidjaja, D., 2000. Neotectonics of the Sumatran fault, Indonesia. J. Geophys. Res. Solid Earth 105, 28295–28326.
Sikumbang, N., 1986. Geology and Tectonics of Pre-Tertiary rocks in the Meratus Mountains South-East Kalimantan. University of London, Indonesia.
Sikumbang, N., Heryanto, R., 1994. Peta Geologi Lembar Banjarmasin, Kalimantan Selatan skala 1: 250.000. Pus. Penelit. dan Pengemb. Geol. Bandung.
Silitonga, P.H., 1981. Geological reconnaissance and mineral prospecting on Bacan Island (Moluccas, Indonesia). The geology and tectonics of eastern Indonesia. Geol. Res. Dev. Centre, Bandung, Spec. Publ. 2, 373–381.
Silver, E.A., Rangin, C., 1991. 1. LEG 124 Tectonic synthesis. In: Proceedings of the Ocean Drilling Program, Scientific Results, pp. 3–9.
Silver, E.A., McCaffrey, R., Joyodiwiryo, Y., Stevens, S., 1983a. Ophiolite emplacement by collision between the Sula Platform and the Sulawesi island arc, Indonesia. J. Geophys. Res. Solid Earth 88, 9419–9435.
Silver, E.A., McCaffrey, R., Smith, R.B., 1983b. Collision, rotation, and the initiation of subduction in the evolution of Sulawesi, Indonesia. J. Geophys. Res. Solid Earth 88, 9407–9418.
Silver, E.A., Reed, D., McCaffrey, R., Joyodiwiryo, Y., 1983c. Back arc thrusting in the eastern Sunda Arc, Indonesia: A consequence of arc-continent collision. J. Geophys. Res. Solid Earth 88, 7429–7448.
Silver, E.A., Gill, J.B., Schwartz, D., Prasetyo, H., Duncan, R.A., 1985. Evidence for a submerged and displaced continental borderland, north Banda Sea, Indonesia. Geology 13, 687–691.
Silver, E.A., Moore, J.C., 1978. The Molucca sea collision zone, Indonesia. J. Geophys. Res. Solid Earth 83, 1681–1691.
Singh, A.K., Chung, S.-L., Bikramaditya, R.K., Lee, H.Y., 2017. New U-Pb zircon ages of plagiogranites from the Nagaland-Manipur Ophiolites, Indo-Myanmar Orogenic Belt, NE India. J. Geol. Soc. Lond. 174, 170–179.
Smith, R.B., Betzler, C., Brass, G.W., Huang, Z., Linsley, B.K., Menill, D., Müller, C.M., Nederbragt, A.J., Nichols, G.I., Pubellier, M., 1990. Depositional history of the Celebes Sea from ODP Sites 767 and 770. Geophys. Res. Lett. 17, 2061–2064.
Smith, R.B., Silver, E.A., 1991. Geology of a Miocene collision complex, Buton, eastern Indonesia. Geol. Soc. Am. Bull. 103, 660–678.
Smith, S.A., Tingate, P.R., Griffths, C.M., Hull, J.N.F., 1999. The structural development and petroleum potential of the Roebuck Basin. APPEA J. 39, 364–385.
Smith, R.B., 1991. Diagenesis and cementation of lower Miocene pyroclastic sequences in the Sulu Sea, sites 768, 769, and 771. Proc. OPD Sci. Results 124, 181–199.
Smyth, H., Hall, R., Hamilton, J., Kinny, P., 2005. East Java: Cenozoic basins, volcanoes and ancient basement.
Smyth, H.R., Hamilton, P.J., Hall, R., Kinny, P.D., 2007. The deep crust beneath island arcs: inherited zircons reveal a Gondwana continental fragment beneath East Java, Indonesia. Earth Planet. Sci. Lett. 258, 269–282.
Smyth, H.R., Hall, R., Nichols, G.J., 2008. Significant volcanic contribution to some quartz-rich sandstones, East Java, Indonesia. J. Sediment. Res. 78, 335–356.
Snyder, D.B., Milsom, J., Prasetyo, H., 1996. Geophysical evidence for local indentor tectonics in the Banda arc east of Timor. Geol. Soc. Lond. Spec. Publ. 106, 61–73.
Socquet, A., Simons, W., Vigny, C., McCaffrey, R., Subarya, C., Sarsito, D., Ambrosius, B., Spakman, W., 2006. Microblock rotations and fault coupling in SE Asia triple junction (Sulawesi, Indonesia) from GPS and earthquake slip vector data. J. Geophys. Res. Solid Earth 111, B08409.
Soeria-Atmadja, R., Maury, R.C., Bellon, H., Pringgoprawiro, H., Polvé, M., Priadi, B., 1994. Tertiary magmatic belts in Java. J. SE Asian Earth Sci. 9, 13–27.
Soesilo, J., Suparka, E., Abdullah, C.I., Schenk, V., 2010. Petrology and Geochemistry of the Quartz-White Mica Schists in the Luk Ulo Melange Complex, Central Java. Bul. Geol. 40, 123–138.
Soesilo, J., Schenk, V., Suparka, E., Abdullah, C.I., 2015. The mesozoic tectonic setting of SE Sundaland based on metamorphic evolution. Proc. Indones. Pet. Assoc. Annu. Conv. 39, IPA15-G-205.
Soesilo, J., 2012. Cretaceous Paired Metamorphic Belts in Southeast Sundaland. Bandung Inst. Technol. Indones.
Sone, M., Metcalfe, I., 2008. Parallel Tethyan sutures in mainland Southeast Asia: new insights for Palaeo-Tethys closure and implications for the Indosinian orogeny. Comptes Rendus Geosci. 340, 166–179.
Spadea, P., D'Antonio, M., Thirlwall, M.F., 1996. Source characteristics of the basement rocks from the Sulu and Celebes Basins (Western Pacific): chemical and isotopic evidence. Contrib. to Mineral. Petrol. 123, 159–176.
Spadea, P., Beccaluva, L., Civetta, L., Coltorti, M., Dostal, J., Sajona, F., Serri, G., Vaccaro, C., Zeda, O., 1991. 19. Petrology of basic igneous rocks from the floor of the Sulu Sea. Proc. ODP Sci. Results 124, 251–269.
Spakman, W., Hall, R., 2010. Surface deformation and slab–mantle interaction during Banda arc subduction rollback. Nat. Geosci. 3, 562–566.
Spencer, J.E., 2010. Structural analysis of three extensional detachment faults with data from the 2000 Space-Shuttle Radar Topography Mission. GSA Today 20, 4–10.
Spencer, J.E., 2011. Gently dipping normal faults identified with Space Shuttle radar topography data in central Sulawesi, Indonesia, and some implications for fault mechanics. Earth Planet. Sci. Lett. 308, 267–276.
Spencer, C.J., Roberts, N.M.W., Santosh, M., 2017. Growth, destruction, and preservation of Earth's continental crust. Earth-Sci. Rev. 172, 87–106.
Srisuriyon, K., Morley, C.K., 2014. Pull-apart development at overlapping fault tips: Oblique rifting of a Cenozoic continental margin, northern Mergui Basin, Andaman Sea. Geosphere 10, 80–106.
Stagg, H.M.J., Colwell, J.B., 1994. The structural foundations of the Northern Carnarvon Basin. In: P.G. & R.R. Purcell (eds.) The sedimentary basins of Western Australia, Proc. Petroleum Expl. Soc. Australia (PESA) Symposium, Perth 1994, 349-364
Standley, C.E., Harris, R., 2009. Tectonic evolution of forearc nappes of the active Banda arc-continent collision: Origin, age, metamorphic history and structure of the Lolotoi Complex, East Timor. Tectonophysics 479, 66–94.
Staudigel, H., Hart, S.R., Richardson, S.H., 1981. Alteration of the oceanic crust: processes and timing. Earth Planet. Sci. Lett. 52, 311–327.
Staudigel, H., Gillis, K., Duncan, R., 1986. K/Ar and Rb/Sr ages of celadonites from the Troodos ophiolite, Cyprus. Geology 14, 72–75.
Stauffer, P.H., Lee, P.C., 1986. Late Paleozoic glacial marine facies in Southeast Asia and its implications. Bull. Geol. Soc. Malaysia 20, 363–397.
Steckler, M.S., Mondal, D.R., Akhter, S.H., Seeber, L., Feng, L., Gale, J., Hill, E.M., Howe, M., 2016. Locked and loading megathrust linked to active subduction beneath the Indo-Burman Ranges. Nat. Geosci. 9, 615–618.
Stern, R.J., 2004. Subduction initiation: spontaneous and induced. Earth Planet. Sci. Lett. 226, 275–292.
Stern, R.J., Bloomer, S.H., 1992. Subduction zone infancy: examples from the Eocene Izu-Bonin-Mariana and Jurassic California arcs. Geol. Soc. Am. Bull. 104, 1621–1636.
Stern, R.J., Reagan, M., Ishizuka, O., Ohara, Y., Whattam, S., 2012. To understand subduction initiation, study forearc crust: To understand forearc crust, study ophiolites. Lithosphere 4, 469–483.
Steuer, S., Franke, D., Meresse, F., Savva, D., Pubellier, M., Auxietre, J.-L., Aurelio, M., 2013. Time constraints on the evolution of southern Palawan Island, Philippines from onshore and offshore correlation of Miocene limestones. J. Asian Earth Sci. 76, 412–427.
Stilwell, J.D., Quilty, P.G., Mantle, D.J., 2012. Paleontology of Early Cretaceous deep-water samples dredged from the Wallaby Plateau: new perspectives of Gondwana break-up along the Western Australian margin. Aust. J. Earth Sci. 59, 29–49.
Su, D., White, N., McKenzie, D.A.N., 1989. Extension and subsidence of the Pearl River mouth basin, northern South China Sea. Basin Res. 2, 205–222.
Sudarmono, 2000. Stratigraphic evolution of the Bone Basin, Indonesia: insights to the Sulawesi collision complex. Proc. Indones. Petr. Assoc. Annu. Conv. 27, 531–543.
Suggate, S.M., Cottam, M.A., Hall, R., Sevastjanova, I., Forster, M.A., White, L.T., Armstrong, R.A., Carter, A., Mojares, E., 2014. South China continental margin signature for sandstones and granites from Palawan, Philippines. Gondwana Res. 26, 699–718.
Sugiaman, F., Andria, L., 1999. Devonian carbonate of Telen River, East Kalimantan. Ber. Sedimentol. 10, 18–19.
Sukamto, R., Westermann, G.E.G., 1992. Indonesia and Papua New Guinea. In: Westermann, G.E.G. (Ed.), The Jurassic of the circum-Pacific pp. 181–193.
Sukanto, J., Nunuk, F., Aldrich, J.B., Rinehart, G.P., Mitchell, J., 1998. Petroleum Systems of the Asri Basin, Java Sea, Indonesia. Proc. Indones. Petr. Assoc. Annu. Conv. 26, 291–312.
Sumarso, Ismoyowati, T., 1975. Contribution to the stratigraphy of the Jiwo Hills and their southern surroundings (Central Java). Proc. Indones. Petr. Assoc. Annu. Conv. 4, 19-26.
Suparka, M.E., 1988. Study on the Petrology and Geochemistry of the North Karangsambung Ophiolite, Luk Ulo, Central Java. PhD thesis, Bandung Inst. Technol.
Suppe, J., 1984. Kinematics of arc-continent collision, flipping of subduction, and back-arc spreading near Taiwan. Mem. Geol. Soc. China 6, 21–33.
Suppe, J., 1980. A retrodeformable cross section of northern Taiwan. In: Proc. Geol. Soc. China, pp. 46–55.
Surmont, J., Laj, C., Kissel, C., Rangin, C., Bellon, H., Priadi, B., 1994. New paleomagnetic constraints on the Cenozoic tectonic evolution of the North Arm of Sulawesi, Indonesia. Earth Planet. Sci. Lett. 121, 629–638.
Surono, Bachri, S., 2002. Stratigraphy, sedimentation and palaeogeographic significance of the Triassic Meluhu Formation, Southeast arm of Sulawesi, Eastern Indonesia. J. Asian Earth Sci. 20, 177–192.
Suwarna, N., Gafoer, S., Amin, T.C., Kusnama, Hermanto, B., 1994. Geology of the Sarolangun Quadrangle. Geol. Res. Dev. Centre, Bandung, Indones.
Suzuki, H., Ja, L., Maung, M., Thin, A.K., Kuwahara, K., 2020. The First Report on Early Cretaceous Radiolaria from Myanmar. Paleontol. Res. 24, 103–112.
Suzuki, S., Takemura, S., Yumul, G.P., David, S.D., Asiedu, D.K., 2000. Composition and provenance of the Upper Cretaceous to Eocene sandstones in Central Palawan, Philippines: Constraints on the tectonic development of Palawan. Isl. Arc 9, 611–626.
Swauger, D.A., Bergman, S.C., Graves, J.E., Hutchison, C.S., Surat, T., Morillo, A.P., Benavidez, J.J., Pagado, E.S., 1995. Tertiary stratigraphic, tectonic, and thermal history of Sabah, Malaysia: results of a 10 day reconnaissance field study and laboratory analyses. ARCO Int. Oil Gas Co. Unpubl. report. TRS 95, 36.
Symonds, P.A., Planke, S., Frey, O., Skogseid, J., 1998. Volcanic evolution of the Western Australian continental margin and its implications for basin development.
Tamayo, R.A., Yumul, G.P., Maury, R.C., Bellon, H., Cotten, J., Polvé, M., Juteau, T., Querubin, C., 2000. Complex origin for the south-western Zamboanga metamorphic basement complex, Western Mindanao, Philippines. Isl. Arc 9, 638–652.

Tamayo, R.A., Yumul, G.P., Maury, R.C., Polvé, M., Cotten, J., Bohn, M., 2001. Petrochemical investigation of the Antique Ophiolite (Philippines): Implications on volcanogenic massive sulfide and podiform chromitite deposits. Resour. Geol. 51, 145–164.
Tamesis, E.V., 1990. Petroleum geology of the Sulu Sea Basin, Philippines. In: 8th Offshore South East Asia Conf. Proc. SE Asia Petroleum Expl. Soc. (SEAPEX), Singapore 9, 45–54.
Tan, D.N.K., 1979. Lupar Valley, West Sarawak; Explanation of sheets 1–111-14, 1–111-15, and 1–111- 16. Geol. Surv. Malaysia Rep. 13, 1–159.
Tate, G.W., McQuarrie, N., Van Hinsbergen, D.J.J., Bakker, R.R., Harris, R., Willett, S., Reiners, P.W., Fellin, M.G., Ganerød, M., Zachariasse, W.J., 2014. Resolving spatial heterogeneities in exhumation and surface uplift in Timor-Leste: Constraints on deformation processes in young orogens. Tectonics 33, 1089–1112.
Tate, G.W., McQuarrie, N., van Hinsbergen, D.J.J., Bakker, R.R., Harris, R., Jiang, H., 2015. Australia going down under: Quantifying continental subduction during arc-continent accretion in Timor-Leste. Geosphere 11, 1860–1883.
Tate, G.W., McQuarrie, N., Tiranda, H., Van Hinsbergen, D.J.J., Harris, R., Zachariasse, W.J., Fellin, M.G., Reiners, P.W., Willett, S.D., 2017. Reconciling regional continuity with local variability in structure, uplift and exhumation of the Timor orogen. Gondw. Res. 49, 364–386.
Taylor, B., Hayes, D.E., 1983. Origin and history of the South China Sea basin. GMS 27, 23–56.
Teas, P.A., Decker, J., Orange, D., Baillie, P., 2009. New Insight Into Structure and Tectonics of the Seram Trough From SeaSeep™ High Resolution Bathymetry. Proc. Indones. Petr. Assoc. Annu. Conv. 33, IPA09-G-091
Tjia, H.D., 1973. Palu-Koro fault zone. Sulawesi. Ber. Direktorat Geol. Geosurvey Newsl. 5, 1–3.
Tjia, H.D., 1996. Tectonics of deformed and undeformed Jurassic-Cretaceous strata of Peninsular Malaysia. Bull. Geol. Soc. Malays. 39, 131–156.
Tjia, H.D., 1972. Strike-slip faults in West Malaysia. In: 24 th IGC 3, pp. 255–262.
Tongkul, F., 1994. The geology of Northern Sabah, Malaysia: its relationship to the opening of the South China Sea Basin. Tectonophysics 235, 131–147.
Tongkul, F., 1997. Polyphase deformation in the Telupid area, Sabah, Malaysia. J. Asian Earth Sci. 15, 175–183.
Tongkul, F., 2006. The structural style of Lower Miocene sedimentary rocks, Kudat Peninsula, Sabah. Geol. Soc. Malaysia, Bull. 49, 119–124.
Topuz, G., Çelık, Ö.F., Şengör, A.M.C., Altintaş, İ.E., Zack, T., Rolland, Y., Barth, M., 2013a. Jurassic ophiolite formation and emplacement as backstop to a subduction-accretion complex in northeast Turkey, the Refahıye ophiolite, and relation to the Balkan ophiolites. Am. J. Sci. 313, 1054–1087.
Topuz, G., Göçmengil, G., Rolland, Y., Çelik, Ö.F., Zack, T., Schmitt, A.K., 2013b. Jurassic accretionary complex and ophiolite from northeast Turkey: No evidence for the Cimmerian continental ribbon. Geology 41, 255–258.
Torsvik, T.H., Cocks, L.R.M., 2016. Earth History and Palaeogeography. Cambridge University Press.
Torsvik, T.H., Amundsen, H., Hartz, E.H., Corfu, F., Kusznir, N., Gaina, C., Doubrovine, P.V., Steinberger, B., Ashwal, L.D., Jamtveit, B., 2013. A Precambrian microcontinent in the Indian Ocean. Nat. Geosci. 6, 223–227.
Toussaint, G., Burov, E., Avouac, J., 2004. Tectonic evolution of a continental collision zone: A thermomechanical numerical model. Tectonics 23, TC6003.
Tsai, C.-H., Iizuka, Y., Ernst, W.G., 2013. Diverse mineral compositions, textures, and metamorphic P-T conditions of the glaucophane-bearing rocks in the Tamayen mélange, Yuli belt, eastern Taiwan. J. Asian Earth Sci. 63, 218–233.
Tsuji, T., Yamamoto, K., Matsuoka, T., Yamada, Y., Onishi, K., Bahar, A., Meilano, I., Abidin, H.Z., 2009. Earthquake fault of the 26 May 2006 Yogyakarta earthquake observed by SAR interferometry. Earth, Planets Sp. 61, e29–e32.
Tun, S.T., Watkinson, I.M., 2017. The sagaing fault, Myanmar. Geol. Soc. Lond., Mem. 48, 413–441.
Udintsev, G.B., 1975. Geological-geophysical Atlas of the Indian Ocean (International Indian Ocean Expedition). In: Udintsev, G.B. (Ed.), Academy of Sciences of the USSR, pp. 150.
Ueno, K., 2003. The Permian fusulinoidean faunas of the Sibumasu and Baoshan blocks: their implications for the paleogeographic and paleoclimatologic reconstruction of the Cimmerian Continent. Palaeogeogr. Palaeoclimatol. Palaeoecol. 193, 1–24.
UN, 1978. Geology and Exploration Geochemistry of the Pinlebu-Banmauk Area, Sagaing Division, Northern Burma. United Nations Dev. Program. Tech. Rep. UN/BUR/72/002 2.
Ustaszewski, K., Wu, Y.-M., Suppe, J., Huang, H.-H., Chang, C.-H., Carena, S., 2012. Crust–mantle boundaries in the Taiwan-Luzon arc-continent collision system determined from local earthquake tomography and 1D models: implications for the mode of subduction polarity reversal. Tectonophysics 578, 31–49.
Vadlamani, R., Wu, F.-Y., Ji, W.-Q., 2015. Detrital zircon U-Pb age and Hf isotopic composition from foreland sediments of the Assam Basin, NE India: Constraints on sediment provenance and tectonics of the Eastern Himalaya. J. Asian Earth Sci. 111, 254–267.
Vaes, B., van Hinsbergen, D.J.J., van de Lagemaat, S.H.A., van der Wiel, E., Lom, N., Advokaat, E.L., Boschman, L.M., Gallo, L.C., Greve, A., Guilmette, C., 2023. A global apparent polar wander path for the last 320 Ma calculated from site-level paleomagnetic data. Earth-Sci. Rev. 245, 104547.
Vaes, B., Van Hinsbergen, D.J.J., Boschman, L.M., 2019. Reconstruction of subduction and back-arc spreading in the NW Pacific and Aleutian Basin: Clues to causes of Cretaceous and Eocene plate reorganizations. Tectonics 38, 1367–1413.
van de Lagemaat, S.H.A., Cao, L., Asis, J., Advokaat, E.L., Mason, P.R.D., Dekkers, M. J., & van Hinsbergen, D.J.J., 2023. Causes of Late Cretaceous subduction termination below South China and Borneo: Was the Proto-South China Sea underlain by an oceanic plateau?. Geoscience Frontiers, in press.
van de Lagemaat, S.H.A., van Hinsbergen, D.J.J., 2024. Plate tectonic cross-roads: Reconstructing the Panthalassa-Neotethys Junction Region from Philippine Sea Plate and Australasian oceans and orogens. Gondw. Res. 126, 129–201.
van de Lagemaat, S.H.A., Swart, M.L.A., Vaes, B., Kosters, M.E., Boschman, L.M., Burton-Johnson, A., Bijl, P.K., Spakman, W., van Hinsbergen, D.J.J., 2021. Subduction initiation in the Scotia Sea region and opening of the Drake Passage: When and why? Earth-Sci. Rev. 215,103551.
van de Weerd, A.A., Armin, R.A., 1992. Origin and Evolution of the Tertiary Hydrocarbon-Bearing Basins in Kalimantan (Borneo), Indonesia (1). Am. Assoc. Pet. Geol. Bull. 76, 1778–1803.
Van de Weerd, A., Armin, R.A., Mahadi, S., Ware, P.L.B., 1987. Geologic setting of the Kerendan gas and condensate discovery, Tertiary sedimentation and paleogeography of the northwestern part of the Kutei Basin, Kalimantan, Indonesia. Proc. Indones. Petr. Assoc. Annu. Conv. 16, 317–338.
Van der Meer, D.G., Van Hinsbergen, D.J.J., Spakman, W., 2018. Atlas of the underworld: Slab remnants in the mantle, their sinking history, and a new outlook on lower mantle viscosity. Tectonophysics 723, 309–448.
van der Vlerk, I.M., Dozy, J.J., 1934. The Tertiary Rocks of the Celebes-Expedition 1929. Verhand. Kon. Nederl. Geol. Mijnb. Gen., Geol. Serie 10, 183–218.
Van der Voo, R., van Hinsbergen, D.J.J., Domeier, M., Spakman, W., Torsvik, T.H., 2015. Latest Jurassic–earliest Cretaceous closure of the Mongol-Okhotsk Ocean: A paleomagnetic and seismological-tomographic analysis. Geol. Soc. Am. Spec. Pap. 513, 589–606.
van der Wal, J.L.N., 2015. The structural evolution of the Bentong-Raub Zone and the Western Belt around Kuala Lumpur, Peninsular Malaysia.
Van der Werff, W., 1995. Cenozoic evolution of the Savu Basin, Indonesia: forearc basin response to arc-continent collision. Mar. Pet. Geol. 12, 247–262.
Van der Werff, W., 1996. Variation in forearc basin development along the Sunda Arc, Indonesia. J. Southeast Asian Earth Sci. 14, 331–349.
van der Werff, W., Kusnida, D., Prasetyo, H., van Weering, T.C.E., 1994. Origin of the Sumba forearc basement. Mar. Pet. Geol. 11, 363–374.
van Gorsel, J.T., 2012. No Jurassic Sediments on Sumba Island?. Ber. Sedimentol. 25, 35–37.
Van Halen, S., 1996. Geochronology and Geochemistry of rocks from Sumba. Indonesia. Internal Report. Institute of Earth Sciences, Utrecht University.
Van Hattum, M.W.A., Hall, R., Pickard, A.L., Nichols, G.J., 2013. Provenance and geochronology of Cenozoic sandstones of northern Borneo. J. Asian Earth Sci. 76, 266–282.
van Hinsbergen, D.J.J., Schouten, T.L.A., 2021. Deciphering paleogeography from orogenic architecture: constructing orogens in a future supercontinent as thought experiment. Am. J. Sci. 321, 955–1031.
van Hinsbergen, D.J.J., Schmid, S.M., 2012. Map view restoration of Aegean-West Anatolian accretion and extension since the Eocene. Tectonics 31, TC5005.
van Hinsbergen, D.J.J., Hafkenscheid, E., Spakman, W., Meulenkamp, J.E., Wortel, R., 2005. Nappe stacking resulting from subduction of oceanic and continental lithosphere below Greece. Geology 33, 325–328.
van Hinsbergen, D.J.J., Kapp, P., Dupont-Nivet, G., Lippert, P.C., DeCelles, P.G., Torsvik, T.H., 2011. Restoration of Cenozoic deformation in Asia and the size of Greater India. Tectonics 30, TC5003.
van Hinsbergen, D.J.J., Lippert, P.C., Dupont-Nivet, G., McQuarrie, N., Doubrovine, P. V., Spakman, W., Torsvik, T.H., 2012. Greater India Basin hypothesis and a two-stage Cenozoic collision between India and Asia. Proc. Natl. Acad. Sci. 109, 7659–7664.
van Hinsbergen, D.J.J., De Groot, L.V., van Schaik, S.J., Spakman, W., Bijl, P.K., Sluijs, A., Langereis, C.G., Brinkhuis, H., 2015. A paleolatitude calculator for paleoclimate studies. PLoS One 10, e0126946.
van Hinsbergen, D.J.J., Lippert, P.C., Li, S., Huang, W., Advokaat, E.L., Spakman, W., 2019a. Reconstructing Greater India: Paleogeographic, kinematic, and geodynamic perspectives. Tectonophysics 760, 69–94. https://doi.org/10.1016/j.tecto.2018.04.006.
van Hinsbergen, D.J.J., Maffione, M., Koornneef, L.M.T., Guilmette, C., 2019b. Kinematic and paleomagnetic restoration of the Semail ophiolite (Oman) reveals subduction initiation along an ancient Neotethyan fracture zone. Earth Planet. Sci. Lett. 518, 183–196.
van Hinsbergen, D.J.J., Torsvik, T.H., Schmid, S.M., Maţenco, L.C., Maffione, M., Vissers, R.L.M., Gürer, D., Spakman, W., 2020. Orogenic architecture of the Mediterranean region and kinematic reconstruction of its tectonic evolution since the Triassic. Gondw. Res. 81, 79–229.
van Hinsbergen, D.J.J., 2022. Indian Plate paleogeography, subduction, and horizontal underthrusting below Tibet: paradoxes, controvercies, and opportunities.
van Leeuwen, T.M., 1981. The geology of southwest Sulawesi with special reference to the Biru area. Geol. Tectonics East. Indones., 277–304.
Van Leeuwen, T., Allen, C.M., Kadarusman, A., Elburg, M., Palin, J.M., 2007. Petrologic, isotopic, and radiometric age constraints on the origin and tectonic history of the Malino Metamorphic Complex, NW Sulawesi, Indonesia. J. Asian Earth Sci. 29, 751–777.
van Leeuwen, T., Allen, C.M., Elburg, M., Massonne, H.-J., Palin, J.M., Hennig, J., 2016. The Palu Metamorphic Complex, NW Sulawesi, Indonesia: Origin and evolution of a young metamorphic terrane with links to Gondwana and Sundaland. J. Asian Earth Sci. 115, 133–152.
van Leeuwen, T.M., Susanto, E.S., Maryanto, S., Hadiwisastra, S., 2010. Tectonostratigraphic evolution of Cenozoic marginal basin and continental

margin successions in the Bone Mountains, Southwest Sulawesi, Indonesia. J. Asian Earth Sci. 38, 233–254.
van Leeuwen, T.M., Muhardjo, 2005. Stratigraphy and tectonic setting of the Cretaceous and Paleogene volcanic-sedimentary successions in northwest Sulawesi, Indonesia: implications for the Cenozoic evolution of Western and Northern Sulawesi. J. Asian Earth Sci. 25, 481–511.
Van Marle, L.J., De Smet, M.E.M., 1990. Notes on the Late Cenozoic history of the Kai Islands, eastern Indonesia. Geol. en Mijnb. 69, 93–103.
van Waveren, I.M., Booi, M., Crow, M.J., Hasibuan, F., Van Konijnenburg-Van Cittert, J.H.A., Perdono, A.P., Schmitz, M.D., Donovan, S.K., 2018. Depositional settings and changing composition of the Jambi palaeoflora within the Permian Mengkarang Formation (Sumatra, Indonesia). Geol. J. 53, 2969–2990.
van Waveren, I.M., Iskandar, E.A.P., Booi, M., van Konijnenburg-van, J.H.A., 2007. Composition and palaeogeographic position of the Early Permian Jambi flora from Sumatra. Scr. Geol. 135, 1–28.
Veevers, J.J., Heirtzler, J.R., 1974. 49. Tectonic and paleogeographic synthesis of LEG 27. Proc. DSDP Init. Results 27, 1049–1054.
Veevers, J.J., Powell, C.M., Roots, S.R., 1991. Review of seafloor spreading around Australia. I. Synthesis of the patterns of spreading. Aust. J. Earth Sci. 38, 373–389.
Verstappen, H.T., 1964. Some volcanoes of Halmahera (Moluccas) and their geomorphological setting. K. Ned. Aardrijkskd. Genoot. 81, 297–316.
Verstappen, H.T., 2010. Indonesian landforms and plate tectonics. Indones. J. Geosci. 5, 197–207.
Vigny, C., Perfettini, H., Walpersdorf, A., Lemoine, A., Simons, W., van Loon, D., Ambrosius, B., Stevens, C., McCaffrey, R., Morgan, P., 2002. Migration of seismicity and earthquake interactions monitored by GPS in SE Asia triple junction: Sulawesi, Indonesia. J. Geophys. Res. Solid Earth 107, ETG-7.
Villeneuve, M., Cornee, J.-J., Martini, R., Zaninetti, L., Rehault, J.-P., Burhanudin, S., Malod, J., 1994. Upper Triassic shallow water limestones in the Sinta ridge (Banda Sea, Indonesia). Geo-Marine Lett. 14, 29–35.
Vissers, R.L.M., Meijer, P.T., 2012a. Mesozoic rotation of Iberia: subduction in the Pyrenees?. Earth-Sci. Rev. 110, 93–110.
Vissers, R.L.M., Meijer, P.T., 2012b. Iberian plate kinematics and Alpine collision in the Pyrenees. Earth-Sci. Rev. 114, 61–83.
Vlaar, N.J., Wortel, M.J.R., 1976. Lithospheric aging, instability and subduction. Tectonophysics 32, 331–351.
Von der Borch, C.C., Grady, A.E., Hardjoprawiro, S., Prasetyo, H., Hadiwisastra, S., 1983. Mesozoic and late Tertiary submarine fan sequences and their tectonic significance, Sumba, Indonesia. Sediment. Geol. 37, 113–132.
von Hagke, C., Philippon, M., Avouac, J.-P., Gurnis, M., 2016. Origin and time evolution of subduction polarity reversal from plate kinematics of Southeast Asia. Geology 44, 659–662.
von Rad, U., Exon, N.F., 1982. In: Watkins, J.S., Drake, C.L. (Eds.). American Assoc. Petrol. Geol. Mem. 34, 253–281.
von Rad, U., Exon, N.F., Haq, B.U., 1992. Rift-to-drift history of the Wombat Plateau, Northwest Australia: Triassic to Tertiary Leg 122 results.Proc. ODP Sci. Results 122, 765–800.
Vozenin-Serra, C., 1989. Lower Permian continental flora of Sumatra. In: H. Fontaine & S. Gafoer (eds.) The Pre-Tertiary fossils of Sumatra and their environments. CCOP Techn. Publ. 19, Bangkok, 53-57.
Wajzer, M.R., Barber, A.J., Hidayat, S., 1991. Accretion, collision and strike-slip faulting: the Woyla group as a key to the tectonic evolution of North Sumatra. J. SE Asian Earth Sci. 6, 447–461.
Wakita, K., 2000. Cretaceous accretionary–collision complexes in central Indonesia. J. Asian Earth Sci. 18, 739–749.
Wakita, K., 2015. OPS mélange: A new term for mélanges of convergent margins of the world. Int. Geol. Rev. 57, 529–539.
Wakita, K., Munasri, Bambang, W., 1991. Nature And Age of Sedimentary Rocks of Luk Ulo Melange Complex in Karangsambung Area, Central Java, Indonesia. In: Symposium on Dynamic of Subduction and Its Product, Yogyakarta.
Wakita, K., Metcalfe, I., 2005. Ocean plate stratigraphy in East and Southeast Asia. J. Asian Earth Sci. 24, 679–702.
Wakita, K., Munasri, Bambang, W., 1994a. Cretaceous radiolarians from the Luk-Ulo melange complex in the Karangsambung area, central Java, Indonesia. J. Asian Earth Sci. 9, 29–43.
Wakita, K., Sopaheluwakan, J., Zulkarnain, I., Mlyazaki, K., 1994b. Early Cretaceous tectonic events implied in the time-lag between the age of radiolarian chert and its metamorphic basement in the Bantimala area, South Sulawesi, Indonesia. Isl. Arc 3, 90–102.
Wakita, K., Sopaheluwakan, J., Miyazaki, K., Zulkarnain, I., 1996. Tectonic evolution of the Bantimala complex, south Sulawesi, Indonesia. Geol. Soc. Lond. Spec. Publ. 106, 353–364.
Wakita, K., Miyazaki, K., Zulkarnain, I., Sopaheluwakan, J., Sanyoto, P., 1998. Tectonic implications of new age data for the Meratus Complex of south Kalimantan, Indonesia. Isl. Arc 7, 202–222.
Walia, M., Knittel, U., Suzuki, S., Chung, S.-L., Pena, R.E., Yang, T.F., 2012. No Paleozoic metamorphics in Palawan (the Philippines)? Evidence from single grain U-Pb dating of detrital zircons. J. Asian Earth Sci. 52, 134–145.
Walia, M., Yang, T.F., Knittel, U., Liu, T.-K., Lo, C.-H., Chung, S.-L., Teng, L.S., Dimalanta, C.B., Yumul, G.P., Yuan, W.M., 2013. Cenozoic tectonics in the Buruanga Peninsula, Panay Island, Central Philippines, as constrained by U-Pb, 40Ar/39Ar and fission track thermochronometers. Tectonophysics 582, 205–220.
Walpersdorf, A., Rangin, C., Vigny, C., 1998a. GPS compared to long-term geologic motion of the north arm of Sulawesi. Earth Planet. Sci. Lett. 159, 47–55.
Walpersdorf, A., Vigny, C., Subarya, C., Manurung, P., 1998b. Monitoring of the Palu-Koro fault (Sulawesi) by GPS. Geophys. Res. Lett. 25, 2313–2316.
Waltham, D., Hall, R., Smyth, H.R., Ebinger, C.J., 2008. Basin formation by volcanic arc loading. Spec. Pap. Soc. Am. 436, 11.
Wang, E., Burchfiel, B.C., 1997. Interpretation of Cenozoic tectonics in the right-lateral accommodation zone between the Ailao Shan shear zone and the eastern Himalayan syntaxis. Int. Geol. Rev. 39, 191–219.
Wang, Y., Qian, X., Zhang, Y., Gan, C., Zhang, A., Zhang, F., Feng, Q., Cawood, P.A., Zhang, P., 2021a. Southern extension of the Paleotethyan zone in SE Asia: Evidence from the Permo-Triassic granitoids in Malaysia and West Indonesia. Lithos 106336.
Wang, Y., Zhang, A., Qian, X., Asis, J.B., Feng, Q., Gan, C., Zhang, Y., Cawood, P.A., Wang, W., Zhang, P., 2021b. Cretaceous Kuching accretionary orogenesis in Malaysia Sarawak: Geochronological and geochemical constraints from mafic and sedimentary rocks. Lithos 400, 106425.
Wang, Y., Wu, S., Qian, X., Cawood, P.A., Lu, X., Gan, C., Asis, J.B., Zhang, P., 2022a. Early Cretaceous subduction in NW Kalimantan: Geochronological and geochemical constraints from the Raya and Mensibau igneous rocks. Gondw. Res. 101, 243–256.
Wang, Y., Liu, Z., Murtadha, S., Cawood, P.A., Qian, X., Ghani, A., Gan, C., Zhang, Y., Wang, Y., Li, S., 2022b. Jurassic subduction of the Paleo-Pacific plate in Southeast Asia: New insights from the igneous and sedimentary rocks in West Borneo. J. Asian Earth Sci. 105111.
Wang, Y., Qian, X., Cawood, P.A., Ghani, A., Gan, C., Wu, S., Zhang, Y., Wang, Y., Zhang, P., 2022c. Cretaceous Tethyan subduction in SE Borneo: Geochronological and geochemical constraints from the igneous rocks in the Meratus Complex. J. Asian Earth Sci. 105084.
Wang, Y., Qian, X., Asis, J.B., Cawood, P.A., Wu, S., Zhang, Y., Feng, Q., Lu, X., 2023a. "Where, when and why" for the arc-trench gap from Mesozoic Paleo-Pacific subduction zone: Sabah Triassic-Cretaceous igneous records in East Borneo. Gondwana Res..
Wang, Y., Gao, Y., Morley, C.K., Seagren, E.G., Qian, X., Rimando, J.M., Zhang, P., Wang, Y., 2023b. Pleistocene accelerated exhumation within the Sumatran fault: Implications for late Cenozoic evolution of Sumatra (Indonesia). Geophys. Res. Lett. 50.
Wang, C.Y., He, X.X., Qiu, S.Y., 1979. Preliminary study on carbonate strata and micropaleontology of Xiyong No. 1 drilling, Xisha Islands. Pet. Exp. Geol. 7, 23–32.
Wang, P.-L., Lo, C.-H., Chung, S.-L., Lee, T.-Y., Lan, C.-Y., Van Thang, T., 2000. Onset timing of left-lateral movement along the Ailao Shan-Red River Shear Zone: 40Ar/39Ar dating constraint from the Nam Dinh Area, northeastern Vietnam. J. Asian Earth Sci. 18, 281–292.
Wang, G., Wan, J., Wang, E., Zheng, D., Li, F., 2008. Late Cenozoic to recent transtensional deformation across the Southern part of the Gaoligong shear zone between the Indian plate and SE margin of the Tibetan plateau and its tectonic origin. Tectonophysics 460, 1–20.
Warmada, I.W., Sudarno, I., Wijanarko, D., 2008. Geologi dan facies batuan metamorf daerah Jiwo Barat, Bayat, Klaten, Jawa Tengah. Media Tek. 2, 113–118.
Watcharanantakul, R., Morley, C.K., 2000. Syn-rift and post-rift modelling of the Pattani Basin, Thailand: evidence for a ramp-flat detachment. Mar. Pet. Geol. 17, 937–958.
Watkinson, I.M., 2009. The kinematic history of the Khlong Marui and Ranong Faults. University of London, Southern Thailand.
Watkinson, I.M., Hall, R., 2011. The Palu-Koro and Matano faults, Sulawesi, Indonesia: Evolution of an active strike-slip fault system. In: Geophysical Research Abstracts. p. 8270.
Watkinson, I.M., Hall, R., 2017. Fault systems of the eastern Indonesian triple junction: evaluation of Quaternary activity and implications for seismic hazards. Geol. Soc. Lond. Spec. Publ. 441, 71–120.
Watkinson, I.M., Elders, C., Hall, R., 2008. The kinematic history of the Khlong Marui and Ranong Faults, southern Thailand. J. Struct. Geol. 30, 1554–1571.
Watkinson, I.M., Elders, C., Batt, G., Jourdan, F., Hall, R., McNaughton, N.J., 2011a. The timing of strike-slip shear along the Ranong and Khlong Marui faults, Thailand. J. Geophys. Res Solid Earth, 116.
Watkinson, I.M., Hall, R., Ferdian, F., 2011b. Tectonic re-interpretation of the Banggai-Sula–Molucca Sea margin, Indonesia. Geol. Soc. Lond. Spec. Publ. 355, 203–224.
Webb, A.A.G., Guo, H., Clift, P.D., Husson, L., Müller, T., Costantino, D., Yin, A., Xu, Z., Cao, H., Wang, Q., 2017. The Himalaya in 3D: Slab dynamics controlled mountain building and monsoon intensification. Lithosphere 9, 637–651.
Webb, M., White, L.T., Jost, B.M., Tiranda, H., 2019. The Tamrau Block of NW New Guinea records late Miocene-Pliocene collision at the northern tip of the Australian Plate. J. Asian Earth Sci. 179, 238–260.
Weissel, J.K., 1980. Evidence for Eocene oceanic crust in the Celebes Basin. Tecton. Geol. Evol. Southeast Asian Seas Islands 37–47.
Wensink, H., 1994. Paleomagnetism of rocks from Sumba: tectonic implications since the late Cretaceous. J. SE Asian Earth Sci. 9, 51–65.
Wensink, H., 1997. Palaeomagnetic data of late Cretaceous rocks from Sumba, Indonesia; the rotation of the Sumba continental fragment and its relation with eastern Sundaland. Geol. en Mijnb. 76, 57–71.
Wensink, H., Hartosukohardjo, S., 1990a. Paleomagnetism of younger volcanics from Western Timor, Indonesia. Earth Planet. Sci. Lett. 100, 94–107.

Wensink, H., Hartosukohardjo, S., 1990b. The palaeomagnetism of Late Permian-Early Triassic and Late Triassic deposits on Timor: an Australian origin?. Geophys. J. Int. 101, 315–328.
Wensink, H., Hartosukohardjo, S., Kool, K., 1987. Paleomagnetism of the Nakfunu formation of Early Cretaceous age, western Timor, Indonesia. Geol. en Mijnb. 66, 89–99.
Wensink, H., Hartosukohardjo, S., Suryana, Y., 1989. Palaeomagnetism of Cretaceous sediments from Misool, northeastern Indonesia. Netherlands J. Sea Res. 24, 287–301.
Wensink, H., van Bergen, M.J., 1995. The tectonic emplacement of Sumba in the Sunda-Banda Arc: paleomagnetic and geochemical evidence from the early Miocene Jawila volcanics. Tectonophysics 250, 15–30.
Westerweel, J., Roperch, P., Licht, A., Dupont-Nivet, G., Win, Z., Poblete, F., Ruffet, G., Swe, H.H., Thi, M.K., Aung, D.W., 2019. Burma Terrane part of the Trans-Tethyan arc during collision with India according to palaeomagnetic data. Nat. Geosci. 12, 863–868.
Westerweel, J., Licht, A., Cogné, N., Roperch, P., Dupont-Nivet, G., Kay Thi, M., Swe, H. H., Huang, H., Win, Z., Wa Aung, D., 2020. Burma Terrane collision and northward indentation in the Eastern Himalayas recorded in the Eocene-Miocene Chindwin Basin (Myanmar). Tectonics 39.
White, L.T., Hall, R., Armstrong, R.A., 2014. The age of undeformed dacite intrusions within the Kolaka Fault zone, SE Sulawesi, Indonesia. J. Asian Earth Sci. 94, 105–112.
White, L.T., Hall, R., Armstrong, R.A., Barber, A.J., Fadel, M.B., Baxter, A., Wakita, K., Manning, C., Soesilo, J., 2017. The geological history of the Latimojong region of western Sulawesi, Indonesia. J. Asian Earth Sci. 138, 72–91.
Whittaker, J.M., Müller, R.D., Leitchenkov, G., Stagg, H., Sdrolias, M., Gaina, C., Goncharov, A., 2007. Major Australian-Antarctic plate reorganization at Hawaiian-Emperor bend time. Science (80-) 318, 83–86.
Whittaker, J.M., Williams, S.E., Müller, R.D., 2013. Revised tectonic evolution of the Eastern Indian Ocean. Geochem. Geophys. Geosyst. 14, 1891–1909.
Widiyantoro, S., van der Hilst, R., 1997. Mantle structure beneath Indonesia inferred from high-resolution tomographic imaging. Geophys. J. Int. 130, 167–182.
Wight, A., Sudarmono, I.A., 1986. Stratigraphic response to structural evolution in a tensional back-arc setting and its exploratory significance: Sunda Basin, West Java Sea. Proc. Indones. Petr. Assoc. Annu. Conv. 15, 77–100.
Williams, S.E., Whittaker, J.M., Müller, R.D., 2012. Full-Fit Reconstructions of the Southern Australian Margin and Antarctica-Implications for Correlating Geology between Australia and Antarctica.
Williams, P.R., Supriatna, S., Harahap, B., 1986. Cretaceous melange in West Kalimantan and its tectonic implications. Bull. Geol. Soc. Malays. 19, 69–78.
Williams, P.R., Johnston, C.R., Almond, R.A., Simamora, W.H., 1988. Late Cretaceous to early Tertiary structural elements of West Kalimantan. Tectonophysics 148, 279–297.
Williams, S.E., Whittaker, J.M., Müller, R.D., 2011. Full-fit, palinspastic reconstruction of the conjugate Australian-Antarctic margins. Tectonics 30.
Wilson, J.T., 1966. Did the Atlantic close and then re-open?. Nature 211, 676–681.
Wilson, M.E.J., Bosence, D.W.J., 1996. The Tertiary evolution of South Sulawesi: a record in redeposited carbonates of the Tonasa Limestone Formation. Geol. Soc. Lond. Spec. Publ. 106, 365–389.
Win, Z., Shwe, K.K., Yin, O.S., 2017. Sedimentary facies and biotic associations in the Permian-Triassic limestones on the Shan Plateau, Myanmar. Geol. Soc. Lond., Mem. 48, 343–363.
Witts, D., Hall, R., Morley, R.J., BouDagher-Fadel, M.K., 2011. Stratigraphy and sediment provenance, Barito basin, Southeast Kalimantan. Proc. Indones. Petr. Assoc. Annu. Conv 35, IPA11-G-054.
Witts, D., Hall, R., Nichols, G., Morley, R., 2012. A new depositional and provenance model for the Tanjung Formation, Barito Basin, SE Kalimantan, Indonesia. J. Asian Earth Sci. 56, 77–104.
Wolfart, R., Čepek, P., Gramann, F., Kemper, E., Porth, H., 1986. Stratigraphy of Palawan Island, Philippines. Newsletters Stratigr., 19–48.
Wu, J., Suppe, J., Lu, R., Kanda, R., 2016. Philippine Sea and East Asian plate tectonics since 52 Ma constrained by new subducted slab reconstruction methods. J. Geophys. Res. Solid Earth 121, 4670–4741.
Wu, S., Wang, Y., Qian, X., Asis, J.B., Lu, X., Zhang, Y., Gan, C., 2022. Discovery of the Late Cretaceous Barru adakite in SW Sulawesi and slab break-off beneath the Central Indonesian Accretionary Complex. J. Asian Earth Sci. 105214.
Xu, C., Shi, H., Barnes, C.G., Zhou, Z., 2016. Tracing a late Mesozoic magmatic arc along the Southeast Asian margin from the granitoids drilled from the northern South China Sea. Int. Geol. Rev. 58, 71–94.
Yan, Q., Shi, X., Liu, J., Wang, K., Bu, W., 2010. Petrology and geochemistry of Mesozoic granitic rocks from the Nansha micro-block, the South China Sea: constraints on the basement nature. J. Asian Earth Sci. 37, 130–139.
Yan, Q., Metcalfe, I., Shi, X., 2017. U-Pb isotope geochronology and geochemistry of granites from Hainan Island (northern South China Sea margin): constraints on late Paleozoic-Mesozoic tectonic evolution. Gondw. Res. 49, 333–349.
Yancey, T.E., Alif, S.A., 1977. Upper Mesozoic strata near Padang. West Sumatra. Bull. Geol. Soc. Malaysia 8, 61–74.
Yang, X., Singh, S.C., Deighton, I., 2021. The Margin-Oblique Kumawa Strike-Slip Fault in the Banda Forearc, East Indonesia: Structural Deformation, Tectonic Origin and Geohazard Implication. Tectonics 40, e2020TC006567.
Yao, W., Ding, L., Cai, F., Wang, H., Xu, Q., Zaw, T., 2017. Origin and tectonic evolution of upper Triassic Turbidites in the Indo-Burman ranges, West Myanmar. Tectonophysics 721, 90–105.
Ye, Q., Mei, L., Shi, H., Camanni, G., Shu, Y., Wu, J., Yu, L., Deng, P., Li, G., 2018. The Late Cretaceous tectonic evolution of the South China Sea area: an overview, and new perspectives from 3D seismic reflection data. Earth-Sci. Rev. 187, 186–204.
Yeats, R., 2012. Active Faults of the World. Cambridge University Press.
Yonemura, K., Osanai, Y., Nakano, N., Adachi, T., Charusiri, P., Zaw, T.N., 2013. EPMA U-Th-Pb monazite dating of metamorphic rocks from the Mogok Metamorphic Belt, central Myanmar. J. Mineral. Petrol. Sci. 108, 184–188.
Yuan, J., Yang, Z., Deng, C., Krijgsman, W., Hu, X., Li, S., Shen, Z., Qin, H., An, W., He, H., 2021. Rapid drift of the Tethyan Himalaya terrane before two-stage India-Asia collision. Natl. Sci. Rev. 8, nwaa173.
Yue, L.-F., Suppe, J., Hung, J.-H., 2005. Structural geology of a classic thrust belt earthquake: the 1999 Chi-Chi earthquake Taiwan (Mw= 7.6). J. Struct. Geol. 27, 2058–2083.
Yui, T.-F., Fukoyama, M., Iizuka, Y., Wu, C.-M., Wu, T.-W., Liou, J.G., Grove, M., 2013. Is Myanmar jadeitite of Jurassic age? A result from incompletely recrystallized inherited zircon. Lithos 160, 268–282.
Yulihanto, B., 2004. Hydrocarbon play analysis of the Bone Basin, South Sulawesi. In: Noble, R.A. et al. (Eds.), Proc. Deepwater and frontier exploration in Asia Australasia Symposium, Jakarta, Indon. Petroleum Assoc. (IPA), p. 333 - 348.
Yumul, G.P., Dimalanta, C.B., Tamayo, R.A., Maury, R.C., 2003. Collision, subduction and accretion events in the Philippines: a synthesis. Isl. Arc , 12, , pp. 77–91.
Yumul, G.P., Dimalanta, C.B., Tamayo, R.A., Maury, R.C., Bellon, H., Polvé, M., Maglambayan, V.B., Querubin, C.L., Cotten, J., 2004. Geology of the Zamboanga Peninsula, Mindanao, Philippines: an enigmatic South China continental fragment?. Geol. Soc. Lond. Spec. Publ. 226, 289–312.
Yumul, G.P., Dimalanta, C.B., Tamayo, R.A., 2005. Indenter-tectonics in the Philippines: Example from the Palawan Microcontinental Block-Philippine Mobile Belt Collision. Resour. Geol. 55, 189–198.
Yumul, G.P., Dimalanta, C.B., Marquez, E.J., Queaño, K.L., 2009a. Onland signatures of the Palawan microcontinental block and Philippine mobile belt collision and crustal growth process: a review. J. Asian Earth Sci. 34, 610–623.
Yumul, G.P., Jumawan, F.T., Dimalanta, C.B., 2009b. Geology, geochemistry and chromite mineralization potential of the Amnay Ophiolitic Complex, Mindoro, Philippines. Resour. Geol. 59, 263–281.
Yumul, G.P., Dimalanta, C.B., Tamayo, R.A., Faustino-Eslava, D.V., 2013. Geological features of a collision zone marker: the Antique Ophiolite Complex (Western Panay, Philippines). J. Asian Earth Sci. 65, 53–63.
Yuwono, Y.S., Priyomarsono, S., Maury, T.R.C., Rampnoux, J.P., Soeria-Atmadja, R., Bellon, H., Chotin, P., 1988. Petrology of the Cretaceous magmatic rocks from Meratus Range, southeast Kalimantan. J. SE Asian Earth Sci. 2, 15–22.
Zahirovic, S., Seton, M., Müller, R.D., 2014. The cretaceous and cenozoic tectonic evolution of Southeast Asia. Solid Earth 5, 227–273.
Zahirovic, S., Matthews, K.J., Flament, N., Müller, R.D., Hill, K.C., Seton, M., Gurnis, M., 2016. Tectonic evolution and deep mantle structure of the eastern Tethys since the latest Jurassic. Earth-Sci. Rev. 162, 293–337.
Zamoras, L.R., Matsuoka, A., 2001. Malampaya Sound Group : a Jurassic-Early Cretaceous accretionary complex in Busuanga Island, North Palawan Block (Philippines). J. Geol. Soc. Japan 107, 316-336.
Zamoras, L.R., Matsuoka, A., 2004. Accretion and postaccretion tectonics of the Calamian Islands, North Palawan block, Philippines. Isl. Arc 13, 506–519.
Zamoras, L.R., Montes, M.G.A., Queano, K.L., Marquez, E.J., Dimalanta, C.B., Gabo, J.A. S., Yumul, G.P., 2008. Buruanga peninsula and Antique Range: two contrasting terranes in Northwest Panay, Philippines featuring an arc–continent collision zone. Isl. Arc 17, 443–457.
Zhang, X., Chung, S., Lai, Y., Ghani, A.A., Murtadha, S., Lee, H., Hsu, C., 2018b. Detrital Zircons Dismember Sibumasu in East Gondwana. J. Geophys. Res. Solid Earth 123, 6098–6110.
Zhang, X., Chung, S.-L., Lai, Y.-M., Ghani, A.A., Murtadha, S., Lee, H.-Y., Hsu, C.-C., 2019. A 6000-km-long Neo-Tethyan arc system with coherent magmatic flare-ups and lulls in South Asia. Geology 47, 573–576.
Zhang, X.R., Chung, S.-L., Ghani, A.A., Rahmat, R., Hsin, Y.-J., Lee, H.-Y., Liu, P.-P., Xi, J., 2023. Time to reconsider the enigmatic tail of eastern Paleo-Tethys: New insights from Borneo. Lithos 442, 107089.
Zhang, X., Chung, S.-L., Tang, J.-T., Maulana, A., Mawaleda, M., Oo, T., Tien, C.-Y., Lee, H.-Y., 2020. Tracing Argoland in eastern Tethys and implications for India-Asia convergence. GSA Bull.
Zhang, Y., Tsai, C.-H., Froitzheim, N., Ustaszewski, K., 2020. The Yuli Belt in Taiwan: Part of the suture zone separating Eurasian and Philippine Sea plates. Terr. Atmos. Ocean. Sci. 31.
Zhang, A., Asis, J. Bin, Fang, X., Li, H., Omang, S.A.K., Chen, M., Fang, Q., Li, D., Peng, T., 2022. Late Cretaceous fore–arc spreading in the northern Kuching Zone of West Borneo, SE Asia: Constraints from the Pakong Mafic Complex. J. Asian Earth Sci. 105189.
Zhang, P., Mei, L., Hu, X., Li, R., Wu, L., Zhou, Z., Qiu, H., 2017b. Structures, uplift, and magmatism of the Western Myanmar Arc: Constraints to mid-Cretaceous-Paleogene tectonic evolution of the western Myanmar continental margin. Gondw. Res. 52, 18–38.
Zhang, P., Miller, M.S., 2021. Seismic imaging of the subducted Australian continental margin beneath Timor and the Banda Arc collision zone. Geophys. Res. Lett. 48.
Zhang, G., Shao, L., Qiao, P., Cao, L., Pang, X., Zhao, Z., Xiang, X., Cui, Y., 2020a. Cretaceous-Palaeogene sedimentary evolution of the South China Sea region: A preliminary synthesis. Geol. J. 55, 2662–2683.
Zhang, J., Xiao, W., Windley, B.F., Cai, F., Sein, K., Naing, S., 2017a. Early Cretaceous wedge extrusion in the Indo-Burma Range accretionary complex: implications

for the Mesozoic subduction of Neotethys in SE Asia. Int. J. Earth Sci. 106, 1391–1408.
Zhang, J., Xiao, W., Windley, B.F., Wakabayashi, J., Cai, F., Sein, K., Wu, H., Naing, S., 2018a. Multiple alternating forearc-and backarc-ward migration of magmatism in the Indo-Myanmar Orogenic Belt since the Jurassic: Documentation of the orogenic architecture of eastern Neotethys in SE Asia. Earth-Sci. Rev. 185, 704–731.
Zhang, J., Xiao, W., Wakabayashi, J., Windley, B.F., Han, C., 2022b. A fragment of Argoland from East Gondwana in the NE Himalaya. J. Geophys. Res. Solid Earth e2021JB022631.
Zhao, D., Ohtani, E., 2009. Deep slab subduction and dehydration and their geodynamic consequences: evidence from seismology and mineral physics. Gondw. Res. 16, 401–413.
Zhao, Q., Yan, Y., Zhu, Z., Carter, A., Clift, P.D., Hassan, M.H.A., Yao, D., Aziz, J.H.A., 2021. Provenance study of the Lubok Antu Mélange from the Lupar valley, West Sarawak, Borneo: Implications for the closure of eastern Meso-Tethys?. Chem. Geol. 581, 120415.
Zheng, H.-W., Gao, R., Li, T.-D., Li, Q.-S., He, R.-Z., 2013. Collisional tectonics between the Eurasian and Philippine Sea plates from tomography evidences in Southeast China. Tectonophysics 606, 14–23.
Zheng, M., Song, Y., Li, H., Guilmette, C., Tang, J., Zhang, Q., Liu, Z., Li, F., 2022. Triassic trachytic volcanism in the Bangong-Nujiang Ocean: geochemical and geochronological constraints on a continental rifting event. Geol. Mag. 159, 519–534.
Zhong, L.-F., Cai, G.-Q., Koppers, A.A.P., Xu, Y.-G., Xu, H.-H., Gao, H.-F., Xia, B., 2018. 40Ar/39Ar dating of oceanic plagiogranite: Constraints on the initiation of seafloor spreading in the South China Sea. Lithos 302, 421–426.
Zhou, M.-F., Robinson, P.T., Su, B.-X., Gao, J.-F., Li, J.-W., Yang, J.-S., Malpas, J., 2014. Compositions of chromite, associated minerals, and parental magmas of podiform chromite deposits: The role of slab contamination of asthenospheric melts in suprasubduction zone environments. Gondw. Res. 26, 262–283.
Zhu, J., Li, S., Murtadha, S., 2022. Oldest Basement (ca. 462 Ma) in Indonesian Borneo and its Implication for Early Paleozoic Tectonic Evolution of SE Asia. Acta Geol. Sin. Ed. 96, 2093–2104.
Zhu, D.-C., Zhao, Z.-D., Niu, Y., Dilek, Y., Hou, Z.-Q., Mo, X.-X., 2013. The origin and pre-Cenozoic evolution of the Tibetan Plateau. Gondw. Res. 23, 1429–1454.
Zillman, N.J., Paten, R.J., 1975. Exploration and petroleum prospects, Bula Basin, Seram, Indonesia. Proc. Indones. Petr. Assoc. Annu. Conv. 4, 129–148.
Zimmermann, S., Hall, R., 2019. Provenance of Cretaceous sandstones in the Banda Arc and their tectonic significance. Gondw. Res. 67, 1–20.

Eldert Advokaat obtained a PhD in Geology at Royal Holloway University of London in 2016, and an MSc in Geology at Utrecht University in 2011. His research includes developing reconstructions of intensely deformed regions, and reconstructing formation and dismemberment of ophiolites using field-based structural geology, paleomagnetism, rock magnetism, and magnetic fabric analysis. His work in SE Asia started with field research on Sulawesi for his PhD project in 2011 and continued in Utrecht in 2016 with field projects in Sumatra, the Andaman Islands, and Borneo, and this reconstruction, which gradually expanded back in time to the Triassic. He is now a research coordinator at Utrecht University.

Douwe van Hinsbergen (PhD, Utrecht University, 2004) is full professor of global tectonics and paleogeography at Utrecht University, the Netherlands, where he has taught since 2012. Van Hinsbergen studies and kinematically reconstructs plate tectonics, orogenesis, and paleogeography across the globe. He closely collaborates with seismologists to reconstruct mantle convection and with modelers of geodynamics and paleoclimate to advance understanding in the physics driving geological processes particularly related to plate tectonics. Van Hinsbergen is author or co-author of over 200 articles in peer-reviewed international journals.